A STUDY OF THE DYNAMICS OF THE BRITISH ICE SHEET DURING MARINE ISOTOPE STAGES 2 AND 3, FOCUSING ON HEINRICH EVENTS 2 AND 4 AND THEIR RELATIONSHIP TO THE NORTH ATLANTIC GLACIOLOGICAL AND CLIMATOLOGICAL CONDITIONS

Sasha Naomi Bharier Leigh

A Thesis Submitted for the Degree of MPhil
at the
University of St. Andrews

2007

Declaration

(i) I, Sasha Naomi Bharier Leigh, hereby certify that this thesis, which is approximately 40,000 words in length (excluding captions and references), has been written by me, that it is the record of work carried out by me and that it has not been submitted in any previous application for a higher degree.

Date Signature of candidate

(ii) I was admitted as a research student in September 2003 and as a candidate for the degree of PhD in September 2004 and changed to the degree of MPhil in September 2005; the higher study for which this is a record was carried out at the University of St Andrews between 2003 and 2005.

Date Signature of candidate

(iii) I hereby certify that the candidate has fulfilled the conditions of the Resolution and Regulations appropriate for the degree of MPhil in the University of St Andrews and that the candidate is qualified to submit this thesis in application for that degree.

Date Signature of supervisor

Unrestricted

In submitting this thesis to the University of St Andrews I understand that I am giving permission for it to be made available for use in accordance with the regulations of the University Library for the time being in force, subject to any copyright vested in the work not being affected thereby. I also understand that the title and the abstract will be published, and that a copy of the work may be made and supplied to any bona fide library or research worker.

Date Signature of candidate

Abstract

A high-resolution investigation into the stratigraphy of core MD95-2006 from the Barra Fan, NW Scottish continental slope, has been carried out. The study focuses on key palaeoceanographic proxies (percentage Neogloboquadrina pachyderma (s), planktonic foraminiferal stable isotopes, planktonic foraminiferal and ice-rafted debris concentrations) throughout the interval between and including Heinrich Event 4 and Heinrich Event 2. A newly constructed age model produced through ties to the GRIP Greenland ice core record places this interval at approximately 20-48 ka BP. The interval covers the end of Marine Isotope Stage 3 and the start of Marine Isotope Stage 2, dating the MIS3/2 transition at 25.34-26.57 ka BP. Results reveal novel information on the dynamics of the British Ice Sheet (BIS) through this period and their relationship with other circum-North Atlantic ice sheets through a particular focus on the structure and provenance of Heinrich Events 2 and 4 within MD95-2006.

The study revealed that at the time of Heinrich Event 4, placed at 36.2-36.7 ka BP, the BIS was of limited extent and significant ice sheet expansion only occurred after ca. 26.5 ka BP, coinciding with the MIS3/2 transition in the MD95-2006 record. It appears that the margin of the BIS reached the continental slope around 25 ka BP and it is likely that the period between 21.5 and 25 ka BP, represents the maximum extent of the NW Scottish ice sheet. At the time of H4, the BIS was of limited extent whereas the Laurentide Ice Sheet (LIS) was already significantly expanded, thus the dominant radioisotopic signal seen in H4 sediment in MD95-2006 is that of LIS icebergs, overcoming the BIS contribution. In contrast, H2 (21.56-21.72 ka BP) occurs at a time of increased delivery of icebergs from all North Atlantic ice sheets however the MD95-2006 record dominated by the influence of the proximal BIS. This is revealed in both the increased background level of IRD delivery and the correspondence of background and peak IRD radioisotopic ratios tending towards British provenance.

Acknowledgements

I would like to thank Rob Ellam and Anne Kelly at The Scottish Universities Environmental Research Centre for willingly giving their time, expertise and facilities throughout the radiogenic isotope preparation and analysis. I am also extremely grateful for all the help I received from Jonathan Wynn and Michael Bird (University of St Andrews) during the stable isotopic analyses procedure and to Angus Calder (University of St Andrews) for all his help with the X-Ray Fluorescence and X-ray Diffraction analyses. Guy Rothwell (National Oceanography Centre, Southampton) was also invaluable for his guidance through the ITRAX procedure. Finally I would like to thank my supervisor Dr William Austin for his support, guidance and encouragement.

Contents

Figures

Tables

1. Introduction

1.1 Abrupt Climate Transitions

Global-scale abrupt climate variability is widely recognised in high-resolution climatic proxies from marine and terrestrial palaeoarchives over the last glacial-interglacial period, in particular within the last 80-100 kyr. Two prominent features of this variability are Dansgaard-Oeschger (D-O) Cycles and Bond Cycles, first recognised in oxygen isotope data from Greenland ice core records (Dansgaard *et al.* 1993, Grootes *et al.* 1993, Grootes and Stuiver 1997), the latter consisting of a series of progressively cooling D-O cycles terminated by an abrupt climatic warming. The ice-core records from the Greenland Summit indicate that transitions between cold stadials and warmer interstadials (the D-O 'events') took place within decades and were accompanied by warmings of ca.10°C (Severighaus and Brook 1999).

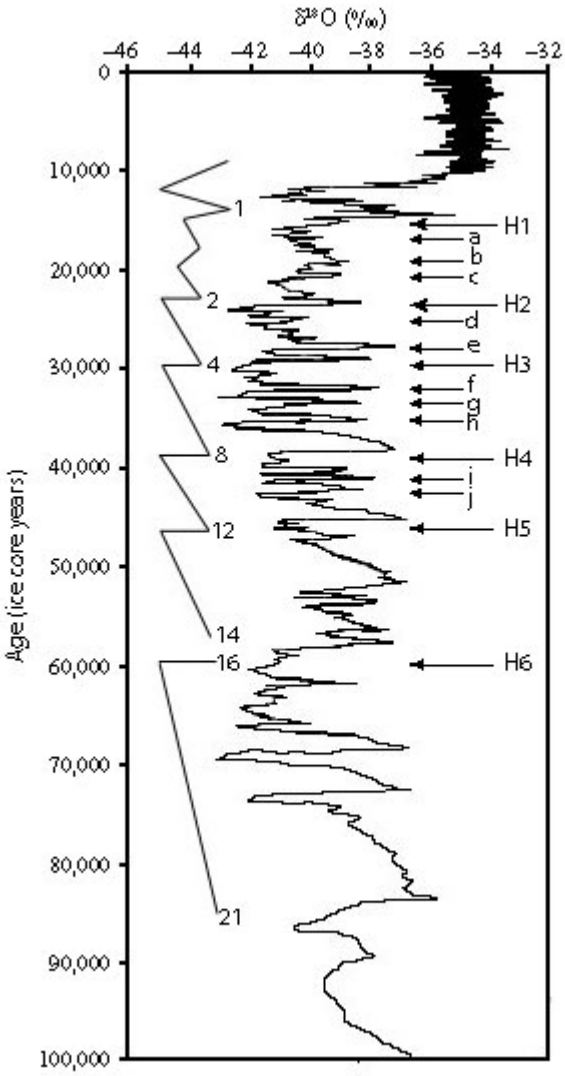

Figure 1.1: Greenland $\delta^{18}O$ record over the last 120 kyr. The timing of Heinrich Events and Detrital Events (lower case letters) are indicated. Longer term cooling cycles (Bond Cycles) are shown on the left along with interstadial numbers (Bond and Lotti 1995).

Records of sea surface temperatures (SSTs) from North Atlantic sediments closely match those of the ice core record (Bond *et al.* 1993, Broecker 1994). In North Atlantic sediments, the end of a 'Bond Cycle' is marked by the appearance of rapidly-deposited, coarse (>125 μm) layers characterised by an increase in percentage of lithic fragments compared to foraminifera and increased magnetic susceptibility, amongst other lithological and geochemical indicators (e.g. Heinrich 1988, Janschik and Huon 1992, Francois and Bacon 1994, Stoner *et al.* 1996, Andrews *et al.* 1998, Grousset *et al.* 1993, 2001). So called Heinrich layers (Heinrich 1988) are attributed to massive discharges of icebergs (Heinrich Events) prior to sudden climatic warming, transporting ice-rafted debris (IRD), scraped from their source areas, across the North Atlantic. D-O cycles are seen as similarly abrupt events in proxy records of North Atlantic sea surface temperature and salinity (e.g. Maslin *et al.* 1995, Elliot *et al.* 1998, Bianchi and McCave 1999, Chapman and Shackleton 1999, Shackleton *et al.* 2000) and are also marked by IRD layers, (Detrital Events, DEs), in the north-east Atlantic with similar sedimentological properties to Heinrich layers (Bond and Lotti 1995, Fronval *et al.* 1995).

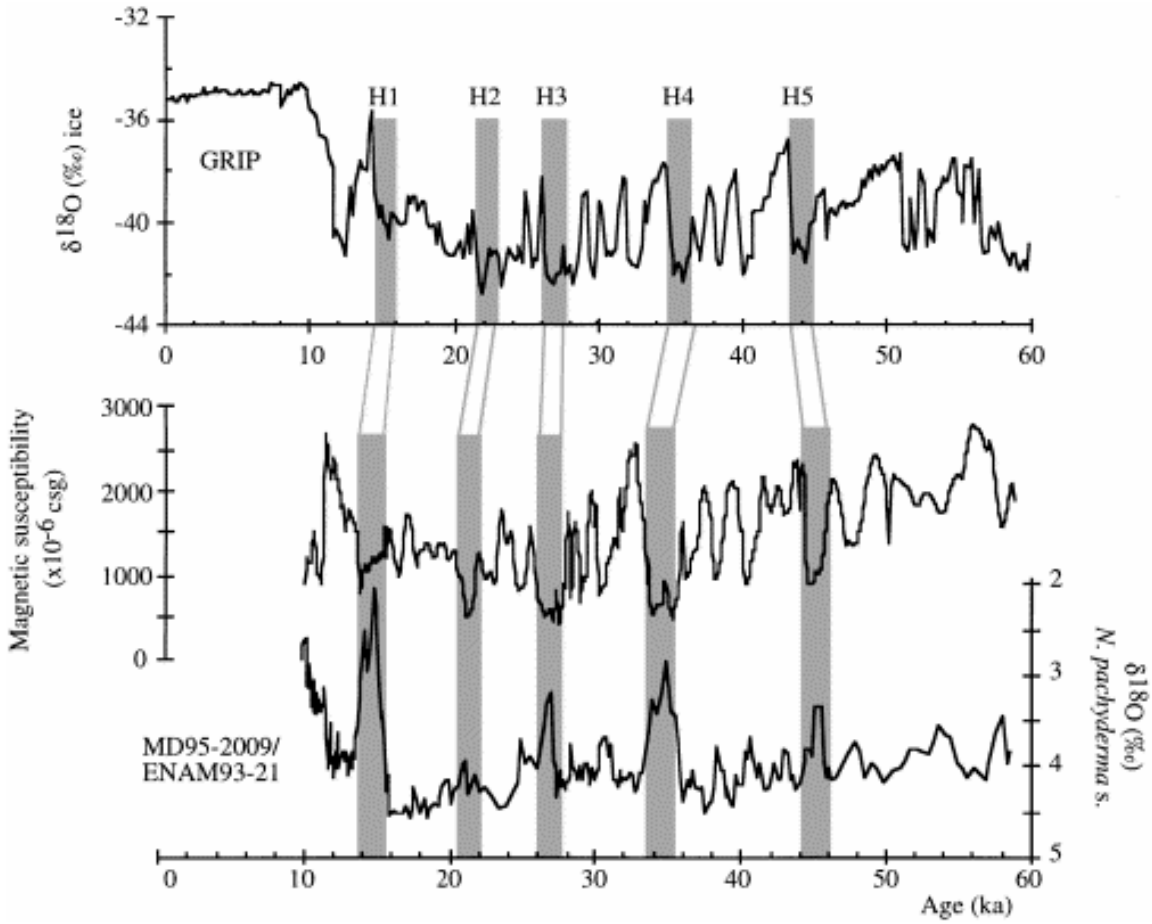

Figure 1.2: An illustration of the correlation between Heinrich Events in a marine core and the GRIP ice core record (after Cortijo *et al.* 2000). From top to bottom: $\delta^{18}O$ of the ice at GRIP site (Greenland) showing the Dansgaard-Oeschger oscillations (Dansgaard *et al.*., 1993); Magnetic susceptibility and *N. pachyderma* s. $\delta^{18}O$ record for core ENAM93-21 (62°N, 3°W) from (Rasmussen *et al.*., 1996a). The Heinrich events are marked by grey rectangle.

1.2 Ice-rafting Events

North Atlantic-wide coarse, sandy layers occurring on millennial timescales within marine sediments were first recognised by Ruddiman (1977) and Heinrich (1988). It was assumed that ice-rafting was the only process able to transport such high volumes of lithic sediment over such a wide spatial area. Ruddiman (1977) identified the zone of maximum thickness of these zones between 40^0N and 55^0N in the North Atlantic, now known as the 'Ruddiman Belt' or 'IRD Belt' and the focus of many of the subsequent palaeoceanographic studies.

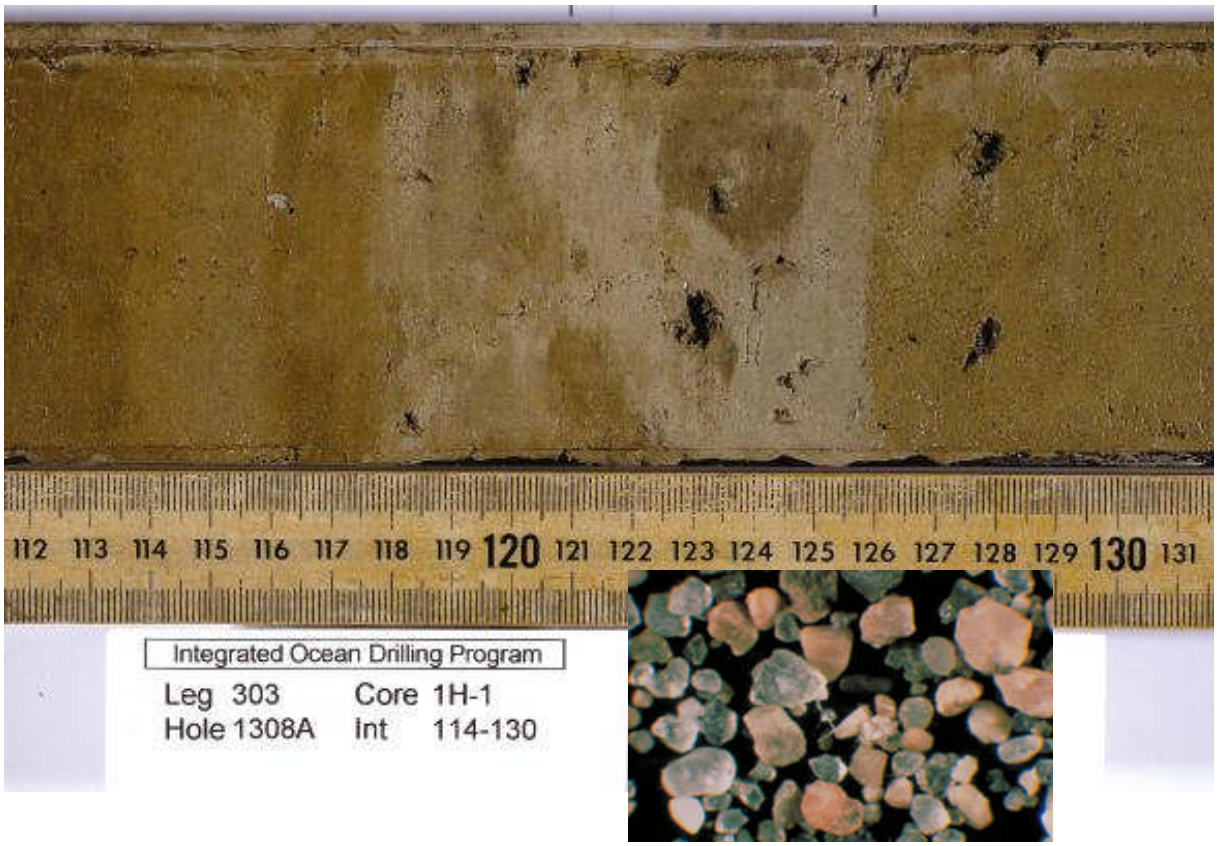

Figure 1.3: Heinrich Event 2 (118-126cm) in new IODP core taken at site 1308, a reoccupation of the site of ODP609.

Note the sharp base at 126cm marking the initiation of the Heinrich Event and the distinct change in sediment colour at this depth from 126 to 118 cm (increasing sediment carbonate content). The upper boundary of the Heinrich Event is marked by a diffuse, bioturbated horizon , burrows extending downward through the Heinrich Layer. Inset: Microscopic photograph of Heinrich Event sediment (>150μm).

These thick, millennial-scale IRD layer occurred late in the course of a Bond Cycle when correlated with the marine cores' $\delta^{18}O$ records, within the coldest oceanic conditions (Zahn *et al.* 1997) and just prior to the maximum atmospheric cold conditions before a sudden warming approaching interglacial conditions (Bond *et al.* 1992, Broecker *et al.* 1992, Bond and Lotti 1995, Maslin *et al.* 1995). These layers were named Heinrich layers after H. Heinrich (1988) and the wide-scale ice-rafting events that produced them are termed Heinrich Events.

1.2.1 Heinrich Events

1.2.1.1 Properties of Heinrich Events

Heinrich Events have been characterised by many different sedimentological properties. The Heinrich Layers are traditionally defined by a high IRD flux and an increase in percentage of lithic fragments compared to planktonic foraminifera. The foraminifera species in these layers are typically dominated by *Neogloboquadrina pachyderma* (s) with light $\delta^{18}O$ values (Bond *et al.* 1992). Other ways Heinrich Events are identified in the marine sedimentary record include increased magnetic susceptibility (Grousset *et al.* 1993, Robinson *et al.* 1995, Stoner *et al.* 1996), relatively high bulk and GRAPE densities (Auffret *et al.* 1996, Chi and Mienert 1996), increased sediment flux recorded in ^{230}Th excess records (Thomson *et al.* 1995) and low organic carbon (Auffret *et al.* 1996) amongst other lithological and geochemical indicators (e.g. Heinrich 1988, Janschik and Huon 1992, Francois and Bacon 1994, Andrews *et al.* 1998, Grousset *et al.* 2001). The assertion that these layers originate from massive iceberg discharges is based on the abrupt increase in coarse detritus thought only to have been feasibly delivered by ice-rafting, in association with a low grain size sorting, thought only to be induced by iceberg discharges (Manighetti and McCave 1995, Revel *et al.* 1996b). Heinrich (1988) demonstrated a series of six main events, occurring every ca.11ka, their timing and duration determined by climatic and oceanographic studies (Bond *et al.* 1992, Grousset *et al.* 1993, Dowdeswell *et al.* 1995, Revel *et al.* 1996, Viega-Pires and Hillaire-Marcel 1999). Heinrich Layers were deposited very rapidly and may have only lasted a few hundred years (Francois and Bacon 1994, Thompson *et al.* 1995, McManus *et al.* 1998). The flux of detritus within Heinrich Layers is dramatically higher than in ambient sediments (Francois and Bacon 1994, Thomson *et al.* 1995,

McManus *et al.* 1998, Viega-Pires and Hillaire-Marcel 1999). Maximum IRD deposition was in the 'IRD Belt' which lies to the north of the location of the polar front during the Heinrich Events (45-50°N), corresponding to the northern limit of warmer, mid-latitude surface waters and thus, the position of maximum iceberg melt (Ruddiman 1977). That said, traces of ice-rafting associated with Heinrich Layers have been found as far south as 30^{0}N (Keigwin and Boyle 1999).

Four (H1, H2, H4, H5) of the six Heinrich Layers contain relatively high (20-25%) contents of detrital carbonate in all grain sizes (Huon *et al.* 1991, Bond *et al.* 1992, Andrews and Tedesco 1992, Stoner and Andrews 1999) with a typical a calcite:dolomite ratio of 2.2+/-0.6; (Andrews 1998). This detrital carbonate is thought to originate from Palaeozoic Canadian Shield Limestones and is nearly absent in ambient glacial sediment (Bond *et al.* 1992). These four Heinrich Layers also show an integrated spatial average thickness of 10-15cm with an overall eastward decay across the North Atlantic (Dowdeswell *et al.* 1995). Studies therefore suggest a main iceberg source from North America, the Laurentide Ice Sheet (LIS), the main iceberg drift-path being the Hudson Strait (Ruddiman 1977, Broecker 1994, Dowdeswell *et al.* 1995, Hemming *et al.* 1998, Revel *et al.* 1996). Chough (1978) and Aksu and Mudie (1985) had earlier noted lithofacies in cores from the southeast Baffin Island Shelf and the floor of the northwest Labrador Sea which were distinctive owing to their high detrital carbonate contents. These were later inferred to be the proximal counterparts of the distal lithic-rich units which characterise Heinrich Events in the deep-sea record (Andrews at al 1998). In addition, model results show that, assuming that glacial and modern icebergs entrain similar volumes of sediment, the ablation of the southern margin of the LIS is an important factor in producing the observed deposition patterns in the glacial North Atlantic (Matsumoto 1997).

These four 'typical' Heinrich Events also contain distinct internal sedimentary patterns (Grousset *et al.* 2001). At least in the Ruddiman Belt, they are generally deposited without any hiatus, erosion surfaces or physical perturbation and are characterised by abundant, poorly-sorted coarse (mm-cm) particle deposits alternating with thin (3-5mm) layers of normal glacial sediments. Bioturbation is only recognised in the latter layers imlying that the Heinrich Layers are deprsited very rapidly (Auffret *et al.* 1996, Grousset *et al.* 2001).

Although Heinrich Layers are often identified through properties of the coarse sediment fraction, an increase in detrital, non-phyllosilicate minerals is also seen in finer (2-16μm) fractions within Heinrich Layers (Janschik and Huon 1992) indicating a change not only in the ice-rafting regime but in sediment transport processes and sources affecting all grain sizes. Indeed, Heinrich Events have not always been unequivocally linked to ice-rafting. Early theories concerning their origin were based on a variety of observations of the properties of Heinrich Layers and alternative explanations of these properties ranged from dramatic decreases in surface water productivity to brief increases in carbonate dissolution on the sea floor.

Although HEs are often grouped together in their classification, each Heinrich Layer can have vastly differing temporal and spatial properties. In initial studies of provenance of IRD from Heinrich Layers, the absence of LIS-sourced material in H3 and H6 compared to the other HEs is particularly noticeable and Heinrich Events were named 'atypical' (H3 and H6) and 'typical' (H1, H2, H4, H5) accordingly. Typical Heinrich Events are dominated by LIS-derived IRD (e.g. Gwiazda *et al.* 1996, Hemming *et al.* 1998, Hemming *et al.* 2002b) and atypical events are thought to reflect more varied, circum-Atlantic origins (Figure 1.4; Huon and Janschik 1993, Grousset *et al.* 1993, Gwiazda *et al.* 1996, Sneockx *et al.* 1999). It is not only in the coarse lithic fraction that such differences are seen. The $\delta^{13}C$ and $\delta^{15}N$ of fine-grained organic matter decrease to minimum values within H1 and H2 compared to the average values for ambient glacial sediment, however there is no significant deviation within H3 (Grousset *et al.* 2001).

All Heinrich Events are characterised by higher abundances of K-feldspar and plagioclase in the clay fraction however high amphibole content is restricted to H1, H2, H4 and H5. Also, although they contain a high IRD percentage, in contrast to the typical Heinrich Layers, H3 and H6 have unremarkable numbers of lithic grains per gram (the relative percentage only increasing due to a lower foraminifera concentration) and sediment flux (McManus *et al.* 1998), little or no apparent increase in detrital carbonate (Bond *et al.* 1992, Bond and Lotti 1995), only minor magnetic susceptibility peaks as shown in Figure 1.4 (Revel *et al.* 1996) and little difference in isotopic

provenance indicators relative to ambient sediments (Janschik and Huon 1992, Grousset *et al.* 1993, Gwiazda *et al.* 1996, Revel *et al.* 1996, Hemming *et al.* 1998). Heinrich Layer 3 is also associated with a gradual transition rather than an abrupt onset (Gwiazda *et al.* 1996c).

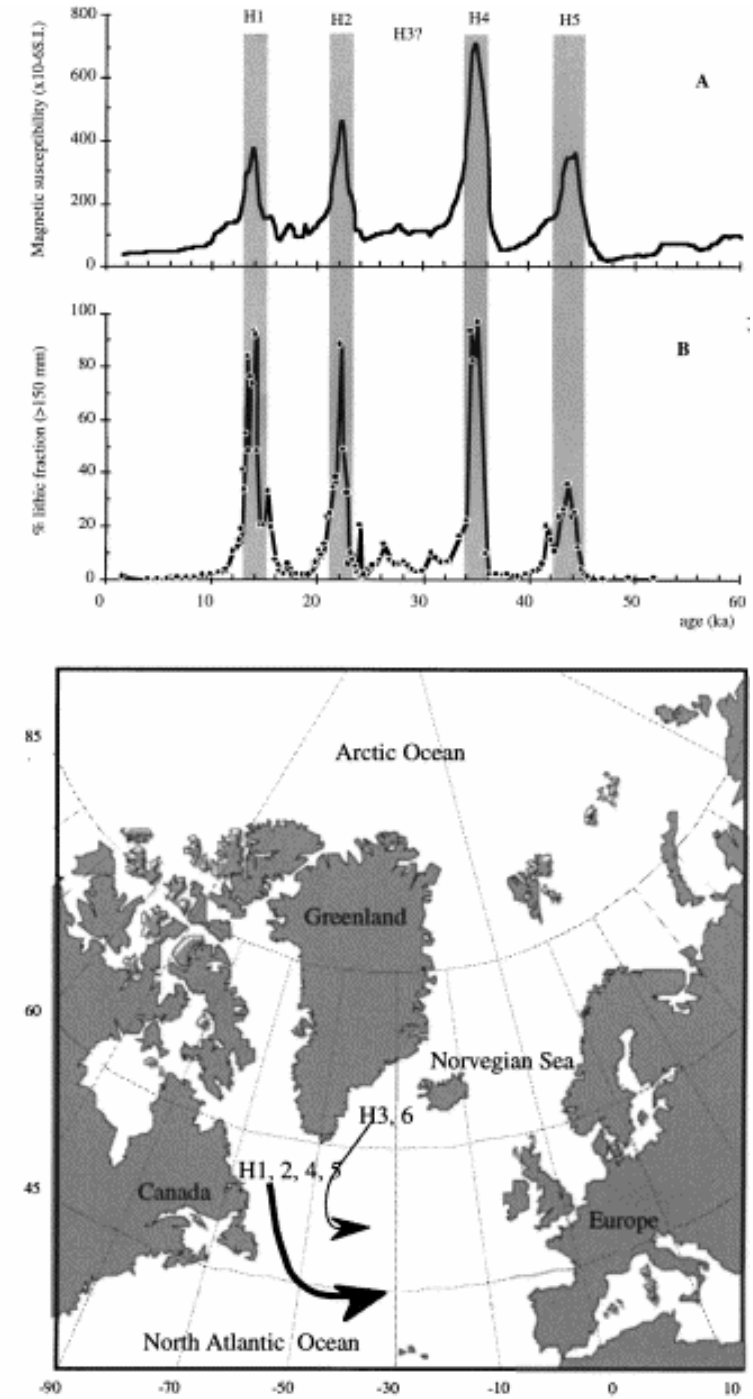

Figure 1.4: (A) Magnetic susceptibility record in core SU90-08 (40°N, 30°W) (Grousset *et al.*., 1993), (B) percentage of the lithic fraction in the same core, (C) sources of the icebergs as defined by (Grousset *et al.*., 1993). The shaded bars in panels A and B identify the Heinrich events (after Cortijo *et al.* 2000).

Sedimentological studies from the SE Baffin Slope and NW Labrador Sea show a poorly-developed and indistinctive H3, indicating that at this time, the NE LIS may have been associated with a different glaciological regime than during the other Heinrich Events, with flow across the Hudson Strait from Ungava-Labrador rather than flow along the axis of the Strait (Andrews and Maclean 2003).

As the depth of study increases, more differences are noted between *all* the Heinrich Layers. Piper and deWolfe (2003) have noted a much higher carbonate sand content but fewer feldspar grains in H2 than in H1, indeed the detrital carbonate content of H1 is around 4-7% less in H1 (Hemming *et al.* 1998). H2 is also seen as a much more pronounced event in both the $\delta^{18}O$ and IRD from sites off the west of Britain (Porcupine Bank, V. Peck *pers. comm*; Barra Fan, L. Wilson *pers.comm.*). Heinrich Events generally occurred late in the build-up to cold phases and were directly followed by brief warm periods, all except H1 after which there seems to be a ca.1000 yr lag between the ice-rafting event and the abrupt warming (Bond and Lotti 1995). Isotopic ratios and inferred ages are similar between the four typical Heinrich Layers (Hemming *et al.* 1998), all except for the εNd(0) which is much less negative (younger model age). Studies of fluxes of lithic fragments and forams within H3 have indicated that the reason for the formation of this layer may not be an increase in the flux of IRD but a decrease in the flux of forams (Bond *et al.* 1992, Higgins *et al.* 1995). Although these assertions are based on radiocarbon dates which have many inherent problems (see Section 1.8.1.3).

Some Heinrich Events have been much more widely studied than others. H2 and H3 are often focused on (e.g. Gwiazda *et al.* 1996, Grousset et al 2001) because of their position within MIS3. MIS3 and MIS2 are the time of peak glacial conditions compared to the position of H1 at the start of deglaciation and H4 which occurred at a time when the Northern Hemisphere ice sheets were still in a phase of growth. MIS3 is within the accurate limit of radiocarbon dating, enabling millennial-scale age control (Hughen *et al.* 2004). MIS3 is often a time of very high sedimentation rates in North Atlantic cores e.g. 24 $cmka^{-1}$ (Kissel *et al.* 1999); >40 $cmka^{-1}$; (Knutz *et al.* 2002), making it ideal for carrying out high-resolution studies and accurate correlations.

1.2.1.2 Duration of Heinrich Events

There is some disagreement about the duration of Heinrich Events and Heinrich Layers, whether they were laid down relatively instantaneously or over 1000 years or more (e.g. Bond *et al.* 1992, Andrews and Tedesco 1992, Grousset *et al.* 2001). Much of this debate stems from the imprecision of the available dating techniques on less than centennial-scale. Some studies have addressed this issue through other methods. Hemming and Hadjas (2003) take the very pure provenance of the Heinrich Layers in an eastern Atlantic core to indicate an instantaneous deposition, thereby swamping out other contributions. Conversely Francois and Bacon (1994) use point by point flux estimates based on ^{230}Th-normalisation to infer maximum durations of 600 and 800 years for H1 and H2 respectively. These durations however are based on the identification of Heinrich Layers by dolomite spikes which, in light of discussions on the probably multi-phase, multi-source structure to Heinrich Events (e.g. Bond *et al.* 1992) is unlikely to encompass the event in its entirety.

The inferred durations of Heinrich Events allows accumulation rates to be calculated. Grousset *et al.* (2001) imply average accumulation rates of 15.3 and 11 $gcm^{-2}ka^{-1}$ for H1 and H2 respectively, in agreement with fluxes calculated using ^{230}Th activity in a core 80 km from their study site: 19 and 11 $gcm^{-2}ka^{-1}$ (Francois and Bacon 1994).

1.2.2 Detrital Events

The debate on North Atlantic ice-rafting events was further complicated by the discovery of layers of IRD with a much higher frequency of occurrence than Heinrich Layers (Bond and Lotti 1995). These so-called Detrital Events (see Figure 1.5) are observed to occur every ca.1500 yr (Bond *et al.* 1999, revised from the original estimates of 2-3 ka; Bond and Lotti 1995), correlating with the D-O cycles seen in Greenland ice cores (Dansgaard *et al.* 1993). Such climate variations have been noted to occur on a global scale (e.g. Denton and Hendy 1994, Behl and Kennet 1996, Little *et al.* 1997). These D-O Cycles correspond to rapid changes in the abundance of polar planktonic and benthic foraminifera and their isotope ratios, lows and highs in magnetic susceptibility and various physical properties (e.g. density, water content, grain size distribution) in North Atlantic cores (Rasmussen *et al.* 1996a, Moros *et al.* 1997). This

indicates that these cycles and associated Detrital Events may have had a similar oceanic influence as Heinrich Events.

Detrital events are noted at the culmination of some (but not all) D-O Cycles, correlating with the D-O cold 'Events' noted in the Greenland Ice core records (Bond *et al.* 1993, Snoeckx *et al.* 1999). Moreover, the IRD layers are spatially variable with a distinct lack of IRD layers between Heinrich Layers in many cores from more southerly locations in the North Atlantic (Grousset *et al.* 2001). The lack of distinctive IRD layers between Heinrich Layers in many cores from more southerly locations in the North Atlantic (e.g. SU90-09; Grousset *et al.* 2001) supports such inferences of a more northerly origin than that for Heinrich Events.

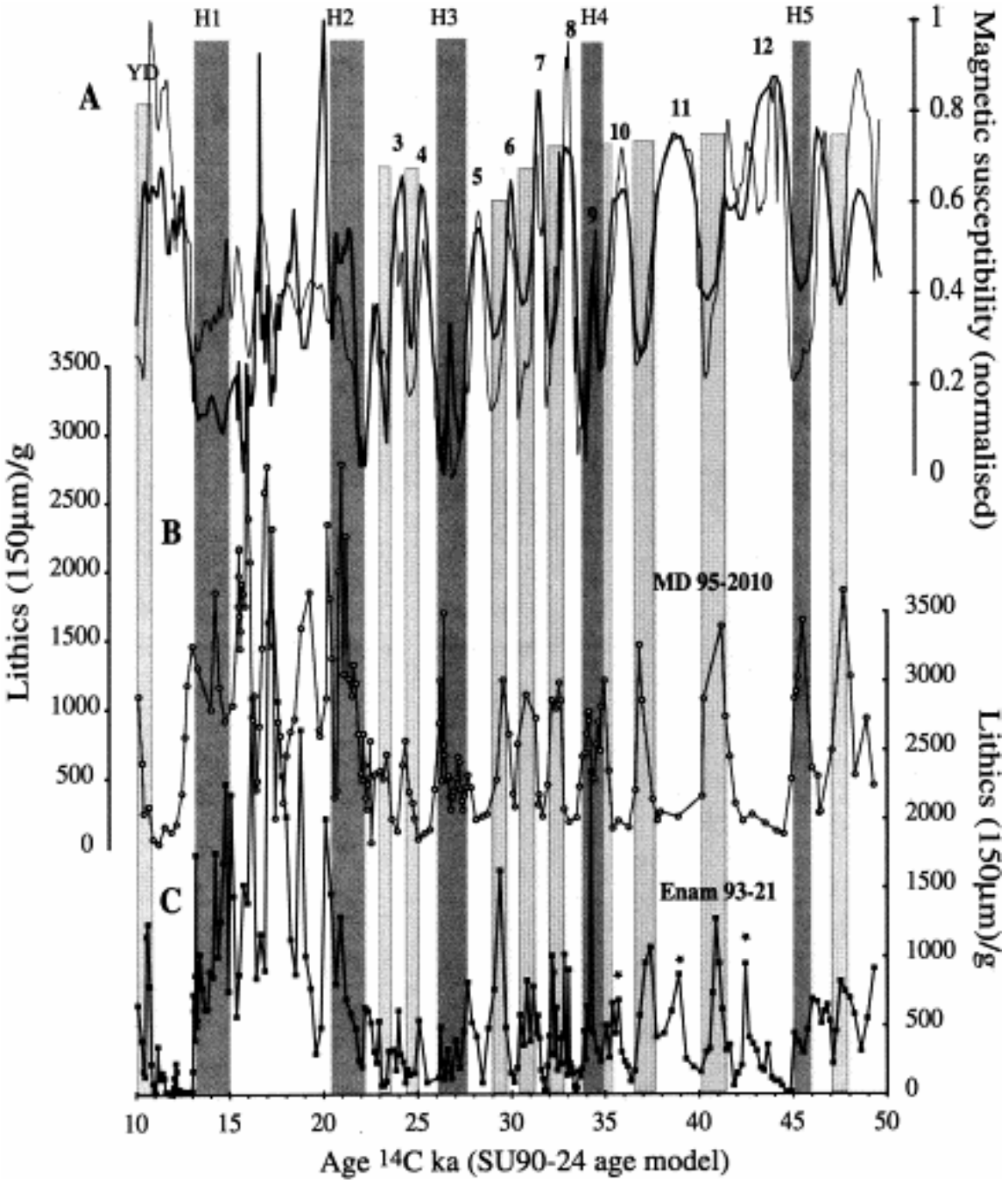

Figure 1.5: Heinrich Events and intervening detrital events in the Norwegian Sea (Elliot *et al.* 2001)

(A) Magnetic susceptibility record; (B) and (C) Coarse lithic content expressed as number of grains (>150 µm) per gram of dry sediment MD 95-2010 and ENAM 93-21. The dark grey bands represent the positions of the HE, the light bands correspond to the positions of the minimum MS values (demarking the DEs) intercalated between the HE.

1.2.3 European precursors

As the temporal (and spatial) resolution of study increased, discrete IRD layers were noted just prior to many Heinrich Layers, seemingly unrelated to the D-O cyclicity of Detrital Events (Revel *et al.* 1996, Snoeckx *et al.* 1999, Elliot *et al.* 1998, Scourse *et al.* 2000). Provenance studies have indicated that these pulses are sourced from Greenland and European ice sheets rather than the LIS.

So-called European Precursor events have been identified in some cores from the IRD belt (including the extensively studied ODP-609 and VM23-81; Bond and Lotti 1995, Bond *et al.* 1999) and in the Irminger Basin (SU90-24; Elliot *et al.* 1998, Bond *et al.* 1999). Similar precursors consisting of European-derived IRD have also been identified along the European margin (MD95-2002 and SU92-28; Grousset *et al.* 2000 and OMEX-2K and –4K; Scourse *et al.* 2000).

Many of the precursor events are enriched in volcanic IRD with a likely Icelandic origin. The spatial and temporal distribution of IRD with $\varepsilon Nd<-15$ suggests that destabilisations of the Fennoscandian Ice Sheet occurred just prior to, the collapse of the Laurentide ice Sheet as recorded in Heinrich Layers 1, 2, 4 and 5 (Grousset *et al.* 2000). The British Ice Sheet has also been implicated in these precursor events with a Campanian chalk peak (characteristic of LGM sediments from the Celtic Shelf; Scourse *et al.* 1990) occurring in the sand fraction of the H2 layer just prior to the main dolomite peak (Scourse *et al.* 2000).

Scource *et al.* (2000) note that the 'precursor' events lead the LIS input by up to 1500 yr. This poses the question of whether these events are in fact Heinrich Event precursors or whether they are simply the previous Detrital Event, which occur on a 1500 yr periodicity (see Section 2.2). Although high-resolution dating suggests that these precursors occur in addition to the more frequent IRD cycles, there still remains the possibility that they are just part of the previous detrital event. Scourse *et al.* (2000) reason that the BIS ‘precursor’ IRD pulse is not the previous detrital event on the basis that the D-O type pervasive periodicity is not observed on the European margin. Wilson and Austin (2002), however, do observe a ca.1500 yr cyclicity in

spetrophotometric records from MD95-2006 and thus, this observation challenges the argument for European precursors based on the reasoning of Scource *et al.* (2000). Data from Goban Spur indicate a lag time (based on ^{14}C dates) of 740-1360yr between the IRD pulse inferred to originate from the BIS and the combined BIS/LIS pulse of the main Heinrich Event 2 (Scourse *et al.* 2000). These studies highlight the extremely dynamic nature of all the circum-North Atlantic ice sheets.

Although detrital events on a D-O cyclicity are essentially absent from more southerly cores, distinctive events lasting 100-200 years and consisting of European-sourced IRD are seen prior to the main Heinrich Layers (Grousset *et al.* 2001). This suggests that precursor events do exist.

The debate surrounding the existence of European precursor events centres on the question of whether there is indeed separate, time-transgressive ice-rafting events comprising the interval within which each Heinrich Event lies or whether the discrete IRD layers are actually a manifestation of the varied response of different sized ice sheets to a common climatic forcing. The response of a large ice sheet like the LIS is likely to be up to 5000 yr whereas that of a small, climatically sensitive ice sheets such as the BIS, is only a few hundred years (Johannesson et al 1989). Discrete ice sheet lobes may even respond faster, especially in a maritime climate regime and if the lobes rest on a deformable substrate (Boulton et al 1985). The lag times of precursor events seem too small to accommodate this hypothesis. European precursors are associated with active THC (i.e. SST maxima) whereas main Heinrich Events are associated with convective shutdown (i.e. SST minima). This raises the question of phasing between glacier dynamics and oceanographic thresholds.

It is the issue of high-resolution dating that provides the real problem in solving the debate over whether precursor events are indeed just that, or whether they are simply the previous detrital event. It is radiocarbon dating that is most applicable to the dating of marine sediments over the past ca.30-40 ka however this dating method is associated with a multitude of complications, errors and uncertainties. If error margins on radiocarbon dates cannot statistically separate the age of a ‘precursor’ event from an age ca.1500 yr before the following HE then it cannot be assumed that the ‘precursor’ is not actually the previous detrital event. Many high-resolution studies do quote relatively

small errors on their radiocarbon dates, sometimes <100yr (Grousset *et al.* 2001). However these dates often contain internal assumptions and uncertainties not quantified in the expressed errors. Apart from factors such as the marine reservoir correction applied (see Section 1.8.1.3), errors can be introduced depending on the method of calibration used. Some studies don't even calibrate their radiocarbon dates at all! This may actually be due to the uncertainty in the calibration curve before ca.40,000 and indeed perhaps even as early as 20,00ka BP but uncalibrated ages are not able to be accurately used for correlation between records.

Comparison of records from different cores is a significant problem with regards to dating errors. Not only do North Atlantic cores show significant spatial differences in the inferred duration of a Heinrich Event but also in the lag-time between the previous minor IRD event (whether a detrital layer or a precursor). The relatively shorter lag-time observed in easterly cores, such as those from the British Margin (eg. 700-1000 yr; Scourse et al 2000) compared to those from the open North Atlantic (e.g. >1000 yr; Grousset et al 2001) poses the question of whether this is due to the same event being diachronous across space (reflecting iceberg trajectory times/differing response of different ice sheets to climatic triggers) or the various cores recording different events altogether. It seems that in all North Atlantic locations the Iceland/Britain IRD pulse is pretty indistinguishable date-wise but the main Heinrich Layer occurs ca.1.2ka earlier in IRD belt core VM23-81 than in cores from the British Margin. If this cannot be explained by ocean circulation patterns and iceberg trajectory times across the Atlantic, it must be due to incompatible dates between cores. There are various possible explanations:

1) The LIS may have surged more than once during a Heinrich Event, with only a late pulse reaching the European Margin – however this does not explain why the initial LIS pulse, a significant event in VM23-81, ca.4800km from the LIS is not observed in cores only ca.900km further to the east.
2) The dates from the British cores are all too young (or other cores too old) and although the precursor events occurred simultaneously, the British precursor occurs before the Icelandic precursor within marine records due to the lag-times associated with iceberg transport to the core site. This adjustment to the age-model of the British cores would then also mean that the time between the precursor and main HE would be reduced, compatible with iceberg transport

times between the sites of VM23-81 and the British Margin and thus the LIS pulse in all cores could realistically belong to the same event. This may be the case but lithological variations between mid- and late-HL IRD in SU90-09 (Grousset *et al.* 2001) both inferred to originate from the LIS indicates that the LIS surged over a longer period of time, perhaps with multiple pulses, delivering material initially from ice marginal geologies and subsequently, material from rocks scraped from under the central part of the ice sheet.

Dowdeswell *et al.* (1999) considered that the deposition of precursor IRD in the Nordic Seas and the North Atlantic were asynchronous, however their conclusions are based on a low-resolution study with limited radiocarbon dates limiting the control on their timescale. Synchronous deposition of material is supported by studies in the Norwegian Sea, Irminger Basin (Elliot *et al.* 2001) and in the main IRD belt (Grousset *et al.* 2001).

1.3 Palaeoclimatic/palaeoceanographic context of ice-rafting events

Due to the focus on orbitally driven climate change that dominated early climatic research, the prominent lithic-rich, foram-poor layers seen in North Atlantic sediments (later to become known as Heinrich Layers; Heinrich 1988, Broecker 1992) were not investigated. It was in fact the possible palaeoclimatic effects of these Heinrich Events: that freshwater discharged during iceberg melt could have disrupted NADW formation with huge implications on climate (Broecker 1992, 1994), that their significance was recognised. However, even after this, progression was hampered by the search for regular cyclicity, early studies attributing a ca.10,000 year spacing between Heinrich Events (Hagelberg *et al.* 1994) influencing theories as to a cause of these events. Further studies have actually revealed a far from regular recurrence interval of 7200 +/- 2400a (Sarnthein *et al.* 2001) between Heinrich Events in marine records with a generally decreasing trend over the course of the last glacial (Broecker 1994). The implications of the phasing of Heinrich Events is discussed in detail in Section 1.4.2. The context of Heinrich events within glacial-interglacial cycles dominated the early literature (e.g. Broecker 1994) and it was only really due to the mainstream shift in interest of abrupt climate change (particularly in relation to future climate prediction), that the potential of these events to record important information on centennial- and millennial-scale climate change was recognised.

The dramatic reduction in foraminifera within Heinrich Layers cannot be solely attributed to a dilution by IRD as the geographical extent of foram-poor sediments is far greater than that of Canadian-derived material (Bond *et al.* 1992, Broecker 1994). This implies that Heinrich Events had wide-reaching effects on north Atlantic palaeoceanography. This assertion is supported by the marine sediment record which records changes in many palaeoceanographic proxies associated with Heinrich Layers. Although the absolute abundance of forams decreases, there is an increase in abundance of the polar-dwelling foraminifer, *Neogloboquadrina pachyderma (s)*, often to 100% of the foram assemblage, indicating a surface water cooling (ranging from 3-5^{0}C; Grousset *et al.* 2001). In addition, the lightening of the δ^{18}O recorded in such species reflects a meltwater influx and corresponding decrease in salinity. Other geochemical changes are also noted within Heinrich Layers. The increase in Cd/Ca ratio of benthic

foraminfera during Heinrich Layer deposition has been interpreted as the result of the reduction of NADW formation and the consequent northward penetration of nutrient-rich waters from the South Atlantic (Bertram *et al.* 1995, Marchal *et al.* 1999).

It has been theorised (Alley 1998) that the larger Bond Cycles observed in the Greenland ice cores can actually be explained by down-wind cooling caused by the expansion of the Laurentide Ice Sheet in the region of Hudson Bay. Each of these periods of expansion was terminated by an episode of ice sheet collapse (the Heinrich Event), releasing a large volume of fresh water into the northern North Atlantic causing a reduction in NADW formation and hence a further intense cold period. This meltwater may have been cause by the melting of a large discharge of icebergs (Broecker 1994) or possibly by an outbreak of freshwater ponded at the base of the LIS (Dowedswell and Siegert 1999) and exiting through the Hudson Strait (Shoemaker 1992). NADW and THC then resumed as the THC 'switch' restarted as the meltwater influence was gradually removed (Broecker *et al.* 1992).

Differences in stable isotope ratios from organic matter between Heinrich Layers and ambient glacial sediment seen in the southern IRD belt have been interpreted to be due to enhanced detrital supply of lithic and/or soil organic matter derived from continental sources of high-latitiudes during Heinrich Events (Grousset *et al.* 2001). This is corroborated by the presence of detrital and continental n-alkane components in Heinrich Layers (Villanueva *et al.* 1998) and the high content of coal seen in some Heinrich Layers (Heinrich *et al.* 1989) and the presence of abundant air-bourne continental material such as spores, pollen and cellulose-rich debris. This continental contribution is supported by the increase of dust associated with Heinrich Events in the Greenland Summit cores (Mayewski *et al.* 1994).

Water column stratification and anoxia during Heinrich Events has also been noted (Rosell-Mele *et al.* 1997, Tamburini *et al.* 2002) and Grousset *et al.* (2001) show that the light excursions in $\delta^{18}O$ reach maxima during the upper part of Heinrich Layers and area associated with a decrease of $3^{O}C$ in mean SST and an estimated 2 decrease in SSS.

Using diatom proxies, Sancetta (1992) proposed that in the glacial Northern Pacific and Atlantic Oceans, the presence of icebergs supported high production owing to physical or biogeochemical mechanisms and this process could be significantly enhanced during Heinrich Events. The increase in nitrogen isotope ratios during H1 and H2 could reflect more efficient surface water nutrient use (e.g. Francois *et al.* 1997).

All these studies indicate a large-scale disruption of the North Atlantic circulation, manifested in both surface and deep waters, correlated to Heinrich Events. Both proxy studies and modelling results have indicated that this is most likely to be attributed to the rapid influx of a large volume of freshwater, perturbing the thermohaline circulation (e.g. Paillard and Labeyrie 1994).

The signature of Heinrich Events has been found not only in Greenland Ice cores and the North Atlantic but also in the Arabian Sea (Schulz *et al.* 1998), South China Sea (Wang *et al.* 1999), Pacific (Chappell 2003) and terrestrial records (e.g. Grimm *et al.* 1993, Lowell *et al.* 1995, Sanchez-Goni *et al.* 2000). The correlation of Heinrich Events to key points in the climatological cycles seen in the Greenland Ice Core records and in marine records inextricably links ice sheet, ocean and climate dynamics. One of the many questions posed by this relationship is whether the large circum-North Atlantic were capable of driving climate change in the region. Feedbacks linking ice sheets and climate may be:

1) The influence of the topography of large ice sheets such as the LIS on the position of the jet stream and the high pressure cell over the North Atlantic and accordingly SSTs.
2) The influence of injections of meltwater into the North Atlantic affecting SST and SSS and hence NADW and the THC conveyor.

The apparent correlation between climatic and North Atlantic oceanographic records has led to speculation that these climate cycles have an intrinsic control in the high latitude North Atlantic and that ice sheet-ocean-atmosphere interactions in the North Atlantic basin drive climate change elsewhere through various feedbacks and amplification mechanisms (Alley *et al.* 1999). P/Et records from lower latitudes (Street-Perrot and Perrot 1990) and Antarctic temperature records (Blunier *et al.* 1998) have also revealed D-O-like oscillations albeit often at a lower amplitude to those from

the North Atlantic. Outwith the North Atlantic, D-O changes seem to be centred on regions with a strong atmospheric link to the North Atlantic such as tropical and sub-tropical monsoon areas of Africa (e.g. Street-Perrot and Perrot 1990) and South America (e.g. Ledru 1993). However, many Southern Hemisphere and Antarctic records appear, as far as dating can constrain and correlate them, to be antiphased with respect to Northern Hemisphere records (Blunier *et al.* 1998). Thus there is still considerable debate as to the causes and mechanisms behind this abrupt climate change.

The question of event synchrony is still ambiguous even between relatively proximal records in the North Atlantic. Short-term variations in magnetic proxies between Heinrich Layers seem to show synchrony across much of the North Atlantic basin (Kissel *et al.* 1999) and with the GISP2 $\delta^{18}O$ record.

The D-O cycles also seem to manifest themselves in downcore physical properties in North Atlantic cores, with sediment density records (strongly correlated to water content) displaying the distinctive saw-tooth pattern, gradually increasing and then suddenly decreasing (Moros *et al.* 1997). However, they are not so apparent in oxygen isotope and NP(s) records suggesting a much less dramatic palaeoclimatic influence. These records correlate well with the corresponding cycles in the GISP2 core although discrepancies occur in the older parts of the record, most likely due to age model uncertainties.

One main discussion point, particularly in relation to ocean modelling is whether the meltwater flux associated with ice-rafting events has even been sufficient to trigger a 'switch-off' of the THC. Comparisons of magnetic properties between cores along the path of the various branches of NADW suggest that rather than the operation of an on-off mechanism, observed changes in deep water circulation were due to stadial-interstadial modulations of its strength, location of origin and patterns of the different branches (Kissel *et al.* 1999). It has tentatively been suggested that the Faroe-Shetland Channel and the Denmark Strait were the only two active paths for overflow water from the Nordic Seas during MIS3 (Kissel *et al.* 1999).

1.4 Causes and Mechanisms

In light of previous discussions, it is clear that deducing the cause of these cycles and events is key in understanding the behaviour of the ice-ocean-climate system.

1.4.1 Theories for the origin of D-O cycles and Heinrich Events

Various theories have been put forward to explain D-O behaviour and Heinrich Events. Both oscillations of the ocean-atmosphere system (Broecker *et al.* 1990, Bond *et al.* 1999) and external forcing mechanisms (Mayewski *et al.* 1997, Keeling and Whorf 2000) have been proposed. Broecker (1994) theorised that D-O cycles can be regarded as a consequence of switches in the North Atlantic's Thermohaline Circulation (THC) which could be triggered by climatically induced freshwater inputs such as ice rafting. However, Bond *et al.* (1992) observed that each HE appeared to be preceded by an oceanic cooling and therefore HEs seem to be a response to, rather than a cause of, climate change. This view is challenged by Broecker (1994) on the basis that mountain glacier advances are observed synchronous with Heinrich Events. He reasons that different sized ice sheets will have different response times following a climatic cooling. This argument may be flawed for various reasons:

1) The assumption of synchrony is based on imprecise radiocarbon dates (+/-300a) and possibly erroneous inter-hemispheric correlation.
2) It assumes that Heinrich Events signify a dramatic ice sheet advance rather than retreat and collapse.
3) It assumes that mountain glaciers will advance in response to a cooling, whereas it may be that in areas controlled by P/Et budget rather than temperature that glaciers actually advance following a climatic warming (and a corresponding increase in precipitation). This, along with imprecise dating opens up the possibility that mountain glaciers advanced due to the rapid warming following a Heinrich Event rather than coeval with the Heinrich Event due to a climatic cooling.

It is interesting, however, that in direct conflict with Broecker's (1994) assertion that different sized glaciers will exhibit different response times to an external (climatic) forcing, Grousset *et al.* (2000) suggest that a synchronous response of circum-North Atlantic ice sheets does indeed implicate an external trigger mechanism for Heinrich Events. Hence it seems that even if a temporally and spatially accurate picture of the

North Atlantic IRD distribution was produced, debates on the forcing mechanism would still remain.

Glaciologists favour the view that Heinrich Events are not climate-triggered but are caused by oscillations intrinsic to the ice sheet system and such internal mechanisms are often favoured as a cause of millennial-scale oscillations. Periodic calving due to internal instabilities of the Laurentide Ice Sheet (LIS; MacAyeal 1993) has been theorised to control the timing of Heinrich Events. This theory asserts that as an ice sheet such as the LIS builds up, thermal energy at its base increases progressively due to pressure melting and the geothermal contribution. A threshold is reached at which basal frictional forces are overcome and the ice sheet surges, discharging icebergs from marginal ice. Based on this internal ice sheet models of MacAyeal (1993) and Alley and MacAyeal (1994), Elliot *et al.* (1998) theorised that the European ice sheets could have oscillated with a 1-2kyr cyclicity and Van Kreveld *et al.* (2000) put forward a similar proposal for the Greenland Ice Sheet, forcing the Detrital Event cyclicity with D-O phasing. The LIS is theorised to discharge icebergs with a periodicity of ca.7200a according to its internal dynamics (MacAyeal 1993, Alley and MacAyeal 1994), whereas the smaller European ice sheets are thought to have oscillated with a periodicity of 1-2ka, coincident with the phasing of D-O Cycles. The production of the large volume of icebergs must have, in turn, led to at least the partial collapse of the ice sheet from which they were derived. Evidence for such a HE-led collapse may reside in the double peak of IRD observed in some Heinrich Layers (e.g. Elliot et al 2001).

Modelling of the Hudson Bay ice streams (e.g. Marshall and Clarke 1997) has supported the idea of a thermomechanical trigger for Heinrich Events however the rate of iceberg production inferred by these models is generally too low to explain the sedimentation rates observed for Heinrich Layers (Dowdeswell *et al.* 1995). This may simply be due to a 'no-analogue' situation where studies of the sediment regime of modern glaciers and ice sheets do not fully represent palaeoconditions (Andrews 2000), in addition, the magnitude of modelled sea level rise is much smaller than is observed (Yokoyama et al 2001, Chappell 2002).

The model of MacAyeal (1993) has been questioned on several other grounds. Firstly evidence has emerged suggesting that debris within some of the Heinrich Layers is not

just sourced from the LIS (e.g. Grousset *et al.* 1993), indicating that several ice sheets may be involved. Bond and Lotti (1995) have indicated that the Icelandic ice sheet underwent synchronous surging with ice in the Gulf of St Lawrence, coincident with D-O coolings affecting unstable ice (Bond and Lotti 1995). The collapse of additional ice sheets may indeed account for the discrepancies in the modelled and observed sea level rises. It is hard to reconcile glaciological mechanisms with the wide-reaching climatic cycles seemingly related to the Heinrich Events and other IRD pulses. Indeed, D-O signals may also appear in western Atlantic sediments (Andrews and Barber 2002). Not only did Bond and Lotti (1995) recognise the D-O cyclicity within North Atlantic IRD events but also presented the first evidence of a multi-phase structure to Heinrich Events with each detrital-carbonate bearing discharge lagging slightly those from other sources. They attribute the former IRD pulses to be part of the D-O-related IRD cycle however subsequent debate and higher-resolution dating has called this assertion into question. In addition, fluctuations in ice volume during and after Heinrich Events appear also to have occurred in the Southern Hemisphere (Lowell *et al.* 1995, Denton *et al.* 1999, Kanfoush *et al.* 2000). This implies that either the North Atlantic events were sufficient to drive global climate change or that both hemispheres were responding to an external forcing. The synchronicity of such interhemispheric events has been widely debated and until these issues are resolved (most likely when the precision and accuracy dating techniques increase sufficiently), the mechanisms and relationships between ice-climate interaction will remain enigmatic.

The debate surrounding European Precursors (Bond and Lotti 1995, Rasmussen *et al.* 1997, Zahn *et al.* 1997, Snoeckx *et al.* 1999, Scourse *et al.* 2000, Grousset *et al.* 2000, 2001) has posed the question of whether these stratigraphically distinct IRD pulses seemingly reflecting asynchronous iceberg discharge from the circum-North Atlantic ice sheets imply a time-lapsed response to a common climatic forcing mechanism or a coincidence of different forcing mechanisms. Snoeckx *et al.* (1999) suggested that changes in the North Atlantic drift may have affected European ice sheets before affecting North America or alternatively that European iceberg discharges could destabilise the LIS through associated sea level rise. However, McCabe and Clark (1998) show that the British Ice Sheet may actually have expanded as a result of the cooling episode induced by a Heinrich Event. According to Alley (1998), the time-transgressive sequences of IRD events, Heinrich Events and precursors challenges the

idea of a global forcing triggering the Heinrich Layers and implicates the role of other processes such as change in the thermocline patterns (Knutz *et al.* 2001) and destabilisation of ice margins (e.g. Scource *et al.* 2000).

It seems instinctively obvious that the Heinrich Events should vary in their properties and perhaps even ultimate cause as they occur at very different stages in the overall glacial cycle, from the period of inception (H6), to the LGM (H2), to deglaciation (H1). There is an obsession particularly within the palaeoclimatic community to attribute discrete mechanisms to observed occurrences, understandable in the light of the present political 'climate' pushing for simple explanations for climate change. Although the principal of Ockham's Razor is a sound one, multiple explanations for the same phenomenon must not be discounted, particularly as boundary conditions change with time.

The question still remains as to whether there is a link between the main Heinrich Events (occurring on Bond Cycle periodicities), Detrital Events and more minor, precursor IRD pulses and their relationship across the North Atlantic. Clearly then, the question of phasing between ice sheets is key in deducing the causes behind the North Atlantic ice-rafting events and their relationship with climate.

Initial studies did not have the temporal resolution or precise enough dating control to resolve issues of cryosphere-climate leads and/or lags however as the temporal and spatial resolution of study increases, so does the potential to unravel these issues.

1.4.2 Pacing of D-O Cycles and Heinrich Events

Controversy surrounding the origin of these climate cycles partly stems from the lack of a universal chronology to which the proxy records can be correlated. This has impeded the quantitative analysis of climate variability for testing the hypotheses proposed to explain D-O behaviour, whether indeed it is cyclic, quasi-periodic or stochastic. The Greenland ice cores are generally thought to have the most reliable age models so other records are often tied to the ice cores to utilise these models.

It has been observed that the D-O cyclicity recorded in Greenland Ice core records falls within a sharp spectral band of ca.1500 yr (Grootes and Stuiver 1997), occurring

prominently within the continuous energy distribution of the climate system (Wunsch 2000). D-O interstadials show a close link to a 1470-yr signal, especially in the interval 15-78 kyr BP (Schulz *et al.* 1999) and the longer lasting D-O events (8, 12, 14, 19, 20) comprise two 1470-yr cycles. This cyclicity has also been observed in proxy records of terrestrial climatic and oceanography change from high and low latitudes (Mayewski *et al.* 1997, Bianchi and McCave 1999, Bond *et al.* 1997, Hinnov *et al.* 2002). In the context of this study it is particularly important to note the work of Bond *et al.* (1997, 1999). They have directly analysed the pacing of the ice rafting events through use of ocean core records of Icelandic glass and haematite-stained quartz grains as petrological tracers assumed to represent ice-rafted debris (IRD) related to D-O events.

Spectral analysis of the record of haematite-stained grains reveals a broad peak centred at ca.1.8 kyr which is similar to both the 1.4 – 1.5 ka spectral peak in glaciochemical time series from GISP2 (Mayewski *et al.* 1997) and power at the 1.5 ka period in sediment grain sizes from south of Iceland (Bianchi and McCave 1999). IRD records from all over the Greenland-Iceland Seas share both common source regions and a common periodicity of 1460-yr (van Kreveld *et al.* 2000). The ca.1470yr signal seems to be insensitive to the sign of the ice sheet growth rate (Schulz *et al.* 1999) which may be attributed to instability caused by the rapid response of ice margins and smaller ice caps. Hence this may provide a reason why the LIS does not contribute to DEs. That said, peaks in freshwater runoff from North America over the last glacial cycle seem to occur at D-O cyclicities (Marshall and Clarke 1999) suggesting that the cause of D-O cycles manifested itself in a different manner with respect to the LIS.

Although statistical studies seem to indicate a regular cycle of 1500 yr, most of these studies focus on spectral analysis as a tool however, this, by nature, smoothes out the climate signal to gain a high signal:noise ratio and therefore essentially produces a result which spectrally ‘averages’ the time series. This acts to output a ‘most likely’ spectral band within which the data falls. If, however, the cyclicity is changing over time, this approach will misrepresent the time series. Such variation is evident in Table 1 which shows a breakdown of the mean pacing of IRD peaks over the last 80000 years. Indeed, it appears that over the long-term, the oxygen isotope record from Greenland ice actually does not have a strict line behaviour (Hinnov *et al.* 2002) and the D-O component slowly oscillates between 0.5 and 0.9 cycleskyr^{-1} (ca.1000-2000yr periods).

In fact, the aforementioned 1470-year signal is actually caused solely by D-O events 5, 6 and 7 (Schulz 2002), which emphasises the non-stationary character of the oxygen isotope time series.

The pacing of HEs is also a matter of debate, varying according to the proxy record studied. Mayewski *et al.* (1997) estimated a 6.1 ka periodicity for HEs in the GISP2 time series however, (although one of the peaks does not have a corresponding HE) whereas estimates from oceanographic records vary between 7200+/-2400a (Sarnthein *et al.* 2001) and 9000a (McIntyre and Molfino 1996).

Table 1.1: Cycle pacing of D-O events for the last 80ka from a northeast Atlantic core (source: Bond *et al.* 1999).

	Time Interval (kyr)	**Mean pacing (+/- kyr)**
Holocene	1.5 – 12	1374 +/-502
Late Glacial	12 – 32	1537 +/-558
Early Glacial	32 – 75	1478 +/-458
12kyr step	13 – 24	1494 +/-624
12kyr step	22 – 34	1631 +/-511
12kyr step	31 – 43	1328 +/-539
12kyr step	43 – 55	1350 +/-302
12kyr step	53 – 64	1443 +/-470
12kyr step	64 – 79	1795 +/-425
Holocene+Glacial	0 – 79	1469 +/-514

Few studies have addressed the relative phasing of D-O cycles and Heinrich Events, most only dealing with the causes of the cycles in isolation. Indeed Hinnov *et al.* (2002) attribute quasi-periodic variations at 9-12 kyr in amplitude of the D-O signal as being related to influences from the half-precession orbital forcing rather than considering an internal influence such as a contribution from the Heinrich Event cyclicity. However, the observed close coupling between HEs and D-O cycles (Bond *et al.* 1993) calls out for a mechanism to reconcile the two together. So far, the most plausible link proposed is that of sea level. It has been hypothesised (Grousset *et al.* 2000, Sarnthein *et al.* 2000) that, whatever the case of D-O cycles and DEs, the

resulting icebergs from the GIS and FIS contribute to a progressively increasing sea level relative to the LIS until a critical point is reached where the relative sea level at the ice margin causes the ice to become decoupled from its bed resulting in a major ice-rafting event. Various positive and negative feedbacks may be involved in this process such as progressive isostatic loading and increased basal temperatures during ice build-up (MacAyeal 1993) further destabilising the ice and ice-marginal isostatic rebound after a discharge event causing relative stabilisation again. The concept that ice sheet instability might be associated with relative sea level change at the ice margin has been addressed in the past (e.g. Andrews 1973, Thomas and Bentley 1978, Pollard 1983). However, the timescale for most of these studies was tuned to the orbital forcing which was the main focus of research at the time.

1.5 Glacial Processes

1.5.1 Circum-North Atlantic Ice Sheet Fluctuations

One of the key areas of understanding in the ice-ocean-climate system is that of glacier dynamics and how these relate to local, regional and global climate change. Until the widescale recognition of abrupt climate change, regional glaciological studies had often focused on glacial-interglacial timescales: the mechanisms and patterns of glacial inception and deglaciation.

Studies have taken various approaches in reconstructing the past dynamics of the North Atlantic Ice Sheets:

1) Traditional, geomorphological approaches, employing terrestrial records
2) Glaciological Modelling
3) Interpretation of submarine sedimentary sequences

The latter method has various benefits over the first two. In general, terrestrial records of glaciation are poorly preserved, successive ice sheets advances and retreats destroying and modifying much of the geomorphological record. Also, dating of such records is often ambiguous, even despite recent advances in cosmogenic isotope dating of exposure ages of glacial features (e.g. Briner et al 2005). Modelling is an extremely useful tool in theory, however a model is only as accurate as its inputs and parameters so without decent control on these, provided by alternative studies, any model is, at best, a good test of the sensitivity of a system to different forcings. Thus models may not provide accurate outputs. Studying marine sediments provide a direct link with the ocean realm for example marrying terrestrial glacier fluctuations with inferred sea ice cover and ocean circulation patterns (e.g. Hebbeln *et al.* 1998). Marine sequences often contain intact stratigraphic sequences extending back to pre-Pleistocene eras. However, the study site must be chosen carefully, for example records of millennial-scale ice sheet oscillations have a low preservation potential along continental margins reflecting the duration and erosional effects of ice cover on the continental shelf. Clearly, if a full picture and understanding is to be built up, a combination of studies is essential (e.g. McCabe and Clark 1998, Olsen *et al.* 2002).

Large ice-rafting events clearly reveal ice sheet instability and are therefore very likely to be associated with ice streams which not only discharge large volumes of ice but also show potential for instability through variations in flow velocity, migration and reorganisation of drainage pathways over time and a potential to switch on and off (Bennett 2003). Theories surrounding the implication of the role of LIS ice streams in Heinrich Events calls for further study into the formation, properties and dynamics of this glacial phenomenon. In the two main theories for formation of ice streams there is strong reason to suspect a geological or substrate control on the initiation of rapid basal motion (Blankenship *et al.* 2001). Thus the sedimentological history of an area is critical in determining the likelihood of streaming (Alley 2000). That said, spatial variation in heat flux may also be of relevance with a correlation between areas of enhanced heat flow and the onset of rapid basal motion (Blankenship *et al.* 1993). Payne and Baldwin (1999) applied a thermomechanical model to the Fennoscandian Ice Sheet which appears to have been characterised by a number of ice streams that traversed the hard rocks of the Baltic Shield and consequently shows little relationship to the outcrop of deformable sediment (Kleman *et al.* 1997, Boulton *et al.* 2001).

1.5.2 Glaciomarine Sedimentation

Ice-proximal sediments of Late Quaternary and Holocene age are preserved on the continental shelves and slopes of all the circum-North Atlantic land masses (Andrews *et al.* 1991, Andrews *et al.* 1996, Piper *et al.* 1991, Vorren and Laberg 1997).

Modern analogue studies are restricted to high-latitudes where ice sheets extend to the present day coastline e.g. Antarctica (e.g.Cooper at al 1991, Kristofferson *et al.* 2000, Eyels *et al.* 2001) Greenland (e.g. Clausen 1998, Solheim *et al.* 1998) and Svalbard (e.g. Solheim *et al.* 1998). Seeing as over 90% of all the ice and sediment discharged by the Antarctic Ice Sheet today flows within its ice streams (Bentley and Giovinetto 1991, Bamber *et al.* 2000), the implication of palaeoicestreams in glaciomarine sedimentation and North Atlantic ice-rafting events is clearly significant.

The interpretation of seismic imaging indicates the large-scale architecture of most glaciated margins comprises of a prograding wedge of glacigenic sediment extending from the continental shelf edge, generally consisting of lensoid debris flows and parallel

to sub-parallel stratified hemipelagic-glaciomarine sediments. An important additional feature is the presence of large glacially-fed Trough Mouth Fans (TMFs; Vorren *et al.* 1988) which are characteristically produced at sites fed by the outlets of ice streams. TMFs consist mainly of stacked debris flows (Dowdeswell *et al.* 1998, Vorren *et al.* 1998) and extend seawards from the shelf edge modifying the wedge-shape progradation. In recent years many TMFs have been investigated with regards to their architecture, sedimentological origin, processes and their potential as palaeoclimatic archives. The debris flows are thought to have originated during periods when the glacier grounding line was near the shelfbreak (Vorren and Laberg 1997) resulting in a very high sedimentation input along the trough mouth, most of the debris flow sediment being derived from glacigenic shelf diamictons deposited mainly during peak glaciations (Vorren *et al.* 1988).

Besides being a locus for sediment deposition, the TMFs were also the main sites of freshwater supply (mainly in the form of icebergs) during the mid-late Pleistocene. Thus TMFs hold the potential for giving information about the various ice streams feeding them with regard to velocity and ice discharge. The sedimentological properties of these TMFs therefore provide significant information regarding the nature of sediment delivery to these sites. The poorly sorted nature of many of the Nordic Sea TMFs implies that deposition was not associated with substantial meltwater in contrast to size-sorted sandy and muddy turbidites and debris flows associated with a well-developed channel system indicating a significant meltwater presence (Dowdeswell *et al.* 1999).

The TMFs along the northwest European margin south of Spitsbergen all seem to have developed later than the early mid-Pleistocene indicating that the European Ice Sheets did not extend to the shelfbreak for any appreciable time before then. This conforms with deep-sea and terrestrial data which show that the mid-Pleistocene was the time of the largest glaciations in northern Europe.

Many studies have highlighted the importance of debris flows and turbidites in glacio-marine processes (e,g. Eyles *et al.* 2001). Deeper settings are complicated by the influence of along-slope contour currents which have the potential to extensively re-work, greatly reduce or even remove packages of sediment.

Early studies of the dynamics of glaciated continental margins were largely based on seismic reflection profiles and short gravity cores (Davison and Stoker 2002) which only allows the characterisation of sedimentary regimes to shallow depths. Accurate interpretation of ancient glaciological successions in the rock record require studies of lower slope and basin floor settings as well as shelf settings. However although deeper-ocean cores are available for analysis, due to the wide spacing of survey lines and the large scale of the margins involved, it is hard to extrapolate the interpretations

TMFs are a significant resource and archive for understanding the potential compositional characteristics of sediment-laden icebergs because they are located in positions of high iceberg production delivering IRD to the North Atlantic and contain source-specific detrital material in highly concentrated accumulations. This is because the composition of the debris flows making up the TMFs mimics that of the tills in the source area and therefore also the composition of the IRD in the calving icebergs, making TMF sediments representative point sources of the glacial drainage area. This of course relies on the assumption that IRD is entrained in an ice sheet throughout its transport path, that basal tills have the same sediment composition as the basally entrained sediment and that a significant portion of the sediments are melted out before the icebergs reach the open ocean. The latter assumption is though to be reasonable (Syvitski *et al.* 1996, Andrews 2000) however there are still questions as to how the composition of IRD changes with distance from its source involving issues of mechanisms of sediment entrainment into icebergs, transport and melt-out dynamics, among other things. Hence, although characterisation of ice-proximal sediments within TMFs may be relatively simple, relating these sediment characteristics to those of distal sediments may prove much more difficult.

1.5.3 Ice-rafted debris

In the past, the climatic fluctuations that occurred in and around the North Atlantic during the last glacial cycle are generally reconstructed by studying the biogenic fraction in marine sediments. This is because they can be used to deduce temperature and salinity among other aspects of the surface and deep water from the $\delta^{18}O$, $\delta^{13}C$ and faunal changes and hence reconstruct past water mass distribution and derive

information on ocean convection. The lithic fraction, however, has the potential not only to be a palaeoclimatic proxy, recording current strength, sediment origin, transport and depositional characteristics, presence of sea ice and icebergs but also, particularly in the case of IRD, allows correlation to terrestrial records. Lithic particles may be transported to the marine realm by wind (aerosols and volcanic ash), surface circulation (IRD and volcanic ash; e.g. Ruddiman 1977), hemipelagic processes and bottom circulation (e.g. Biscaye and Ettreim 1977).

The interest in variations in grain size and grain size distribution in North Atlantic sediments stems from investigations of orbital cyclicities and Milankovich forcing on ice sheets and climate (Ruddiman 1977, Fillon *et al.* 1981, Heinrich 1988). Initial studies focused on turbidites and their onshore origins (e.g. Chough and Hesse 1987) before the emphasis shifted towards studies of IRD and Heinrich Layers and in particular the dating of such sediment sequences, previously deemed a low priority in comparison to spectral analyses. Ruddiman (1977) produced the first distribution maps (spatial record) of coarse sand (>200μm) in the North Atlantic during the last glacial period showing that the highest fluxes were along a west-east band around 45^0N, the so-called 'Ruddiman (or IRD) Belt.' In the 1980s Fillon and Duplessy produced one of the first downcore (temporal) records from the Labrador Sea however due to the lack of dates for the record, millennial-scale changes were not noted. The absence of AMS dates often led to vastly underestimated sedimentation rates (Andrews *et al.* 1994) so the potential for higher-resolution studies was not recognised. IRD is one of the main proxies (along with stable isotopes, from both marine and ice cores) that triggered and subsequently aided more recent investigations into millennial- and centennial-scale climate variability and it now seems that these investigations must be combined with the knowledge of turbidite sequences in order to fully understand the processes occurring on glaciated continental margins.

Ruddiman (1977) showed that the flux of IRD during the last glacial cycle is correlated to the extent of ice sheets in the Northern Hemisphere. The occurrence of IRD in marine sediments outlines the former presence of ice sheets that extended to the edges of continental shelves and the occurrence of both sea ice and iceberg IRD indicates the geographic extent of drifting ice (Smythe *et al.* 1985). IRD studies also lend themselves

to studying the evolution of ice sheets but only as the glaciers extend into the marine realm and begin to release icebergs. However, sometimes the relationship between IRD and ice extent is not simple. It has been noted that IRD sedimentation rates were actually lower during glacials than interglacials in the western and central Arctic (Darby *et al.* 1997, Nordgaard-Pedersen *et al.* 1998). This could be due to the trapping of Arctic icebergs close to shore by the presence of sea-ice and shallow continental shelves, low temperatures preventing iceberg melt in northerly locations or discharge into floating ice tongues where basal melting could rapidly strip debris (Hulbe 1997).

In order to document the relative IRD contribution of the different North Atlantic ice sheets it is necessary to constrain the compositions and relative timing along different ice sheet margins. One of the first in-depth studies to focus on the grain size characteristics of glacio-marine sedimentation from different sites is that carried out by Dowdeswell and Principato (2002).

If a sample has a low abundance of grains >150μm but a high % sand-sized lithic fragments (63-150μm), it may indicate sea ice rather than icebergs i.e. related to cold climates without extensive ice sheets. Indeed Heinrich Layers within the IRD belt are often characterised by the reverse: a high lithic abundance in the >150μm fraction and a low fraction of >63μm material relative to bulk sediment (e.g. Hemming and Hadjas 2003). This spatial variation in the expression of Heinrich Events is also exemplified in areas close to probable sources of the icebergs (NW LIS) where changes are poorly defined by the sand-sized fraction but appear in dramatic variations in the input of fine-grained detrital carbonate (Andrews 2000).

It is important to note that an increase in IRD from a particular source does not in itself require or even suggest the collapse of a particular ice sheet. Heinrich Layers H1, H2, H4 and H5 have been attributed to major ice sheet collapse but only through combining IRD records with other observations such as greatly increased sediment flux in the deep sea (e.g. Francois and Bacon 1994, Thomson *et al.* 1995, Viega-Pires and Hillaire-Marcel 1999), highly distinctive provenance (e.g. Jantschik and Huon 1992, Grousset *et al.* 1993, Gwiazda *et al.* 1996, Hemming *et al.* 1998) and the role of oceanic fronts in the control of glacial and iceberg melting history.

Heinrich Layers are generally defined by an increased flux of IRD however it is important to note that this property could be caused by various situations:

(a) Increased iceberg flux with constant sediment content and melting rate
(b) Increased sediment content with constant iceberg flux and melt rate
(c) Change in melt rate or zone of melting due to changing SSTs and ocean circulation patterns.

1.5.3.1 Defining IRD

Ice-rafted debris is often defined by the weight percentage of counts of mineral grains within certain size fractions. It is well known that icebergs generally entrain sediment of sand-size and above; indeed in studies of marine cores from the Labrador Sea Fillon *et al.* (1981) state that "…the coarseness of much of the dispersed sand and gravel certainly suggests that ice rafting has been an important mechanism of sediment transport…" and indeed using specific sand-sized fractions as an indication of IRD stems back to the early 1970s (see Fillon *et al.* 1981). Hemming *et al.* (1998) state unequivocally that "analysis of individual grains within the >150μm fraction allows evaluation of sediment sources that are clearly of ice rafted origin" and Gwiazda *et al.* (1996) justify the cut-off grain size of >150μm with the assertion that "no mechanism other than ice-rafting can account for the delivery of grains this large." Most studies, by convention, select this grain size of >150μm as defining the IRD fraction according to Bond *et al.* (1992). However some studies employ somewhat different cut-off points in distinguishing the IRD component from other types of sediment (see section on glacio-marine sedimentation). In his pioneering study, Heinrich (1988) defined IRD as >180μm but cut off points as low as >63μm have been used to infer an ice-rafted origin (Manighetti and McCave 1995, Revel *et al.* 1996a). This method of defining IRD is dangerous for various reasons:

1) It does not differentiate between different size-fractions above the cut-off point and hence ignores varying grain-size distributions inherent to different depositional processes.
2) It assumes that all sediment over and above the cut-off grain size is ice-rafted and all that smaller than the cut-off is delivered through other processes.

3) Even using a single cut-off point, this is likely to vary in different settings e.g. mid-ocean versus ice-proximal.

Lack of a universal protocol on IRD characterisation has meant that many different practical methods have been employed in counting IRD. These vary from hand-picking lithic grains >150μm using a light microscope (e.g. Bond and Lotti 1995), counting >2mm particles on X-radiographs (e.g. Stein *et al.* 1996), calculating weight percentages of IRD size-fractions. There is a distinct lack of correlation between results from these various methods, indicating not only the need for consistency of methodology but also further investigation into the actual properties of IRD and factors affecting these properties in space and time.

Material in the sand-sized class (63-2000μm) is the least represented size fraction in typical glacial sediments (Drewry 1986) and in addition, studies of glacial and glaciomarine sediments indicate poor correlation between the weight percentage in different sand-sized classes (Andrews 2000). The bulk of glacially-derived sediments are actually silts and clays (<63μm). The size-spectra of glacial sediments seems to depend strongly on the mineralogy of the sediment, that is, crystal configuration and relative rock weaknesses (Slatt and Eyles 1981). Hence some of the inferred spatial variation in IRD across the North Atlantic may actually be due to varying source area geology rather than ice-rafting *per se*.

The absolute sand content within a sediment core is dependent on the input rate of sand from ice-rafting, the overall sediment accumulation rate (i.e. input of non-sand-sized components), the transport of sand by contour currents (strongly dependent on along-current topography) and the winnowing capacity of bottom currents (i.e. the potential to winnow out fine grains to produce 'lag' deposits and hence increase sand content).

Different grain-size distributions are therefore likely to result from different erosional, transport and depositional processes, different bedrock lithologies of source areas and variations in the mineral grain sizes. The effects of the latter two influences could be investigated by comparing mineralogies and/or isotopic characteristics of the different size fractions at one site, and those of the same size fraction at different sites. At present, such studies are far too spatially limited to provide any kind of useful reference

database. IRD is also observed to be very poorly sorted (Grousset *et al.* 1993) and thus the sorting (often quantified by the standard deviation around the mean grain size; e.g. Revel *et al.* 1996b) of different size fractions may reveal whether they were indeed ice-rafted or deposited by a different mechanism (e.g. contourite deposits, turbidites).

A key issue, particularly in ice-proximal sites is distinguishing the ice-rafted signal from other mechanisms capable of transporting coarse sediment to a site. This is vital if an accurate palaeoclimatic signal is to be deduced from the sedimentary record. This will help not only answer questions about glacio-marine sedimentation but also address the issue of whether IRD events are representative of a glacial response to a climate signal or a function of local ice sheet dynamics, or even possibly a balance between the two over time.

The issue of defining the grain size cut-off for IRD is even more significant in provenance studies. The sortable silt sized sediment (10-63μm) is extremely sensitive to changes in bottom current strength (McCave *et al.* 1995) and thus incorporation of this size fraction into samples used to study IRD provenance may mean that the signal reveals changing provenance of particles, possibly induced by a change in transport mechanisms, rather than IRD patterns. It would of course be preferable to use the coarsest possible cut-off to minimise problems of mixed signals, however, there is always the possibility of finer IRD and that this will exclude important provenance signals recorded therein. Also, often sample material is limited so there may not be sufficient material to produce statistically valid results if a coarser cut-off size is used. Problems such as this may be overcome through carefully considered site selection. Trends in the sortable silt fraction in cores from the main Atlantic sediment drifts (e.g.Gardar Drift, south of Iceland) are controlled primarily by changes in bottom current strength (ISOW) rather than to changes in sediment supply i.e. ice-rafting and turbidity currents (Revel *et al.* 1996b). Thus sites such as these are not necessarily an ideal location to study IRD.

1.5.3.2 Why study IRD?

IRD constitutes an essential part of the ice-ocean-climate story and IRD studies have the potential to shed light on many different aspects of the ice-ocean-climate system (Table 1.2).

Table 1.2: The properties of IRD horizons within a core record and their potential diagnostic applications

Application	Property Studied
Correlative tool	Matching IRD layers
Palaeoclimatic indicator	IRD concentration
Reconstructing past ocean circulation	Spatial distribution and thickness of IRD layers along with provenance indicators
Reconstructing glacier dynamics	IRD concentration and provenance indiactors
Ice sheet fluctuations	IRD concentration and provenance coupled with accurate age models
Modes of glacial sediment entrainment and transport	Grain size distribution within IRD layers

IRD distributions are often used to justify qualitative schemes for glacial ocean circulation states and verify quantitative model constructions. For all these reasons, an accurate knowledge of the relative iceberg sources and iceberg fluxes are an essential palaeoceanographic requirement.

1.5.3.3 Entrainment and release of IRD

If IRD records are to be interpreted properly, knowledge of the processes and pattern of the initial debris entrainment into ice is vital as the quantity and pattern of sediment release is controlled by the distribution of sediment within icebergs. The main control on sediment distribution within glacier ice is though to be the basal thermal regime of the ice mass (Boulton 1972, Alley and MacAyeal 1994). The major source of sediment for large ice sheets is from basal erosion of bedrock, providing that the glacier is at pressure melting point (Drewry 1986). Thus thick sequences of glacial debris are most common below warm-based glaciers. However even then, sediment is commonly concentrated in a basal layer 1-3 m thick with virtually debris-free ice above (Dowdeswell 1986). In general, studies of present day icebergs indicate that entrained sediment constitutes an extremely small fraction of the total volume of calved ice (Andrews 2000). This may be due to the aforementioned 'no-analogue' situation.

Indeed, sediment erosion may be related to the stage of glaciation and thus at the present position in time (recovery from the last glaciation), glaciers may have proportionally less basal debris available to them.

The pattern of IRD release depends on the distribution of sediment within the iceberg, the rate of melting and the oceanographic conditions in the vicinity of iceberg release. At times of widespread sea-ice, iceberg transport from the ice margin to the open ocean may be restricted and much of the debris will thus be deposited near the outlet terminus (e.g. Syvitski *et al.* 1996). Iceberg drift in the open ocean is largely controlled by surface currents and past IRD distribution may therefore provide valuable information to enable the reconstruction of palaeocirculation. However, one of the main methods of accomplishing this is through the mapping of spatial IRD isopachs and so circular reasoning becomes a distinct possibility.

The estimated melt rate in water of 0^0C varies between 0.01-0.1 m per day (Dowdeswell and Murray 1990) indicating that a 3m-thick layer of basal debris would be melted out in around 1-10 months.

1.5.3.4 Modelling IRD

There have been limited attempts to model the patterns of iceberg drift, decay and IRD release (Bigg *et al.* 1997, Matsumoto 1997) and the models are primarily dependent on the choice of ocean and atmospheric flow fields. Therefore the accuracy of the model relies on knowledge of past circulation patterns and climatic conditions: two of the variables which palaeoceanographic studies, using proxies such as IRD, aim to reconstruct. The possibility of circular argument is therefore a key consideration in the interpretation of the model results. Therefore the most beneficial way to employ such models is investigating their sensitivity and consequently the sensitivity of IRD delivery to various parameters rather than using them as a reconstructive tool *per se* (Matsumoto 1997).

Even with significant alterations to model boundary conditions, results produce an IRD distribution pattern consistent with the spatial extent of the IRD Belt but falling ca.5^0 south of the 50^0N limit of the "basic glacial" IRD deposition (Ruddiman 1977). It seems that the basic glacial IRD distribution almost agrees totally with the CLIMAP

(1981) reconstructed sea ice limit and this may suggest that a large amount of glacial IRD was delivered by sea ice instead of icebergs. However, the sea ice limit may provide an oceanographic limit to iceberg survival, coinciding with the meltzone's boundary. This model does however only use two modes of ocean circulation (modern and LGM) so the results may simply indicate that there were significant changes in ocean currents between these two states over the last glacial period. Even this is an important conclusion as it demonstrates the highly variable nature of the North Atlantic environment over this time period.

1.5.4 Distal vs. Proximal Sites

In general, ice-proximal areas are defined as being less than 100 km from glacier margins (Andrews and Principato 2002). Such site offer the potential to compare and match available terrestrial data for certain time periods and then at times when terrestrial data is lacking, marine data can be used to infer information about glacial history and also test terrestrial-based theories with regards to glacier extent and the timing of the fluctuations of ice.

One of the main advantages of ice-proximal sites is the potentially high-resolution records existing there. Sites such as the Barra Fan offer sedimentation rates of >50cmka^{-1} (Knutz *et al.* 2001). The most reliable data sets are from cores where the sediment accumulation rate is high enough to reduce the influence of bioturbation.

The advantage of higher resolution offered by many ice-proximal sites can sometimes be shadowed by the complex nature of the sedimentological signal recorded at such sites. The Barra Fan is characterised by large glacigenic debris flows which consist, at least during intervals of greater BIS extent, of packages of thin-bedded sandy turbidites (Knutz *et al.* 2002). These can act to obscure possible IRD layers due to the inherent coarseness of the sediment associated with both processes. Turbidite emplacement may also erode underlying sediment layers leading to stratigraphical gaps and may also cause possible redeposition of older sediments within the turbidites. This can cause large problems when it comes to the high-resolution dating of such sequences. The diversity of sedimentary processes operating in proximal sites may be unravelled if proximal cores can be correlated accurately with cores from more distal locations at

which a single sedimentological process may exert a dominant influence and thus provide the potential to isolate the effects of this process over time. For example, it is thought that bottom currents exert a primary control on parts of the contourite drift sediments of the Northeast Atlantic outwith the main IRD belt (Revel *et al.* 1996b). Thus studies of cores from these locations can reconstruct changes in bottom currents over time (e.g. McCave *et al.* 1995, Revel *et al.* 1996b) and if correlated to ice-proximal cores, may provide the potential to remove the bottom current signal from these records.

The complex regime of glaciomarine sedimentation in ice-proximal sites means that discrete IRD events are often not able to be distinguished from background glacial sedimentation. Heinrich Layer sediments off Hudson Strait not only contain an abundance of sand-sized particles but include massive deposits of fine-grained silts and clays (Hesse and Khodabakhsh 1998) which could feasibly be from icebergs or suspended sediment plumes.

In studying ice-proximal sites in relation to on-shore glacier and calving dynamics various elements of the terrestrial-marine system must be examined. These include reconstructing ice flow trajectories and extents of the palaeogrounding line and sedimentological mapping and dating of onshore tills and moraines.

The literature from ice-distal locations considers Heinrich Events to be characterised by an abrupt increase in IRD (Heinrich 1988, Bond *et al.* 1992). However, such a characterisation does not prevail at sites close to former ice fronts such as the margin of the LIS or that of the BIS. Proximal Heinrich Layer units are usually massive to laminated clayey-silts with some IRD (Kirby amd Andrews 1999). At ice-proximal sites the association of IRD and Heinrich Events is far from obvious. Such observations indicate that Heinrich Events are associated with processes other than an "…iceberg calving, drift and melting sedimentological regime" (Andrews and MacLean 2003). The fine-grained laminated nature of Heinrich Events, particularly evident in Hudson Strait sediments (Andrews and MacLean 2003) and large negative excursions in marine $\delta^{18}O$ records (e.g. Cortijo et al 2000) suggests deposition associated with large amounts of meltwater in surface meltwater plumes and turbidite flows (Hillaire-Marcel *et al.* 1994).

Ice-proximal sedimentary sequences in the northwest Atlantic have already revealed complex, dynamic links between different ice streams draining the same ice sheet (Andrews and MacLean 2003) however such studies from adjacent to some of the smaller circum-North Atlantic Ice Sheets are much more limited. Ice proximal studies have the added advantage that they can be directly compared and correlated to their terrestrial counterparts. However, as previously discussed, most terrestrial records of millennial-scale climate change and particularly of glacier dynamics in the North Atlantic have low preservation.

Studies of marine sediments near to the Fennoscandian and Svalbard-Barents Ice Sheets have attempted to reconstruct terrestrial ice fluctuations with IRD (Richter *et al.* 2001) but few, if any studies have done this for the British Ice Sheet. A British origin for all Heinrich Layers has been inferred from isotopic ratios within a core from the eastern IRD belt attributed to an advance of the BIS (Revel *et al.* 1996a), however this assertion is based on bulk sediment analyses and thus further study is needed to confirm this. Due to the ice-proximal location of the Barra Fan, it can be assumed that the dominant IRD source during glacial times will be the British Land Mass, however variations in IRD provenance can still be used to represent variations in the extension of ice into the marine environment (see Hemming *et al.* 2000).

A disadvantage of studying Heinrich Events in ice-proximal locations is that, specifically in locations close to the source of these events, they may not appear as well-defined IRD spikes, and thus IRD patterns may not be diagnostic of Heinrich Events (Dowdeswell *et al.* 1999). Release of sediment from icebergs close to ice sheet margins is likely to have been a pervasive feature of glacial periods. In addition, away from the proximal canyon systems, turbiditic activity is only effective for water depths > 4400 m (Janschik and Huon 1992) so distal sites <4400 m have the potential to display continuous stratigraphic records with less variation in sediment accumulation rates.

1.6 NW Scotland Continental Margin

1.6.1 The last British Ice Sheet

Despite a wealth of studies, significant debate has surrounded the timing of the initial expansion of the last BIS ranging from before 40 kaBP (Bowen *et al.* 2002) to after 26ka BP (Atkinson *et al.* 1986, Lawson 1984). An interstadial period dated at ca.30^{14}C ka BP is widely recognised across Europe, thought to immediately pre-date the advance of the last major NW European Ice Sheets (Ran 1990, Valen *et al.* 1996) and tentatively correlated with Greenland Interstadial 8 (Whittington and Hall 2002). The majority of existing evidence corroborates this age as a maximum date for initial ice sheet build-up. Pollen records from ^{14}C-dated organic sediments on the Isle of Lewis, Outer Hebredes indicate that the area was ice-free before 28.7 ^{14}C yr BP (32 cal yr), the preceding interstadial period correlating with interstadials in both Norway and The Netherlands. U-series dates on speleothems and ^{14}C dated remains in caves in Assynt indicate that ice sheet build-up occurred after ca.26 kaBP (Atkinson *et al.* 1986, Lawson 1984). Marine evidence also indicates ice-free conditions in the North Sea around 30 kaBP (Sejrup *et al.* 1994, 2000) and westwards ice expansion across the outer continental shelf break only after 30 kaBP (Wilson *et al.* 2002).

At its maximum extent, the last (Late Devensian) Scottish/British Ice Sheet covered around two thirds of the present British land mass. The southern limits are quite well-constrained (Bowen *et al.* 1986, Ehlers *et al.* 1991) and although it is thought that the northern ice sheet descended west to northwest-wards from the mainland, the offshore limits of the northern BIS still remain uncertain. Various authors have suggested that Outer Hebredean ice terminated on land in N or NW Lewis (e.g. Sutherland and Walker 1984) and reached no further west than the North Minch basin (Sutherland 1984). However Hall (1995) proposed that all of Lewis was ice covered during the Late Devensian and Stoker *et al.* (1993) conclude that the ice sheet terminated to the north or northwest of the isle, the northern ice limit extending as far as Orkney and Caithness (Hall 1996). The western extent of the Outer Hebrides ice sheet is still unconstrained. The presence of morainal banks and iceberg plough marks on the Hebridean Shelf margin provide evidence of off-shore glacial activity (Austin and Kroon 1996). It is thought that the ice terminated at submarine morainal banks south of St Kilda (which

was ice free during the Late Devensian; Sutherland *et al.* 1984) and that a broad lobe of confluent ice streams from the mainland and Hebrides extended southwest across the continental shelf (Boulton *et al.* 1985, Ballantyne *et al.* 1998, Whittington and Hall 2002), possibly reaching the shelf edge at its maximum extent (Anderson 1981, Boulton *et al.* 1995, Wilson *et al.* 2002).

The last Scottish Ice Sheet is now thought to have been much thinner than previously modelled due to its warm-based nature and a bed of deformable sediment. Evidence from some erratics suggests that there may have been a thicker pre-Late Devensian ice sheet reaching a maximum at >ca.59 kaBP which may have encroached on the Outer Hebrides (Ballantyne *et al.* 1998). Ballantyne *et al.* (1998) suggested that this may even have been responsible for the sub-marine end moraines, glacigenic sediments and glacial scour marks at the edge of the Hebrides shelf, however recent palaeoceanographic evidence suggest that the BIS expanded westwards to the outer-continental shelf break only after 30 kaBP. It is thought that the North Sea was ice free around 30kaBP but at some stage between 29-22 kaBP, the FIS and BIS were confluent (Sejrup *et al.* 1994, 2000).

The Outer Hebrides supported an independent ice cap at the LGM (e.g. Peacock 1984, 1991) that was confluent with mainland ice in The Minches. Low gradient ice streams are likely to have extended north of Lewis (Stoker and Holmes 1991) and near to the shelf margin south of the Hebridean platform, across the Hebridean Shelf offshore (Peacock *et al.* 1992). In addition, a locally nourished ice dome was centred on the mountains of south-central Skye, diverting mainland ice north and south. Trimline evidence indicates only a single glacial maximum in NW Scotland (Ballantyne *et al.* 1998) although this maximum, as defined by greatest ice sheet thickness is likely to have been spatially diachronous.

Erosional destruction of much of the terrestrial evidence has precluded extensive studies to be carried out for pre-LGM times, although even the time at which the last BIS reached its maximum extent is uncertain. In England, ice sheet maximum has been conventionally dated to 18ka BP (during the Dimlington Stadial; Rose 1985), although evidence suggests that this post-dates the ice sheet maximum in the NW Scottish highlands (Sutherland 1991). Glaciological modelling indicates that the last BIS

reached maximum volume at ca. 22 ka BP (Lambeck 1993, 1995) although the lateral extent seems to be underestimated with respect to the geomorphological evidence. The glacial history of the North Sea implies that maximum glaciation along the NW European seaboard may have occurred prior to 22 ka BP (Sejrup *et al.* 1984) suggesting that the European Ice Sheet reached its maximum prior to the BIS. This is supported by evidence indicating that the northwestern BIS margin reached maximum extent between 21-17 ka BP (Wilson *et al.* 2002). In reality, the greatest lateral extent of different ice margins and ice streams are likely to have been diachronous (Ballantyne *et al.* 1998), possibly not even co-inciding with the 'true,' climatic LGM. This caveat should be recognised when correlating different terrestrial records and between the terrestrial and marine realms.

Ice-proximal marine sediment cores are ideally located to chart changes in glacial sediment delivery from the adjacent land mass and also provide the necessary high-resolution to place these changes on millennial- and centennial-timescales.

The British Ice Sheet is thought to have been influenced by a more temperate climatic regime compared to other circum-north Atlantic ice sheets due to its position relative to the north-flowing Gulf Stream. Indeed there has been much debate as to whether the often-used modern analogue of the present day Svalbard glaciers is indeed appropriate (S. Lukas *pers. comm.*). Temperate glaciated continental shelves are a complex end-member of glacio-marine environments having not only typical siliciclastic processes acting to produce a sedimentary record and depositional architecture but they also have glacial action superimposed on this.

Studies from SW Ireland have the advantage of a fairly well-constrained onshore glacial reconstruction and chronology (e.g. Wintle 1981, Scourse 1991, Lambeck 1996) whereas the extent and fluctuations of the Scottish Ice Sheet are still fairly speculative, with on-going studies still addressing key issues (e.g. Ballantyne and Hallam 2001). This has two main implications on the proposed study:

1) Interpretation of results are hampered by the lack of a robust terrestrial record to be tied to and verified against
2) It may aid the progress of terrestrial glacial reconstructions

Hence the progression of marine- and land-based studies should prove mutually beneficial.

In general, very little is known about the pre-LGM BIS. Therefore, studies addressing questions concerning both the timing and dynamics of the build-up of the BIS are extremely important, in circum-North Atlantic and more regional contexts.

1.6.2 The Barra Fan

Stoker (1995) found three main depositional settings on the continental margin of northwest Britain:

1) Two discrete fans (the Sula Sgeir and Barra Fans) on the Hebrides slope covering respective areas of 400km^2 and 700km^2 with radii of ca.50 km and relatively steep slopes (1-4°).
2) The 'between fan' area including the Geikie Escarpment
3) The more laterally persistent outer shelf/upper slope wedge west of Shetland.

The Barra Fan is one of the North Atlantic TMFs and is the main depocentre for material transported to the continental shelf-slope from the British Ice Sheet. The Barra Fan consists of Neogene-Pleistocene sediments which thicken seawards in a progradational wedge, to a thickness of over 600 m (Stoker 1995). The Barra Fan is part of the southernmost glacigenic fan system of the European continental margin and progrades into the Rockall Trough from the continental slope of western Scotland. The site is at a key position in the water-mass exchange between mid- and high-latitudes: on the main north-ward course of the NAC towards the sinking site in the Nordic Seas and also on the return trajectory of the NADW during the last glacial although this is likely to have changed over the course of the last glacial cycle which make the site particularly useful in charting variations in these currents. Due to the British Ice Sheet's location in direct influence of the 'Gulf Stream' and its relatively small size, it is most likely out of all the circum-North Atlantic ice sheets to show abrupt fluctuations in glacial regime forced by changing ocean and atmospheric circulation. Sedimentation rates reach over 50cmka^{-1} (Wilson *et al.*. 2002) in IMAGES core MD95-2006 (57^{0}01.82N, 10^{0}03.48W, 2130m), providing the necessary resolution to study centennial-and millennial- (and possibly even decadal-) scale variations. This site is uniquely located to study changing

ocean, atmosphere and ice sheet dynamics and their relationships over the last glacial cycle.

Few detailed provenance studies have been carried out at sites to the west of Britain, most of these focusing on the area off SW Ireland (e.g. Snoeckx *et al.*. 1999). These studies have mainly employed lithological tracers to identify broad zones, often attributing, for example, the presence of dolomite as an indicator of an LIS source. However, since dolomitic limestone constitutes a significant proportion of Irish bedrock (Charlesworth 1966), it may be highly problematic and potentially disastrous to attribute such lithologies to a LIS source.

The diversity of geology traversed by the British Ice Sheet (Figure 1.6) provides the scope to use both visual identification of different lithologies within the IRD and quantitative isotopic analyses to accurately match the offshore sediment record with geological terrains and even pinpoint sediment delivery sources from specific ice streams and lobes to the Barra Fan site. This diverse geology may be used not only to provenance IRD across Heinrich Layer intervals but also to study the overall evolution of the British Ice Sheet.

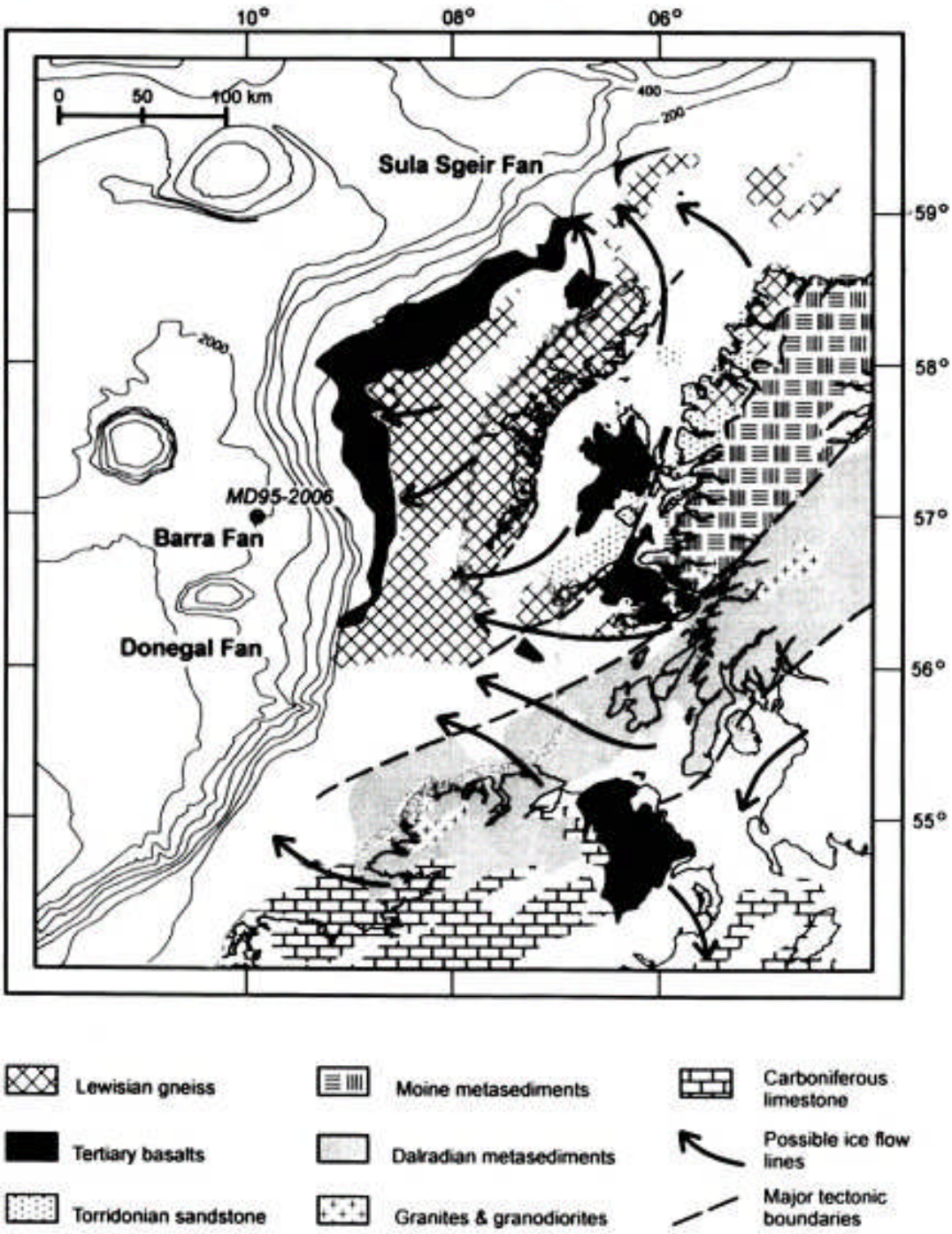

Figure 1.6: The Geology of NW Britain, proximal to MD95-2006 and arrows indicating likely direction of flow of the British Ice Sheet (Knutz *et al.* 2001).

1.6.3 MD95-2006

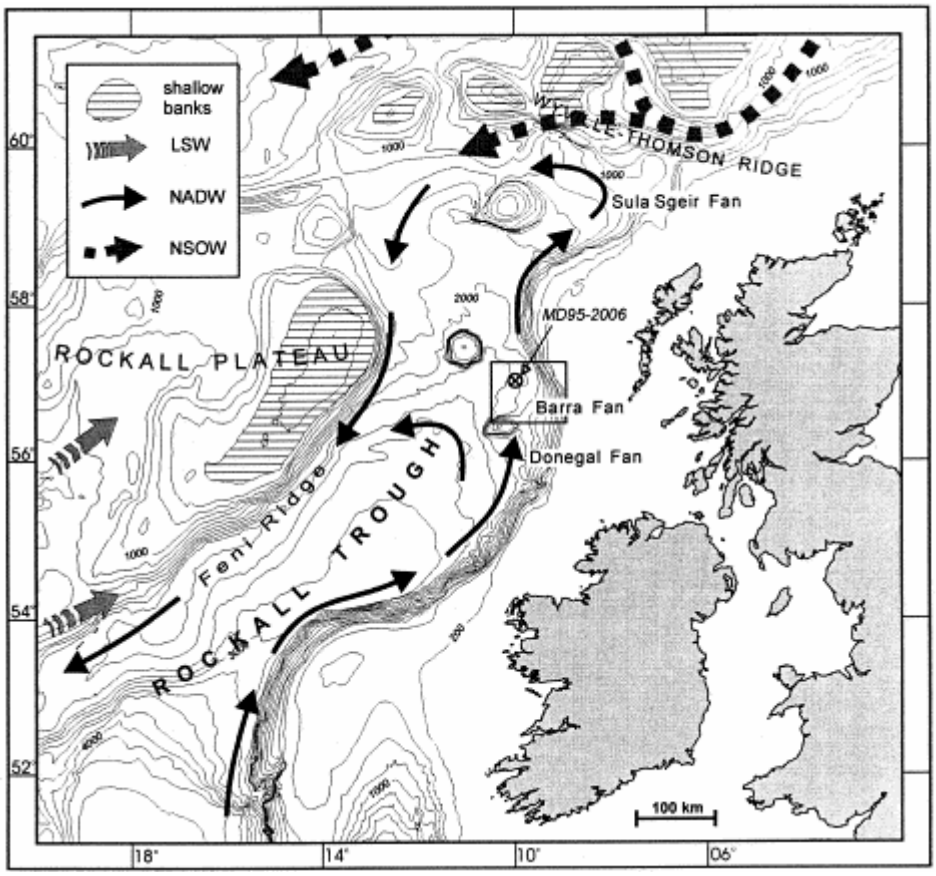

Figure 1.7: Location of the Barra Fan and MD95-2006 (Kroon *et al.* 2000, Knutz *et al.*).
Local Bathymetry and ocean currents affecting the site are also indicated.
(LSW:Labrador Sea Water; NADW:North Atlantic Deep Water; NSOW:Norwegian Sea Overflow Water).

MD95-2006 is a 30 m long piston core recovered by RV Marion Dufresne during IMAGES cruise 101. The coring operation formed part of the UK's North East Palaeoceanography and Climate Change Program (NEAPACC). The core was taken at 57°01.82'N; 10°03.48'W at a water depth of 2120 m on the northern edge of the Barra Fan (Figure 1.7). The corer penetrated a well-layered and laterally continuous acoustic sequence interpreted as contourites and distal marine sediments (Figure 1.8; Howe *et al.* 1998).

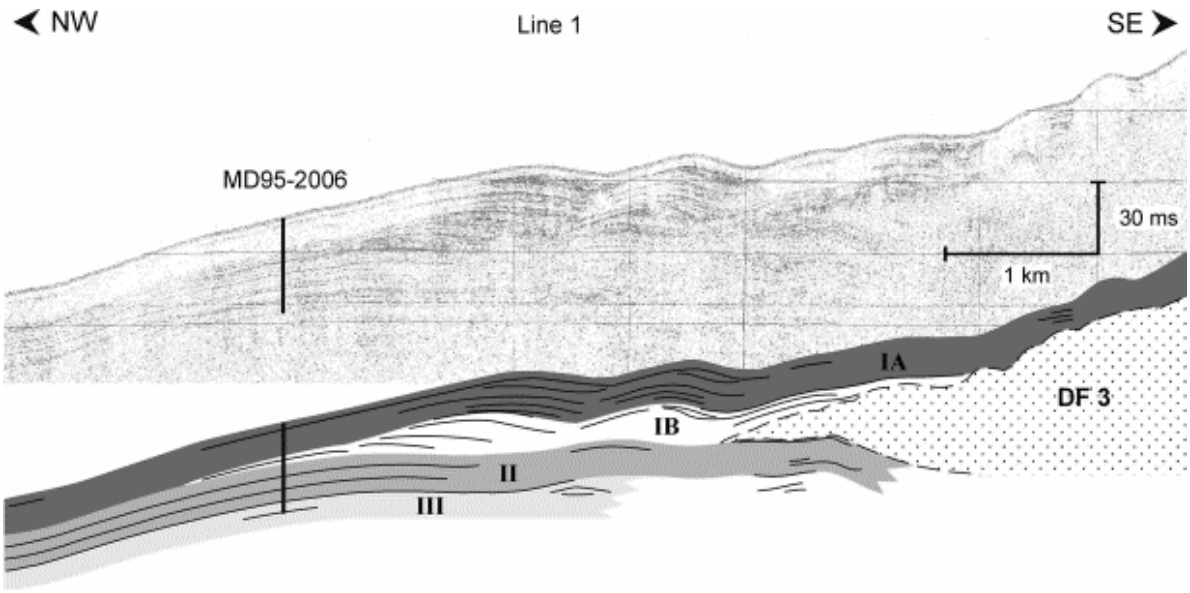

(A)

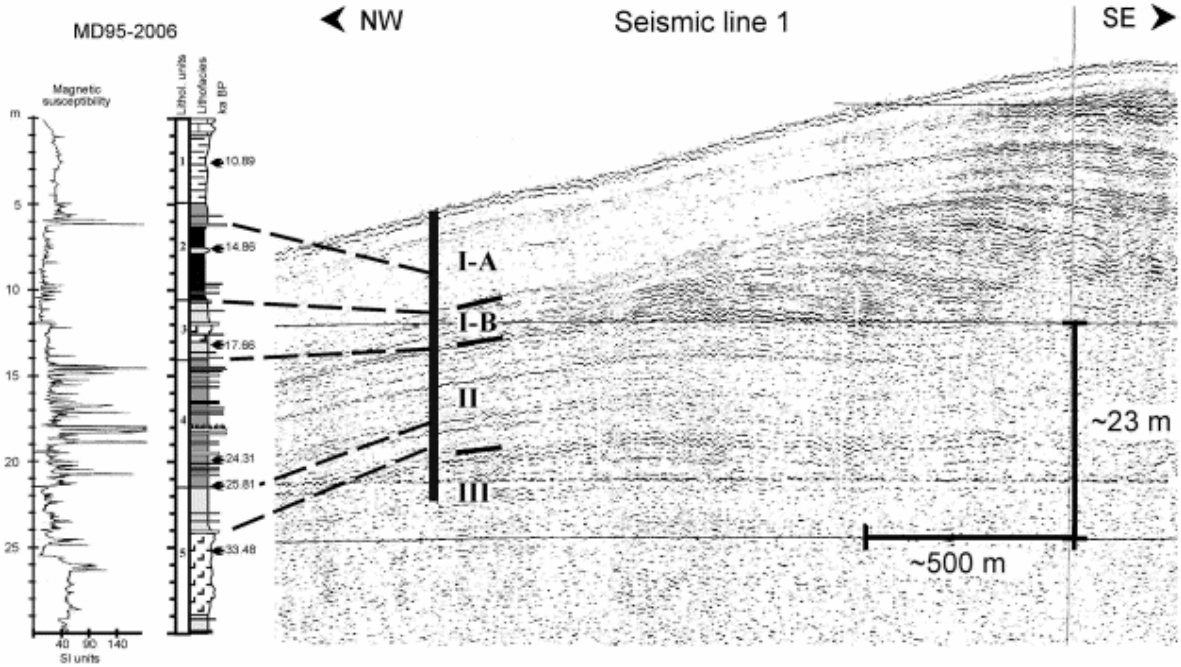

(B)

Figure 1.8:

(A) Seismic line taken across the site of MD95-2006. Different seismic units representing separate sedimentary packages are shown (IA-III). After Knutz *et al.* 2002.

(B) MS, lithostratigraphy and chronology from core MD95-2006 correlated with boomer line 1. The correlation is based on an acoustic velocity of 1525 m/s (30 ms scale bar corresponds to ~23 m), which was derived from P-wave velocity data (not shown). Seismic units I–III are indicated.

The lithology of MD95-2006 was initially described by Kroon *et al.* (2000). Due to the core's generally high sedimentation rates the initial 10 cm sampling resolution was enough to reveal significant fluctuations in terrigenous input and sea surface temperature, correlative with the Greenland ice core records. However, the initial age model was only based on 7 radiocarbon dates, the position of NAAZI in the core record and tentative correlation with dated horizons in two nearby vibrocores. It was therefore impossible to date the higher frequency events and constrain the phasing of the cycles that seemed apparent in some of the proxy records. The sampling resolution of the core record was improved by Knutz *et al.* (2001) who concentrated on characterising the pattern and nature of the lithic sediment fraction delivered to the core site although the age control remained poor as no additional ages were added to the radiocarbon-based age model. This study did, however, begin to reveal the possible millennial- and centennial-scale cycles in sediment delivery that appear in the Hebridean margin record, related to the dynamics of the British Ice Sheet. Due to the poor age control, it remained difficult to correlate the MD95-2006 record with that from other North Atlantic cores. Through studies of the sediment magnetic susceptibility, grain size distribution, colour variation and calcium carbonate content, Wilson *et al.* (2002) and Wilson and Austin (2002) confirmed the correspondence between the Barra Fan sediment cycles and the 1500 yr D-O phasing tentatively suggested by Knutz *et al.* (2001). They produced a higher-resolution (10cm for grain size and %$CaCO_3$; 1-5cm for MS and colour) lithostratigraphy. This was constrained by an new age model based on 14 radiocarbon dates and including the position of NAAZII near the base of the core (Austin *et al.* 2004), indicating that the core basal sediment is 8.3ka older than previously thought (Wilson and Austin 2002) and delimiting the previously unconstrained position of Heinrich Event 5 at ca.2800 cm. These studies demonstrate two clear transitions within the core record: one at 11 ka BP delimiting the start of the Last Glacial-Interglacial Transition (LGIT) and one indicating the transition between MIS3 and MIS 2 at around 30ka BP (27.9ka BP in this study: see Section 4.1). The latter is very important at this site and indeed across the North Atlantic.

Although the general North Atlantic stratigraphy can be gleaned from the Barra Fan record, still to be determined, however, was the position and nature of all the Heinrich Events in MD95-2006. H4 had been identified at ca.24.7 m as the only one of the IRD

events to contain the characteristic dolomitic carbonate but uncertainty regarding H2, H3 and H5 still remained (Wilson and Austin 2002).

Employing IRD records for correlations between Atlantic continental margin and open ocean sites have been dismissed due to the likely overwhelming regional influence that the local ice sheet is likely to have on the lithic record, particularly in the case of smaller ice sheets such as the BIS. However, the petrologic signal is seemingly more robust in North Atlantic records, possibly as it is not subject to biological imprints that tend to complicate other proxies (Bond *et al.* 1999). The delivery of IRD to the North Atlantic is also unique as it can be charted and interpreted through its source area and the North Atlantic surface circulation pattern.

Wilson and Austin (2002) cite the need for identifying a distinctive LIS geochemical signature in the Barra Fan record in order to facilitate amphi-Atlantic correlations. In addition to this, a well-constrained and accurate age model is needed for correlation with other marine cores as the often time-transgressive nature of IRD events such as Heinrich Events precludes their use as robust circum-North Atlantic isochrons.

1.7 Sediment Provenance

The main way to deduce phasing of the different IRD events is through studying the provenance of the IRD layers and how it varies both spatially and temporally. As discussed in Section 2, it is thought that the LIS is the main supplier of IRD to the 'typical' Heinrich Layers whereas the 'atypical' Heinrich layers had a different (possibly European) origin. This assertion was initially based on qualitative lithological analyses of the Heinrich Layer sediment (Bond *et al.* 1992, 1993, Bond and Lotti 1995) but gained support from quantitative, radioisotopic characterisation of the same sediment (e.g. Grousset *et al.* 1993, Revel *et al.* 1996). However the identification of material from ice sheets other than the LIS in the typical Heinrich Layers raised the question of participation of other circum-North Atlantic ice sheets in these events: whether all ice sheets surged simultaneously (Bond and Lotti 1995), possibly disproving the binge/purge mechanism for the initiation of Heinrich Events (MacAyeal 1993), or with associated lag times (Snoeckx *et al.* 1999, Elliot *et al.* 1998, Bond *et al.* 1999, Grousset *et al.* 2000, Scourse *et al.* 2000). Further to this, IRD with a Scandinavian (European) origin has now been identified even within typical Heinrich Layers in more northerly cores located in the Norwegian Sea (Grousset *et al.* 1998, Snoeckx *et al.* 1999) inferring that even these events had a more diverse origin than cores in the main Atlantic basin may record. Clearly then, studies must address both the temporal and spatial dimensions in order to produce an accurate picture of these events.

Although there is extensive literature on the sedimentlogical and lithological characteristics of the stratigraphy of glacio-marine sequences, the majority of these do not address the issue of the provenance of the sediment other than perhaps mentioning the dominant lithologies of the lithic grains and clasts (e.g. Davison and Stoker 2002).

A wide range of methods have been employed in the past to investigate the provenance of north Atlantic IRD. These include using characteristic minerals such as haematite-coated quartz grains (Bond and Lotti 1995, Grousset *et al.* 2001), radioisotopic tracers such as Strontium and Neodymium (eg. Revel *et al.* 1996, Scource *et al.* 2000), magnetic properties (Robinson *et al.* 1995, Stoner *et al.* 1996), K-Ar ages (Jantschik and Huon 1992, Huon and Ruch 1992) and ^{40}Ar-^{39}Ar ages (Hemming *et al.* 1998). Until recently, characterisation of IRD provenance has relied on visual lithological

identification and in general only distinguishes between broad rock types (e.g. quartz, feldspar, mica, rock fragments, detrital carbonate, volcanic glass). Bond and Lotti (1995) and Bond *et al.* (1999) interpreted the increase in haematite-stained grains in Heinrich Event IRD to a Gulf of St Lawrence origin and volcanic glass to Iceland.

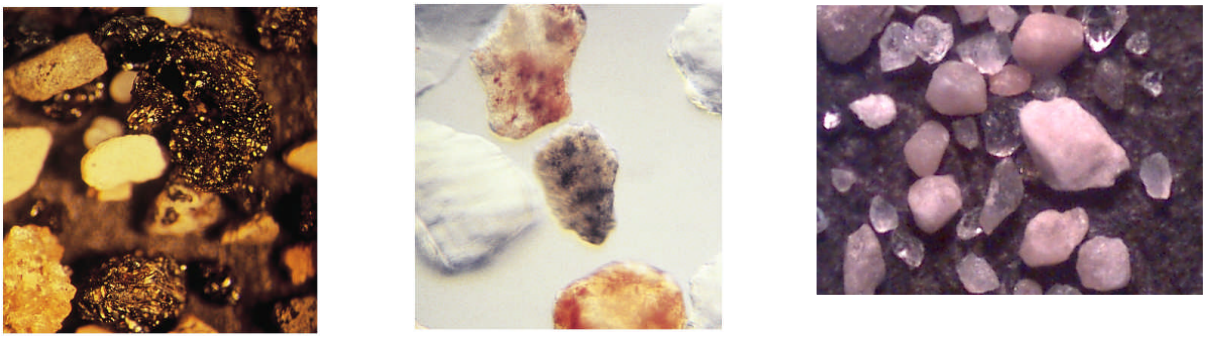

Figure 1.9: Left: Basaltic, volcanic grains; Middle: Haematite-stained grains; Right: Detrital, dolomitic carbonate (large white/pink grain to right of centre)

Broad lithologies can reveal certain information, for example Iceland and the mid-Atlantic ridge can be ruled out as influential quartz sources due to their >90% basaltic composition indeed, XRD spectra reveal an increase in the quartz:plagioclase (of bytownite composition, thought to originate from basaltic areas) during Heinrich Events suggesting that contributions from these sources was minimal or much diluted at least during the main IRD intervals (Moros *et al.* 2004).

Although such an approach is able to address issues of relative fluctuations of such lithologies within and between Heinrich Layers, it still remains highly qualitative in comparison to other potential methods and such compositional data does not in fact rule out iceberg discharges from the Greenland, Barents Sea and Scandinavian Ice Sheets. Detrital carbonate and haematite-stained grains have been attributed to LIS and Greenland/Svalbard source areas respectively (Bond *et al.* 1992, 1997). Recently, however, the origin of the latter has become more controversial, with possible sources identified in Canada (Bond 1998 cited by Snoeckx *et al.* 1999) and indeed detrital carbonate is not restricted to the Baffin Bay area but also occurs in areas as far away from the LIS as the dolomitic limestones of Ireland. Hence lithology alone clearly cannot distinguish between source areas.

Radioisotopic characterisation of certain fractions of the sediment provides a more quantitative and accurate method of determining the sediment provenance. The use of isotopic ratios as an indicator of provenance of Heinrich Layer debris can allow the isotopic composition of the Heinrich Layer sediment to be plotted against that of potential source areas (Gwiazda *et al.* 1996, Hemming *et al.* 1998) and in theory, the isotopic ratio of a mineral sample can be matched to a specific source area defined by identical isotopic ratios (Steiger and Wasserburg 1969).

Although a large amount of recent work has focused on the provenance of IRD, there has been little consistency in the specific areas studied and in the analytical techniques used. Initial geochemical and isotopic provenance studies were based on analysis of fine-grain or bulk sediment fractions. Conclusions reached by such studies are not entirely consistent with implied source areas ranging from multiple sources (Revel *et al.* 1996) to dominantly one source (Gwiazda *et al.* 1996), for the typical Heinrich Layers. The need for studies based on the analysis of single, coarse grains in order to isolate the IRD isotopic signal was recognised by Gwiazda *et al.* (1996).

Although isotopic techniques have been taken further in recent years in order to study Heinrich Events, most of these studies focus on Heinrich Layers within the IRD belt in cores with relatively low overall sedimentation rates (e.g. Hemming *et al.* 1998). This means that although a good control can be gained on the general sources of IRD in a Heinrich Layer, there is little potential to address the varying provenance of IRD within the Heinrich Layer horizon. Ice-proximal sites with high sedimentation rates allow for such expanded resolution studies. As long as comparable techniques are used, studies from within the IRD belt can then act as a basis for comparison of results, possibly leading to a distinction being made between actual Heinrich Layer IRD and adjacent IRD layers.

The main uncertainty involved in deducing the provenance of IRD through isotopic ratio signatures is in the methods used in matching the IRD signal with that of source area. In general, isotopic ‘fields’ are determined for each potential source area from isotopic databases as described above. The isotopic ratios for each sample of IRD are then plotted on the same chart to see which field they lie within. In cases where

particles originate from one of two source regions, the isotopic ratios are spread along a straight line linking their end members and their respective contribution to the mixture can be quantified from their position on the calculated mixing line (Langmuir *et al.* 1978). This presents an initial problem in that bulk Heinrich layers' compositions plot amid the isotopic compositions of all source areas (ie a result of mixing among more than two end members) and thus single sources cannot be distinguished and only the 'dominant' source can be identified (e.g. Revel *et al.* 1996). The analysis of single grains overcomes this 'mixing' problem, however, the parallel geological histories of many circum-North Atlantic terrains (see Section 1.7.1) means that they often have overlapping isotopic fields. Hence a single sample analysis cannot usually unequivocally point to a single source region. Gwiazda *et al.* (1996) note that the highest certainty in identifying a single source is if isotopic analyses of a number of grains tend to fill the field of only one source area. This assertion is valid in principal but as yet, no studies have adopted a quantitative statistical approach to address this issue. Revel *et al.* (1996) tackled this by weighting sediments more heavily than bulk rock ratios in calculating the mean ratio for each potential source area. Although this attempts to better define the ratios of potential source areas, it vastly simplifies the source area signal and still avoids the issue of accurately matching distinct areas to IRD data.

The present methods only really allow relative contributions from different areas to be deduced e.g. decreasing Sr ratios indicate an increasing contribution from volcanogenic relative to continent-derived material. A quantitative method of data analysis may enable isotopic fields to be spatially weighted in order to determine a 'most likely' position of IRD composition within the field. This can then be complimented with multiple isotopic analyses and descriptions of the petrologic composition of the IRD. The accuracy of any technique is directly proportional to the number of samples analysed, thus, time permitting, as many data points as possible should be acquired. In the case of provenance studies, the more samples whose isotopic ratios plot within the characteristic field of a particular source area, the higher the certainty that they can actually be attributed to that source (Gwiazda *et al.* 1996).

There is a distinct lack of information on the isotopic characteristics of glacially derived siliciclastic detritus actually delivered to the North Atlantic and thus, until recently,

provenance determinations have generally been based mainly on comparison of the isotopic ratios of IRD with the isotopic characteristics of basement rocks now exposed in circum-North Atlantic terrains. Future studies should aim to include isotopic analyses of the fine sediment fraction both through the IRD intervals and within ambient sediment. This will (a) characterise the 'background' sediment signal of the study site and (b) start to work towards a general inventory of the isotopic signals contained in glacial sediment across the North Atlantic. In particular, this inventory needs to bracket sedimentological end members characterising the sediment delivered by different ice-stream outlets around the North Atlantic. This can be achieved through looking at the isotopic ratios of sediment collected from the specific areas in which material from each outlet is focused. This approach has been tackled only recently and so far only the Hudson Strait outlet has been studied in any real detail (Farmer *et al.* 2003). Grousset *et al.* (2001) have begun to compile a base of ice-proximal sediment isotopic ratios, isolating the carbonate-free, >63 μm fraction.

Due to the nature of variations in the isotopic signal of the different size fractions within a bulk sediment sample it is necessary for different studies to select the same size fraction in order to produce comparable results. This is particularly important in the context of circum-North Atlantic studies addressing interrelated processes which affect the whole region. Using ice-proximal sites is also preferential as studies of transport distance of distinctive rock types show that the concentration of a particular diagnostic mineralogy falls off exponentially over a characteristic 'half-distance' of a few tens of kilometres (Clark *et al.* 1987). Therefore products of basal erosion should mirror rock types found within ca.50-100 km of a specific ice margin. The trough mouth fans around the North Atlantic provide ideal areas for such inventories to be built from. The Barra Fan is the main depocentre for material transported to the continental shelf-slope from the British Ice Sheet and therefore is one of these key sites.

The Barra Fan is likely to be dominated by IRD and indeed ambient glacial sediment, from the area drained by the British and Irish Ice Sheets, however this signal may be affected by influxes of 'foreign' IRD at key times in the past, in particular during Heinrich Events and the adjacent sediment. Collecting data on the bulk amounts of sediment >150 μm (assumed rightly or wrongly to be IRD) may provide information on

the timing of iceberg release from the British Ice Sheet and other contributing sources as broad lithologies can be distinguished (quartz, feldspar, basaltic grains, mica, composite sedimentary grains etc.) however due to the wide occurrence of such lithologies across the North Atlantic, it does not allow unequivocal correlation of the IRD with specific source areas. Isotopic analyses, in theory, enable IRD to be matched with the geology from specific source areas characterised by identical isotopic ratios or model ages. It has been argued that isotopic measurements on single IRD grains such as hornblende for $^{40}Ar/^{39}Ar$ (e.g. Hemming and Hadjas 2003) or feldspars for Pb isotopes (e.g. Gwiazda *et al.* 1996) are superior to bulk sample analyses as the latter may contain a mixture of isotopic signals from different sources. However, it could be that the different mineral fractions of the IRD have different and contrasting isotopic properties. This could be because:

(a) Different mineral grains have been delivered from different sources i.e. the IRD interval contains IRD of heterogeneous source area.

(b) Orogenic events, polymetamorphic histories and/or cooling patterns have generated isotopic differences in co-existing minerals from the same source area, subsequently delivered to the ocean via ice-rafting. For example younger $^{39}Ar/^{40}Ar$ ages would be expected from feldspar and biotite than from hornblende due to their lower blocking temperature for diffusion of Ar (McDougall and Harrison 1988). Ages could be possibly ca.400 Ma younger in the Churchill province (Hemming and Rasbury 2000).

Ideally then, different mineral grains within the same core horizon should be analysed for the appropriate isotope to investigate the sample heterogeneity. However, expense and time constraints may mean this is not possible and then single grain analyses could be compared to down-core changes in bulk sample analyses which should provide information on the changing relative contribution of material from the different end member sources. A key question, however, is whether isotopic compositions of sediments from particular sources vary with grainsize, indeed the case may even be different for ice-proximal versus ice-distal sites (e.g. Innocent *et al.* 2000). Although it seems that the Pb-Nd-Sr isotopic compositions of the typical Heinrich Layers indicate a consistent source across the spectrum of grain sizes (Hemming *et al.* 1998), further studies are required to address this issue.

The diversity of geology traversed by the British Ice Sheet provides the scope to use both visual identification of different lithologies within the IRD and quantitative isotopic analyses to accurately match the sediment with geological terrains and even pinpoint sediment delivery sources from specific ice streams and lobes to the Barra Fan site. This diverse geology can be used not only to provenance IRD across Heinrich Layer intervals but also to study the overall evolution of the British Ice Sheet. Hemming and Hadjas (2003) compared the relative contribution of North American terrains with different Ar-Ar ages to the IRD record of an east Atlantic core over the last 43 ka to infer information about the latitudinal extent of the LIS.

In order to be able to directly relate all circum-North Atlantic data, analyses need to be carried out with the same methodology. This includes the types of samples used, analytical techniques employed, statistical verification, methods of data display etc. This caveat has not been adhered to in the past. Although related, some of the studies address distinct issues so it may be argued that the methodologies chosen should be inherently different. However the need for decent spatial knowledge of ice-rafted sediment across the North Atlantic requires the ability to compare and correlate these studies. The type of samples used in isotopic provenance determinations varies from <63μm (Farmer *et al.* 2003), >63μm (Revel *et al.* 1996, Snoeckx *et al.* 1999, Grousset *et al.* 2001), >150μm bulk sediments to analyses on isotopes from single mineralogies such as Ar on hornblendes (Gwiazda *et al.* 1996, Hemming *et al.* 1998, Hemming and Hadjas 2003) and mica (Hemming *et al.* 2002), Pb on feldspars (Gwiazda *et al.* 1996) and Sr/Nd (Grousset et al 2001). The question of whether the absolute isotopic composition of sediments derived from particular sources varies as a function of sediment grain size still remains unanswered (Farmer *et al.* 2003) hence the sediment grain size selected for analysis may be key in the implications of the study. The dangers of using different grain sizes is illustrated by the fact that single coarse grains from H2 sediments indicate the main source to be the Churchill Province (Gwiazda *et al.* 1996a), supported by an eastward decay in thickness of H2 (Dowdeswell *et al.* 1995), abundant detrital carbonate (Bond *et al.* 1992) and a surge route along the Hudson Strait (MacAyeal 1993). However Sr and Nd analyses of the bulk silicate fraction do not plot within the Churchill province field (Grousset *et al.* 1993), most likely due to the fact

that bulk sediment includes sediments transported by wind, surface and bottom currents as well as IRD. More recent studies seem to indicate that in the IRD belt, all size fractions are dominated by the same source (Hemming *et al.* 1998, 2002). However this actually seems highly unlikely during Heinrich Events and may not be the case in ice-proximal areas.

The assertion that atypical Heinrich Layers contain a dominant European, Fennoscandian or Icelandic signature in contrast to the LIS-dominated material from the typical Heinrich Layers (Grousset *et al.* 1993, Revel *et al.* 1996) was initially based on the isotopic characterisation of the bulk lithic fraction of the sediment which allows the possibility that the isotope variation may be due to variations in grain size caused by changing amount of coarse material rather than a change in source area. Hence, it may be preferable to concentrate on carefully selected grain size intervals depending on the desired objectives of the study.

Often the sand-sized fraction (>63μm) is used as it thought to isolate the ice-rafted fraction (McCave and Manighetti 1995) and it is thought to avoid the effects of size and mineral fractionation of the isotopic signal which may occur over a wider range of particle sizes, particularly within the Sr isotopic system (Dasch 1969, Snoeckx *et al.* 1999).

The <63μm fraction is thought to represent the integrated erosional signature of ice-proximal sediments in areas of former ice streams (e.g. Clark *et al.* 1999). However in the deep ocean, this fraction can be transported by a variety of processes so it is often the coarse fraction that is analysed, indeed in the case of Sr and Rb/Sr, coarse-grained fractions are actually more likely to retain the ratios of their source regions (Famer *et al.* 2003). However, due to the multi-modal distribution between different sand-size classes of glaciomarine sediment and the dominance of the silt- and clay-sized fractions in the bulk sediment, there is some validity in basing provenance studies on the <63μm fraction as the most representative of sediment source (Andrews 2000).

It has also been shown that within the IRD belt, K-Ar ages of the clay-sized fractions is mainly related to the ^{40}Ar contribution from continent-derived micas (and to a lesser

extent, amphiboles and feldspars) with other mineral phases having little influence (Janschik and Huon 1992), whereas the ^{87}Sr:^{86}Sr ratios allow a better estimation of the smectite contribution with mixed oceanic and continental signatures (Huon and Ruch 1992). Even in the clay-sized fraction (<16μm), there is also distinctive mineralogical differences between size fractions with mica, chlorite, smectite and kaolinite concentrated in the <2μm fraction and quartz, K-feldspar, plagioclase and amphibole in the 2-16μm fraction (Janschik and Huon 1992); a suggestion of cold and arid weathering conditions at high latitudes (Singer 1984). In addition to this, these two fine-grained fractions show remarkably different behaviour with respect to some analytical techniques, such as incremental heating during $^{40}Ar/^{39}Ar$ age determination (Hemming *et al.* 200). If such variation is possible even on this scale, the potential variation in mineralogy across the whole size spectrum is even greater. However, if such effects are studied and quantified, they may actually reveal subtle ways in which to interpret provenance.

The nature of the samples analysed is also relevant when comparing ratios from sediment cores with those of potential source areas. Grousset *et al.* (2001) base their conclusions on matching ratios obtained through the analysis of the >63μm fraction to those from bulk sediment sampled from potential source areas. In light of the above discussion, this opens up the possibility of inferring erroneous matches/mismatches and emphasises the need for consistent methodologies both within and between studies. This further emphasises the need for consistency between studies, both in the context of comparisons of provenance between cores and in matching sediment signatures to that of potential source areas.

Although this discussion has highlighted the dangers of using different grain size fractions for provenance studies, the inherently different information which they record may also be beneficial in separating out the dynamics of climatic/oceanic/glaciological processes.

Different studies have employed different radioisotopes to characterise source areas in order to provenance the IRD signal. These include $^{39}Ar/^{40}Ar$ (Hemming *et al.* 1998,

Hemming and Hadjas 2003), Sr-Nd (e.g. Revel et al 1996, Snoeckx et al 1999, Grousset et al 2001) and Pb-isotopic ratios (e.g. Gwiazda et al 1996a).

The most abundant published isotope measurements for North Atlantic sediment samples are Sr isotopes, closely followed by Nd (Grousset *et al.* 1993, Revel *et al.* 1996) and the Sr-Nd isotopic composition of circum-Atlantic source regions have been extensively documented (e.g. Sinko 1994, Revel 1995). In the surface sediments of the North Atlantic, the geographic distributions of the isotopic ratios of Sr and Nd reflect both source areas and the present-day hydrographic and atmospheric circulation patterns (Revel *et al.* 1996a). Both the Rb-Sr and Sm-Nd isotopic systems within surface sediments have been used to reconstruct Atlantic circulation patterns (Dasch 1969, Biscaye *et al.* 1996, Grousset *et al.* 1988). It should therefore be possible to use downcore ratios to reconstruct such palaeoclimatic changes in the past. For example, changes in Sr and Nd isotopes in bulk sediment from the northern Gardar Drift display distinct glacial-interglacial shifts (Revel *et al.* 1996b). The large range in $^{87}Sr/^{86}Sr$ (ca.0.703-0.743) seen in sediments from across the North Atlantic make this isotopic system extremely useful in provenance studies.

Although the Sr isotopic system is highly useful in provenance determinations care must be taken that the Sr signal from seawater associated with the sediments analysed is completely removed through sediment leaching in the sample preparation process. Incomplete removal may result in erroneously high $^{87}Sr/^{86}Sr$ values which may hamper the interpretation (e.g. Farmer *et al.* 2003). Even if leaching of biogenic carbonates is 100% successful, the residue may still contain some opaline silica. However, Sr and Nd contents in marine biogenic opal are low (>5ppm) so this is not considered a serious problem (Revel *et al.* 1996). Leaching may also affect fragile clay minerals and introduce bias into the Sr results. There has also been concern in the past about the mobility of Sr within marine sediments after burial and also the effects of grain size variation on isotopic compositions, particularly of $^{87}Sr/^{86}Sr$ which has shown increasing ratios (more radiogenic) and higher [Sr] with decreasing grain size (Dasch 1969, Revel *et al.* 1996). Thus any grain size fractionation or winnowing during transport or after deposition of the sediment may critically affect the Sr ratios recorded.

Due to the above reasons, εNd values are often quoted as being more reliable than Sr ratios (Goldstein *et al.* 1984, Grousset *et al.* 1992) as εNd(0) does not record such grain size fractionation in river sediment, loess or aerosols (Goldstein *et al.* 1984, Grousset *et al.* 1992), although this assertion has yet to be proved unequivocally for marine sediments. Nd isotopes have long been used to delineate crustal age and to trace sediment provenance. They provide a measure of upper continental crust compositions integrated over their large source areas and to determine the average 'crustal age' of a sample. Sr and Nd record contrasting aspects of sedimentary provenance and are often combined to compliment each other. Sr and Nd isotopes are well-correlated, although the correlation breaks down for samples with εNd<-20 (or $^{87}Sr/^{86}Sr>0.71$;Hemming and McLennan 2001).

Rb and Sr have very different geochemical behaviour which can lead to decoupling of the Sr and Nd isotopes, particularly in terrigenous sediments. Due to the large geochemical contrast between Sr and Rb, the Sr composition of terrigenous clastic sediment is sensitive to:

1) The Rb/Sr ratio
2) The initial Sr isotopic composition
3) The age of the source

However, Sm and Nd behave relatively similarly so the most important control on that isotopic system is the time of extraction from the mantle (DePaolo 1988). Under most conditions, metamorphism, transport and weathering do not significantly alter the REE patterns of the resulting materials. Therefore the Sm-Nd depleted-mantle model age of sediment is thought to be a good estimate of the average mantle extraction age of the mixture of sediment sources.

The U-Th-Pb isotope system is particularly good for sedimentary provenance studies for various reasons:

(a) Differences in Th/Pb, U/Pb and Th/U over time occur due to the substantial fractionation of Th, U and Pb during both continental crust formation and igneous differentiation of the crust.

(b) Compared to Nd, Sr or Hf, the upper continental crust is far more enriched in Pb than the primitive mantle. Thus Pb isotopes are highly sensitive to crust-mantle interactions and therefore produce much more distinctive isotopic compositions.

(c) Pb ratios ($^{208}Pb/^{206}Pb$, i.e. Th/U ratios) from the depleted mantle are often very different (lower Th/U) than primitive mantle values leading to potentially different isotopic characteristics in the resulting magmas.

(d) Pb can be used to constrain the age of post-sedimentary effects such as U depletion through oxidation or U-enrichment in black shales due to $^{208}Pb/^{204}Pb$ reflecting the time-integrated Th/U ratio and $^{207}Pb/^{204}Pb$ and $^{206}Pb/^{204}Pb$ reflecting the time-integrated U/Pb ratio.

(e) Pb isotopes clearly distinguish between ancient upper continental crust and younger terrains, particularly in terms of the $^{207}Pb/^{204}Pb$ ratios, both key distinctive geological associations of different circum-North Atlantic land masses.

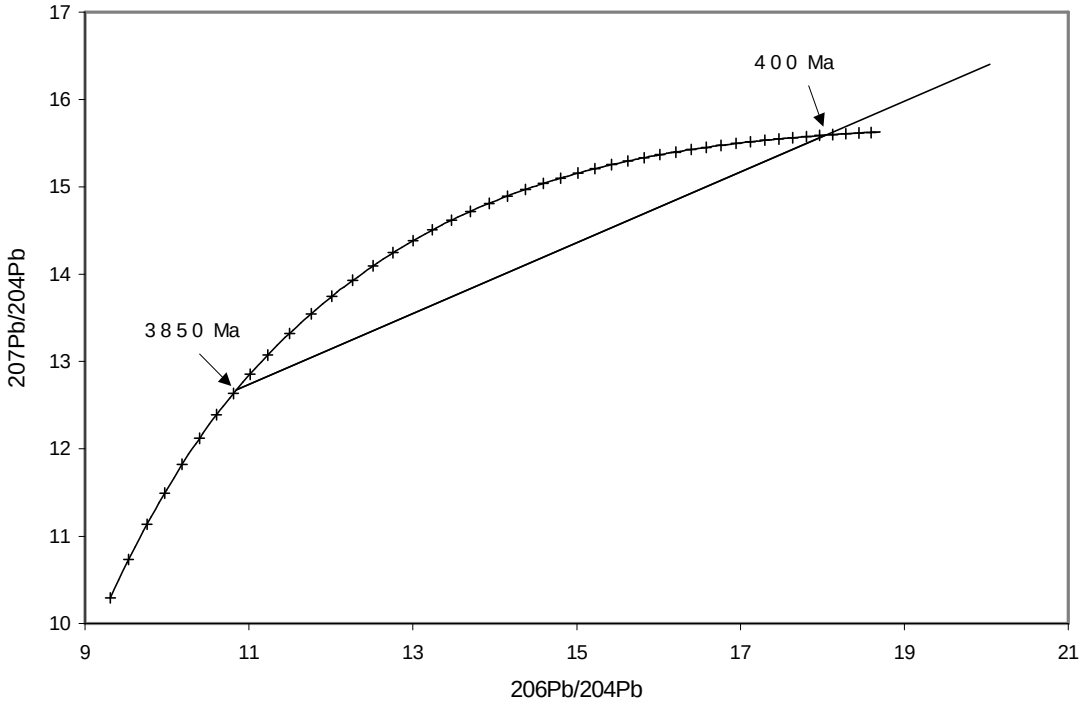

Figure 1.10: Two-Stage Mantle Evolution Curve (Stacey and Kramer 1975).

- Stacey and Kramer (1975) revised the original mantle evolution model constructing a Two-Stage Mantle Evolution Model taking into account differentiation of the promordial (4.57Ga) mantle at 3.7Ga to produce a more accurate age model than the original Single-Stage Model.
- Curve has been plotted using the Standard Growth Equations and other parameters (initial isotopic ratios, μ, decay constants) outlined in Appendix 1.
- Tick-marks have been plotted every 100Ma

Isotopic composition can be altered by metamorphism but in theory, the timing of the metamorphic event can be calculated from new isotopic ratios. Newly formed feldspars incorporate lead with the composition of the host rock (containing lead from both U-rich and U-poor minerals). Thus, on a geographic scale, heterogeneities between the metamorphosed feldspars and the host rock are produced. When plotted onto the Lead Evolution Curve, samples from the metamorphosed terrane form a linear array representing different degrees of mixing of the U-rich and U-poor rock components. This line therefore intersects the Evolution Curve (of the original mantle reservoir) at the ages of original rock crystallisation and subsequent metamorphism (Gwiazda et al. 1996).

Straight line represents the mixing line of a system which crystallised from a reservoir at 3.85Ga and underwent a metamorphic event at 400Ma (eg. A Caledonian Terrain)

Due to the tendency for feldspar (particularly K-feldspar) to sequester Pb and exclude U and Th from the crystal structure, the Pb isotopic composition is a good measure of the initial Pb composition at the time of crystallisation. Thus Pb ratios from feldspars are excellent tracers of their sources. Pb ratios, however are affected by metamorphic events which allow mixing of radiogenic Pb of uranium-rich minerals with the Pb of uranium-depleted minerals. On a large-geographic scale such as many of the circum-North Atlantic terrains, differences in the uranium content of the rock create differences in the Pb composition of the whole rock and the metamorphosed feldspars. These Pb ratios plot along a mixing line which intercepts the Pb evolution curve of the original mantle reservoir at the ages of crystallisation and metamorphism (see Figure 1.10). Thus, as long as the evolution curve is modelled accurately, Pb model ages can still be well constrained. If samples plot along a line which has a zero age intercept on the lead evolution curve, this indicates than the line is in fact an isochron and in this case, the isotopic composition of the initial lead is the Pb isotopic ratio of the least radiogenic

feldspars (Gwiazda *et al.* 1996). High radiogenic values tend to suggest either a high uranium content (very rare in feldspars) or a multistage history.

Most previous Pb-based studies of IRD provenance in the North Atlantic have used the 'common' Pb in feldspars as a basis for comparing isotopic compositions between IRD and potential source areas (e.g. Gwiazda *et al.* 1996). This is not necessarily a correct representation of the Pb composition of sediments. It is thought that whole rock material (containing both radiogenic and common Pb) is best represented in the bulk sediment fraction <63μm (Grousset *et al.* 1993, Revel *et al.* 1996, Hemming *et al.* 1998, Farmer *et al.* 2003).

Pb isotopic compositions measured on bulk sediment integrate that of the detrital (mostly clays) and authigenic (carbonate and Mn/Fe-oxide coatings) fractions of the sediment (Abouchami and Zable 2003). Therefore, variations in bulk sediment Pb isotopic compositions could feasibly be attributed to changing proportions of carbonate and detrital fractions rather than changing sediment source areas. Hence it is preferable to carry out isotopic analyses on the carbonate-free fraction (Abouchami and Zabel 2002). Of course, analysis of single grains avoids all of these problems. Having said this, it is still necessary to analyse a statistical minimum amount of single grains in order to find rare lithic fragments originating from minor sources (Gwiazda *et al.* 1996a). This problem is avoided by analysing composite samples (combining >200 grains) ensuring with 95% confidence that sources that contributed as little as 1.5% to the total sediment are included in the sample.

Whole rock Pb isotopic data from basement rock surrounding the North Atlantic demonstrate that unlike common Pb measurements, whole rock material from Archean, Proterozoic and Cenozoic rocks have overlapping Pb isotopic compositions (Gariepy and Allegre 1985, Anderson *et al.* 2001). In addition, the intersection of the Pb-isotopic fields of the Early Proterozoic terrains of Greenland and the Churchill Province line mean that lead isotopes alone cannot be used to discriminate between these two areas (Gwiazda *et al.* 1996a). As a result, whole rock Pb analyses do not allow the discrimination of potential source areas as readily as Nd and Sr isotopic data.

1.7.1 Potential North Atlantic Source Areas

The major circum-North Atlantic land masses that were ice covered during the last glacial period have similar geological histories and were subsequently separated by the opening of the Atlantic Ocean. They are composed of an Archean core (ca.2.7-2.9 Ga) and underwent metamorphism during the early Proterozoic (ca.1.7-1.9 Ga). The margins were affected by the Grenville Orogeny (Middle Proterozoic; 0.9-1.2 Ga) and by the Caledonian Orogeny (Palaeozoic; 450 Ma).

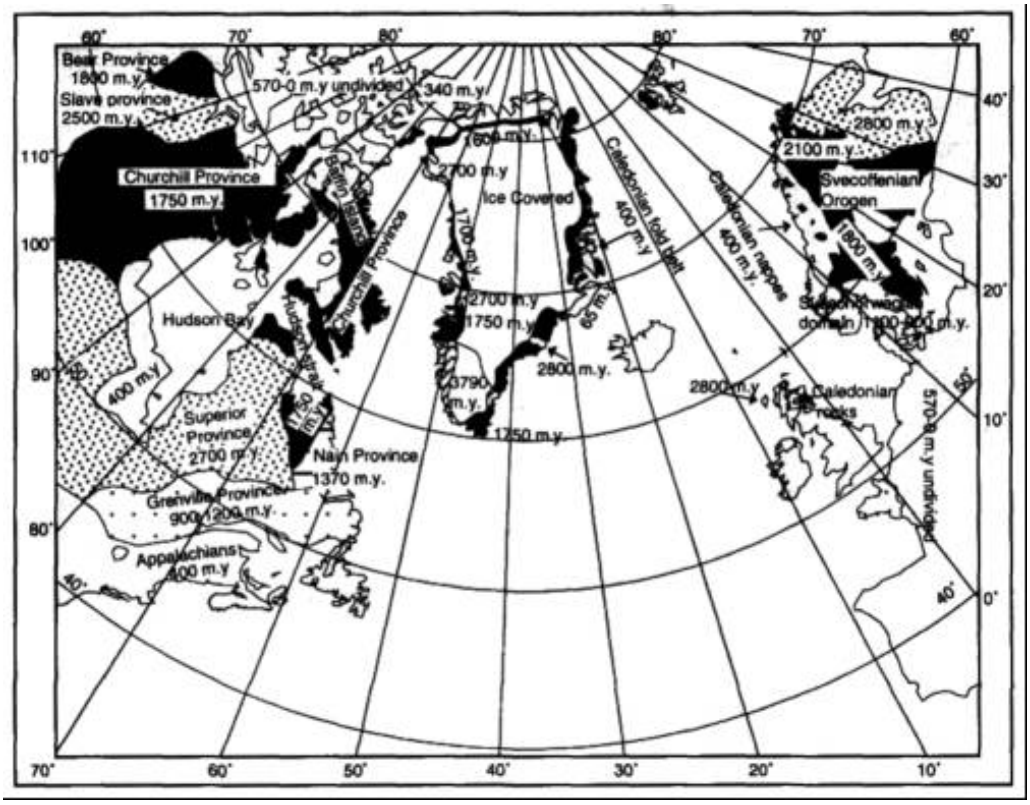

Figure 1.11: The main geological Terrains of the North Atlantic (Gwiazda *et al.* 1996) Main geological units of different ages are drawn with different patterns and the age corresponding to each pattern is shown on the map. These are: Archean Core Rocks (2.5-2.8 Ga); Early Proterozoic Metamorphic Terrains (1.7-1.9 Ga); Middle Proterozoic Terrains (Grenville Orogeny, 1.2-0.9 Ga); Caledonian Terrains (Caledonian Orogeny, 450 Ma)

Silicoclastic material in the North Atlantic should essentially be dominated by very old detrital minerals; peripheral landmasses being predominantly made up of Precambrian and Palaeozoic rocks. Sediment transport processes should theoretically supply 250-

3800 Ma old minerals according the weathering and erosion processes prevailing on the continents, however orogenic events, polymetamorphic histories and cooling patterns can generate distinct age differences between co-existing minerals. The only sources of younger rock are the Tertiary-Quaternary volcanic province of Iceland and SE Greenland, the Tertiary igneous province in NW Britain and Ireland originating from a range of tholeiitic and olivine-basalt magmas (Preston 1982) and the mid-Atlantic ridge system.

The eastern USA is very good for the application of isotope provenance determinations because a large database exists for the terrains and the isotopic composition of the crust at the margin of the continent varies with North-South position. Thus it is possible to distinguish between sediment sources at a high spatial resolution. The increasing terrain age from south-north is borne out in both bulk sediment Nd isotopic composition and ^{40}Ar:^{39}Ar ages of hornblende grains from marine sediment samples taken from the east coast of North America. Samples from near the Hudson Strait show a dominant Palaeoproterozoic population with subordinate Late Archean grains in contrast to samples from the Gulf of St Lawrence which have ages between 0.9 and 1 Ga, i.e. dominated by Grenvillian sources (Hemming *et al.* 2002, Farmer *et al.* 2003) possibly affected by the Appalachian Orogeny as indicated by Rb/Sr ratios plotting on an ca.470Ma reference isochron (Farmer *et al.* 2003).

The similar geological histories of terrains across the north Atlantic pose problems for identification of provenance through radioisotopic ratios from bulk sediment. Given the degree of overlap of the isotopic fields of coeval terrains (Figure 1.12 and 1.13), the highest certainty in the identification of a specific source would be obtained when isotopic analyses fill the field of only one source or fall directly along a mixing line between two sources. This is rarely the case with core sediments as they are often extremely distal to the proposed glacial sediment sources and the isotopic characteristics of source areas' bedrock may not be representative of the true sub-glacial or ice-proximal sediments. Detailed knowledge of the appropriate provenance sediment signature from well-defined sources is, at present, lacking. Revel *et al.* (1996) believe that bulk lithic samples provide a better estimate of the averaged composition of a given source region than do individual rock samples from restricted geological rock units. It would therefore be preferable to weight the mean values for each source area more

heavily towards bulk sediment ratios (e.g. Snoeckx *et al.* 1999). The use of an average value to represent sources areas as large as those discussed is a considerable simplification, however, such approximations are required for discussion of the data from MD95-2006.

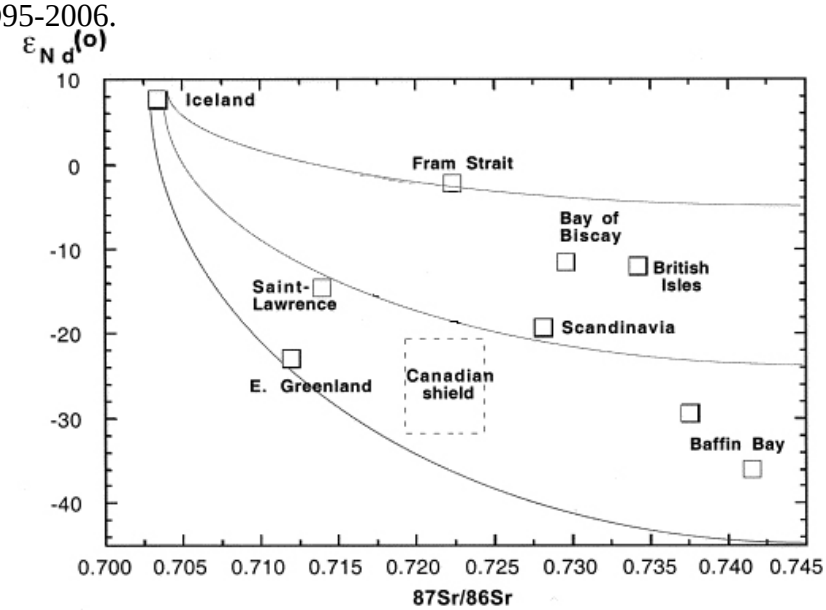

Figure 1.12: Sr-Nd signatures of North Atlantic Potential Source Areas. Squares represent average compositions from all samples from each area (Snoeckx *et al.* 1999).

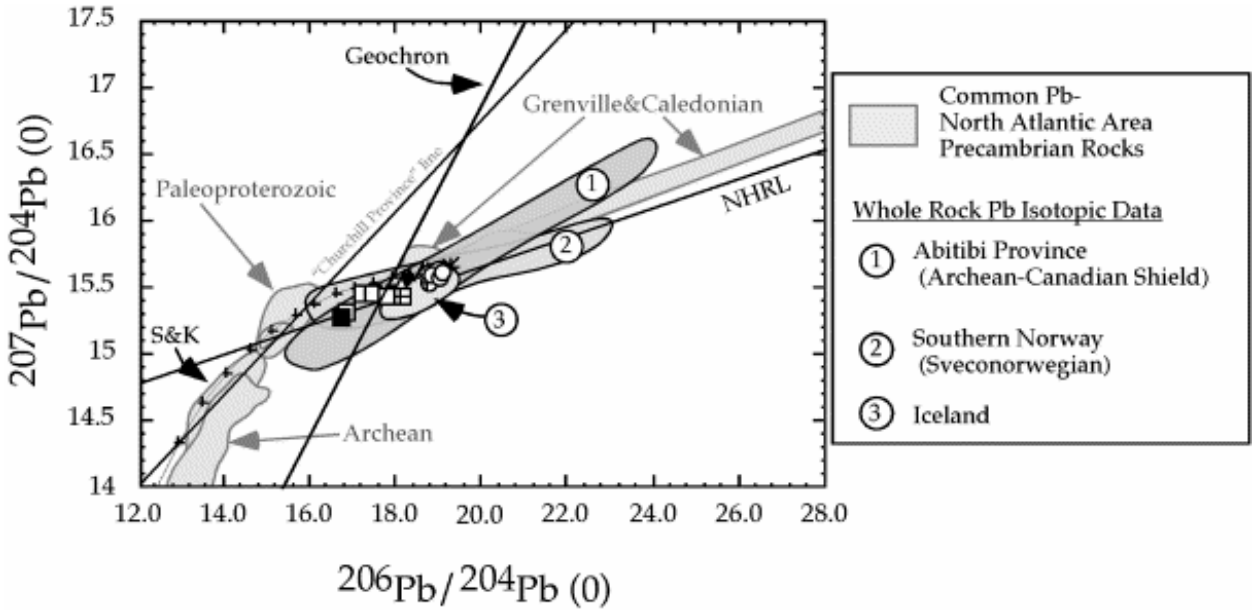

Figure 1.13: $^{207}Pb/^{204}Pb$ vs. $^{206}Pb/^{204}Pb$ isotopic compositions of 'common Pb' from potassium feldspars in circum-northern Atlantic Precambrian crustal rocks and for whole rocks from Precambrian crustal rocks and Iceland basalts. 'Churchill Province' line and Stacey–Kramers two-stage Pb growth curve (S&K) are also shown. From Farmer *et al.* (2003) and referenced therein.

1.7.2 Sediment End-Members

The isotopic method of determining provenance relies on an adequate database of isotopic ratios characterising the different source regions. In the majority of past studies provenance determinations have been based largely on comparisons of the isotopic compositions and/or ages of IRD and the known isotopic and age characteristics of basement rocks (in many cases Precambrian in age) now exposed in the circum-North Atlantic area. However, the provenance of glacial marine sediments in the North Atlantic can be more accurately determined by comparing the isotopic characteristics of the IRD with those of Late Quaternary ice-proximal sediments present around the northern Atlantic margins because such sediments provide information on the isotopic characteristics of siliciclastic material actually delivered to the North Atlantic. Revel *et al.* (1996) analysed not only literature data on terrestrial rocks and sediments from around the North Atlantic but also analysed the bulk lithic fraction of sediments from beaches, estuaries, continental shelves and slopes and Grousset *et al.* (2001) went even further, basing their potential source area data exclusively on sediment samples.

In general it is thought that ice-proximal sediments deposited throughout the Northern Atlantic were derived from glacial erosion of immediately adjacent crustal rocks and do not represent far-travelled detritus produced by glacial erosion at the interior of the ice sheets (Farmer *et al.* 2003). Although this assertion is based primarily on the isotopic analysis of fine-grained sediments and so may not hold true for North Atlantic IRD, there is a characteristic half-distance fall out for diagnostic mineralogies (Clark 1987, Andrews 2000) and this may suggest that icebergs calving from a specific margin should also carry primarily local materials. However, meltwater plumes and debris flows may transport material much further and complicate this signal. Although there is no evidence to suggest that these processes deliver significant amounts of sediment to ice-marginal sites (Farmer *et al.* 2003), this assertion is based on sediment from discrete time intervals and may therefore be a poor representation of ice sheet-sediment dynamics of a lot of the last Glacial period.

The limited isotopic data from ice-proximal sediments agrees with the expected pattern of north-south younging of the North American terrains (Farmer *et al.* 2003). Hornblende grains from Hudson Strait sediments have a dominant Palaeozoic age

population with a subordinate Late Archean population (Gwiazda *et al.* 1996a, Hemming *et al.* 2000, Hemming *et al.* 2002) whereas sediment from the Gulf of St Lawrence show a dominant Grenvillian age population (0.9-1Ga; Hemming *et al.* 2002). Such a latitudinal pattern is not as prominent in Norwegian terrains. Although there is a west-east longitudinal progression from younger to older terrains, the westwards flow of ice across Scandinavia renders it harder to characterise Norwegian sea ice-rafted sediments in terms of distinctive isotopic compositions. The south coast of Norway is underlain by Mesoproterozoic crust with the west coast having been overprinted by the Caledonian Orogeny. Palaeozoic and Archean crust lie to the east of the Caledonides. Ages of hornblendes from sediments along the mid-Norwegian margin range from 385-847Ma (Hemming *et al.* 2002), dominated by younger, Paleozoic ages. This mirrors up-stream geology: Cambrian-Silurian metasediments with Caledonian igneous intrusions. Sediments from the Bear Mouth Fan are poor in datable mineral grains, making characterisation of the sediment difficult (Hemming *et al.* 2002). Rare grains yield ages of ca.1.6-2Ga i.e. Palaeoproterozoic-Archean suggesting an origin from similar aged rocks in northern Fennoscandia and NW Russia but the presence of abundant black shale and carbonaceous grains suggest that some of the sediment originates from the Cenozoic and Mesozoic sedimentary rocks in the Barents Sea. The diversity of geologies within Bear Island Fan sediments indicates a complex sedimentary regime and thus distinguishing between sediment from separate Scandinavian Ice Streams has proved complicated (Figure 1.14). Farmer *et al.* (2003) have distinguished between the ambient (fine grained) sediments from the mid-Norway continental shelf and those from the Bear Island TMF on the basis of both εNd and Pb ratios. Unlike studies from the western Atlantic margin (e.g. Hemming *et al.* 2000, Farmer *et al.* 2003), limited work has been done on separating out the different Scandinavian signatures, or indeed spatial signatures from most of the margins of the eastern Atlantic.

Even once extensive studies have been carried out, complications may still exist. For example, although the εNd isotopic signal from the Gulf of St Lawrence can be separated from that of Hudson Strait, it is indistinguishable from glacial detritus delivered to the Norwegian Sea by the western Fennoscandian Ice Sheet (Farmer *et al.*

2003). This calls for provenance studies to employ more than one method in defining a specific source signal within IRD.

Isotopic signatures from sediments off Greenland prove as complicated to unravel as those in the rest of the GIN Seas. There is much overlap in geological ages with Greenland and thus isotopic dating alone may not be enough to distinguish between different sources both in Greenland and between Greenland and other landmasses (Figure 1.14). Sediments off southern Greenland contain populations indistinguishable from Churchill sources and sediments from off northeast Greenland are indistinguishable from both Norwegian Caledonian and the Laurentide Appalachian age spectra (Hemming *et al.* 2000, Hemming *et al.* 2002). Further petrological work is needed in order to start to distinguish between sediments from these various sources. Darby and Bischof (1996) and Bischof and Darby (1999) have begun to carry out this type of work on the contribution of Canadian Arctic Island sediment to Arctic IRD but as yet, a similar focus has not been taken for many other circum-North Atlantic sites. Table 1.3 provides approximate Sr and Nd isotopic values for various source areas.

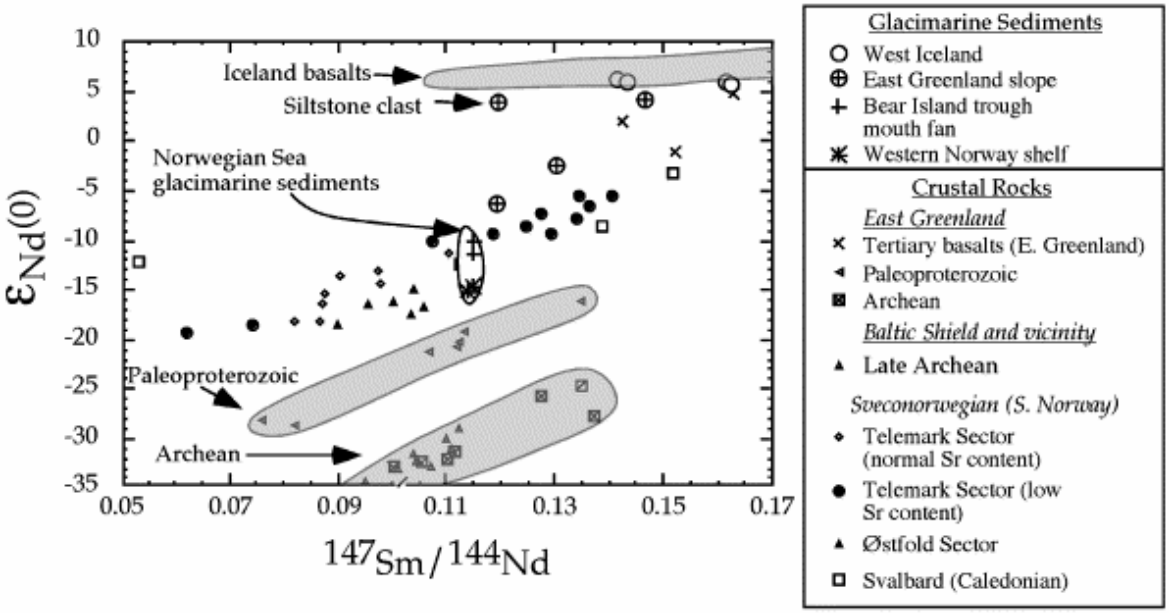

Figure 1.14: εNd(0) vs. $^{147}Sm/^{144}Nd$ for glacimarine sediments in Iceland, East Greenland and eastern Norwegian Sea in comparison to whole isotopic compositions of exposed crustal rocks in Greenland, Iceland and Fennoscandia/Svalbard. From Farmer *et al.* (2003) and references therein.

Table 1.3: Sr and Nd isotopic values for various North Atlantic source areas.

Source	$^{87}Sr/^{86}Sr$	$^{143}Nd/^{144}Nd$	εNd(0)
Revel *et al.* (1996b)			
Bay of Biscay	0.730700	0.512050	-11.6
British Isles	0.734254	0.512019	-12.1
Norwegian Margin	0.728200	0.511644	-19.3
Iceland	0.703450	0.513050	8.0
Grousset *et al.* (2001) – >63μm sediment samples			
Fram Strait	0.71818	0.511980	-12.8
Fram Strait	0.721620	0.512000	-12.4
Voring Plateau	0.7229	0.511903	-14.3
Voring Plateau	0.7235	0.512057	-11.3
Oslofjord	0.725039	0.512077	-10.9
Sogrefjord	0.735614	0.511923	-13.9
Rockall Trough	0.724352	0.512062	-11.2
Rockall Trough	0.724012	0.512001	-12.4
Irish Shelf	0.721308	0.511998	-12.4
Irish Channel	0.729787	0.512011	-12.2
Celtic Sea	0.720651	0.511965	-13.1
British Isles (mean)	0.732519	0.511966	-13.1
Bay of Biscay (mean)	0.730650	0.512030	-11.9
SW Portuguese Shelf	0.723874	0.512054	-11.4
NW Protuguese Shelf	0.723285	0.511919	-14.0
Iceland (mean)	0.70345	0.513924	7.6
Azores	0.704172	0.512890	4.9
Faroe Islands	0.704637	0.512905	5.3
Faroe Islands	0.705334	0.512966	6.2
Faroe Islands	0.703887	0.513037	7.6
Baffin Bay	0.74287	-	-33.0
Baffin Bay	0.73156	-	-27.4
St Lawrence	0.720113	0.511738	-17.5
Milnes Seamount	0.72836	0.510991	-32.1
GRIP bedrock	0.7288	0.510403	-43.5
GISP bedrock	0.73167	0.510739	-37.0
East Greenland Shelf	0.713495	0.512094	-10.6
Farewell Cape	0.71111	0.511483	-22.5

1.7.3 North Atlantic Sediment

The 'background' (fine-fraction) of Holocene and glacial sediment from cores in the northeast Atlantic is a mixture of an acidic and a basaltic component, yielding a K/Ar age of 440+/-50 Ma, though to be representative of the acidic, continental contribution (Jantschik and Huon 1992, Huon and Ruch 1992). The ages of Heinrich Layers are significantly older (990-1340 Ma) reflecting an increased contribution from one or several Precambrian terrains.

Studies up to present indicate that Nd isotopic ratios of IRD within the IRD belt can be divided into two groups: εNd values <-15 or >-15. Values of <-15 being products of erosion of the Canadian Shield by the LIS (Fagel *et al.* 1999, Farmer *et al.* 2003). Furthermore, Farmer *et al.* (2003) use Nd and Sr isotopic compositions to narrow down the source area for the typical Heinrich Layers (H1, H2, H4, H5) to be the Hudson Strait rather than further south (e.g. Gulf of St Lawrence) confirming the implications of many earlier studies (e.g. Bond *et al.* 1992, Broecker *et al.* 1992), although the isotopic ratios of H1 are slightly different possibly implying a contribution from a number of source areas. Values of >-15 are harder to resolve. They were initially inferred to require a Fennoscandian (Snoeckx *et al.* 1999) or an Icelandic, volcanic source (Grousset *et al.* 2001) however recent data has shown that Sr and Nd data from ice-proximal sediments deposited in the St Lawrence seaway are indistinguishable from those in the Norwegian Sea and indeed also from the IRD (>150μm) comprising atypical Heinrich Events H3 and H6 (Farmer *et al.* 2003). There still remains the possibility that these potential source areas may be able to be resolved through using criteria other than Sr and Nd isotopes and through combining different distinguishing methods. It has been shown that H3 IRD layers increase in thickness from west to east supporting a European source for this Heinrich Event (Grousset *et al.* 1993) however this is still a relatively qualitative method and further work is needed in separating out isotopic signatures particularly when addressing the question of precursor events; whether the εNd values of >-15 observed prior to the main Heinrich Layers H1, H2 and H4 (Grousset *et al.* 2000, 2001) are indeed due to a European (Scandinavian) source or whether they are a signal of material delivered by a surge of the southern LIS, which is known to have delivered icebergs to the North Atlantic (Hemming *et al.* 2000), prior to the main Hudson Strait surge.

Outwith the IRD belt the clear distinction between high and low εNd values breaks down due to the significant input of detritus from Tertiary volcanic rocks of Iceland (Revel *et al.* 1996, Grousset *et al.* 2001) and SE Greenland (Farmer *et al.* 2003). Thus both areas must be considered as potential sources of high εNd material to proximal areas of the North Atlantic.

Studies on modern deep sea turbidites have shown a much greater spread of Pb isotope ratios from North Atlantic sites in relation to those from the Pacific and Indian Oceans (Hemming and McLennan 2001). This means that bulk samples are less likely to fall into a discrete isotopic field. Thus the large contrasts in age and geological history of the circum-north Atlantic terrains can be both a blessing and a hindrance depending on the methodology employed in provenance studies.

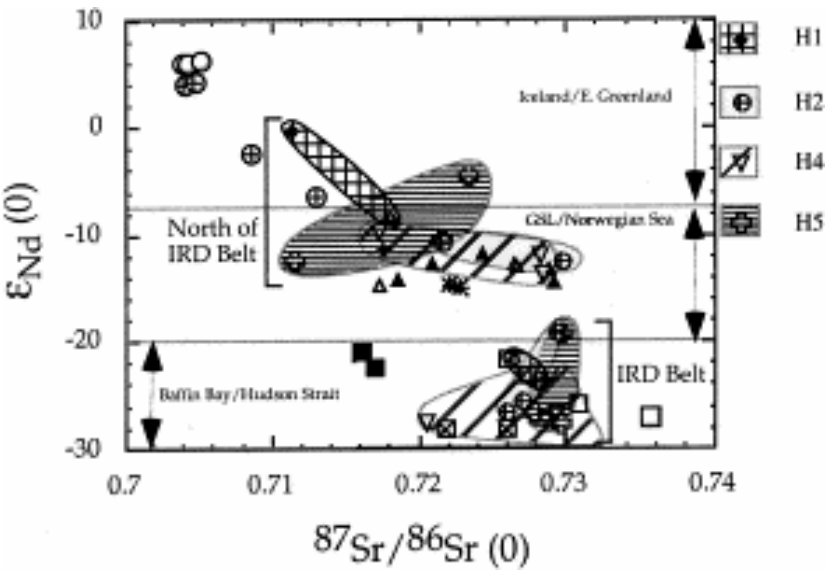

Figure 1.15: εNd(0) vs. $^{87}Sr/^{86}Sr$ for bulk sediment and >63 μm sediments from H1, H2, H4 and H5 in North Atlantic compared to ice-proximal glacimarine sediments. Data from Farmer *et al.* (2003) and references therein.

1.8 Major Questions facing the palaeoceanographic community

1.8.1 Methodological

There is a need for consistency between methods in order to have comparable studies. This consistency extends to the criteria used to identify IRD and source region characteristics, analytical techniques, methods of displaying data, the data precision and all statistical techniques employed as means of data comparison.

1.8.1.1 Sample Collection: coring methods

Accurate interpretations of down-core properties require prior distinction between primary stratigraphic features and secondary artifacts introduced in the coring and sampling processes. This is particularly important in the context of the rapid changes of sediment flux associated with Heinrich Events and other ice-rafting events. Up to a 50% 'shortening' of gravity cores has been noted (Emery and Dietz 1941), with the effect varying from approximately linear down-core (Lebel *et al.* 1982) to intermittent shortening (Parker 1991), effects being different depending on the interactions between core dimensions and sediment characteristics (Blomquist 1985, Parker and Sills 1990). Furthermore, sediment 'lengthening,' or 'over-sampling' has also been observed to occur not only in the top of piston cores (Thouveny *et al.* 2000) but also in both the middle and base, probably due to cable recoil and sediment plugging respectively (Skinner and McCave 2003). This can lead to effects such as double penetration, leading to the repetition of down-core trends. This is particularly problematic in studies aimed at identifying cyclic variations in core properties.

Attempts to minimise these problems have been made through the development of new coring techniques such as Advanced Piston Coring (APC), stationary piston coring (STACOR) and Giant Piston Coring. However the more advanced coring techniques often suffer practical drawbacks such as time-consuming deployment and complexity of design.

Placing different types of core on the same timescale provides a direct method of stratigraphic comparison (Skinner and McCave 2003). This indicates that in situ stratigraphic dimensions are most faithfully represented in the upper portions (10-12m)

of large-diameter (20-30cm), square barrel gravity-type corers and in the lower portions of cylindrical piston corers. Hence the most accurate representation of a sedimentary sequence is likely to result from the splicing together of different records.

1.8.1.2 Proxies Studied

There are inherent problems involved in assuming what proxies actually represent, particularly with regards to Heinrich Layers. For example MS is often used as a means of identifying Heinrich layers within marine core stratigraphies. Bulk sediment analyses have shown that the MS signal in North Atlantic cores covering a wide spatial area is actually mainly from low Ti-bearing magnetites with the subtle trends in susceptibility due to variations in the magnetite grain size (Rasmussen *et al.* 1996a, Moros *et al.* 1997, Kissel *et al.* 1999). In dramatic contrast to the susceptibility peaks associated with Heinrich Events in much of the IRD belt (e.g. Grousset et al 1993), these studies have correlated Heinrich Events to magnetic minima.

In addition, redox enrichments at the base of Heinrich Layers may lead to ambiguous signals in the records of redox metals such as Fe, Ni and V. Thus using these elements as any kind of palaeoclimatic indicator may be problematic.

1.8.1.3 Dating and Resolution

Studies of millennial-, centennial- and decadal-scale climate variability require the appropriate resolution to be able to distinguish such abrupt events within the record. However, the resolution is only as good as the dating and hence stratigraphic control of the record.

The most widely used dating method in the marine environment is the measurement of the ratio of $^{12}C/^{14}C$ in foraminifera tests within sediment to determined the age at which they ceased CO_2 exchange with the surrounding water (i.e. age of death). The use of Accelerator Mass Spectrometry (AMS) to measure very small concentrations of ^{14}C has led to significant improvements in the accuracy, precision and dating age range of ^{14}C-dating, however, there are still many problems inherent in the technique, particularly when applied to the marine environment.

In calculating radiocarbon dates obtained by conventional methods, laboratories compare sample activities to a modern reference standard; the modern level of activity of the NBS oxalic acid standard. Isotopic fractionation occurs during the natural reduction of CO_2 to C during photosynthesis meaning that lighter carbon isotopes will react preferentially to heavy. Fractionation is mass dependent and therefore if the $^{13}C/^{12}C$ ratio of samples is measured, the equivalent fractionation of $^{14}C/^{12}C$ can be calculated. The $^{13}C/^{12}C$ ratio is compared with a standard (the PDB limestone belemnite carbonate) and values are cited as deviations from this standard:

$$\delta^{13}C = \left(\frac{^{13}C/^{12}C_{sample}}{^{13}C/^{12}C_{PDB\ standard}} - 1\right) * 1000$$

There are 3 main assumptions inherent in calculating the conventional radiocarbon age:

1) The atmospheric ^{14}C production has been constant over time
2) The dynamics of atmosphere-ocean CO_2 exchange have been both temporally and spatially constant.
3) The dynamics of surface-deep ocean water exchange have been both temporally and spatially constant.

There is a transferral time of ^{14}C from atmosphere to surface ocean and subsequently slow circulation from surface ocean to deep waters. Therefore both the ^{14}C ages of shallow and particularly deep water, appear older than is the case. The surface water 'apparent age' at present ranges up to 580 years in parts of the equatorial Pacific (Shackleton et al 1988). Thus, the 'apparent age' of seawater will change over time according to levels of atmospheric production, rate of uptake by the surface oceans and dynamics of ocean circulation. Therefore a 'reservoir correction' must be added to any ^{14}C age based on the time taken for CO_2 exchange between surface and deep waters to occur.

In general a reservoir correction of 400a is assumed over the whole North Atlantic, however this has the potential to lead to errors of up to 1500a (Kissel *et al.* 1999), rendering less than millennial-scale correlations using a ^{14}C-based chronology impossible. Not only is there a varying marine reservoir effect to contend with but there

is also the inherent age of the mixed sediment (Manighetti and McCave 1995). The age of this mixed layer at the time of Heinrich Event 2 is <620yr (Hall and McCave 1998) and this has large implications on the dating of precursor events.

Linear interpolation is usually used between age control points in the construction of age models. A better approach would be to weight the interpolation so that transitions between different sedimentation rates are taken into account. Heinrich Events are actually inherently characterised by abrupt increases in the flux of sediment to the core site and hence the assumption of linear sedimentation rates between dated control points is essentially invalid. This poses large problems when it comes to high-resolution dating as even slightly varying sedimentation rates can introduce a large offset to the age-depth model used. Heinrich Event 4 is seen as a very large event in the Mg:Al and Zr:Al record in piston core KL1 from Bengal, NE Atlantic, causing large deviations from the mean sedimentation rate (Hinrichs *et al.* 2001).

Problems of down-core changes in abundance of foram species used for dating Heinrich events is potentially a huge problem when it comes to inferring dates and durations of these events. Bioturbation mixes younger sediment into old down to the depth of the mixed layer and thus mixing above a foram-poor Heinrich Layer will lead to artificially young ages above the event whereas a fossilised mixed layer below the event will lead to erroneously old ages at this horizon (Manighetti and McCave 1995).

1.8.2 Glaciological Processes

1.8.2.1 Glacial sediment entrainment

More information is needed regarding glacial sediment entrainment mechanisms and the translation of this into iceberg debris. Is there a vertical size fractionation in icebergs? What, if any, is the characteristic grain size spectrum within an iceberg? For example a low IRD total within a core horizon may reflect a decrease in iceberg flux or simply a decrease in the amount of debris entrained within icebergs.

Dowdeswell *et al.* (1995) suggested that Heinrich Events were associated with an overall glacial erosion rate of between 0.8 and 0.08mma^{-1}. With warm-based and

rapidly moving ice streams it would normally be considered that the basal traction layer was <10m (Andrews 2000) and that sediment composition would reflect a characteristic half-distance fall-off in the range of 50-100km (Clark 1987). This raises the question of how the carbonate values of >40% in the Heinrich Events in the Labrador Sea and >20% in the IRD belt (Bond *et al.* 1999) can be maintained solely from iceberg transport and melting. It seems necessary that the glacially eroded carbonate sediments are transferred from the basal traction zone into a significant portion of the ice column: the mechanisms through which this may be achieved are still under debate.

Various studies have tackled the question of the total amount of sediment deposited during each Heinrich Event (e.g. Dowdeswell et al 1995) and this has raised issues on how the resulting large volumes of sediment produced could have been delivered to the North Atlantic by icebergs alone. Alley and MacAyeal (1994) have demonstrated how the binge/purge model can explain how the large amount of debris (0.1-1km^3) making up the Heinrich Layers could have been frozen into basal ice and MacAyeal (1993b) suggest that during Heinrich Events, Hudson Strait could produce an iceberg flux of 2800km^{3}yr^{-1}.

Modelled estimated total northern Hemispheric LGM iceberg flux outwith Heinrich Events is 3500-4000km^{3}a^{-1} (Bigg and Wadley 2001), demonstrating the massive nature of iceberg delivery during each Heinrich Event.

1.8.2.2 Source to sink sediment pathways

Further to Section 9.2.1, a better understanding of pathways of sediment source to sink is needed (eg see Schaefer-Neth and Stattegger 1999). Is there a difference between sediment grain size deposited by icebergs in ice-proximal vs ice-distal locations? Do icebergs oveturn, thus producing a more 'random' element to IRD deposition? Past studies seemed to focus a lot more on past ocean circulation and paths of icebergs which now seems to be almost overlooked in most recent papers. A tracer approach to IRD must be combined with studies of past ocean circulation (and sediment delivery) in order to fully understand what was going on at different time intervals.

Modelling work has been carried out on modern iceberg drift (e.g. Bigg *et al.* 1997). Such studies have addressed questions concerning the factors that control iceberg drift directions and melt rates. Iceberg motion can potentially be affected by not only water

advection (currents) and air from drag (wind speed and direction) but also water-, ice- and wave-drag (Bigg *et al.* 1997). Little is known about the details of individual iceberg trajectories over long distances, apart from general conceptions of large-scale movements (e.g. Marko *et al.* 1994). It has been shown that climatological factors in ocean and atmosphere circulation play as an important role in iceberg trajectories as the seasonal variation in calving (Bigg *et al.* 1997). It appears that ocean currents exert a first order control on iceberg trajectories, subsidiary to that of prevailing wind patterns (Matsumoto 1997).

Modelling studies show that the maximum lifetime of modern icebergs is ca.5 years (Bigg *et al.* 1997) with only around 1% of total iceberg release lasting over 5 years. Obviously the survival time of an iceberg is strongly dependent on size, showing an exponential distribution.

Icebergs all seem to overturn during their lifetime, the stage at which this happens being dependent on the regional atmospheric, oceanic and wave climate. Smaller bergs will overturn sooner in their lifetime and there is a tendency for icebergs to roll over more frequently as they get smaller. This does not, however apply to large tabular icebergs or sea-ice rafts (Andrews 2000) so consequently if the nature of sediment release is to be determined, accurate knowledge of the type of iceberg in question is vital.

In most models, it is assumed that IRD is essentially contained in the outer shell of icebergs so that most debris is released early in the decay of the iceberg (Matsumoto 1997). If the assumed mechanisms of debris entrainment are incorrect, this renders much of the reconstructed IRD-deposition pattern incorrect as well.

Many studies overlook the terrestrial record altogether when addressing iceberg release and volume. It is valuable to look at the palaeogeography and palaoglaciology affecting the study site (terrestrial sediment pathways, shelf break environments, palaeochannels, buried sandbanks, deltas etc., TMFs, proglacial lakes and drainage). Indeed, it has been proposed that one reason why the Hudson Ice Stream might be inherently more unstable (and hence be responsible for the Heinrich Event signal) than other circum-North Atlantic ice streams associated with large TMFs, might be the great depth of the shelf

break off Hudson Strait (600m water depth) and the deep basin on the shelf, seaward of the Precambrian sill (Andrews and MacLean 2003).

It is also important to resolve issues concerning the path of iceberg drift across the North Atlantic and the relative time taken for icebergs to reach a particular location from a particular ice sheet. This is especially important in deducing possible leads and lags of iceberg discharge from the circum-North Atlantic ice sheets and hence implicating forcing mechanisms for the IRD Events. Paradoxically it is often IRD records that are used to address such issues thus resulting conclusions may actually be based on a circular argument. For example, palaeocirculation studies imply that the observed lag time of a few centuries between European IRD and LIS IRD in H4 on the Portuguese continental margin is too long to be accounted for purely by the longer time needed for LIS icebergs to reach the site. Hence Snoeckx *et al.* (1999) argue against synchronous iceberg release from all North Atlantic ice sheets. However, if the reconstructed circulation patterns at the time and models of iceberg drift and survival are wrong, then this conclusion could be too.

1.8.3 Provenance Studies

1.8.3.1 Constraining North Atlantic PSA isotopic signatures

At present there is a dearth of detailed knowledge constraining appropriate provenance sediment signatures from well-defined sources (see Section 1.7.1). Thus, future studies should aim to include isotopic analyses of the fine sediment fraction both through the IRD intervals and within background glacial sediment. This will (a) characterise the 'ambient' sediment signal of the study site and (b) start to work towards a general inventory of the isotopic signals contained in glacial sediment across the North Atlantic. In particular, this inventory needs to bracket sedimentological end members characterising the sediment delivered by different ice-stream outlets around the North Atlantic. This can be achieved through looking at the isotopic ratios of sediment collected from the specific areas in which material from each outlet is focused. Due to the nature of variations in the isotopic signal of the different size fractions within a bulk sediment sample it would be highly advantageous if different studies selected the same size fraction and isotopic system. This approach would enable cross-comparison of

results, particularly important in the context of circum-North Atlantic studies which address interrelated processes affecting the whole region.

Ideally, unique tracers for different source areas are needed. The carbonate content of Heinrich Events consists primarily of calcite with some dolomite but as yet, no distinctive provenance signature has been provided for the carbonate fraction. Significant progress has been made however, in characterising the isotopic composition and geochemical signature of the non-carbonate sediment fraction. The most accurate constraints on sediment provenance are likely to result from using a combination of complimentary techniques. For example an inferred provenance of IRD from material of tertiary ages may be verified by an abundance of smectite in the corresponding clay-fraction as this clay is largely produced from the weathering of basaltic material.

1.8.3.2 Matching sediment to source

The point of sediment entrainment mechanisms is also relevant in provenance determinations: Glaciological studies note the large distances which glacial erratics can be transported relative to only a few tens of kilometres for fine-grained sediment (Clark 1987). This is in agreement with isotopic studies which suggest that fine-grained ice-proximal sediment is generally sourced from directly adjacent crustal areas and do not contain material eroded from under the ice sheet interior (Farmer *et al.* 2003). This, along with the characteristic half-distance fall out suggests that icebergs calving from a specific margin should also carry primarily local materials. However, meltwater plumes and debris flows may transport material much further and complicate this signal. Although there is no evidence to suggest that these processes deliver significant amounts of sediment to ice-marginal sites (Farmer *et al.* 2003), this assertion is based on sediment from discrete time intervals and may therefore be a poor representation of ice sheet-sediment dynamics of a lot of the last Glacial period.

Many studies to date have simply used visual identification of broad lithological groups as a basis for IRD provenance studies (e.g. Scource *et al.* 2000). This poses all sorts of problems. It is generally assumed that the presence of dolomite (or high-Mg calcite) is an clear indication of an LIS origin. It seems, however, that this is a huge and not necessarily correct assumption to make. No-one has really addressed this issue and

many large-scale, and now generally accepted theories have been based on this assumption (e.g. Bond and Lotti 1995, Bond et al 1992, 1993).

Volcanic glass is often used as an indication of the presence of material derived from Iceland, likely to be tephra from one of the Icelandic volcanic systems. This in itself is a valid assumption, however, there remains the problem of distinguishing between ice-rafted glass and air-fall deposits. Larger shards at sites distal from Iceland are unlikely to have been direct air-fall deposits however they could be secondary deposits, initially erupted onto sea ice or true IRD, entrained into icebergs from Iceland. Distinguishing between these processes is vital if inferences about the dynamics of the Icelandic Ice Sheet and the timing of icebergs released are to be made. One way to do this is to study the size distribution of the Icelandic material within bulk sediment. This has been done within NAAZII (Wilson and Austin xxxx) but as yet it seems as if no-one has studied the size distribution of Icelandic volcanic material within the bulk sediment of an IRD layer.

1.8.4 Interpretational

1.8.4.1 Sea ice vs. debris flows

As mentioned in Section 1.5.4, one of the main problems affecting ice-proximal sites is distinguishing between the true IRD signal and coarse mass-flow deposits delivered to the core site. Multi-proxy studies provide the potential to combine charactersitics within each proxy to define a unique combination of properties within each proxy record that can aid the distinction between sediment delivery through different mechanisms.

Isotopic studies may not only be useful for provenancing IRD but also may provide the potential to distinguish between turbidite flows and IRD. In ice-proximal sites, turbidite flows are likely to produce a strong sporadic increase in local material (i.e. a local isotopic signal) in all size fractions whereas a local IRD signal is only likely to be revealed in the coarse fraction, and vary independent of other size fractions. Hence it is vital not only to combine mineralogical and isotopic studies but also to examine variations in these characteristics in different size fractions over time.

However, processes like winnowing are able to remove the fine fractions thereby accentuating the isotopic signal from size fractions of silt and above. Interpretation of results must therefore bear this effect in mind.

1.8.4.2 IRD Records

Andrews (2000) addresses some of the main issue surrounding the interpretation of IRD records in the North Atlantic. Concurring with the issues outlined in Section 1.5.3, he identifies four main criteria that must be reconstructed if an accurate interpretation is to be made:

1) The past volume of icebergs calved into the North Atlantic basin.
2) The sediment distribution within these icebergs.
3) The trajectories and melt history of these icebergs.
4) The characteristics of the sediment transported in these icebergs.

   However, Andrews (2000), fails to address certain problems related to the interpretation of the records of IRD once laid down in marine sediments.

One such question is what potential information the shape of IRD records may hold. IRD spikes are open to different interpretations than longer intervals of coarse lithic delivery, possibly a representation of local versus regional ice-rafting. (e.g. Knies *et al.* 2001).

In addition, there have been few, if any, studies looking at the lateral variability of IRD on scales of centimeters and metres (Andrews 2000). New coring techniques using large-volume box core material may provide the scope to address this issue.

1.8.4.3 Signature of glacial retreat vs. glacial advance

How can we distinguish an IRD pulse related to glacier advance from one due to glacier retreat? This question may be able to be answered if IRD studies are complimented with detailed sedimentological analysis (e.g. Powell and Cooper 2002). Although the IRD records of many Heinrich Events are comparable in deep-sea sediments, studies have revealed markedly different responses, encompassing both glacial advances and retreats of circum-North Atlantic ice margins during at least Heinrich Event 1 (e.g McCabe and Clark 1998).

Solving this question will have a direct effect on the attribution of mechanisms behind ice-rafting events as a retreat of one ice sheet at the same time as the advance of another is not necessarily an argument against a climatic forcing of Heinrich Events. For example, a climatic warming could potentially trigger an initial advance in a small maritime ice sheet such as the BIS due to enhanced moisture supply but a retreat in a larger ice sheet such as the LIS, which has more of a temperature-related control on mass balance.

1.8.4.4 Signature of Heinrich Events

Auffret *et al.* (1996) raise the question of whether Heinrich Layers are more to do with a concentration of IRD *per se* or a balance between increased IRD and the potential for the Heinrich Layer to survive relative to other facies within the sediment column. Janschik and Huon (1992) note that one mineralogical difference (an elevated amphibole content in the clay sized fraction) seen only in horizons corresponding to 'typical' Heinrich Events also corresponds to the only four cemented marl horizons in the core (ME-68-89, Grosser Dreizak). Further to this, Bond *et al.* (1992) note that there is significant dissolution of foraminifera within H3 compared to well-preserved microfossils in the other Heinrich Layers. This tends to suggest that certain features may be better preserved due to diagenetic/authigenic effects producing these cemented layers.

1.9 Aims and Objectives

The specific aims of this study have been formulated mainly to focus on the above site-specific issues but also to address some of the broader questions outline in sections 1.8.

1) To chart the dynamics of the BIS through MIS3-2: ice sheet growth through the last glacial cycle.
2) To investigate the structure and signal of Heinrich Events as recorded on the Barra Fan: an ice-proximal location.
3) To define the provenance of the IRD delivered in each Heinrich Event and any changes in this source through the Heinrich Layer.
4) To distinguish between true IRD layers and turbidites/mass flow deposits in this continental slope location.

2. Materials and Methods

2.1 Sample acquisition

Giant piston core MD95-2006 (57°01.82 N, 10°03.48 W, 2120m) was retrieved in 1995 by the research vessel *Marion Dufresne* as part of the IMAGES programme from the Barra Fan on the continental slope of NW Scotland. The core was recovered using the giant piston (Calypso) corer consisting of a 40-60 m lance and an internal high-pressure PVC liner of 10cm diameter. MD95-2006 consists of 30 m of Pleistocene (<50,000yr BP) glacio-marine sediments.

Initial sampling of the working sections of the core was carried out at 10 cm resolution by William Austin and Cecelia Taylor for micropalaeontological counts, AMS ^{14}C dates, coarse lithic counts and stable carbon and oxygen isotope analysis. Further sampling was done for water content, combined bulk density, environmental magnetics, grain size and geochemical analysis (Knutz *et al.* 2001, Wilson *et al.* 2002). Sampling for this study was carried out at 1cm resolution across Heinrich Events 2 and 4 and at 4 cm resolution in the intervening 769 cm of the core (see Section 3.# for explanation behind the choice of these intervals). Samples were taken from the centre of the working half in order to avoid contamination from above and below each sample due to smearing of the core sediment down the barrel sides during core retrieval (e.g. Austin 1994).

2.2 Whole-core Analysis

2.2.1 Acquisition of previous data

Extensive work has been done over the entire core record (Kroon *et al.* 2000, Knutz *et al.* 2001, Bossenkool 2001, Wilson and Austin 2002, Wilson *et al.* 2002, Austin *et al.* 2004) enabling this higher resolution study to be carried out in the context of a well-constrained stratigraphy and existing age model.

2.2.2 ITRAX X-ray fluorescence

ITRAX XRF analysis was carried out on the archive sections of MD95-2006 at BOSCORF, Southampton Oceanography Centre. ITRAX XRF is a relatively new, automated, non-destructive core scanning instrument that records optical, density and elemental variations from sediment half cores up to 1.8 metres long at a resolution as fine as 100 micrometers. An intense micro X-ray beam focused through a flat capillary waveguide is used to irradiate samples to enable both X-radiography and X-ray fluorescence (XRF) analysis. Data are acquired incrementally by advancing a split core, via a programmable stepped motor drive, through the flat, rectangular-section X-ray beam. Whereas traditional XRF determination of element composition in sediments provides high quality data, it takes a considerable time and normally consumes gram quantities of material that is often available in limited quantities. The ITRAX core scanner collects non-destructively, optical and X-radiographic images and provides high-resolution elemental profiles that are invaluable for guiding sample selection for further (destructive) detailed sampling.

Prior to analysis, the surface of each section was scraped with a clean glass slide to remove any mould/contamination that would affect the XRF reading. Each section was then run through the ITRAX scanner with a 2 mm resolution and a 30 second count time. These two parameters must be chosen carefully in order to maximise both the accuracy of the method (higher count times and resolution increases accuracy) and the time efficiency of the process of analysis (lower count times and resolution increase time efficiency).

Scanning XRF is in its infancy and thus there are still many uncertainties involved in the interpretation of such records. The results are produced in counts rather than absolute values, the general intensity of peaks determined by the exposure time and are therefore relative and only semi-quantitative.

2.3 Sample preparation and processing

High resolution (4 cm) records of IRD concentration, planktonic foraminiferal concentration, percentage *Neogloboquadrina pachyderma* (sinistral), $\delta^{18}O$ and $\delta^{13}C$ N. *pachyderma*(s) have been generated across the core interval between H2 and H4 within MD95-2006 (1600-2520 cm) and even higher resolution studies (1 cm) carried out across the core intervals containing H2 (1600-1670 cm) and H4 (2439-2520 cm).

Having been stored at <4°C, most samples were dried to constant weight at ca.40°C. This drying temperature is maintained at below 60°C in order to prevent further fractionation of the stable isotopes within the $CaCO_3$ shells of the foraminifera. However, repeat analyses at 40°C and >70°C on foraminifera tests picked from the same sample produce similar stable isotopic ratios suggesting that this effect may not be significant at the exposure temperatures (Table 2.1). The remaining samples were freeze-dried overnight before processing.

Table 2.1: Repeat stable isotopic analyses of planktonic foraminifera samples at 70°C and <40°C

Sample (depth and temperature)	$\delta^{18}O$ VPDB (‰)	$\delta^{13}C$ VPDB (‰)
1610 at 70^{0}C	3.974 ±0.022	-0.504 ±0.005
1610 at <40^{0}C	-0.146 ±0.014	3.966 ±0.003
1625 at 70^{0}C	3.240 ±0.019	-0.544 ±0.012
1625 at <40^{0}C	3.189 ±0.010	-0.733 ±0.012
1634 at 70^{0}C	3.444 ±0.016	-0.973 ±0.008
1634 at <40^{0}C	3.234 ±0.030	-0.823 ±0.010
1643 at 70^{0}C	4.242 ±0.018	-0.438 ±0.012
1643 at <40^{0}C	4.227 ±0.026	-0.668 ±0.008
1656 at 70^{0}C	4.223 ±0.017	-0.524 ±0.005
1656 at <40^{0}C	4.217 ±0.009	-0.474 ±0.016
1664 at 70^{0}C	4.185 ±0.016	-0.297 ±0.012
1664 at <40^{0}C	4.265 ±0.019	-0.299 ±0.009

Samples were wet-sieved on a 63 μm mesh in order to separate the sand fraction for foraminiferal and lithic analysis. The >63 μm residue was then dried at 40°C. Samples were weighed before and after sieving and weights recorded in order to calculate the >63 μm residue weight as a percentage of the dry sediment processed. Residues were then dry-sieved through a >150 μm sieve to separate out the coarse fraction, thought to represent that which can only be transported by ice-rafting processes (see Section 1.5.3.1).

2.4 Single Sample analysis

All grain counts were carried out using a Zeiss Stemi SV11 binocular microscope. Each sample was split in half progressively until the material was sufficient to be spread evenly and thinly across a counting tray consisting of a grid of 42 squares. Squares were picked at random and all grains (planktic foraminifera or lithic grains) within each square were counted until >300 grains (forams or lithics) had been counted. Concentrations were calculated from the acquired data using the following formula:

$$\text{Concentration (grains g}^{-1}) = \frac{\text{total grains x (42/no of squares counted)*(2)}^{\text{no. of splits}}}{\text{total dry sed weight (g)}}$$

2.4.1 Foraminiferal counts

Counts of all planktonic foraminifera were made as above. The number of *Neogloboquadrina pachyderma* (s) were then counted and their fraction calculated as a percentage of total planktic foraminifera in each sample.

Repeat counts of 5 samples were carried out in order to assess the inherent counting error. These repeat counts and associated errors are shown in Table 2.2.

20-30 monospecific planktonic foraminifera (*Neogloboquadrina pachyderma* (sinistral) or *Globigerina bulliodes*) were picked for stable isotopic analysis.

2.4.2 Lithic grain counts

Counts of total lithic grains >150 μm were carried out as above. Repeat counts of 5 samples were carried out in order to assess the inherent counting error (see Table 2.2).

For the 1 cm resolution data within Heinrich Events, lithological counts were also undertaken. Of the >300 lithic particles counted for each sample, all different lithologies were distinguished, in particular quartz, feldspars, dolomitic carbonate, haematite-stained grains, micas, metamorphic and volcanic grains. The concentrations of each type of lithic grain within the sediment was then calculated:

$$\text{Concentration (grains g}^{-1}) = \frac{\text{total grains x (42/no of squares counted)*(2)}^{\text{no. of splits}}}{\text{total dry sed weight (g)}}$$

and the fraction of each lithology calculated as a percentage of total lithic grains >150μm.

Table 2.2: Repeat grain counts and statistical analysis of counting errors

Sample	Foram counts	Np(s) counts	%Np(s)	IRD counts	IRD #g^{-1}	Foram #g^{-1}	IRD:Forams
2218	39	36	92.308	517	970	57	107
2218	40	31	77.500	806	1134	72	101
2218	41	33	80.488	818	1151	85	120
Average	*40.00*	*33.33*	*83.43*	*713.67*	*1085*	*71.33*	*109.26*
Standard Deviation	*1.00*	*2.52*	*7.83*	*170.42*	*99.99*	*14.01*	*9.37*
% error			*9.39*		*9.22*		*8.57*
1882	18	12	66.667	585	536	18	16
1882	23	18	78.261	575	527	23	21
1882	31	21	67.742	826	504	31	19
Average	*24.00*	*17.00*	*70.89*	*662.00*	*522.18*	*24.00*	*18.82*
Standard Deviation	*6.56*	*4.58*	*6.41*	*142.12*	*16.17*	*6.56*	*2.29*
% error			*9.04*		*3.10*		*12.17*
2066	238	10	4.202	157	193	238	292
2066	288	9	3.125	203	187	288	265
2066	91	1	1.099	216	199	323	297
Average	*205.67*	*6.67*	*2.81*	*192.00*	*192.66*	*283.00*	*284.64*
Standard Deviation	*102.40*	*4.93*	*1.58*	*31.00*	*5.98*	*42.72*	*17.28*
% error			*56.09*		*3.10*		*6.07*
2314	32	29	90.625	195	190	81	79
2314	42	33	78.571	287	224	113	88
Average	*37.00*	*31.00*	*84.60*	*241.00*	*207.34*	*97.00*	*83.70*
Standard Deviation	*7.07*	*2.83*	*8.52*	*65.05*	*23.89*	*22.63*	*6.49*
% error			*10.07*		*11.52*		*7.76*
2338	25	22	88	449	464	108	112
2338	20	20	100	409	423	80	83
Average	*22.50*	*21.00*	*94.00*	*429.00*	*443.27*	*94.00*	*97.13*
Standard Deviation	*3.54*	*1.41*	*8.49*	*28.28*	*29.23*	*19.80*	*20.46*
% error			*9.03*		*6.59*		*21.06*
Average Error			**18.72**		**6.71**		**11.13**

2.5 Analytical Techniques

2.5.1 X-ray diffraction

XRD was run on all samples within the H4 window. All samples were first crushed in acetone to <10¼ μm using an agate ball mill. Samples were then dried for 20 minutes at 90^0C. They were then back-packed into standard Philips sample holders to produce maximum random orientation. Typical detection limits are 0.5±2% depending on the bulk matrix. Samples are placed into a sample holder ensuring it is perfectly flat and level with the top of the sample holder. XRD analysis was carried out using a Philips PW1050/ Hiltonbrooks DG2 with a cobalt anode.

The Rietveld Method (Rietveld 1967, 1969) was used for calculating the mineralogy of XRD scans from the fundamental crystallographic data: The sample is scanned by XRD and the minerals present are identified. A computer-based task is then sent up to include all the minerals present. These minerals are included in a database where fundamental crystallographic data taken from published data is stored. A synthesised pattern is calculated from the "task" and a least squares regression is used to calculate mineral concentration. The Rietveld method corrects for preferred orientation, mass absorption, line overlaps, grainsize, unit cell and crystallinity. As the method relies on fundamental data, starting from an ideal model of the phases to be quantified, it is standardless. Typical relative errors are 5 - 10%.

2.5.2 Single sample X-ray fluorescence

XRF was run on all samples within the H2 window. All samples were first crushed in acetone to <10¼ μm using an agate ball mill. Samples were then dried for 20 minutes at 90^0C. ~0.8 g of sample was fused for 12 minutes in a platinum crucible at 1100^0C using 3.6 g sodium metaborate flux and 0.01mg ammonium iodide. The molten solutions were allowed to cool into solid glass disks ready for analysis.

Loss on ignition (LOI) was measured on a separate sample fraction in order to calculate the carbonate percentage within each sample. 1 mg of sample was heated in a porcelain crucible for 40 minutes at $>1000^0$C and weighed before and after in crucible (Sample wt.(S) + Crucible wt. (C) in grams). LOI was calculated using the formula:

$$\% \text{ LOI} = [(S+C_{\text{before heating}}-S+C_{\text{after heating}})/\text{Sample weight}]*100$$

Repeat analyses (n=16) of a standard of known composition were run to test instrument accuracy and to estimate precision. Results of standard runs are shown in Table 2.3. The penultimate row of Table 2.3 indicates the precision and the final row, the accuracy, of each of the elemental determinations.

Table 2.3: XRF analyses of Standard samples and calculated errors											
	Na_2O	MgO	Al_2O_3	SiO_2	P_2O_5	SO_3	K_2O	CaO	TiO_2	MnO	Fe_2O_3
	%	%	%	%	%	%	%	%	%	%	%
STD 1	4.08	2.54	11.69	59.65	0.53	0.17	4.22	8.27	0.15	0.35	6.50
STD 2	4.20	2.54	11.71	59.49	0.54	0.16	4.21	8.26	0.14	0.35	6.50
STD 3	4.07	2.56	11.68	59.66	0.53	0.15	4.22	8.28	0.15	0.35	6.50
STD 4	4.19	2.55	11.66	59.61	0.53	0.15	4.21	8.26	0.15	0.35	6.49
STD 5	4.16	2.56	11.64	59.64	0.53	0.15	4.21	8.26	0.15	0.35	6.48
STD 6	4.10	2.60	11.71	59.56	0.53	0.16	4.22	8.28	0.15	0.35	6.49
STD 7	4.10	2.61	11.67	59.47	0.54	0.15	4.26	8.38	0.15	0.36	6.61
STD 8	4.09	2.60	11.65	59.48	0.54	0.15	4.27	8.37	0.15	0.36	6.61
STD 9	4.13	2.59	11.66	59.51	0.54	0.15	4.24	8.35	0.15	0.36	6.61
STD 10	4.13	2.62	11.60	59.51	0.54	0.16	4.25	8.36	0.14	0.36	6.62
STD 11	4.07	2.62	11.66	59.53	0.54	0.15	4.26	8.35	0.15	0.36	6.63
STD 12	4.09	2.61	11.70	59.78	0.54	0.15	4.18	8.24	0.15	0.35	6.49
STD 13	4.05	2.61	11.79	59.74	0.54	0.15	4.19	8.23	0.15	0.35	6.49
STD 14	4.06	2.57	11.70	59.84	0.54	0.15	4.20	8.22	0.14	0.35	6.50
STD 15	4.08	2.58	11.69	59.86	0.54	0.16	4.18	8.22	0.15	0.35	6.48
STD 16	4.10	2.58	11.67	59.85	0.53	0.16	4.20	8.25	0.15	0.35	6.53
3sd	0.13	0.08	0.12	0.42	0.01	0.01	0.08	0.17	0.01	0.01	0.18
max	4.05	2.54	11.60	59.47	0.53	0.15	4.18	8.22	0.14	0.35	6.48
min	4.20	2.62	11.79	59.86	0.54	0.17	4.27	8.38	0.15	0.36	6.63
Average	**4.11**	**2.58**	**11.68**	**59.64**	**0.54**	**0.16**	**4.22**	**8.29**	**0.15**	**0.35**	**6.53**
CERTIFIED	**4.11**	**2.57**	**11.74**	**59.62**	**0.54**	**0.13**	**4.23**	**8.26**	**0.15**	**0.32**	**6.49**
% Analytical ERROR	2.18	2.19	0.70	0.47	1.86	5.51	1.33	1.35	4.86	1.72	1.81
% Accuracy	-0.09	0.51	-0.51	0.03	-0.80	19.68	-0.25	0.32	-1.34	10.34	0.67

2.5.3 Stable Isotopic Analysis

Stable isotope analyses were carried out at The University of St Andrews, Scotland by Sasha Leigh (samples 1600-1670cm and 2551-2520cm at 1 cm resolution), The University of Cardiff, Wales by Giancarlo Bianchi (samples 1670-2434cm at 4 cm resolution) and The University of Bergen, Norway by Lindsay Wilson (10 cm resolution 0-3000 cm) and William Austin (samples 2438-2500cm at 1 cm resolution).

Stable isotopic analysis carried out by L. Wilson were measured using a ThermoFinnigan MAT 251 Isotope Ratio Mass Spectrometer. Samples in the weight range 60-100μm produced a reproducibility of 0.07‰ for $\delta^{18}O$ and 0.06‰ for $\delta^{13}C$ based on replicate measurements of the NBS-19 standard (0.1±0.05mg).

Approximately 10 (Cardiff) and 20-30 (St Andrews) *Neogloboquadrina pachyderma* (sinistral) or *Globigerina bulliodes* tests were picked from the dry-sieved >150 μm fraction of the remaining samples. Sample weights ranged from ca.0.125-0.25 mg. The foraminifera were transferred to clean plastic vials and ca.1 ml methanol was added for cleaning the sample. Samples were then placed in an ultrasonic bath for ca.2 minutes and a fine syringe used to remove the excess methanol plus any small particles dislodged from the foraminifera tests. The samples were then dried at 40^0C overnight. Samples were then transferred into glass autosampler vials and these placed into the mass spectrometer with Gasbench II at the University of St Andrews. Samples were analysed on a ThermoFinnigan Deltaplus XP Isotope Ratio Mass Spectrometer.

To monitor the machine precision and accuracy, standards were interspersed between the MD95-2006 samples. The two standards analysed were NBS-19 and a Carrara marble (see Table 2.4).

Table 2.4: Stable Isotopic Standards' Isotopic Composition

Standard	**$\delta^{18}O$ VPDB (‰)**	**$\delta^{13}C$ VPDB (‰)**
Carrara Marble	-0.179‰	+2.01‰
NBS-19	-2.2‰	+1.95‰

Within the initial run, a sequence of 8 standards were analysed at the start of the run with progressively increasing weights (from 0.03-0.5 mg). This was done to monitor the instrument linearity across a full range of potential sample weights. After this three standard samples (1xNBS-19 and 2xCarrara) were placed after every 10 MD95-2006 samples to monitor the mass spectrometer throughout the stable isotope analysis and ensure any adjustments can be made for possible instrumental drift. Precision of the analyses is typically 0.13-0.19‰ for $\delta^{18}O$ and 0.12‰ for $\delta^{13}C$ based on replicate measurements of the two standards (Table 2.5)

Table 2.5: Replicate analyses of standards for stable isotopic compositions

Standard	Number of replicates (n)	Average $\delta^{18}O$	Standard Deviation	Average $\delta^{13}C$	Standard Deviation
Carrara	47	-1.79	0.13	+2.01	0.12
NBS-19	13	-2.18	0.19	+2.0	0.12

2.5.4 Radioisotopic Analysis

2.5.4.1 Sample Selection

Pb, Sr and Nd analyses of selected samples were carried out on the >63 μm bulk sediment fraction. This grain-size fraction was chosen in order to be consistent and hence comparable with previous data obtained on the same fraction in other studies (Grousset *et al.* 2001, Snoeckx *et al.* 1999, refs).

2.5.4.2 Sample preparation

1mg of each sample was weighed out to ensure it would be sufficient for parallel Sr and Nd analysis. Samples were leached in 2 ml 2.5M HCl for ~2hr to remove the carbonate fraction and then washed 3 times in ultrapure, deionised water, centrifuging between each wash. Leachates were retained for Sr extraction and analysis. All chemistry was done with purified reagents in a clean laboratory under controlled conditions at the Scottish Universities Environmental Research Centre, East Kilbride.

2.5.4.3 Chemical preparation and elemental separation

Lead

To verify low background laboratory levels of lead, a blank was prepared for each batch of samples, maintaining Pb levels of ca. 1ng. (Blank #1=107ng). The Pb separation chemistry was first detailed by Manhes *et al.* (1978). Samples were dissolved sequentially in a series of acids overnight at 150°C and dried between each stage: HF-HNO_3 mixture (conc HF, 16M HNO_3), HNO_3, HCl, HBr. It was noted that samples were not digesting as they should (possibly higher in organics than expected) so an extra acid digestion stage was included. A perchloric acid stage was added after initial dissolution in HF+HNO_3. Pb was separated on 15 μm of strongly basic, macroporous anion exchange resin in a polypropylene column. Columns were washed in 6M HCl and H_2O and samples were loaded in a 1MHBr solution. Samples were eluted three times with 1M HBr and finally once with 1.5M HCl. The eluted fraction was retained for Sr and Nd extraction and analysis. Pb samples were collected in PTFE beakers using 6M HCl and dried ready for analysis. Prior to analysis, Pb concentrations were checked to ensure accurate levels of dilution for ICP-MS loading. This was done by adding 1 ml of NIST 997 (5ppb Tl) to the dried sample and extracting an aliquot of 50 μl. This was made up to 0.5 ml by adding a further 450 μl of Tl solution. These were then run on the ICP-MS to measure Pb concentrations within each sample.

Strontium

Sr was separated from the carbonate leachates using HNO_3 (Otto *et al.* 1988) as this allows much better separation of Sr and Ca because the solubility of Ca under such conditions causes it to remain dissolved. The method used is a modification of the method of Sr extraction detailed by Henderson *et al.* (1994). Columns were cleaned twice with 0.01 M HNO_3 and the resin conditioned with 1 ml 8 M HNO_3. Samples were then loaded in solution with 8M HNO_3 and eluted with 1 ml and 5 ml 8 M HNO_3 and then twice with 5 ml 3 M HNO_3. Sr was then collected into PTFE beakers using 5 ml 0.01 M HNO_3 and evaporated to dryness and columns were cleaned with 8 M HNO_3. Sr was separated from the Pb elutes on cation exchange columns pretreated with 2x5ml 2.5 M HCl. Samples were loaded in solution with 2 ml 2.5 M HCl and washed with 2x1 ml 2.5 M HCl. Samples were eluted with 72 ml 2.5 M HCl and then Sr was collected using 14 ml 2.5 M HCl. Subsequent to Sr collection, samples were eluted in 18 ml 2.5

M HCl and then 43 ml 3 M HNO_3 before Rare Earth Elements (REEs) were collected in 47 ml 3 M HNO_3 and evaporated to dryness. Columns were then washed in 30ml 6M HCl, H_2O, 60ml 6M HCl and 30ml 2.5M HCl. The above method was used for the first 6 samples run (2474, 2479, 2481, 2482, 2483 and 2497cm) however on analysis with Thermal Ionisation Mass Spectrometer (TI-MS), two of the samples had very high levels of Rb contamination and thus Sr was unmeasurable. Thus, the remainder of the samples were separated from the Pb residues using Henderson *et al*.'s (1994) method of Sr extraction on Sr-spec columns. The eluted fraction was retained for Nd separation on REE columns. Blanks were maintained at negligible levels ($<5x10^{-11}$g for sample sizes of $5x10^{-8}$g of Sr (e.g. Musgrove and Banner 2003). Sr samples from carbonate leachates were loaded onto Re filaments with a Ta/HF mixture and other Sr samples were loaded onto Ta filaments with 0.1M H_3PO_4 loading medium. This was done for the first 6 samples but the remainder were all loaded onto Re filaments as above. Sr ratios were measured on a multiple-collector TI-MS. Instrument performance was monitored by measuring the NBS-987 Sr standard (ref) under identical run conditions to the samples. Most recent Sr studies report a range of $^{87}Sr/^{86}Sr$ values for NBS-987 from 0.7102-0.7103 (Banner 2004).

Neodymium

Nd was separated from the remaining REEs in a procedure similar to that outlined by O'Nions *et al.* (1977). Ba was eluted using a solution of 90% ethanol and 10% 5M HNO_3 and the REEs were collected with 0.05M HNO_3. An anion exchange column was used to separate Nd from Sm using methanol-ethanol-H_2O-5M HNO_3. The sample was then eluted again with ethanol-5M HNO_3. Nd isotopes ratio analyses were measured on a multiple-collector thermal ionisation mass spectrometer and the $^{143}Nd/^{144}Nd$ ratios were corrected for mass fractionation using $^{146}Nd/^{144}Nd = 0.7219$.

εNd(0) was calculated using the following formula:

$$\varepsilon Nd(0) = \left(\frac{^{143}Nd/^{144}Nd}{0.512636} - 1 \right) \times 10000$$

2.6 Radiocarbon chronology

The latest chronology for MD95-2006 is based on seventeen calibrated ^{14}C dates (Table 2.6; Austin *et al.* 2004) calculated from the analysis of monospecific foraminiferal samples of *Globagerina bulloides* and *Neogloboquadrina pachyderma* (sinistral) and further constrained using two tephra layers: 1 Thol. 2 Ash, constraining the Younger Dryas period and North Atlantic Ash Zone II, dated at 52-53 2660ka BP through correlation with the ash zone in the Greenland Ice Cores (Mayewski *et al.* 1997).

Table 2.6:
Radiocarbon ages of MD95-2006 (Wilson *et al.* 2002)

* Calibrated using Calib4.2
** Calibrated using U/Th ages and second order polynomial equation

Core Depth (cm)	Conventional Radiocarbon age (^{14}C yr BP ± 1σ)	Calendar Age (years)	Species sampled
0.5	2799 ±44	2526	*G. bulloides*
164.5	10270 ±73	11153	*G. bulloides*
323	11960 ±120	13442	*G. bulloides*
770	15260 ±140	17664	*N. pachyderma* (s)
1175.5	17390 ±190	20115	*N. pachyderma* (s)
1340	18060 ±130	20886	*N. pachyderma* (s)
1411	18680 ±130	21600	*N. pachyderma* (s)
1591.5	20390 ±150	23567	*N. pachyderma* (s)
1941.5	22720 ±130	26740	*N. pachyderma* (s)
2020.5	24710 ±280	29022	*N. pachyderma* (s)
2173.5	26210 ±270	30726	*N. pachyderma* (s)
2288	29400 ±370	34305	*G. bulloides*
2418.5	29730 ±470	34672	*G. bulloides*
2539	33880 ±610	39229	*G. bulloides*
2653.5	42500 ±1800	48361	*G. bulloides*
2728.5	47100 ±3000	53052	*G. bulloides*
2860	44430 ±2000	50345	*G. bulloides*

The implications of using such a chronology based on ^{14}C ages and their calibration have been mentioned in Section 1.8.1.3 Thus, this study takes a different approach in constructing the chronology as explained and discussed in Section 3.3.

3. Results

3.1 Lithostratigraphy

Core MD95-2006 has been sub-divided into five lithological units (Figure 3.1; Kroon *et al.* 2000, Knutz *et al.* 2002) based on visual sediment description (colour, texture, structure) and from this, interpretation of general depositional environments through the core record have been proposed (Wilson and Austin 2002). Results from all the main non-destructive analytical techniques for the whole-core record parallel these lithological divisions and provide evidence for a changing glacio-marine sedimentary regime at this core site since MIS 3.

Lithological Unit 5 (ca.2150-3000cm) is characterised by silty and muddy contourites and hemipelagic sediments. Within this unit there is considerable, high-amplitude, seemingly cyclic variation in all proxies, notably %$CaCO_3$ and absolute Ca content, L* and reflectance (400-700 nm), silt and sortable silt (10-63 μm) and %>63μm (Figures 3.1 and 3.2). Elevated levels of calcium carbonate content (20-28%) coincide with peaks in L* and sortable silt and troughs in %>63 μm. MS is low throughout this unit, indicating little variation in terrigenous input. Clay content is also relatively low (<ca.20%) but variable, correlative with sortable silt which also displays lower values in relation to the rest of the core record (fluctuating around an average of ca.20% compared to ca.30%).

The transition into Lithological Unit 4 (2150-1400 cm) is marked by a change to glacio-marine muds. All proxies are highly variable within this unit, and bioturbation is rare to absent (Knutz *et al.* 2002), consistent with the presence of coarse-grained turbidites and high sediment accumulation rates. The former is particularly evident in the significantly higher average MS values and significantly higher (and more variable) Fe-content, Si/Al and Ti/Al ratios obtained through single sample XRF analysis. Following an abrupt increase in L* at the top of unit 5, L* follows a prominent decreasing trend from ca.2040-1700 cm (Figure 3.1 (c)) displaying the typical saw-toothed shape seen in many other glacial proxy records (refs). Ca and %$CaCO_3$ do not display this pattern despite

following the same decreasing trend over this interval. Clay content appears to increase at the expense of the silt fraction towards the top of unit 4. Clearly there are some highly significant changes occurring in the marine environment at this time and these are discussed in greater detail within Sections 3.2 and 4.

Lithological Unit 3 (1400-1050 cm) is bracketed by two intervals of coarser average grain size (with lower % silt and clay, higher %>150 μm and higher MS). Within Unit 3, classified as a silty-muddy contourite, the carbonate content (L*, %$CaCO_3$, Ca) is low with low amplitude variation while sortable silt and clay are high (at around 45% and 30% respectively). a* and b* both display increasing trends through Unit 3 with highs at the Unit 3/2 transition before decreasing through Unit 2.

Lithological Unit 2 (1050-500 cm) comprises of mainly glacio-marine muds and clays. Carbonate content and MS reach their lowest values within this interval, whilst clay % reaches its highest values at ca.35%. The horizon at the top of Unit 2 is much coarser grained, fining upwards and has significant amounts of larger dropstones within its coarse base. This is likely to correspond to the gravely layer observed at around 300 cm in core MD04-2823 and thus may represent a regionally extensive mass flow deposit. Calcium carbonate content, Si/Al, Ti/Al and % silt all rise into the transition into Unit 1 (Hemipelagic muds grading up to a muddy contourite) in opposite trend to that of MS and clay content.

Unit 1 (0-500 cm) is characterised by dramatic increasing trends in calcium carbonate, L*, reflectance and silt content towards the core top, again converse to the trends in MS and %clay. A short-live reversal, or at least an abrupt interruption of the general trend, in many proxies occurs between ca.200-300cm, the transition commencing around 300 cm.

The stable isotope records of planktonic foraminifera for MD95-2006 fit the lithologically-defined framework only loosely (See Figure 3.1). A short-term decreasing trend (from 4 to 2.6‰) in $\delta^{18}O$ at the core base is replaced by a gradual increase of ca.1‰ through Units 5 to 3: these changes are thought to represent the transition from MIS 4 to 3 and subsequent cooling through MIS3 (Wilson *et al.* 2002).

A sudden increase to 4.2‰ at ca.1250 cm commences an interval of significantly heavier $\delta^{18}O$ into Unit 2. This interval is abruptly interrupted by a rapid transition to a low of 2.6‰ within the coarser-grained interval at the top of Unit 2. Unit 1 $\delta^{18}O$ values are generally lighter, at ca.2.8‰ relative to the whole-core record.

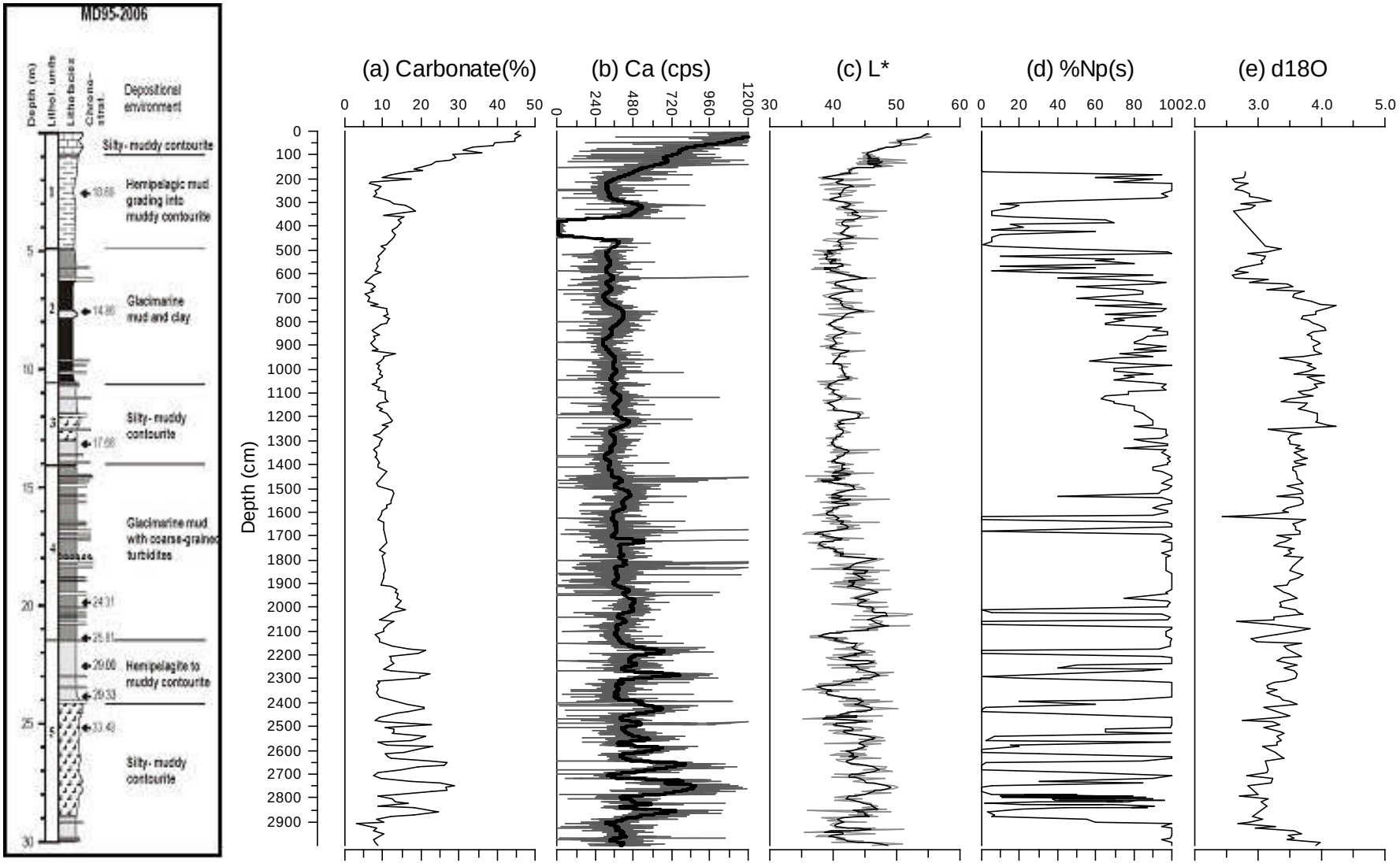

Figure 3.1: Stratigraphic Log of core MD95-2006. Graphic Log is from Kroon *et al.* (2000). (a) Weight % $CaCO_3$; (b) ITRAX Ca counts per second with smoothing line; (c) Sediment lightness with smoothing line; (d) Neogloboquadrina Pachyderma (s) as % of total planktic foraminifera >150µm; (e) Planktonic foraminiferal $\delta^{18}O$ (‰). (a), (c), (d) and (e) from Wilson (2003), Wilson et al (2002).

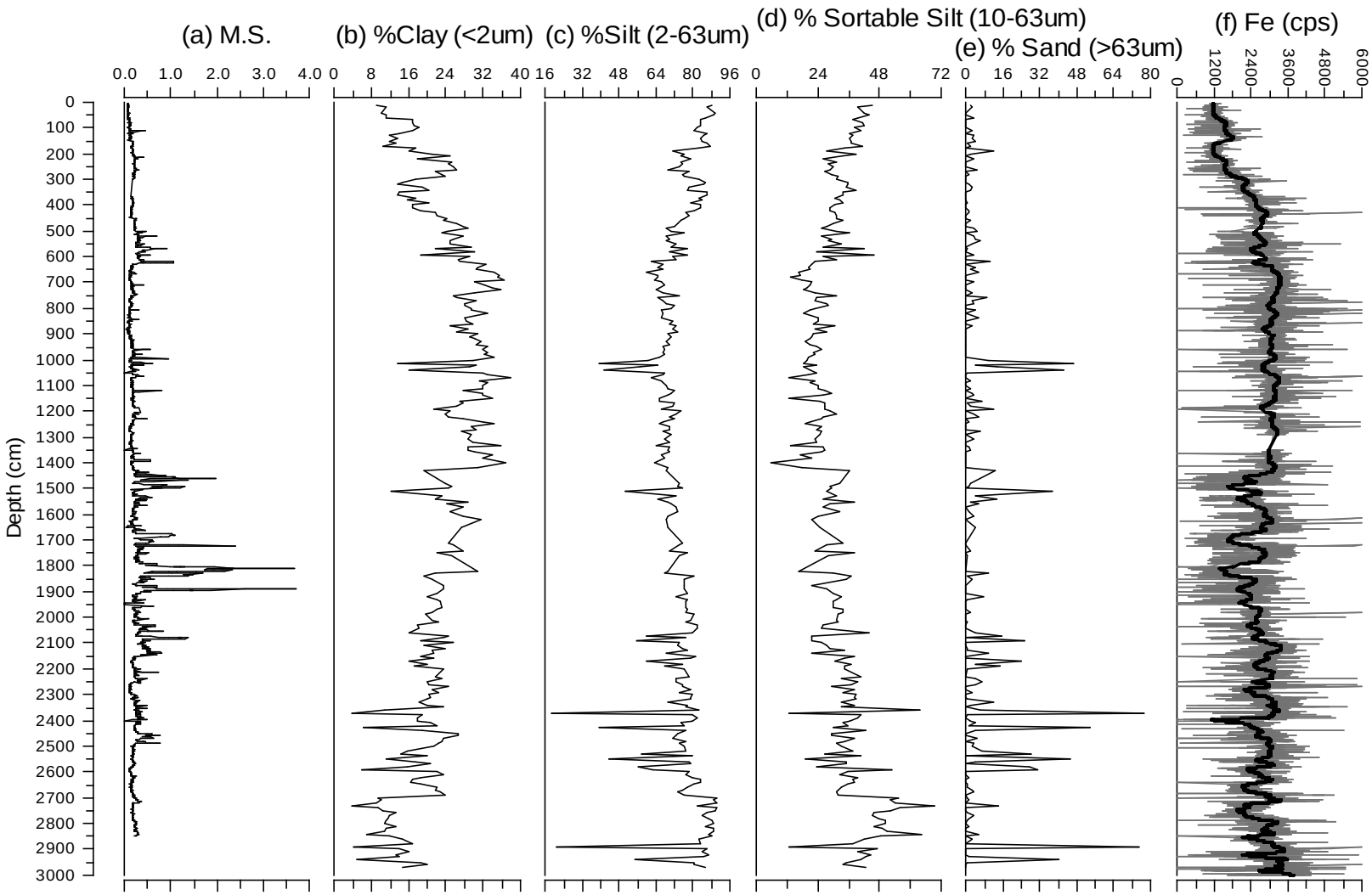

Figure 3.2: Stratigraphic Summary of MD95-2006. (a) Bulk sediment Magnetic Susceptibility (units); (b)-(e) Volume % of sediment grain size fractions; (f) ITRAX Fe counts per second with lowess smoothing line. (a)-(e) from Wilson (2003).

3.2 High-resolution Investigation

3.2.1 ITRAX Ca and Fe

The nature of the ITRAX analytical technique (see Section 2.2.2) precludes the discussion of the absolute variations in the sediment calcium content, however the overall trend and higher-resolution fluctuations appear to be robust and valid. The ITRAX XRF Ca counts (step size 2mm) display higher amplitude variations with a clear cyclicity (short-lived highs and broader lows with an amplitude of ca.500 cps) below ca.2150 cm i.e. Lithological Unit 5. These cycles are correlative with the cycles in %Np(s) and in sediment Ca content determined through single sample XRF (Figure 3.3). The agreement between results from single sample XRF and the ITRAX XRF provide strong evidence that the latter, non-destructive, more time efficient method of analysis is a legitimate equivalent technique in providing comparable data. Within this core interval (1550-2550 cm), six pronounced peaks in %$CaCO_3$ are observed centred at 2010 cm, 2184 cm, 2288 cm, 2420 cm, 2493 cm and 2539 cm. These peaks reach values of up to 22.75% and below 2150 cm (Lithological Unit 5), they coincide with well-defined peaks in Ca (cps) and lows in %Np(s). Above 2150 cm there is less variation in Ca content. Between 2150 and 1900 cm, despite a reasonably symmetrical increasing-decreasing trend in Ca content centred on 2010 cm, the superimposed variations in Ca seems highly irregular. Significant increases are seen, notably at 2066 cm and 2014 cm. Low Ca content (ca.350 cps) prevails after 1900 cm until ca.1620 cm after which Ca begins to increase again. These changes are illustrated in Figure 3.3.

The earlier peaks in Ca within the more cyclic interval (below 2150 cm), coincide with troughs in the core Fe content measured through both single sample XRF and ITRAX, however above ca.2150 cm, the Fe signal is complicated by the influence of the sedimentary regime, in particular the presence of turbiditic horizons noted in Section 3.1. Fe content follows a clear but fluctuating decreasing trend from ca.2150-1900 cm. There are three distinctive troughs in Fe content at ca.1700, 1830 and 1897 cm. These directly coincide with the intervals of high >63 μm% (see Section 3.2.2) with the intervening intervals having higher Fe content. Fe content decreases diametrically to Ca above ca.1620 cm.

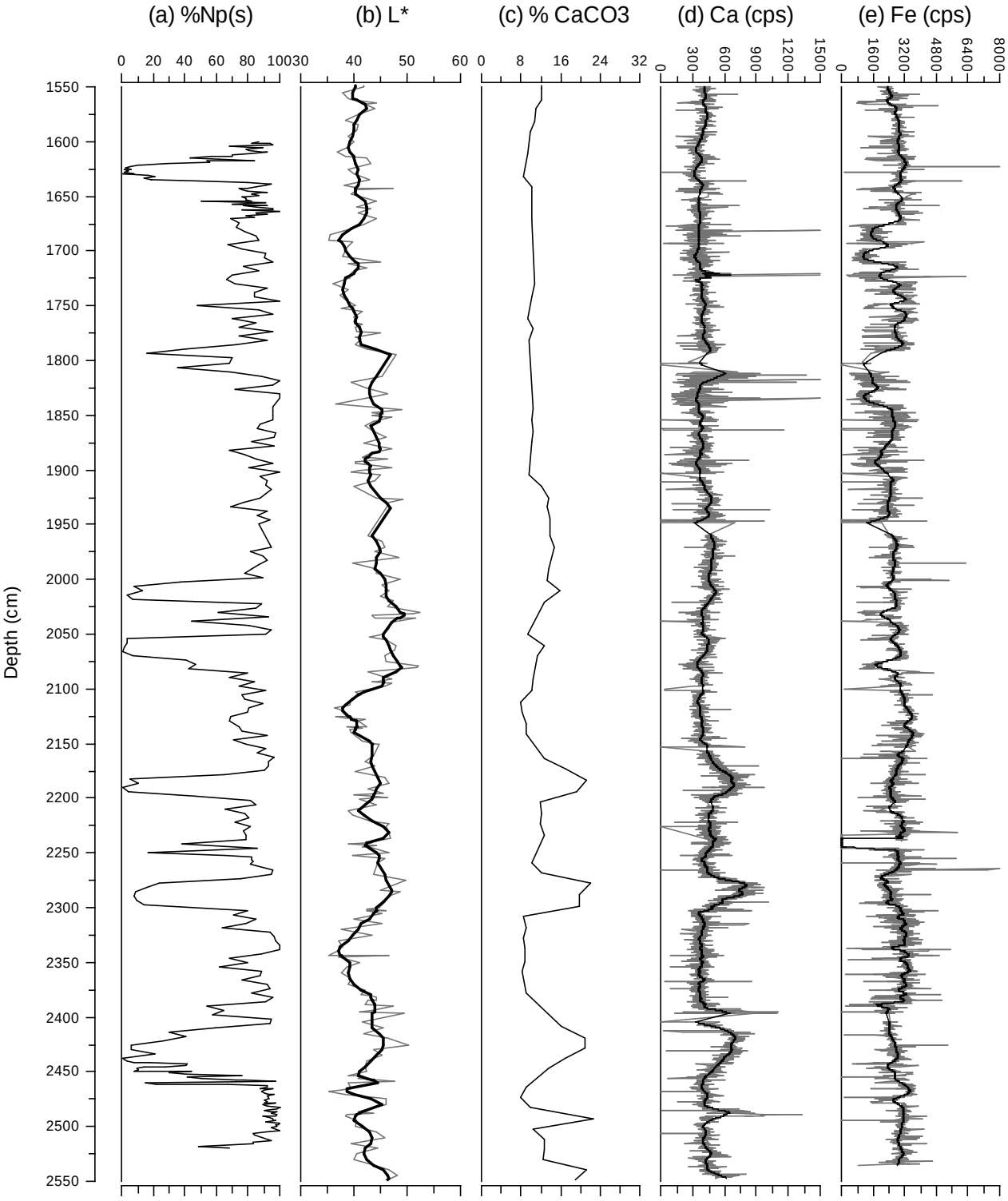

Figure 3.3: Sediment properties of interval 1550-2550cm in MD95-2006. (a) *Neogloboquadrina pachyderma* (s) as % of total planktic foraminifera >150μm; (b) Sediment lightness; (c) Weight % $CaCO_3$; (d) ITRAX Ca counts per second; (e) ITRAX Fe counts per second. (b) and (c) from Wilson (2003).

3.2.2 <63μm fraction

There are large and irregular variations in percentage clay, silt and sortable silt (SS) below 2378 cm (Figure 3.4). Two prominent lows occur at 2455 cm and 239 6cm where the silt:clay ratios are the highest in the entire core section (at 7.5 and 6.2 respectively; see Figure 3.4). Above the trough at 2396 cm there is an abrupt peak in SS (at 2388 cm) where % clay (and %2-10 μm) remains low as % silt dramatically increases. From 2378-2233 cm, all grain size fractions <63 μm remain relatively high and stable with averages of 21.44% clay, 76.07% silt and 36.24% SS and only 4-9% variation around the mean. Between 2233 cm and 2050 cm clay, silt and SS all show irregular fluctuations, % silt being the most irregular. SS and clay seem to show an opposing trend: an increase in the former and a decrease in the latter. A peak in SS of 44.2% at 2091 cm, the second highest peak in the whole core section, coinciding with a low of 16.22% clay. Below 2050 cm, when % >63 μm increases, % silt (and also sometimes % clay) decreases. Above 2050 cm, silt and clay are in opposition, clay gradually increasing and silt decreasing. This trend is interrupted at 1920 cm with diametric fluctuations in % silt and clay around 1650-1920 cm which are accentuated in the SS record. Broad lows in SS and silt correspond to highs in the %>63 μm and >150 μm fraction by volume and the more dramatic highs in >63 μm fraction by weight. That said, the trends in the former two proxies are more ambiguous due to the much lower average percentage volume of >63 μm and >150 μm (1.75% and 0.39% respectively) and lower variation around the mean. Above ca.1640 cm, percentage clay and silt fall lower (as do all size fractions <63 μm) whereas SS increases.

3.2.3 >63μm fraction

3.2.3.1 Weight % >63μm

Below ca.2000 cm the >63 μm fraction reveals regular fluctuations at relatively low values (average 6.96%) with short-lived peaks, usually consisting of just a single data point (maximum ca.20-50%) and troughs (minimum ca.1-2%). From 2000-1650 cm there are highly irregular, larger, broader peaks reaching a maximum of 95%. Many of these coincide with the interval of turbidites noted in Section 3.1 and indicate a period of prolonged delivery of large volumes of sand to the core site.

However, within this interval of elevated sand-sized content, there are distinctive differences between the peaks in >63 μm fraction. Peaks at 1894 cm, ca.1830 cm and 1680-1706 cm highlight these differences (Figure 3.4). The former appears similar in shape to the more abrupt events earlier in the core record whereas the latter two events are wider and in particular, the event around 1830 cm has a sharp base and an upper tail. Section## examines possible reasons behind these differences and the contrasting sedimentary regimes that may be in operation through this time over the core site. Above 1650 cm, the sediment sand content falls dramatically into another broad minimum centred around 1630 cm.

3.2.3.2 Volume % >63μm

Although sampled at a much lower resolution, the %volume trend is remarkably different to that of %wt (see Figure 3.4). Below ca.2375cm this proxy shows high amplitude fluctuations with highs reaching 50-80%, notably at 2396cm and 2455cm. The interval 2250-2375cm is characterised by a reduced sand content with a maximum of <10% sand by volume. The amplitude of variation increases again between 2250-2050cm with two distinct maxima of ca.25% at 2122cm and 2203cm. Above 2050cm the sampling resolution is often sparse, precluding any detailed discussion, however it seems that the highs in >63%vol. do not exceed ca.13%. In general, intervals of lower sand % volume occur in sediment with lower $CaCO_3$, content suggesting that intervals with a greater concentration of foraminifera have a finer-grained lithic fraction. Indeed, this assertion does agree with the number of foraminifera g^{-1} counted in the >150μm fraction (see Section 3.2.5.#).

A comparison of the %vol. data to %wt. data through this core interval reveals two distinctive horizons: below 2050cm, higher amplitude variation in %vol and lower in %wt and vice versa above 2050cm. These data suggest that the absolute proportion of the sand-sized fraction increases above 2050cm but because samples are dominated by silt and clay throughout, the relative proportion of sand appears higher below 2050cm because of occasional and pronounced reductions in silt and clay content.

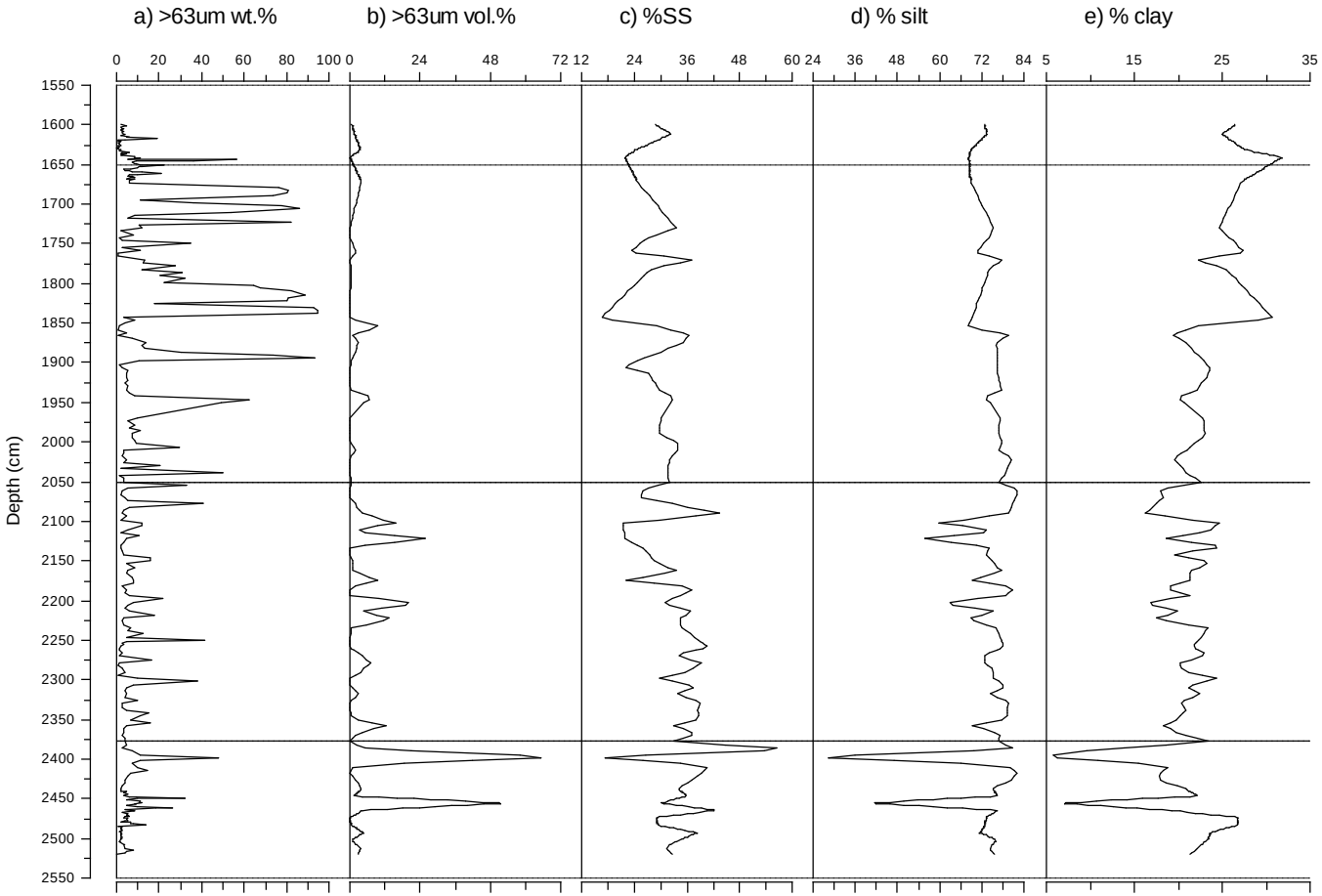

Figure 3.4: Grain size analyses from 1550-2550cm in MD95-2006.

(a) Weight % >63µm of total dry sediment; (b)-(e) Volume % of total de-carbonated sediment as determined from laser particle sizer (W. Austin/C. Taylor, Edinburgh).

Dashed lines indicate key horizons mentioned in the text: 1650cm, 2050cm, 2375cm

3.2.4 >150μm fraction

3.2.4.1 Volume % >150μm

This proxy is again distinctly different below and above ca.2050 cm. Below this depth, peak values are much higher, maximum values reaching 17.59%. There are two intervals of lower values between 2250-2350 cm and 2418-2520 cm. Above 2050 cm >150 μm fraction by volume is much lower. This size fraction seems to start to increase above ca.1650 cm with a fairly prominent peak of 8.23% at 1561 cm.

3.2.4.2 Lithic grains >150μm

Below ca.1920 cm, variations in the lithic fraction >150 μm (grains g^{-1}) fall into a pattern of generally low values (with an average of ca.1117±75 grains g^{-1}). There is however, distinct variation around these low values with lower concentrations coinciding with high %Np(s) and low %$CaCO_3$. The interval of lowest lithic concentration is 2310-2390 cm with an average of only 438 grains g^{-1}. Higher average concentrations (1065 grains g^{-1}) are seen between 2110 cm and 2298 cm, bracketed by two distinct peaks of ca.3500 grains g^{-1}. Pronounced, discrete peaks always appear to fall just prior to or during the transition into periods of lower %Np(s) and $CaCO_3$. The highest peaks fall at 2398 cm and 2078 cm and 1950 cm with values of 7652, 21755 and 11375 grains g^{-1} respectively. Within this interval dramatic cycles occur in the percentage lithics of the total count of the >150 μm fraction (see Section 3.2.5), generally intervals of higher percentages lithic fraction >150 μm coincide with more prominent peaks in% >150 μm (and >63 μm) by volume. In addition, the aforementioned peaks in >150 lithics g^{-1} all coincide with high points in the cycles in percentage lithics.

Above 1920 cm (to ca.1670 cm), average values of >150 μm lithics per gram are a factor of ten higher (10273 grains g^{-1}) with maxima of up to four times the value of the highest peak below 1940 cm. During this interval of higher >150μm lithic grains g^{-1}, the % lithics of total counts >150μm remains high at >90%. Above 1670 cm the average value falls to an equivalent level of below 1950 cm (at 1382 grains g^{-1}).

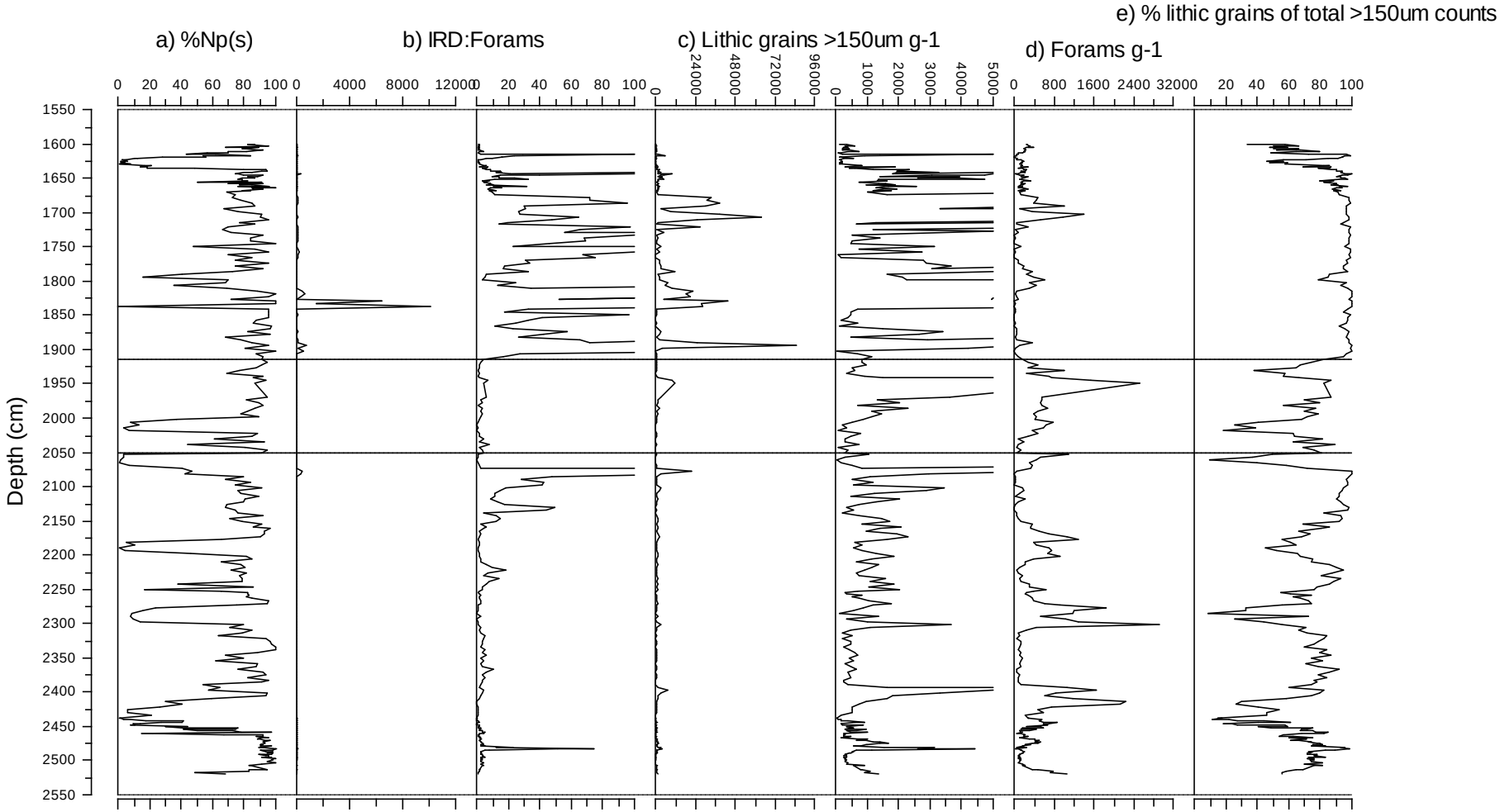

Figure 3.5: Foraminiferal and lithic grain counts from MD95-2006 core section 1550-2550cm.

(a) *Neogloboquadrina pachyderma* (s) as % of total planktic foraminifera >150μm; (b) Lithics;Foram ratio plotted on large-scale (left) and expanded x-axis scale (right); (c) Number of lithic grains >150μm g^{-1} sediment plotted on large-scale (left) and expanded x-axis scale (right); (d) Number of planktonic foraminifera >150μm g^{-1} sediment; (e) % lithic grains of the total counts (lithics plus forams) of the >150μm sediment fraction.

3.2.5 Foraminiferal Data

3.2.5.1 Planktonic foraminifera >150μm

There is a significant cyclicity recorded in the foraminiferal abundance in the >150 μm fraction (Figure 3.5d). Highs in forams coincide with high % $CaCO_3$ and absolute Ca content. Despite this, only the lower two intervals of high foram content in the >150 μm fraction coincide with significantly high L*, suggesting that the latter proxy is influenced by other factors such as clay content (Wilson and Austin 2001). Prior to ca.2050 cm, all increases in forams g^{-1} coincide with the decreasing limb of the %Np(s) curves at each period of warming (interstadial). During most of these highs, a double spike is seem in foram abundance each high coinciding respectively with the transitions in and out of the warm period as recorded in the %Np(s) curve. Two exceptions to this trend are during the first and fifth interstadials of this core interval (1550-2550 cm) where there is only a really significant increase in forams towards the end of the interstadial with a gradual or no increase at the start and/or during the first half of the warm interval. These two interstadials are associated with significantly higher IRD:Foram ratios.

Above ca.2050 cm there is no clear relationship between foraminifera content and any other proxy. However the cyclicity in foraminiferal concentration still appears to exist above ca.2050 cm but this is not recorded in the %Np(s) record. For example, two of the highs in foraminiferal concentration (1702 cm and 1950 cm) are not associated with any significant warming trend. The exception to these assertions is the brief warming period around 1794 cm during which foram content >150 μm, Ca, %$CaCO_3$ and L* all increase: the same correlation as below 2050 cm. Again above, as below 2050 cm, during the interval associated with the Heinrich Event (H2), it is only right at the end of the period of warming that there is any significant increase in number of forams g^{-1}. However, the maximum here is still minor (at <400g^{-1}) compared to earlier in the core record where forams reach a maximum of nearly ten times as high.

3.2.5.2 % lithics of bulk sediment >150μm

There are distinct cycles in the respective dominance of lithic grains or forams within the >150 μm size fraction (Figure 3.5e). All minima (ie. dominance of forams) of these

cycles directly coincide with minima in %Np(s). There is one exception to this where lows in % lithics at 1930 cm do not have a corresponding trough in %Np(s). It does however occur on a prominent falling limb of the $\delta^{18}O$ curve. A number of the cycles in % lithics reveal a distinctive saw-tooth shape with abrupt decrease and more gradual increase. For the most part, this trend seems to be governed by the changing number of foraminifera per gram with a significant exception of the lithic event around 1680-1710 cm which overwhelms the high foraminiferal count across this interval.

3.2.5.3 IRD:Foraminifera Ratio

There is a clear divide at ca.1914 cm below which the IRD:Foram ratio is on average over twenty times lower than above but with a variation around this mean of only ca.7%, significantly less than above. Below 1914 cm, cycles in IRD:Foram ratio are observed with higher values generally coinciding with intervals of high %Np(s). From ca.2420-2050 cm, each cycle reaches progressively higher ratios until a maximum of 368 is reached at 2078 cm after which ratios fall dramatically. The overall correspondence between %Np(s) and IRD:foram ratio continues above 2050 cm however the absolute correlation is much more equivocal above ca.1914 cm. Here, four significant peaks in IRD:Foram ratio occur at 1644 cm, 1818 cm, 1830-1838 cm and 1894-1902 cm and lower ratios are associated with the significant excursions to low %Np(s) between 1786-1810 cm and 1620-1636 cm.

3.2.6 Temperature and Salinity Indicators

3.2.6.1 Percentage Neogloboquadrina pachyderma (sinistral)

Neogloboquadrina pachyderma (sinistral) is a species of planktonic foraminifera which lives in cold, polar waters in temperatures of <6^0C. Thus the dominance of this foram calculated as a percentage of total planktic species in a sediment sample is widely used as a proxy for sea surface temperature (SST) over the core site. The high-resolution record of %Np(s) from the 10m core interval in MD95-2006 is defined by distinct excursions to values of less than 10% over intervals of 10-40cm (Figure 3.6a). Seven of these excursions are observed with an additional low of ca.16% around 1794cm. Most of these excursions have well-defined transitions (consisting of only one or two data points) down to and up from low values. However, the first and last intervals of low %Np(s) are associated with more complicated, fluctuating transitions. This is likely to reflect the higher sampling resolution within these two intervals (1cm cf. 4cm) increasing the potential for 'noise' to disturb the record. The intervening intervals are characterised by generally higher values with high-frequency variations between ca.60-100%. Clearly this proxy records shorter-lived warm intervals within a background of generally cold SST.

'Noise' in the record may be partly due to counting errors which are on average 18.7% of the quoted value (see Section 2.4), however, there are also particularly low concentrations of foraminifera in some samples and therefore the signal to 'noise' ratio may be particularly low in these intervals. An example of this is sample 1838 cm which only contained a single foraminifer that was not Np(s), hence an anomalously low value of zero %Np(s). Such data points, where obvious, are excluded.

The warm stages in the %Np(s) record can be correlated with Greenland Interstadials 8-2 as shown in Figure 3.6 (See Section 3.3 for further discussion of this).

3.2.6.2 Planktonic Stable Isotope Ratios

There is a general trend of lightening isotopic ratios from 2380-1718 cm, with on average a 0.013‰ increase in $\delta^{18}O$ per 10 cm. Superimposed upon this trend are fluctuations: higher amplitude and seemingly more regular below ca.2002 cm and lower

amplitude and irregular above. There are broad troughs in $\delta^{18}O$ prior to 2380 cm and above 1640 cm, from a maximum of 4.6‰ at 1718 cm, ratios begin a decreasing trend into a dramatic excursion to some of the lightest values in the whole core interval. The start and indeed end of this excursion (1639 cm and 1617 cm) exactly coincide with the equivalent in %Np(s). In fact, on close examination of the planktic $\delta^{18}O$ record, there is a decrease and subsequent increase exactly coinciding with the transitions in and out of every excursion in %Np(s). Low values at these points vary from 3.2‰ to a minimum of 1.77‰ during GIS 4. However, the initial, longest warm period at the base of this core interval (GIS 8), is again an exception to this pattern with the interval of heavier $\delta^{18}O$ preceding that of low %Np(s), occurring within a period of very stable, high (average 90%) %Np(s); also coinciding with a peak in IRD:Foram ratio.

Many of the excursions in the $\delta^{18}O$ record are also observed in the planktic $\delta^{13}C$ record: below 2002cm, every significant excursion to lower %Np(s) exactly coincides with an excursion to lighter $\delta^{13}C$, except for the initial excursion, in this case, the lightening of carbon isotope ratios post-ceding the transition into the warm period as recorded in %Np(s). A notable anomaly to this correlation occurs just above this warm interval (at ca.2400-2410 cm), lighter $\delta^{13}C$ values actually coincide with a significant peak in %Np(s). Above 2002cm, any trends are less obvious however a distinct trend to lighter $\delta^{13}C$ is seen over the same depths as the warm period between ca.1786-1810 cm. There is however an interval around 1950cm (similar to that ca.2400-2410 cm) where a dramatic lightening in $\delta^{13}C$ occurs at a time of high %Np(s).

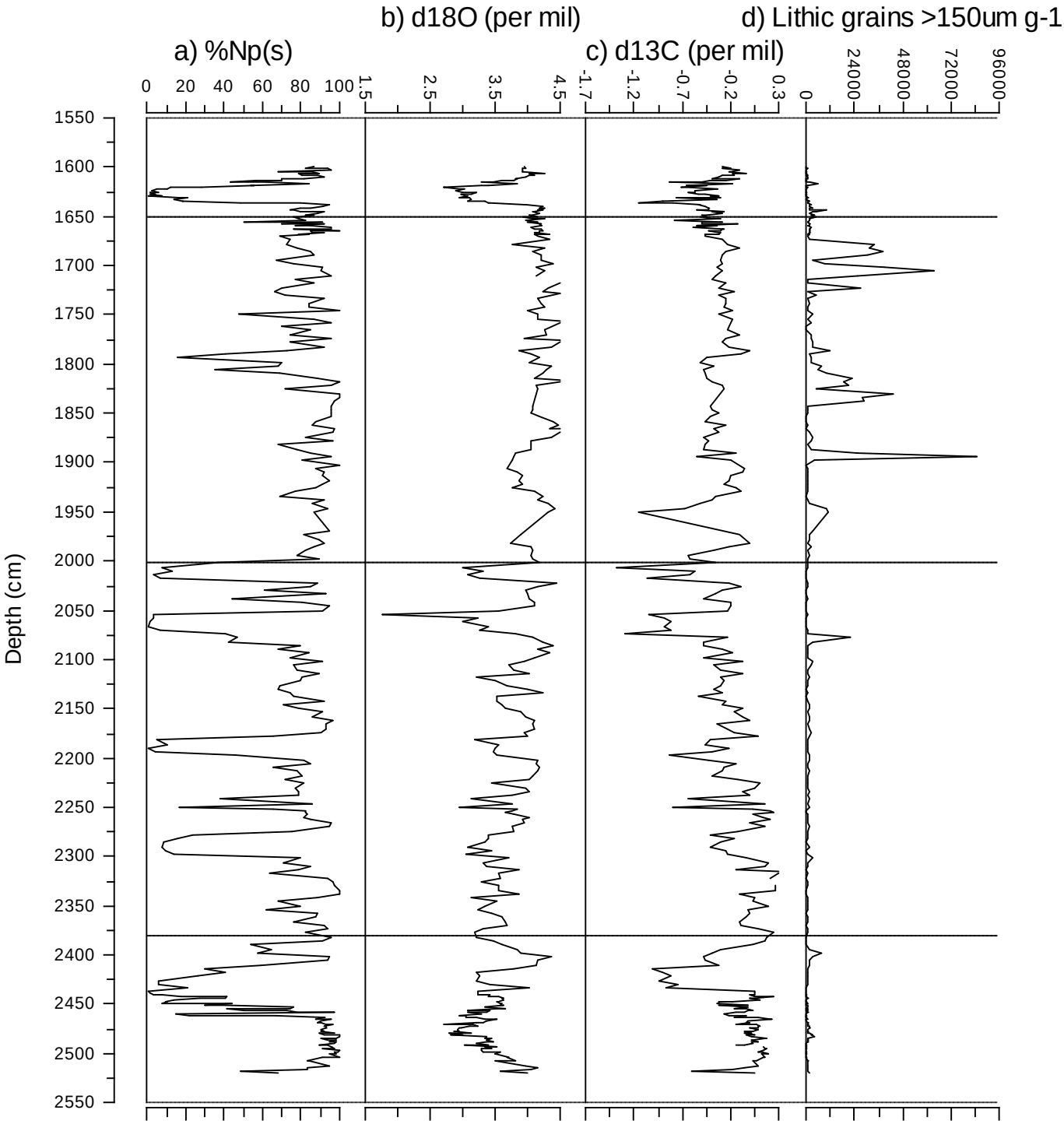

Figure 3.6: Key proxies from MD95-2006 1550-2550cm discussed in the text. (a) *Neogloboquadrina pachyderma* (s) as % of total planktic foraminifera >150μm (with Greenland Interstadials labelled); (b) Planktonic foraminiferal $\delta^{18}O$ (‰); (c) Planktonic foraminiferal $\delta^{13}C$ (‰); (d) Number of lithic grains >150μm g^{-1} sediment. Dashed lines indicate significant horizons mentioned in the text: 2380cm, 2002cm and 1650cm.

3.3 Chronostratigraphy

3.3.1 Radiocarbon Chronology

There are a significant number of AMS radiocarbon dates available over this core interval (Section 2.6), however they are not considered to be the most reliable base from which to construct an absolute age-depth model. This is due to two main reasons: firstly, there are intrinsic problems associated with radiocarbon ages in general but particularly those determined from marine sediments (see Section 1.8.1.3). Secondly, the radiocarbon calibration curve remains poorly constrained beyond ca.24 cal yr BP, precisely the interval on which this high-resolution study focuses. Figure 3.8 demonstrates the significant differences obtained when using the calibrated radiocarbon ages compared to the event stratigraphic method described in Section 3.3.2.

3.3.2 Event Stratigraphy

The chronostratigraphy for 1550-2550cm in MD95-2006 is based on an event stratigraphic approach, correlating the palaeoclimatic events recorded in sediment proxy records with the well-established Greenland ice core $\delta^{18}O$ record.

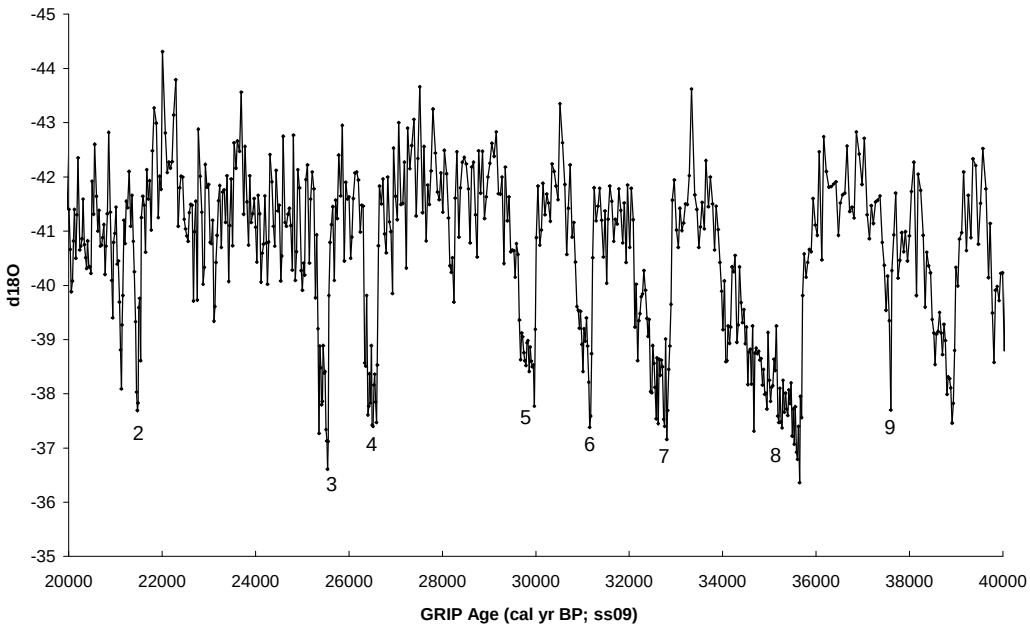

Figure 3.7: Detail of GRIP $\delta^{18}O$ record corresponding to approximately H4-H2 (ca.20-40 ka BP). Greenland Interstadials (GIS) are numbered according to Dansgaard *et al.* (1993) and Bond *et al.* (1992), (1993).

For nearly a decade, the Greenland ice core records have been the most widely used reference point for correlation of palaeoceanographic and palaeoclimatic data not only

in the North Atlantic but globally. The ice core data provide a sensitive, high-resolution and, most importantly due to the common occurrences of hiatuses within marine (and terrestrial) sediment, a continuous record of atmospheric changes over Greenland and the North Atlantic (e.g. Dansgaard *et al.* 1993, Hughen *et al.* 1996, Taylor *et al.* 1997). The ice cores can also be dated independently (Gronvold *et al.* 1995, Meese *et al.* 1997). It has therefore been widely accepted that, in particular the GRIP record be used as a 'stratigraphic template' for rapid climatic change in the North Atlantic region (Bjork *et al.* 1998, 2001, Lowe *et al.* 2001). Through this 'Event Stratigraphic' approach, millennial- and centennial-scale changes recorded in the marine record can be correlated to this well-dated template avoiding some of the pitfalls of absolute dating in the marine environment. Subsequently, this enables all such records to be compared on the same timescale (in this case, GRIP ss09; Johnsen *et al.* 1997). This method correlates 'events' or "short-lived occurrences that have left some trace in the geological record and can therefore be used as a means of correlation" (Bjork *et al.* 1998).

The events used for correlation in this study are the Greenland interstadials or the D-O 'events' (Dansgaard *et al.*, 1993). There is often some confusion in the terminology as it is actually the cooling into the stadials that are referred to as the D-O events in the marine record. Thus a clear and well-defined event stratigraphic approach can avoid such confusion when tie-points are being chosen for correlation. This method of course relies on identifying and matching the exactly equivalent events in both records. This initially involved assigning the correct number to each interstadial in the MD95-2006 record. Percentage *N. pachyderma* (s) was chosen as the most reliable proxy on which to base the correlation because the planktic $\delta^{18}O$ record at this site is complicated by the influence of salinity as well as temperature. There are clearly eight well-defined troughs in the %Np(s) curve (see Figure 3.6a). The overall core stratigraphy (see Section 3.1) places this core interval between H4 and H2 and therefore a record of GIS 8-2 would be expected (Wilson *et al.* 2002); furthermore, the position of NAAZII at 2817 cm provides a further stratigraphic constraint (Austin *et al.*. 2004). Ambiguity falls in deciding whether the brief low at 2242-2250cm is indeed an interstadial or a minor, un-numbered warming. If the latter is the case, then the low in %Np(s) recorded at 1794-1806cm might, based on the same criteria, represent an unumbered interstadial between GIS 3 and GIS 2 in the MD95-2006 record (see Firgure 3.6). In fact marine

records from further south on the European margin (e.g. de Abreu *et al.* 2003, Moreno *et al.* 2002, Wansard 1996) also reveal an un-numbered warming event (in %Np(s) if not in $\delta^{18}O$) between GIS 3 and GIS 2 (at around 23 cal ka BP) suggesting that this warming - northward migration of the polar front - is a robust feature of the surface North Atlantic but was highly subdued in polar areas due to the occurrence of this event at a time of generally very low North Atlantic temperatures during the LGM.

Tie-points between the core record and the ice core record were based on transitions into and out of the interstadials, the mid-point of each transition generally providing the anchor point. These tie-points and the equivalent GRIP ss09 ages are tabulated in Table 3.1 along with sedimentation rates calculated between each transition. Some interstadials, such as GIS 7 have clear, associated transitions, however others are more ambiguous and so assigning tie-points proved more problematic. One example of this is GIS 8. This interstadial is unusual in the MD95-2006 record, being the only warming which is not recorded simultaneously in the planktic $\delta^{18}O$ and percentage Np(s). In fact, the Np(s) record shows a highly fluctuating warming transition into this interstadial and a distinctive reversal in %Np(s) at 2270-2390cm. The correlation is further complicated by the extremely pronounced saw-tooth shape of GIS 8 in the GRIP $\delta^{18}O$ record (Figure 3.7) raising uncertainty as to where exactly on the gradual, extended cooling transition to place the tie-point. The tie-point eventually chosen into GIS 8 from the MD95-2006 record was placed on the final, most pronounced falling limb towards the lowest values and the same approach was taken in assigning a tie-point out of GIS 8 in the GRIP record, choosing a point on the limb rising up to lightest $\delta^{18}O$ values after the interstadial. In order to constrain ages and sedimentation rates into and out of this core section, two tie-points were chosen: one during the transition out of GIS 9 and the other at the minimum point of GS-2b (Greenland Stadial sub-event b, as identified by Bjork *et al.* 1998) and correlated with the corresponding events in the whole-core MD95-2006 %Np(s) record (see Figure 3.1).

Table 3.1: Tie-points used for MD95-2006 age model and associated sedimentation rates.			
GIS Transition	**MD95-2006 depth (cm)**	**Age (GRIP ss09 ka BP)**	**Sedimentation rate (cm ka^{-1})**
GIS-2b	1125.5	17.687	}-----132.80
2 (end)	1619.5	21.407	}-----110.74
2 (start)	1636	21.556	}-----96.27
3 (end)	2000	25.337	}-----85.47
3 (start)	2020	25.571	}-----41.67
4 (end)	2052	26.339	}-----76.39
4 (start)	2074	26.627	}-----35.87
5 (end)	2178	29.526	}-----41.07
5 (start)	2198	30.013	}-----50.24
6 (end)	2240	30.849	}-----32.52
6 (start)	2252	31.218	}-----25.75
7 (end)	2276	32.15	}-----32.17
7 (start)	2300	32.896	}-----101.76
8 (end)	2410	33.977	}-----23.00
8 (start)	2450	35.716	}-----37.82
9 (end)	2516	37.461	

Once tie-points were selected at specified depths in the MD95-2006 record, GRIPss09 ages were assigned and interpolation was carried out between the resulting ages in order to produce a high-resolution, linear, step-wise age-depth scale (Figure 3.8). Alternative age models (also illustrated on Figure 3.8) were produced by:

1) Assigning tie-points according to the minima (maximum warming) in the proxies at each interstadial.
2) Assigning tie-points based on the transitions into each interstadial anchored at the mid-point between the preceding stadial maxima and the interstadial minima in the proxy records (Method as employed by Rahmstorf 2004).
3) Calibration of available radiocarbon dates (see Section 2.6) and subsequent interpolation between these.
4) Assigning additional tie-points as discussed below.

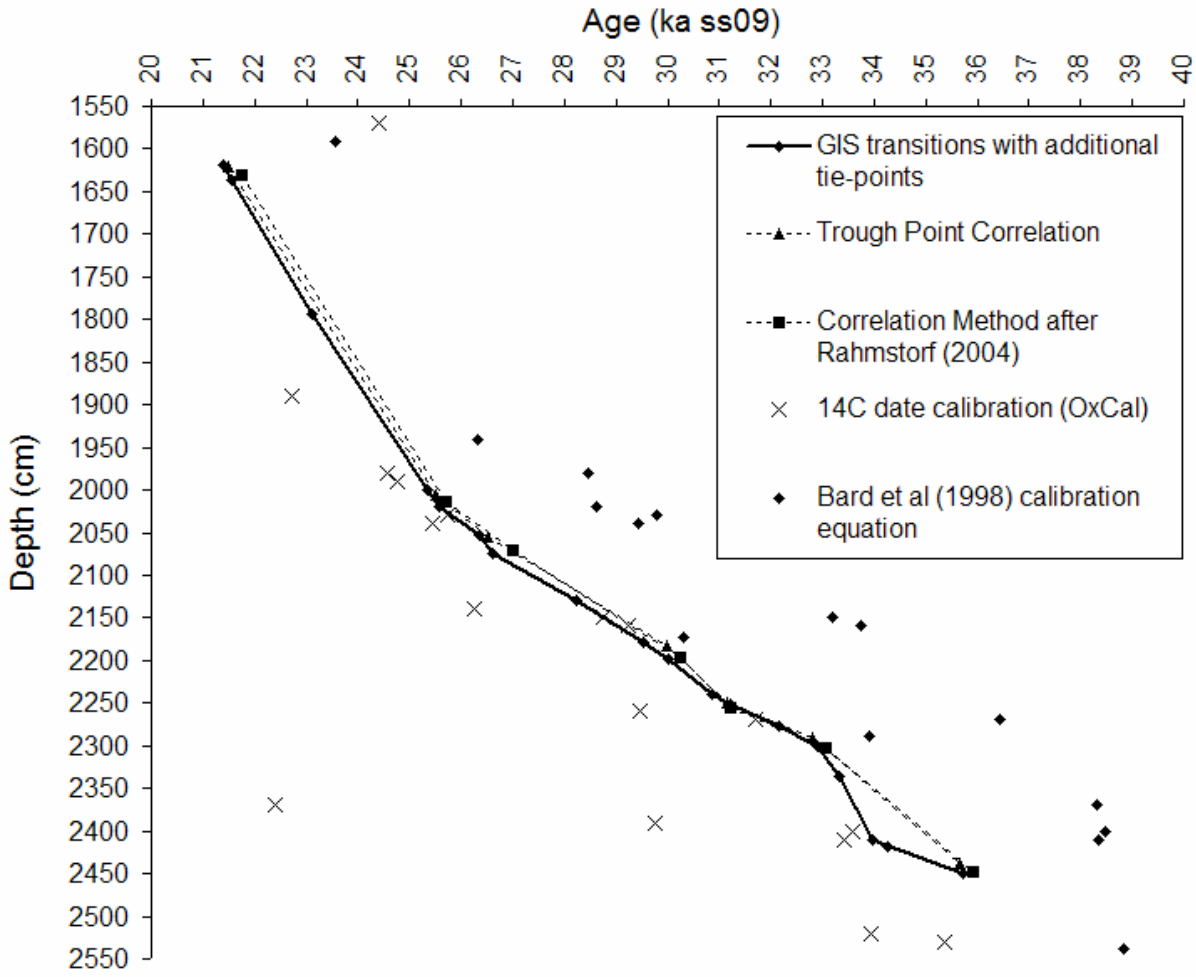

Figure 3.8: Age-depth curves produced from the different methods (see text).

This method has been used extensively in the past to construct age models for marine core records however few, if any, have pursued any subsequent improvement in the resolution of the chronostratigraphy past the millennial-scale tie-points afforded by the D-O cyclicity. The high-resolution data produced in this study presents the possibility of increasing the number of tie-points constraining the age model by identifying and correlating robust highs and lows within stadials revealed in both the ice core and marine core records and adding them to the age model for additional age control. This enables an investigation into changing sedimentation rates within stadials as well as contrasting those of stadials and interstadials. In the context of this study, this is highly beneficial. Table 3.2 lists the additional tie-points used (this time tying the maximum or minimum points of the tied event), Figure 3.9 demonstrates the correlation between the MD95-2006 %Np(s) record and GRIP $\delta^{18}O$ curve and the age-depth curve produced is shown in Figure 3.8. The initial additional tie-point used is the aforementioned un-numbered warming event, dated independently at ca.23ka BP from European Margin records and thus, actually correlating with the slight warming seen in the GRIP $\delta^{18}O$ record at this time (see Figure 3.9).

Table 3.2: Tie-points added to basic age model (Table 3.1)
Resulting adjustments to the sedimentation rates are shown in Figure 3.3.3

MD95-2006 depth (cm)	**Age (GRIP ss09 ka BP)**
1794	23.109
2130	28.248
2336	33.335

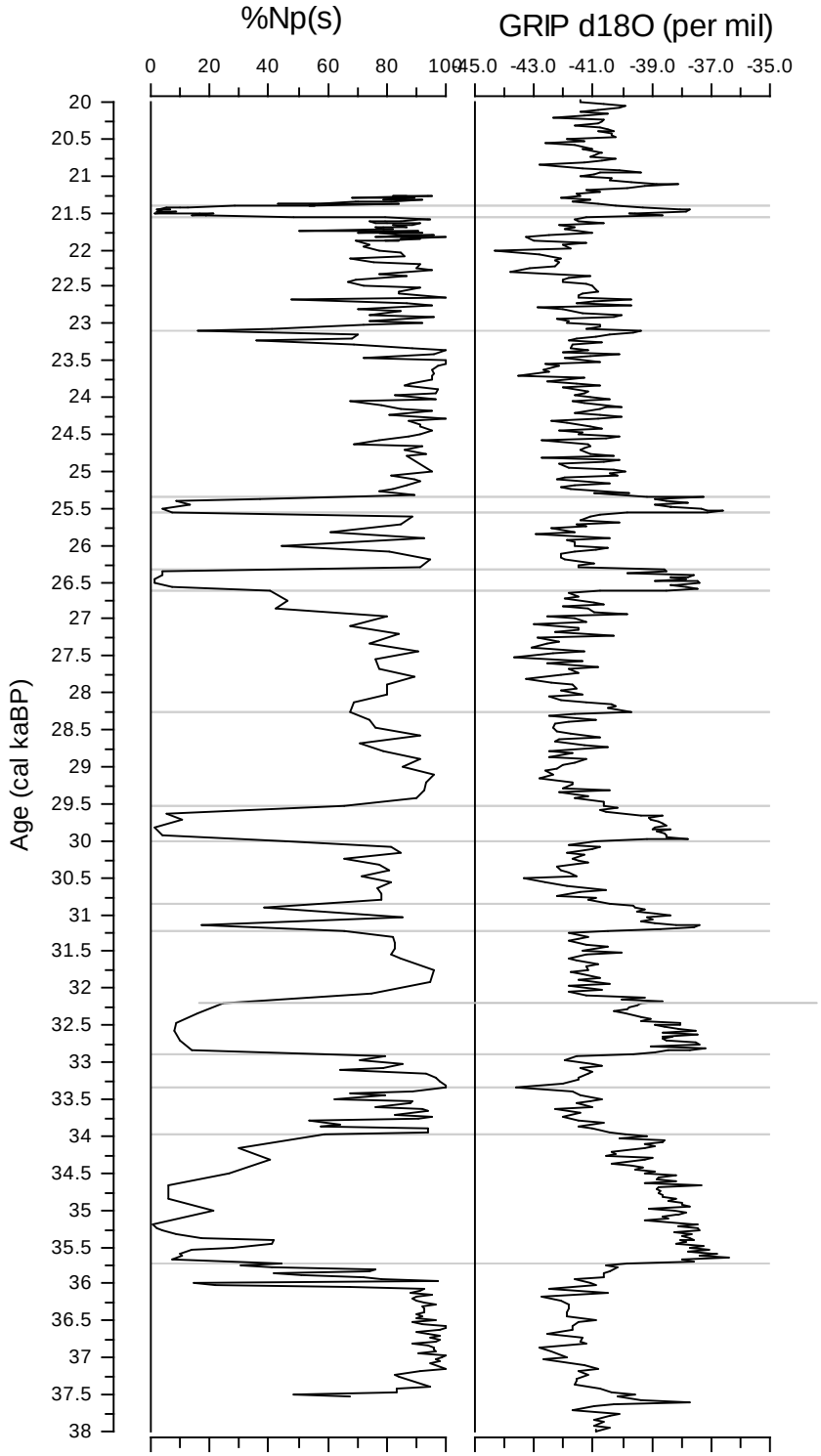

Figure 3.9: GRIP $\delta^{18}O$ and MD95-2006 %Np(s) curves shown on a common age scale. Age scale is GRIP ss09 (ref). Horizontal lines indicate the tie-points used to correlate the MD95-2006 record to the GRIP age model.

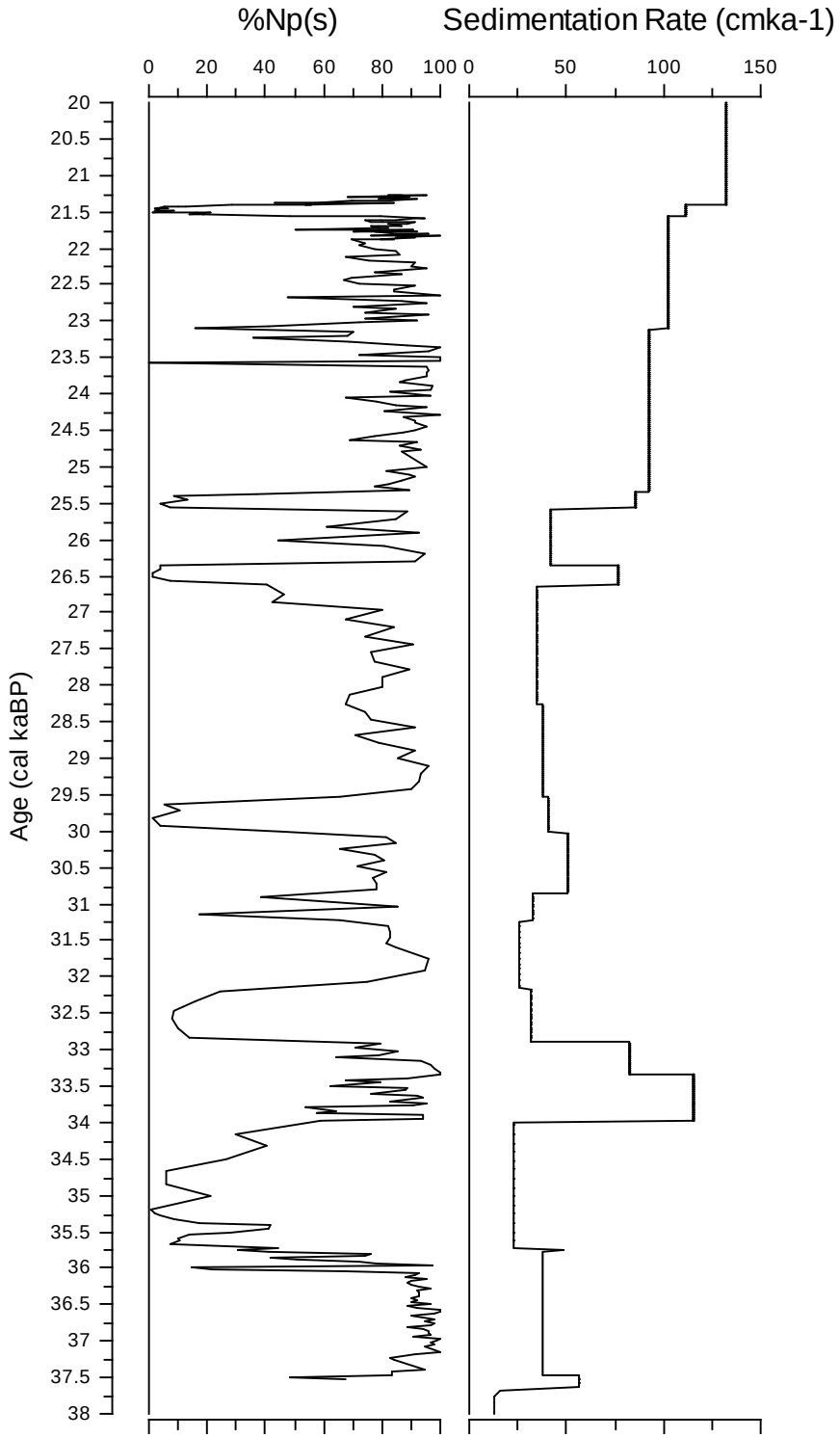

Figure 3.10: %*N. pachyderma* (s) curve and changing sedimentation rates through time shown on new timescale (this study) from 20-38 ka BP.

3.3.3 Sedimentation Rates

Figure 3.10 clearly shows the changing sedimentation rates through this core section. In general, an increasing sedimentation rate is observed throughout this core section, reaching a maximum of 133cmka^{-1} after ca.21.5ka BP. Sedimentation rates during interstadials increase progressively from GIS 8 (23cmka^{-1}) through to GIS 2 (111cmka^{-1}) however there does not seem to be any clear correlation between sedimentation rates and stadial/interstadial variations, interesting since Austin and Wilson (2002) argued that there should be changing sediment accumulation rates. Prior to GIS 3, stadials typically have sedimentation rates of between 25.6 and 48.8cmka^{-1}. The exception is the stadial following GIS 8, which records an extremely high initial sedimentation rate of 116cmka^{-1}. The sedimentation rate decreases during the latter stages of the stadial period, a pattern which is repeated in the stadial following GIS 5 (although absolute sedimentation rates are lower at 37.5-34.5cmka^{-1}). The stadials with higher sedimentation rates (those bracketing GIS 8 and between GIS 6 and GIS 5) directly coincide with the intervals of higher lithic concentration (grains g^{-1}) in the >150μm fraction, higher % lithics and higher IRD:foram ratios. It therefore seems that, at least between H4 and H2, sedimentation rates at this location are governed predominantly by the delivery of lithic/terrestrial material to the core site from ice-rafting processes rather than surface ocean productivity and $CaCO_3$ production or by material advected by bottom currents.

The average sedimentation rate throughout this core section is 64.67cmka^{-1}. This is significantly higher than the average rate for the whole core (50cmka^{-1}; Knutz *et al.*. 2001, Wilson and Austin 2002). Sedimentation rates and age models can be verified through reference to an independently dated isochron. Tephra horizons are ideal: NAAZII has been used to produce a more accurate chronology for MD95-2006 (Wilson and Austin 2002).

3.4 Heinrich Events

Heinrich Events 4 and 2 are generally observed to occur just prior to GIS 8 and 2 respectively (Bond *et al.* 1992, 1993, 1999). Table 3.3 shows age estimates of H2 and H4 from published circum-North Atlantic studies. These two intervals of intense ice-rafting occur at contrasting stages of the glacial cycle with respect to the British Ice Sheet: H4, occurring at a time of ice sheet build up and H2 at a time of maximum ice sheet extent (Wilson *et al.* 2002). Based on preliminary stratigraphic investigations (Wilson *et al.* 2002, Knutz *et al.* 2001) a high-resolution focus on these two events was aimed at two intervals (1600-1670cm: H2 and 2438-2520cm: H4) in order to compare and contrast the signature of such North Atlantic-wide events in the context of a site proximal to on of the smallest (i.e. British) North Atlantic ice sheet through the last glacial cycle.

Table 3.3: Compilation of Heinrich Event 2 and 4 Ages from North Atlantic sources

Heinrich Event	^{14}C Age (ka BP)	Duration	Cal. Age (ka BP)	Duration	Reference
2	20±1	-	-	-	Bond *et al.* (1992)
2	21	-	23	-	Bond *et al.* (1993)
2	-	-	23.6-24.8	1.2	Moros *et al.* (2002)
2	20.42-21.96	1.54	-	-	VM23-81; Bond *et al.* (1999)
2	20.55-22.38	1.83	-	-	DSDP 609; Bond *et al.* (1999)
2	-	-	22-23	1	GRIP
2	-	-	24	-	GISP2
2	-	-	24.3	-	Curry *et al.* (1999)
2	20.4-22.1	1.7	23.65-25.62	1.97	Elliot *et al.* (2001)
2	-	-	24-24.8	0.8	Wilson *et al.* (2002)
2	-	-	-	2.1	Grousset *et al.* (2001)
2	-	-	-	0.8	Francois and Bacon (1994)

4	41	-	-	-	Bond *et al.* (1992)
4	35	-	37	-	Bond *et al.* (1993)
4	-	-	37.7-39.7	2	Moros *et al.* (2002)
4	-	-	33-35	2	Cortijo *et al.* (1995)
4	-	-	35.5-36.5	2	VM23-81; Bond *et al.* (1999)
4	-	-	39.9	-	Curry *et al.* (1999)
4	-	-	38.5-39.6	1.1	GISP2 (Grootes and Stuiver 1997)
4	-	-	36.7-38	1.3	Wilson *et al.* (2001)
4	33.9-34.9	1	38.85-39.93	1.08	Elliot *et al.* (2001)

3.4.1 Heinrich Event 4

In the MD95-2006 record, the main peak in lithic fraction >150 μm (4440 grains g^{-1}) just prior to GIS 8 occurs at 2483 cm (36.59 ka BP) with generally high lithic grain concentration (average 1157.8 grains g^{-1}) prevailing from 2467-2491 cm (ca.36.2-36.8 ka BP) and a secondary, broad high centred on 2474cm (36.35 ka BP; Figure 3.11). The maximum peak in IRD occurs at a time of >90% Np(s), approximately 0.87ka prior to the transition into GIS 8. It has previously been noted that the transition into GIS 8 is unusual with respect to the rest of the MD95-2006 record in that it is not seen simultaneously in the *% N. pachyderma (s)* and $\delta^{18}O$ records (see Section 3.3), with the decrease in $\delta^{18}O$ (meltwater?) preceding that in *% N. pachyderma (s)* (warming?) by up to ca.1.5ka. In fact there is a distinct trough in $\delta^{18}O$ exactly coinciding with the interval of increased IRD, a pronounced shift to lighter $\delta^{18}O$ occurring coeval with peak IRD delivery.

The initial and highest IRD peak is also associated with high IRD:Foraminifera ratios and high lithic % of total >150 μm counts. This is not seen in the secondary IRD peak at 2474 cm (36.35 ka BP), which occurs at a time of higher planktic foraminiferal concentrations and hence low IRD:Foraminifera ratio and on a decreasing trend in % lithic grains as a percentage of total >150 μm counts. There are four smaller peaks in IRD and slightly elevated lithic concentrations (average 513.2 grains g^{-1}) between 2442 cm and 2460 cm (ca.35.4 and 36.0ka BP) coinciding with gradually increasing

foraminifera concentrations and fluctuations in *% N. pachyderma (s)* on a general decreasing (warming) trend through the transition into GIS 8. Interestingly, these peaks

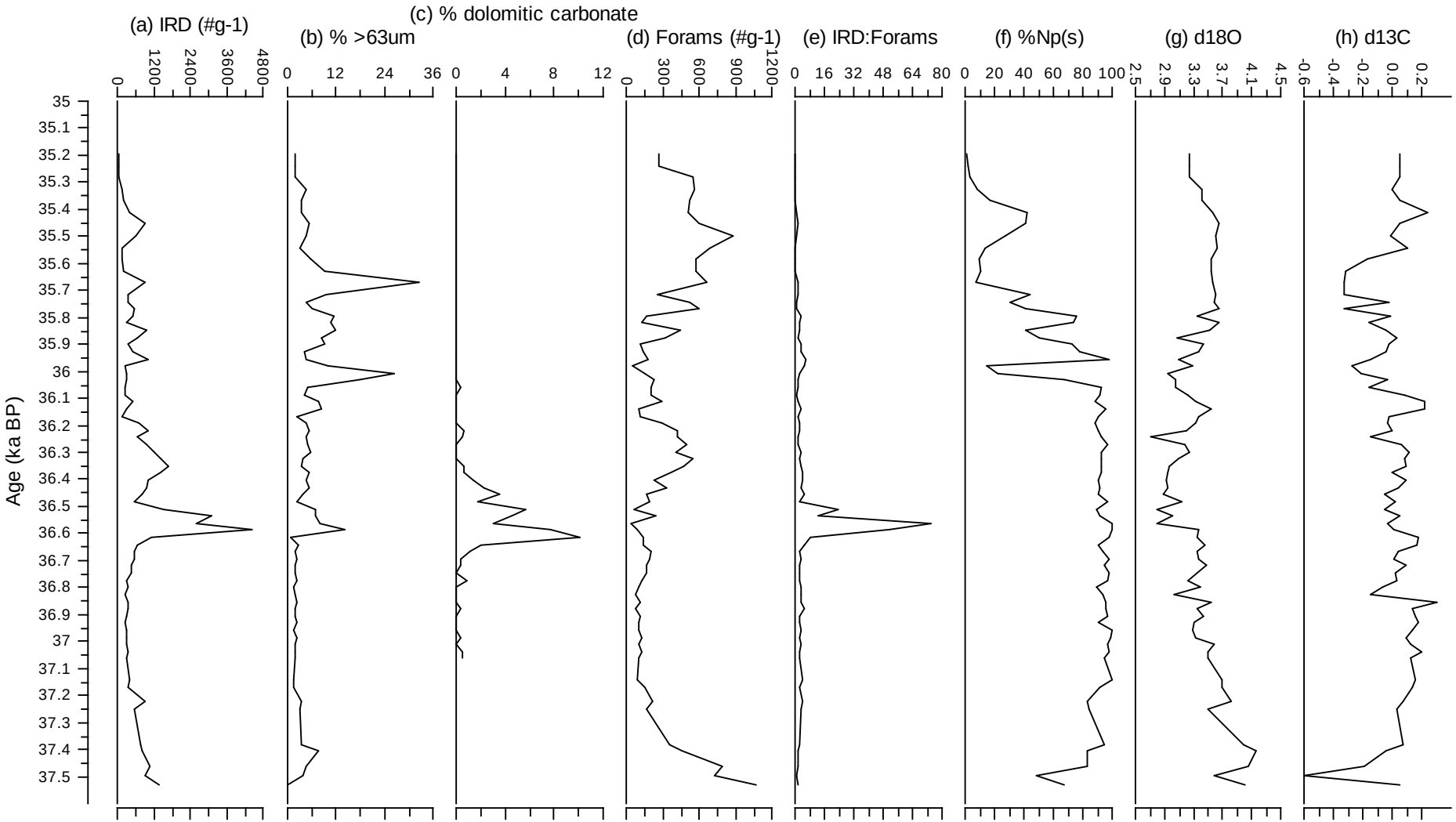

Figure 3.11: Heinrich Event 4 window in MD95-2006. (a) Concentration of lithic grains >150 μm g^{-1}; (b) Weight % >63μm fraction; (c) d.c. grains as % of total IRD; (d) Planktic foraminifera concentration (tests g^{-1} >150μm); (e) IRD:Foram ratio; (f) *Neogloboquadrina*

pachyderma (s) as % of total planktic foraminifera >150μm; (g) Planktic foraminiferal $\delta^{18}O$ (‰); (h) Planktic foraminiferal $\delta^{13}C$ (‰).

in IRD also coincide with peaks in and overall higher weight percentage of total sediment in the >63 μm fraction, reaching a maximum of 32.56% (and a significant peak of 54% volume of lithic sediment >63 μm) whereas the %>63 μm fraction is less than half this value (14.12 weight % and <1 volume %) during the main IRD event and actually falls to 3.55% during the secondary IRD peak. Samples with higher weight % >63 μm fraction are also defined by significant peaks in magnetic susceptibility whereas magnetic susceptibilty seems to show no correlation to IRD concentrations.

There is a general decrease of ca.1.5‰ in $\delta^{18}O$ from ca.36.4-36.2 ka BP. The initial, more rapid decrease in $\delta^{18}O$ from 37.4 ka BP to 37 ka BP is accompanied by increasing *% N. pachyderma (s)* until the latter reaches stable high values of >90% after 37 ka BP. There is a distinct step in the $\delta^{18}O$ trend at ca.36.57 ka BP with an abrupt drop of 0.56‰, exactly coinciding with the main IRD peak. After 36.2 ka BP, $\delta^{18}O$ starts to increase again, a more pronounced, regular increase occurring at ca.36 ka BP where *% N. pachyderma (s)* begins to decrease marking the warming into GIS8. There are distinct fluctuations in *% N. pachyderma (s)* throughout this warming interval which takes place over ca.1500 years, the most notable being an abrupt and short-lived excursion to 36% at 36 ka BP. After ca.35.25 ka BP, the *% N. pachyderma (s)* and $\delta^{18}O$ both follow a decreasing trend reflecting the main interstadial and subsequent increase indicating cooling into the following stadial after ca.34.5 ka BP. $\delta^{13}C$ increases coeval with the more rapid decrease in $\delta^{18}O$ following GIS9. Subsequent to this, $\delta^{13}C$ follows a general decreasing trend (of ca.0.9‰) from ca.36.9-36 ka BP. $\delta^{13}C$ then follows a fluctuating, irregular pattern during the transition into GIS8 until 35.2ka BP where $\delta^{13}C$ decreases abruptly at the peak of GIS 8, only increasing again during the transition out of the interstadial.

Notable events are recorded in the stable isotope record through the H4 interval. There are short-lived but distinctive excursions in both $\delta^{18}O$ and $\delta^{13}C$ at 2492cm (36.83 ka BP) and 2470cm (36.24 ka BP) but no similar signal in $\delta^{13}C$ corresponding to the shift in $\delta^{18}O$ during the main IRD event. There is, however, a broad trough in $\delta^{13}C$ between 2446 cm and 2551 cm (ca.35.54 - 35.74 ka BP). This event corresponds to low *% N. pachyderma (s)* and a peak in IRD but has no signal in the $\delta^{18}O$ record.

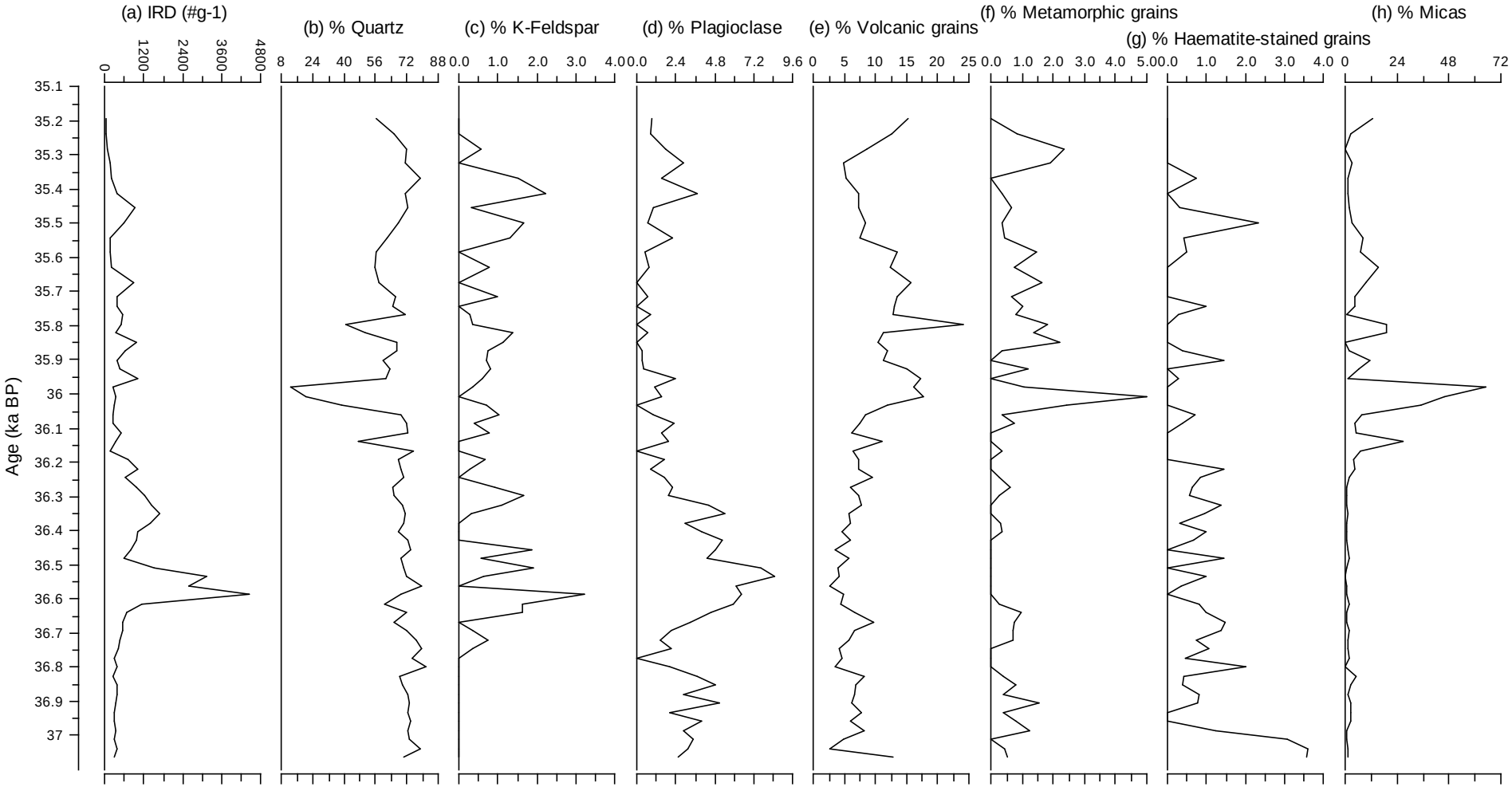

Figure 3.12: Heinrich Event 4 window in MD95-2006 (2438-2520 cm).

(a) Concentration of lithic grains >150 μm g^{-1}; (b)-(h) Lithological grain counts expressed as % of the total lithic grains >150μm.

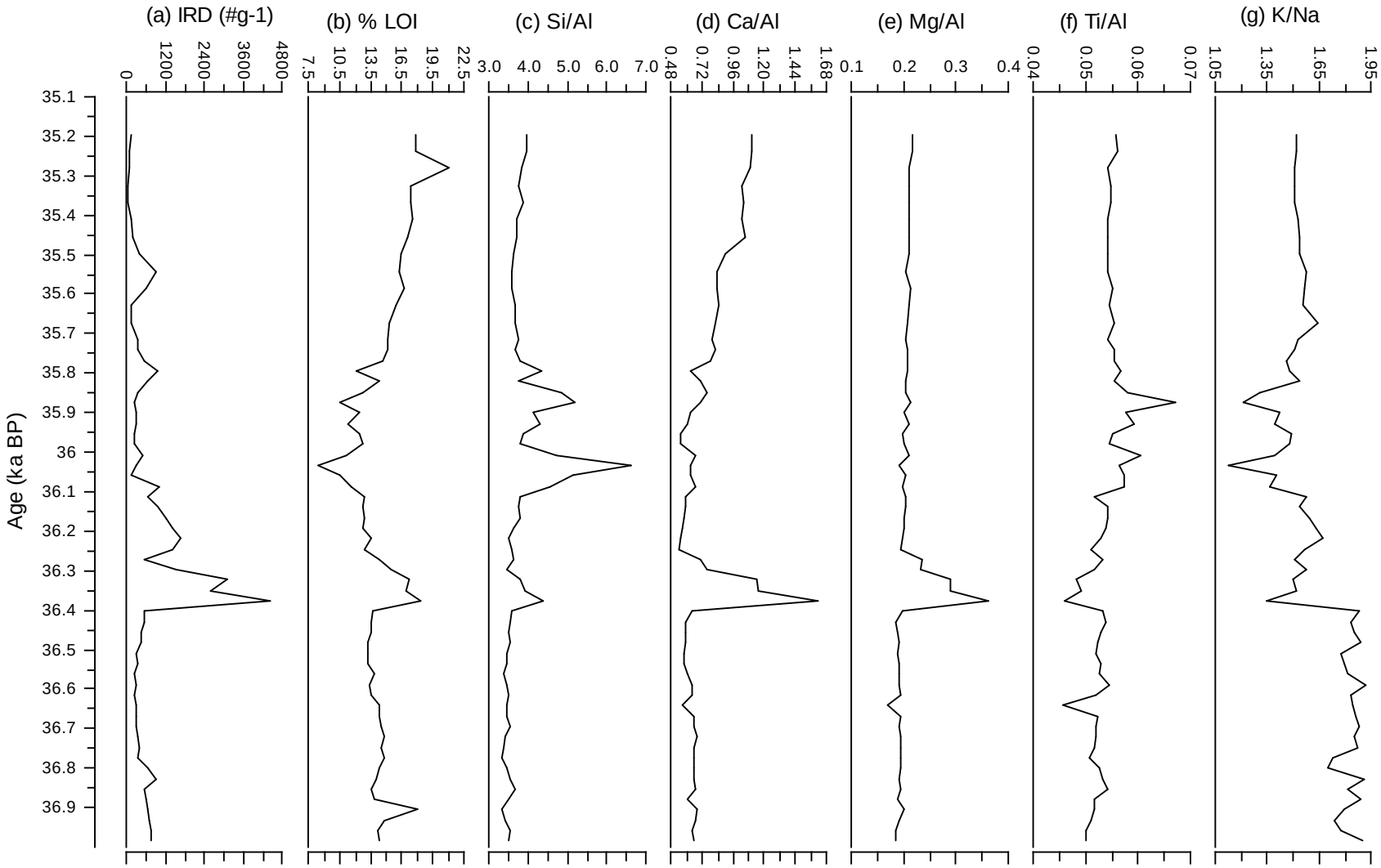

Figure 3.13: Heinrich Event 4 window in MD95-2006 (2438-2520 cm).

(a) Concentration of lithic grains >150 μm g^{-1}; (b) Bulk sediment % loss on ignition; (c)-(g) Bulk sediment normalised XRF ratios

Quantitative lithological grain counts within the >150 μm (Figure 3.12) over the interval of high IRD (ca.36.2-36.8 ka BP) reveal that the IRD is dominated by quartz, plagioclase and K-feldspar grains with much lower concentrations of volcanic and metamorphic fragments and micas (muscovite and biotite) relative to the rest of this core interval. The initial, higher IRD peak (2483 cm, 36.59 ka BP) does, however have a distinctively different composition to that of the secondary IRD peak (2474 cm, 36.35 ka BP) with much higher dolomitic carbonate and haematite-stained grain concentrations and generally a much lower diversity of lithologies distinguished.

XRF analysis was carried out on the bulk de-carbonated fraction and therefore results reveal slightly different but complimentary trends (Figure 3.13). Peak organic carbonate content occurs within the initial IRD peak (LOI=17.2%) but this also sees the highest detrital carbonate contents revealed both in normalised (Ca/Al and Mg/Al) and absolute percentage of calcium and magnesium (CaO and MgO). All of these parameters fall dramatically - by up to a third of the magnitude - in the secondary IRD peak. Si/Al is also higher within the first IRD peak although higher values are observed in the core interval where Si/Al and %SiO_2 reach their highest magnitude (6.64 and 65.65% respectively) at 36.14 ka BP. This sample (at a depth of 2466 cm) also reveals a dramatic low in Cl/Al and a peak in $\delta^{18}O$. K/Na reaches a low value of 1.35 within the initial IRD peak but increases slightly to 1.68 within the secondary peak. However K/Na is generally lower within the whole IRD interval compared to the rest of this core section. Ti/Al also falls to a low value of 0.05 within the main IRD peak but then shows a steady increase (along with K/Na) after this point until ca.35.85 ka BP (2455 cm) where both ratios reach generally steady values.

The Pb, Sr and Nd radioisotopic ratios of the sand-sized sediment fraction reveal the highly distinctive nature of the sediment composing the main IRD peak. Figure 3.14 shows the distribution of the sediment Pb-ratios relative to each other. Clearly the main IRD event is characterised by much lower $^{206}Pb/^{204}Pb$ and eNd(0) than the rest of the H4 window. eNd(0) values of the >63 μm fraction are between ca.-25 and –35 for samples within the main IRD peak but –10 to –15 for other samples. eNd(0) progressively decreases and $^{87}Sr/^{86}Sr$ increasing (Figure 3.14) closer to the sample of maximum IRD concentration (with eNd(0)=-32.01 and $^{87}Sr/^{86}Sr$ = 0.727164). The sample with the

highest $^{206}Pb/^{204}Pb$ (18.0766) is made up of higher % quartz, volcanic and micaceous grains and lower % feldspar grains (of which K-feldspar dominates over plagioclase). The opposite is true of the sample with lowest $^{206}Pb/^{204}Pb$. Lithological and radioisotopic data therefore indicates that during the main interval of IRD delivery to the core site, this sediment is sourced mainly from a more ancient, crustal terrain. Interestingly, the main IRD peak (and most negative eNd(0)) does not coincide with the lowest $^{206}Pb/^{204}Pb$ which occurs 2 cm higher. The Pb signal is generally carried in the feldspar fraction (ref) and the main IRD peak contains a higher percentage of K-feldspar and lower plagioclase grains in the >150 μm fraction compared with the sample of lowest $^{206}Pb/^{204}Pb$ indicating that the K-feldspar is sourced from much older terrains than the plagioclase fraction. All but two of the MD95-2006 samples fall along the trend of the two-stage Pb evolution curve (Figure 3.15B). Two samples deviate to much lower $^{207}Pb/^{204}Pb$ than the evolution curve would predict. One of these samples is the secondary IRD peak at 36.35 ka BP (2427 cm). This indicates that these two samples are likely to be influenced by the contribution of material from a terrain which formed (crystallised) much earlier and/or underwent one or more metamorphic events much later in its geological history than the sources of the material from the other samples.

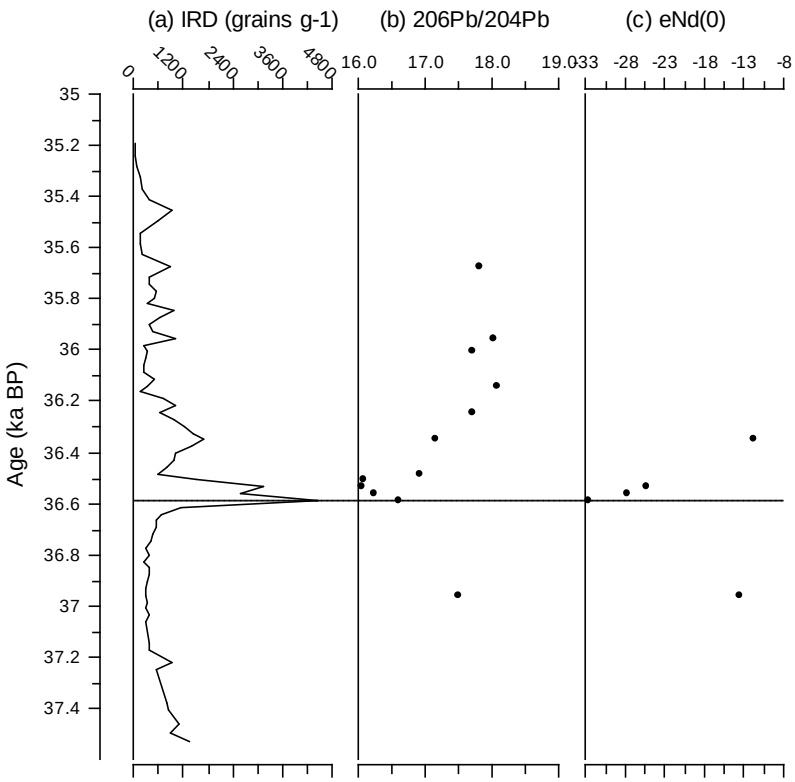

Figure 3.14: Heinrich Event 4 window in MD95-2006 (2438-2520 cm). (a) Concentration of lithic grains >150 μm g^{-1}; (b) >63μm fraction $^{206}Pb/^{204}Pb$ ratios; (c) >63μm fraction εNd(0). Errors are smaller than symbols.

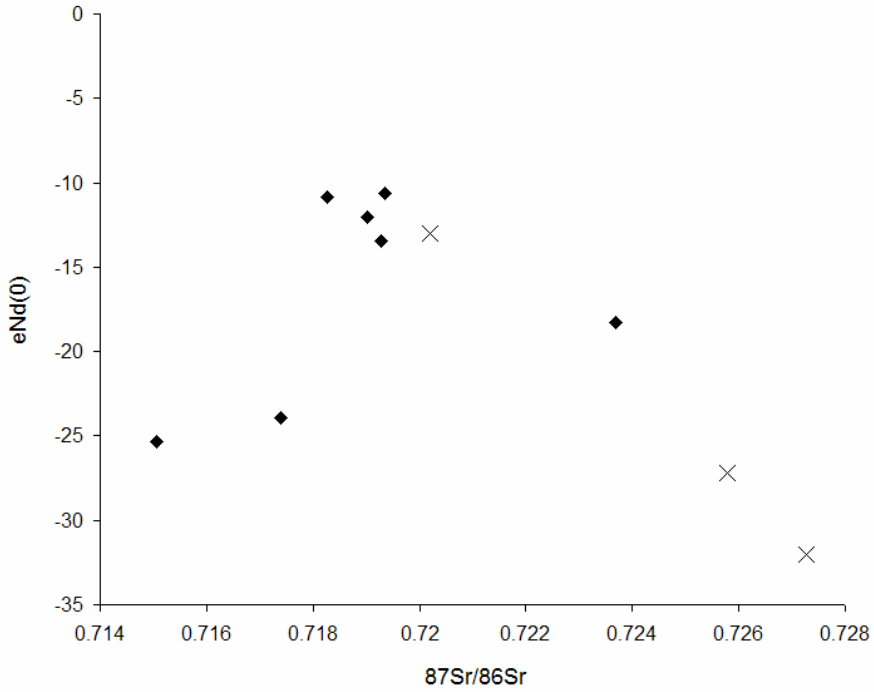

(A)

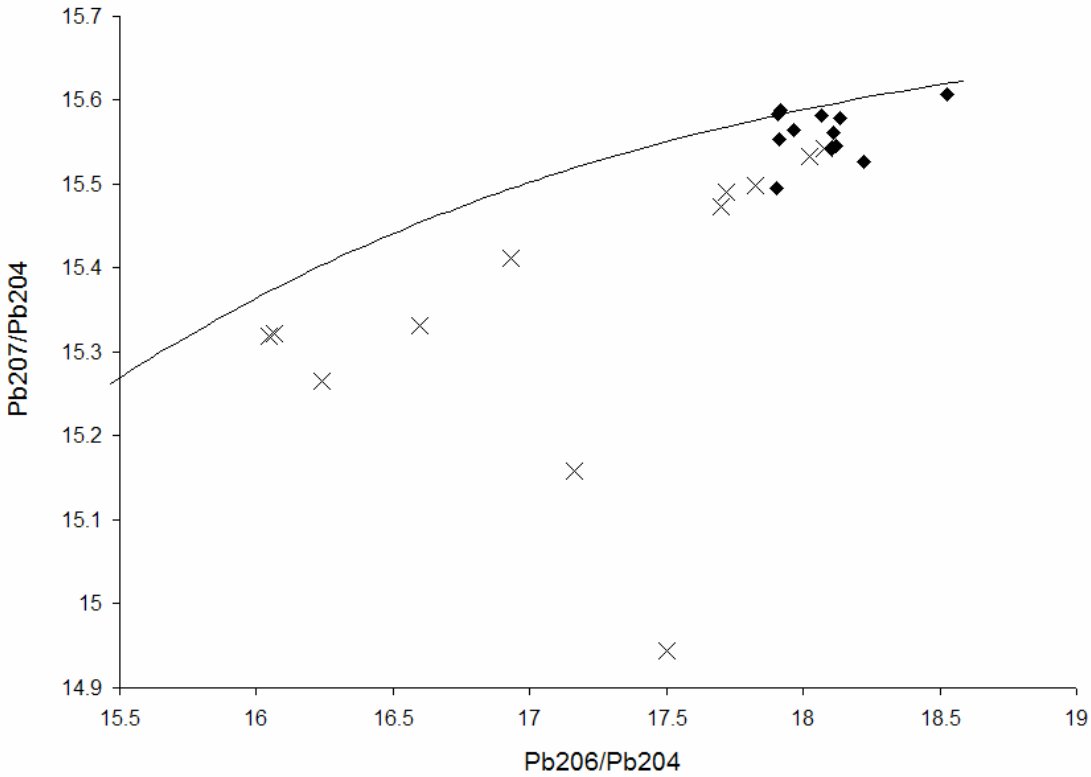

(B)

Figure 3.15: Heinrich Event 4 (2438-2520 cm, 35.19-37.53 ka BP) and Heinrich Event 2 (1600-1670 cm, 21.26-21.89 ka BP) samples' radioisotopic distribution.
H4 samples are represented as crosses and H2 samples are represented as black diamonds
(A): Sr-Nd plot; (B): Pb-plot. Errors are smaller than symbols. Curve is the Stacy-Kramer 2-Stage Pb evolution curve (Stacey and Kramer 1975).

3.4.2 Heinrich Event 2

Heinrich Event 2 occurs between 1600-1670 cm (21.26-21.89ka BP). Two distinctive events are seen in the concentration of lithic grains >150 μm and weight % >63 μm: a broader interval of high lithic concentration from 1637-1653 cm (ca.21.57-21.72 ka BP; average 3164 g^{-1}) with a maximum of 10379 g^{-1} at 1644 cm (21.63 ka BP) and a more discrete, shorter-lived event with a peak of 5969 lithic grains g^{-1} at 1617 cm (21.39 ka BP). The discrete IRD events exactly at these two peak values are also recorded in the IRD:foraminifera ratios (see Figure 3.16). The former event occurs at a time of high but fluctuating (mean=83.2% ±9.8%) *% N. pachyderma (s)*, just prior to the warming into GIS 2 as recorded in both the *% N. pachyderma (s)* and $\delta^{18}O$ records. IRD then falls to much lower concentrations within the interstadial. $\delta^{18}O$ values within GIS 2, although generally lighter throughout the interstadial, show a significant shift to lighter values at 1626 cm (ca.21.47 ka BP). This exactly coincides with a shift to much lower planktonic foraminiferal concentrations and the start of a shift toward higher overall lithic grains as a percentage of the total >150 μm fraction. The peak in this lattermost parameter (>99% lithics) exactly coincides with the second IRD event. This IRD event occurs during the cooling trend out of GIS 2, actually coinciding with a short-lived, significant peak in $\delta^{18}O$ and *% N. pachyderma (s)* on the generally more gradual overall cooling transition. Foraminiferal concentrations then increase significantly after this event.

Unlike H4, *% N. pachyderma (s)* and $\delta^{18}O$ records follow broadly similar trends throughout the H2 window, both are high and relatively stable before GIS2 (although more fluctuations are seen in *% N. pachyderma (s)* than prior to GIS 8 and H4), decreasing into and increasing out of the interstadial. A significant peak is seen in both proxies at 21.39 ka BP (1617 cm) directly coinciding with the secondary, short-lived IRD peak (and peak IRD:Foram ratio). However the finer details are slightly different between the two proxies. $\delta^{18}O$ begins to decrease at 21.6 ka BP, ca.20 yr prior to the start of the warming trend seen in *% N. pachyderma (s)* and the warming in the latter proxy begins at ca.21.45 ka BP, ca.40 yr before $\delta^{18}O$ starts to increase out of GIS 2. In addition, $\delta^{18}O$ follows a decreasing trend throughout the interstadial, reaching a minimum just prior to the abrupt increase at the end of the interstadial whereas, *% N. pachyderma (s)* fall to and remains at low values (<22%) throughout GIS 2. It seems

that the 'true' H2 event correlates with the initial and highest IRD peak (21.63 ka BP) as all other North Atlantic records place H2 prior to GIS2 at the culmination of the Bond Cycle between GIS 4 and 2. Again, the %lithics >150μm reveal a saw-toothed shape during GIS 2 (see Figure 3.5e) with a gradual decrease from a high at the H2 IRD peak over ca.160 yr and a more abrupt increase to the subsequent maximum coinciding with the secondary IRD peak at 1617 cm (21.39 ka BP).

Prior to the H2 IRD peak there are two distinct lithic peaks (recorded in all of the >63 wt% and IRD grains g^{-1} and IRD:foraminifera ratios). These are also revealed as having a significantly higher magnetic susceptibility signal. The two main IRD peaks also coincide with peaks in MS. However, unlike H4, the >63 μm weight percentage follows the same pattern as that of the concentration of lithic grains per gram >150 μm so it may be that the dominating MS signal is actually carried in the >63 μm fraction rather than the IRD fraction.

The two main IRD peaks have contrasting lithological compositions (Figure 3.17) but this appears to be due largely to the changing composition of the lithic fraction from before GIS 2, through the interstadial into the subsequent stadial period. The second IRD peak has a much more diverse composition than the former. Although all the IRD throughout the H2 window is dominated by quartz grains, there is a distinct decrease in % feldspar and increase in % volcanic grains, glass and haematite-stained grains with time, through this interval. The initial IRD event also exhibits lower concentrations of metamorphic quartz and micas compared to the secondary IRD event. Both, however, coincide with peaks in dolomitic carbonate grains. These trends are mirrored in the XRD results from the bulk de-carbonated fraction (Figure 3.18): all IRD peaks have high % quartz, both plagioclase and K-feldspar decrease through the H2 window but the two samples with peak IRD concentration both have higher percentage feldspar in the bulk sediment fraction. One interesting trend is a distinct decrease in dolomite within bulk sediment during the interval of highest IRD concentration. During GIS 2, the bulk sediment contains much lower quartz concentrations (and lower quartz:plagioclase ratio) but higher calcite, illite/mica and chlorite contents.

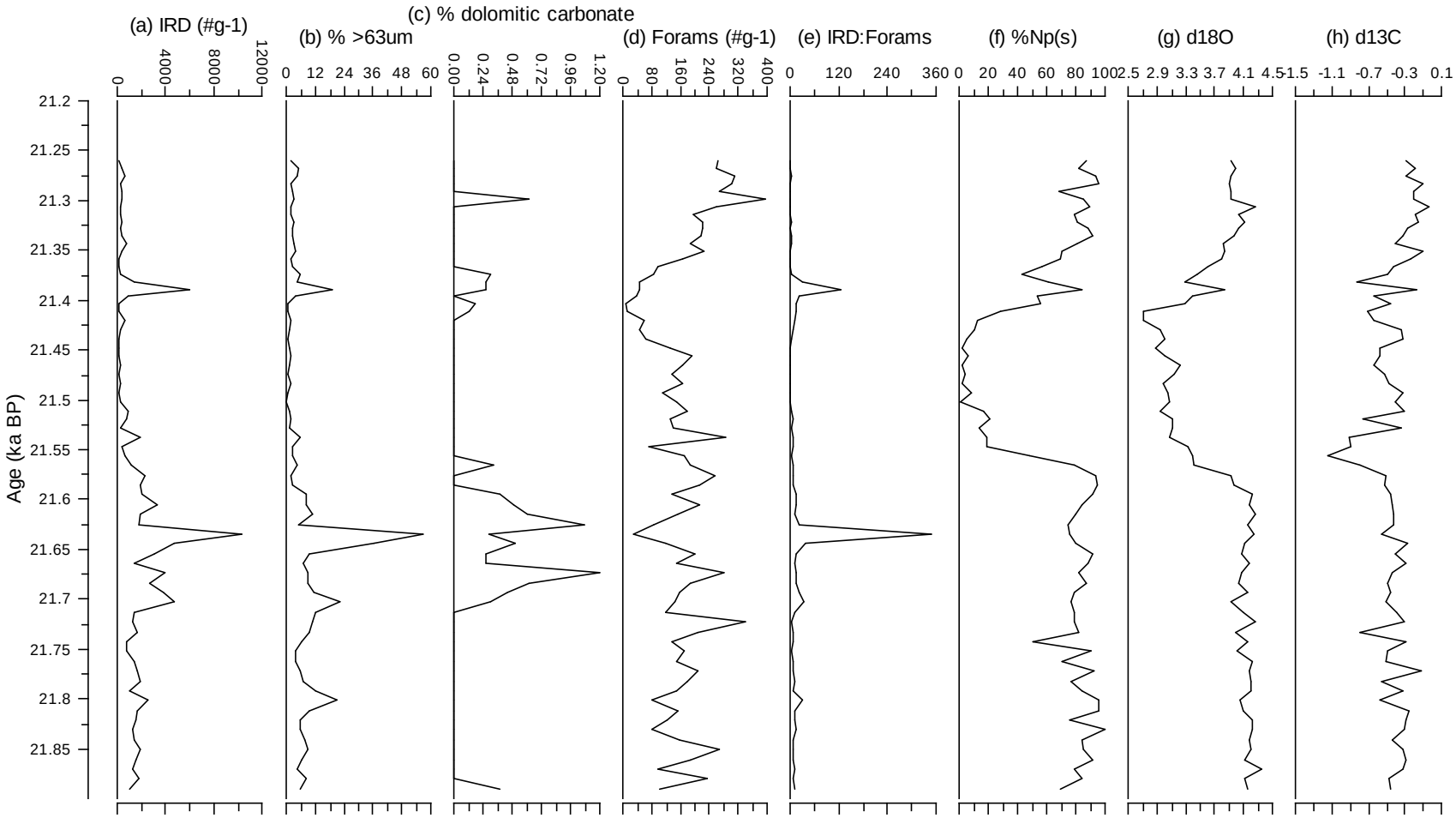

Figure 3.16: Heinrich Event 2 window in MD95-2006 (1600-1670 cm). (a) Concentration of lithic grains >150 μm g^{-1}; (b) Weight % >63μm fraction; (c) d.c. grains as % of total IRD; (d) Planktic foraminifera concentration (tests g^{-1} >150μm); (e) IRD:Foram ratio; (f) *Neogloboquadrina pachyderma* (s) as % of total planktic foraminifera >150μm; (g) Planktic foraminiferal $\delta^{18}O$ (‰); (h) Planktic foraminiferal $\delta^{13}C$ (‰).

Compositional differences between the two main IRD events are clearly illustrated in the Pb isotope ratios of the sand fractions (Figure 3.19): the initial higher magnitude IRD peak showing considerably lower $^{206}Pb/^{204}Pb$ than the later IRD peak (17.9016 and 18.2205 respectively). This suggests that the former IRD peak contains a higher proportion of sand from more ancient terrains. This is corroborated by the previously discussed lithological evidence demonstrating a shift from crustally-derived feldspars to higher volcanic content of the IRD. One caveat to consider is that the Pb-ratios are not measured on single grains so the relative radioisotopic ratios reflect changing mixing ratios of different end members rather than absolute distinction between the contribution of different mineral fractions to the marine sand.

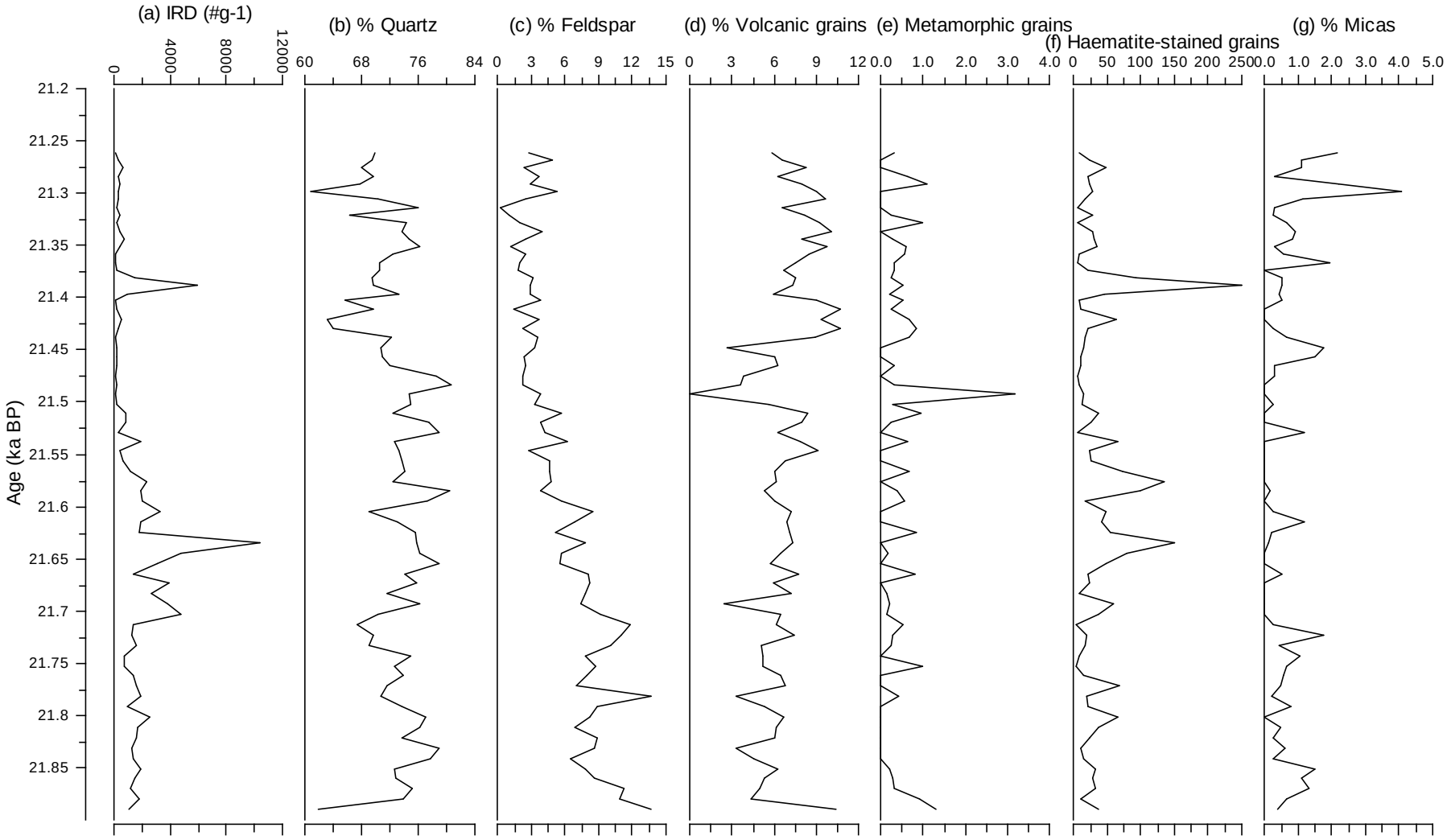

Figure 3.17: Heinrich Event 2 window in MD95-2006 (1600-1670 cm).

(a) Conentration of lithic grains >150 μm g^{-1}; (b)-(h) Lithological grain counts expressed as % of the total lithic grains >150μm.

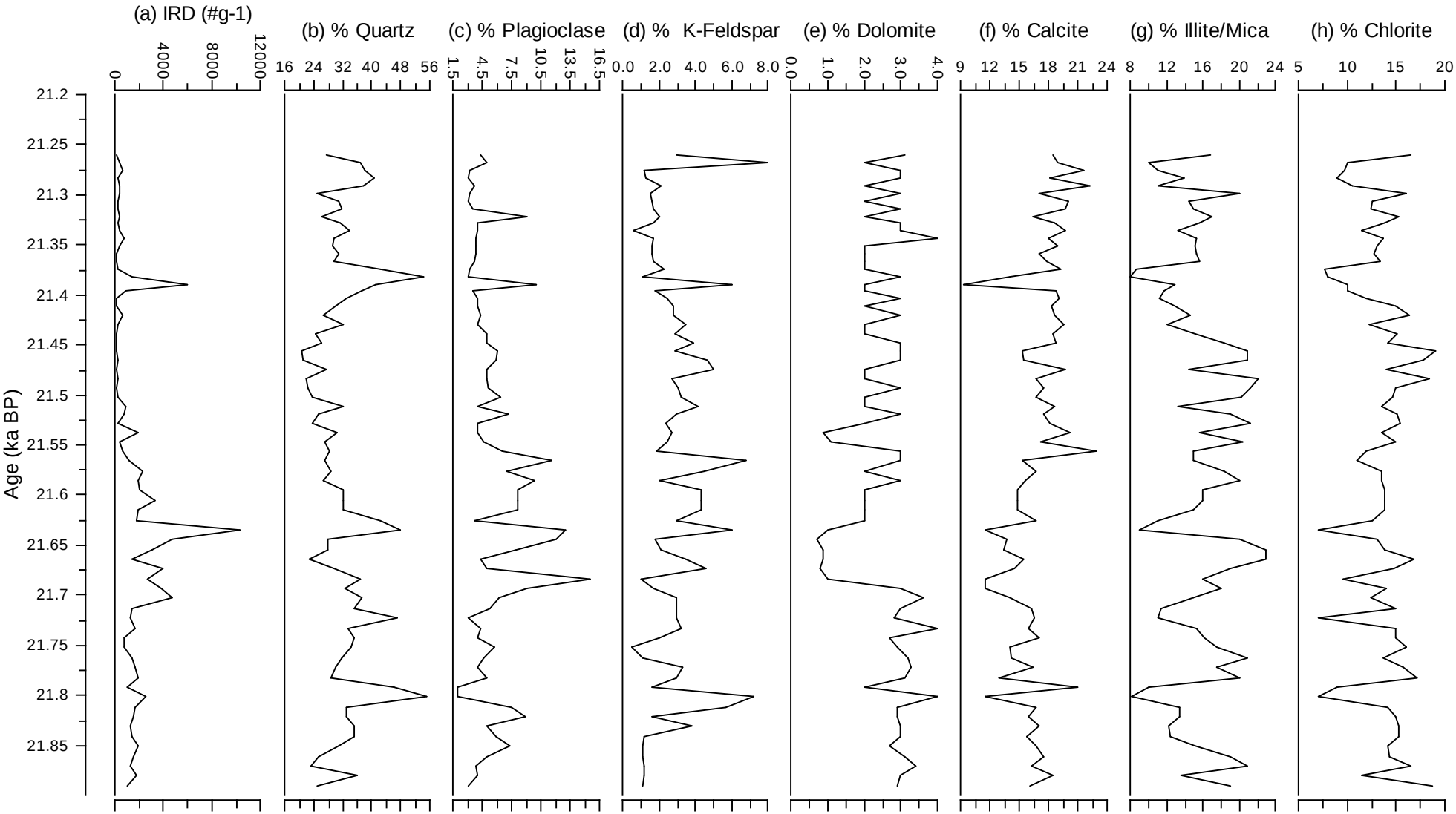

Figure 3.18: Heinrich Event 2 window in MD95-2006 (1600-1670 cm).

(a) Concentration of lithic grains >150 μm g^{-1}; (b)-(h) Bulk sediment XRD mineral percentages

The changing provenance of the sand fraction is illustrated in the changing radioisotopic ratios although there is much less of an obvious pattern through the H2 window compared to that of H4 and the dolomitic carbonate contribution during H2 is nearly an order of magnitude less (1.2% cf. 10%). Twelve samples from through the H2 window fall within different characteristic groups illustrated in Figure 3.15. The main cluster has εNd(0) between ca.-10 to –15 and $^{86}Sr/^{87}Sr$ between 0.718275 and 0.719357; Pb^{206}/Pb^{204} between 17.9097 and 18.1367 and Pb^{207}/Pb^{204} between 15.5420 and 15.5872. The oldest sample from H4 (36.9587 ka BP, 2497 cm) actually plots adjacent to this cluster indicating a similar isotopic

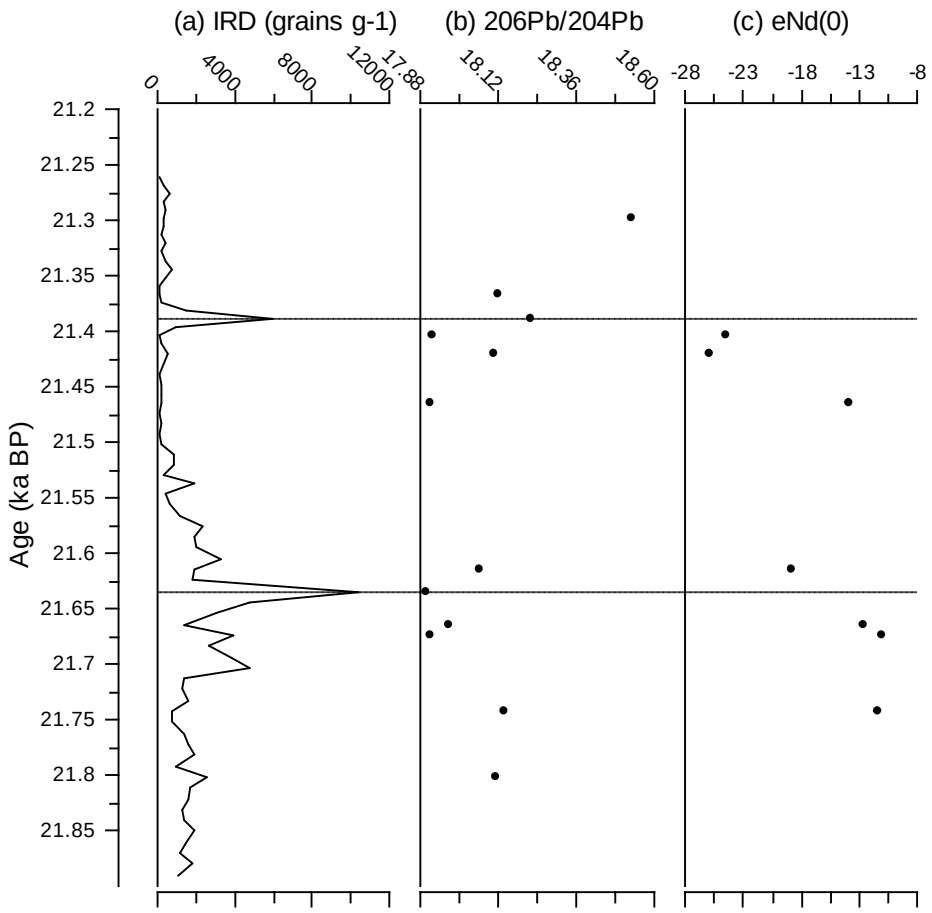

Figure 3.19: Heinrich Event 2 window in MD95-2006 (1600-1670 cm). (a) Concentration of lithic grains >150 μm g^{-1}; (b) >63μm fraction $^{206}Pb/^{204}Pb$ ratios; (c) >63μm fraction εNd(0). Errors are smaller than symbols.

composition likely to be the background signal at this location. There are two H2 samples distinctive from the main cluster in Pb-ratios: that of the main IRD peak having much lower Pb-ratios and the youngest sample in the twelve having much higher ratios. The secondary IRD peak falls just outwith the main cluster in a position in Figure 3.15B, falling further from the Pb evolution curve which suggests less of an influence of radiogenic lead within this sample.

Despite the samples at 1648 cm (21.67 ka BP) and 1644cm (21.63 ka BP) appearing similar with respect to $^{206}Pb/^{204}Pb$, the former has significantly higher $^{207}Pb/^{204}Pb$, demonstrating clear changes in sediment composition within the initial interval of higher IRD concentration. This is confirmed by the Sr-Nd data, these two samples showing distinctively less negative εNd(0). However, these samples fall within the main cluster on the Sr-Nd plot (Figure 3.15A), also plotting close to the 'background' sample from the H4 interval (2497 cm, prior to the increase in IRD).

Within the two intervals of significant IRD delivery within the H2 window, εNd(0) falls to more negative values and these samples plot outwith the main cluster on the Sr-Nd plot, the samples from the main IRD interval tending towards higher $^{87}Sr/^{86}Sr$ and the other two tending towards lower $^{87}Sr/^{86}Sr$. The sample from within the main IRD peak plots towards the main H4 samples, however the samples from higher in the H2 window, at the termination of GIS 2 and adjacent to the second IRD peak have significantly different Sr-Nd ratios (see Figure 3.15A). These two samples have similar εNd(0) to the two H4 samples but lower $^{86}Sr/^{87}Sr$, these 4 samples therefore plotting along a mixing line indicating a mixing of Archean age sourced with a range of Rb/Sr.

4. Discussion

4.1 MD95-2006 Stratigraphy (20-38ka BP)

Section 1.9 outlines some of the results from the extensive work already carried out on MD95-2006 and emphasises the need for improved age control in order to study high-frequency palaeoclimatic fluctuations and short-lived events such as Heinrich Events. This study provides improved constraints on the MD95-2006 age model, placing the MIS3/2 transition (ca.2000-2070cm: the base of Lithological Unit 4) at 25.34-26.57ka BP, more than 3.5ka later than previous studies (e.g. Wilson *et al.* 2002). The generally quoted age for the end of MIS 3 is 29 ka BP (25 ^{14}C ka BP): the transition from H3 to GIS 4 (Voelker et al 1998, van Kreveld et al 2000). These other studies, however, are based on ties to the GISP2 age model which dates MIS 2 and 3 interstadials significantly older than the GRIP ss09 age model used in this study. However, even if this study had employed the GISP2 age model, the MIS3/2 transition would still be dated at >1000 years younger than that of Wilson et al (2002).

The latitude of the Barra Fan is ideal for constructing *N. pachyderma (s)* records during glacial periods as the polar front is likely to have shifted regularly north- and southwards across these latitudes following the rapid climatic changes at this time, the latitude of MD95-2006 even recording minor latitudinal shifts in the polar front during MIS3 and MIS2. The core stratigraphy is well-delimited by the % *N. pachyderma (s)* record. This reveals short-lived interstadials lasting between 0.12ka and 1.74ka (Table 4.1).

Discounting the longest interstadial the interstadials' duration only varies by 56% around a mean of 0.39ka. The intervening stadials are of much longer and more variable duration lasting between 0.75ka and 3.77ka (with >80% variation around the mean). Most stadials reveal unstable SSTs, with highly variable % *N. pachyderma (s)* but some stadials, such as that prior to GIS8 have much more stable, low temperatures (i.e. high % *N. pachyderma (s)*). The counting errors (average 19%) allow for this variation to be noise in the record but the overall stadial-interstadial trend and shape of the % *N. pachyderma (s)* curve is robust (see Figure 3.9 and 4.1). This is confirmed

through the agreement of transitions within the % *N. pachyderma (s)* and the $\delta^{18}O$ records. With a unique exception of GIS8, every transition into and out of an interstadial is marked by coeval decreases in % *N. pachyderma (s)* and $\delta^{18}O$, both recording the climatic warming signal is the ocean surface waters. In general, however, the $\delta^{18}O$ record exhibits an overall cooling trend from ca.33.73ka to 22.36ka BP reflecting the North Atlantic cooling into the LGM and a likely ice-volume component to global $\delta^{18}O$. The relatively longer length of the stadials recorded in % *N. pachyderma (s)* during MIS2 (2.5ka compared to 0.8ka in MIS3) reflects this climatic cooling as % *N. pachyderma (s)* does not reflect temperature changes below ca.5°C (i.e. stadial temperature are therefore <5°C). Below this, the species saturates the planktic population (Pflaumann *et al.* 1996). Also by shifting growth seasons and depth habitats, the species can maintain optimum growth temperatures (Sarnthein *et al.* 1995). Thus any slight temperature fluctuations, although possibly revealed in other proxies, is unlikely to be present in the %*N. pachyderma (s)* record during times of regionally cold temperatures.

Table 4.1: Stadial and Interstadial durations as calculated from the stadial-interstadial transitions noted in Table 3.1.

Stadial between GIS	Stadial Duration (ka)	GIS	Interstadial Duration (ka)
2-3	3.781	2	0.149
3-4	0.768	3	0.234
4-5	2.899	4	0.288
5-6	0.836	5	0.487
6-7	0.932	6	0.369
7-8	0.642	7	0.746
		8	1.739
Average duration	1.64±1.35		0.57±0.55
Average Duration (MIS2)	2.27±2.13		0.22±0.07
Average Duration (MIS3)	1.33±1.05		0.84±0.62

As the chronology of this section of the core is produced by ties to the stadial-interstadial pattern in the GRIP ice core record (Section 3.3), any comparison of the phasing of these cycles in the core record is not possible. However cycles in proxies other than % *N.pachyderma (s)* can be examined. The two proxies which reveal the strongest periodicities during MIS 2 and 3 are the minima in the cycles of %lithics >150 μm and maxima in planktonic foraminifera concentrations; both pervasive throughout the period from 40-20 ka BP, even during the prolonged stadial between GIS 3 and 2 (Figure 4.1). Cycles in % lithics have an average of 1.56±0.77 ka; (MIS 3 average = 1.76±0.95 ka; MIS 2 average = 1.3±0.45ka) and cycles in planktonic foraminifera have an average of 1.36±0.73ka (MIS 3 average = 1.35±0.83 ka; MIS 2 average = 1.39±0.38 ka). Bond et al (1999) found that the 1-2ka cycle recorded in lithological data did indeed persist through prolonged stadials such as between GIS2 and 3 and GIS 4 and 5. In fact, North Atlantic petrologic records reveal a much more regular cyclic pattern than the more irregular D-O events seen in the Greenland records (Pisias et al 1973, Keigwin and Jones 1989, Bond et al 1999, Elliot et al 1998, 2000). Cycles in other proxies within MD95-2006 are generally irregular with no strong periodicity although, on average, cycles are shorter with smaller percentage deviations during MIS 2. Although highly irregular and at low amplitude, the MD95-2006 IRD record also reveals continued fluctuations in lithic concentrations during these prolonged stadials.

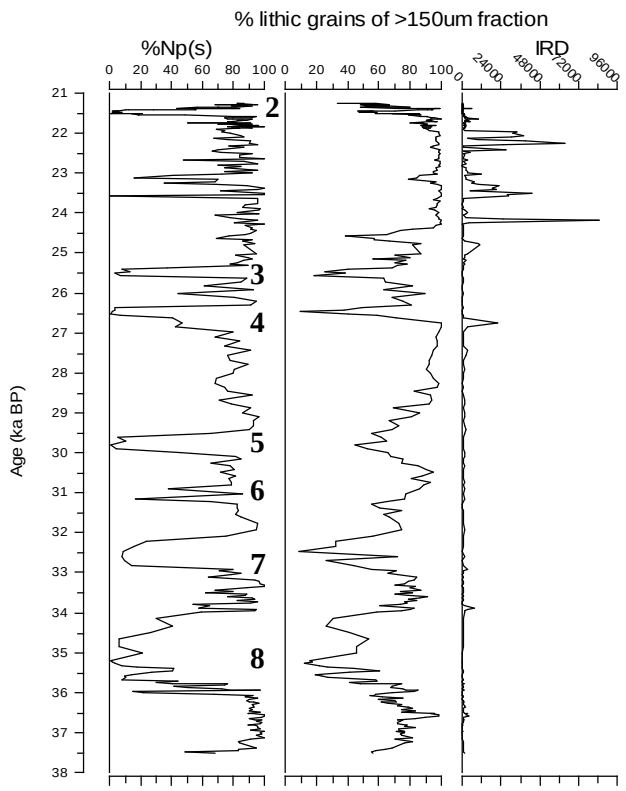

Figure 4.1: The main cyclic proxies recorded in MD95-2006 from 20-40 ka BP recording D-O-like cyclicity as discussed in text. GIS numbers are labelled.

Cyclicities of 1.3ka, 1.5ka, 1.8ka, 2ka and 2.6ka have all been recognised in different climatic proxies (Elliot et al 1998, Bond et al 1999). A strong periodicity of 1.46ka has been recognised in Irminger Sea records during MIS3 (van Kreveld et al 2000). During MIS3 in the MD95-2006 record, a strong periodicity of 3.077ka has been recognised in %$CaCO_3$ and reflectance and one at 3.125ka in lightness (Wilson and Austin 2002). Longer periodicities have been noted in the sediment silt and clay fractions (9.524ka and 4.878ka respectively). All proxies reveal a significant but weaker periodicity of 1.98ka during MIS3. Cycles during MIS2 are weaker but at a higher frequency although clay, silt and %$CaCO_3$ all show a maximum power at a periodicity of 2.5ka (Wilson and Austin 2001).

Most IRD events within MIS3 in MD95-2006 coincide with a stadial-interstadial shift. The relationship between climate and IRD delivery within MIS2 is much more complicated. The occurrence of an IRD event with nearly every D-O event during MIS3 led Bond et al (1999) to call these 'mini' Heinrich Events, triggering abrupt warmings and rapid switches to stronger North Atlantic oceanic overturning. It seems that this may also be recorded in the Barra Fan record however, although IRD concentrations (lithic grains g^{-1}) are higher during stadials, there are not significant 'events' before either GIS 6 or 5. This is also observed in the record of haematite-stained grains in VM23-81 (Figure 4.2) where significant increases are associated with GIS 8 and 7 but the record is more stable, and slightly more ambiguous between GIS 7 and H3 (see Figure 7 p. 45, Bond et al 1999). IRD:Foram ratios reveal a slightly different pattern, still indicating high ratios within stadials and low during interstadials. There seems to be no correspondence between lithic concentration >150μm and IRD:Foram ratio, the latter proxy remaining low (at <15) throughout most of the lithic cycles. The exception to this is during the Heinrich Events which are defined by peaks in both proxies, significant peaks in IRD:Foram ratio only occurring at these horizons. The patterns revealed by these two proxies therefore confirm the highly unique nature of Heinrich Events and the contribution of terrestrial/glaciological factors (ice stream surging, nature of ice sheet substrate, internal ice sheet mechanics i.e. MacAyeal 1993) against the background signal controlled mainly by oceanographic conditions (influenced by climate, ocean circulation). In addition, inter-Heinrich IRD events seem to be controlled in the most part by glaciological mechanisms (although influenced by

climatic controls), however the true Heinrich Events have much more of a climatic influence both in their cause and effect.

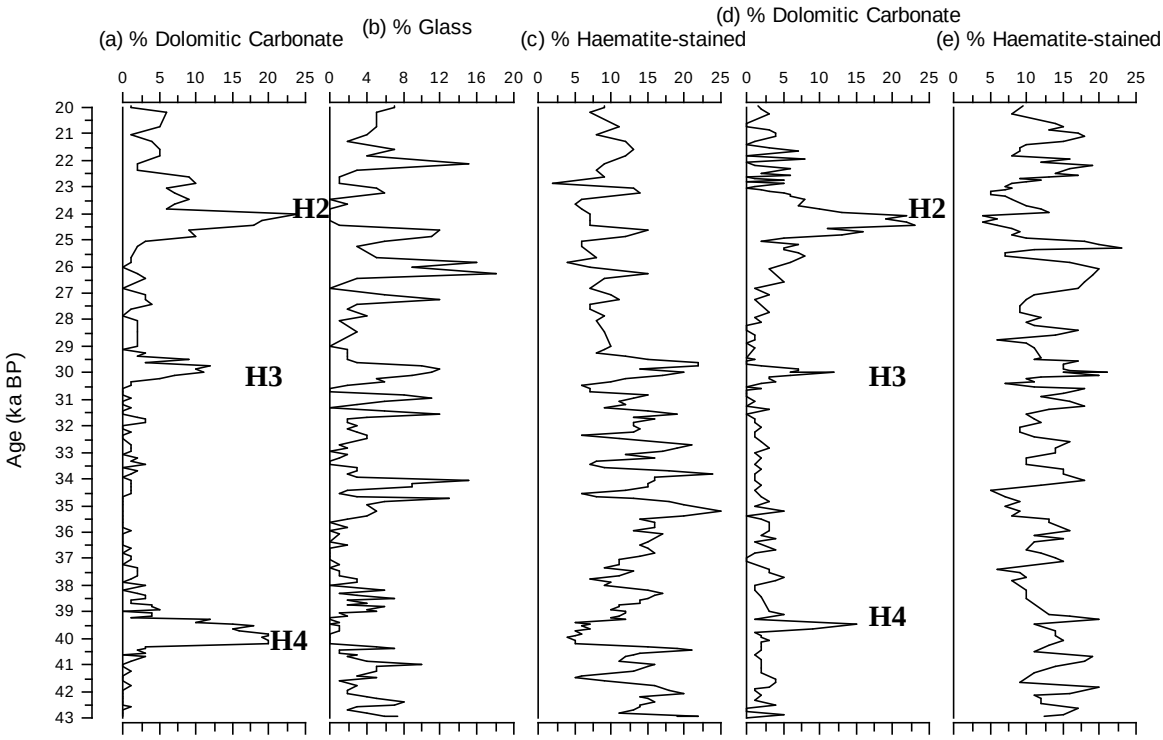

Figure 4.2: Petrologic tracers as identified by Bond et al (1999) in cores from the central IRD belt (DSDP 609; a-c) and the open NE Atlantic (VM23-81; d-e) over the period from 20-40 ka BP. Heinrich Events are labelled.

The robust cycles in % lithic grains of total >150μm counts exactly coincide with those in %*N. pachyderma (s)*: Lithic concentration falling during interstadials and increasing during stadials (Figure 4.1). The saw-toothed shape of the former cycles suggests that atmospheric, climatic factors have a stronger influence considering the coincidence and correlation of the saw-toothed shape with that of the Greenland $\delta^{18}O$ records. In addition, not every maximum in % lithics (this proxy controlled mainly by changes in foraminiferal concentration as discussed in Section 3.2.5.2) coincides with a distinctive IRD peak, thus adding *gravitas* to the theory that inter-Heinrich IRD events are, in the most part, glaciologically-driven.

There is, however, a significant difference between % lithic grains and concentration expressed as number per gram of sediment. Quoting percentages (e.g. Lackschewitz *et*

al.. 1998) opens the data interpretation up to dilution effects rather than absolute sedimentological changes, particularly in ice-proximal locations which are subject to sudden influxes of continent-derived debris. At some sites in the North Atlantic the argument can be made that during HEs there is relatively little change in lithic flux but there is a dramatic decrease in foraminifera numbers. This could be explained by a dilution due to a rapid pulse of sediment (Thomson *et al.*. 1995) or by a real reduction in foraminifera possibly associated with a meltwater cap. In these cases, quoting lithic and foram abundances as percentages may lead to erroneous conclusions as to the processes operating. It is preferable to evaluate inputs in absolute rates of accumulation ($gcm^{-1}a^{-1}$). This, however, requires a very accurate, high-resolution age model. In addition, the rate of sediment accumulation during a Heinrich Event is, at present, not known better than a factor of around 5 (250 versus 1250 years) nor are changes in sediment density (Andrews 2000), hence flux calculations remain poorly constrained. Progress could be made by combining measurements such as flux and number of lithics per gram of sediment.

SST reconstructions from foraminiferal assemblages below H4 (A. Dixon, MSc Thesis 2004) do not reveal a saw-toothed shape, however, the temperature changes within each cycle appear more gradual with respect to the %*N. pachyderma (s)* record demonstrating the gradual change in foraminiferal assemblage with response to temperature, a characteristic that is likely to continue through the rest of the core record. This pattern agrees much more with that of planktic foraminiferal abundance indicating the coeval response of surface ocean productivity to stadial-interstadial temperature fluctuations.

4.2 Marine Isotope Stage 3

There is a clear evolution of the sedimentary regime through the core record. During MIS3, cyclic, high-amplitude variation is seen in all proxies. The climatically-driven signal is evident in the covariation of %*N. pachyderma (s)*, planktic foraminiferal concentration, $\delta^{18}O$ and % lithic grains of total >150μm fraction. The shapes of the curves of the proxies reveal different properties of the signals they record. % *N. pachyderma (s)* both increases and decreases abruptly reflecting the immediate response of the foraminiferal assemblage to the polar front passing to and fro over the core site,

correlative with the cooling and warming within each D-O cycle. The cycles in $\delta^{18}O$ also reflect these frontal migrations but instead record both the changing influence of fresher polar waters with more saline waters from the south and changing SSTs, the opposing effect of these two factors on the $\delta^{18}O$ values reflected in the damped amplitude of the $\delta^{18}O$ cycles.

In general, planktic foraminiferal concentration seems to be controlled by stadial-interstadial variations, SST and the climatic effect on surface ocean productivity as all peaks coincide with warmer periods as recorded in % *N. pachyderma (s)* during MIS 3. Despite this general increase in foraminiferal concentrations within interstadials, double peaks are observed: the first coinciding with the warming transition and the second with the cooling. This is most likely due to the polar front, a major area of oceanic overturning and hence higher productivity, passing over the core site at these times. The only exceptions to this pattern are in GIS8 and GIS4, those following the two Heinrich Events (H4 and H3 respectively) where the foraminiferal concentration only starts to increase in the middle of the interstadial due to the huge dilution of forams by IRD (high IRD:foram ratios).

The sedimentation rates within MIS 3 (Figure 3.10) are invaluable in revealing information regarding the relationship between BIS dynamics and the continental margin sedimentary regime. The limited extent of the BIS would have enabled terrestrial sediment to be trapped on the continental shelf. This, in combination with increased bottom current strengths during MIS3 interstadials (Curry *et al.* 1999) would have led to the highly reduced sedimentation rates observed on the Barra Fan at this time. Periods of high carbonate content occur during the interstadials and coincide with peaks in sortable silt (Figures 3.1 and 3.2) reinforce the evidence for enhanced bottom current strengths along the British margin during warmer periods. Clay content is also relatively high during these intervals but this is likely to be an effect of vastly reduced volumes of sand delivered to the core site during interstadials, as clay content is generally low in MIS3 compared to the rest of the core record (Figure 3.2).

Higher sedimentation rates are observed during certain stadials during MIS 3: those bracketing GIS 8 and between GIS 6 and GIS 5. These directly coincide with the

intervals of higher lithic concentration (grains g^{-1}) in the >150μm fraction, higher % lithics and higher IRD:foram ratios. It therefore seems that, at least between H4 and H2, sedimentation rates at this location are governed predominantly by the delivery of lithic/terrestrial material to the core site from ice-rafting and mass transport processes rather than surface ocean productivity and $CaCO_3$ production or by material advected by bottom currents. The stark exception to the generally low sedimentation rates is during the stadial directly following GIS 8 where sedimentation rates reach 116 $cmka^{-1}$, the highest in all of the studied core section. This stadial also records unusually low and stable IRD and planktonic foraminifera conentrations in the size fraction > 150μm. Despite this, there is not a significant increase in the lithic silt- and clay-sized fractions. This is likely to be a result of a combination of the abrupt sea level rise that would have accompanied H4 freeing up an increased amount of coastal sediment and the post-H4 BIS expansion entraining a significant sediment load from the shelf which would largely have been removed and therefore not available during the build-up to H4. This mechanism is also likely to confirm and explain similarly anomalously high sedimentation rates during the stadial following H3.

The percentage of lithic grains of total >150μm fraction is the only proxy that shows a saw-toothed shape (Figure 4.3): abrupt decrease (warming) followed by more gradual increase (cooling). Each IRD event always coincides with the maximum cold stage (maximum lithic %), exactly the same pattern as that recorded in D-O cycles in so many Atlantic cores (e.g. Bond et al 1992, 1993, Elliot et al 1998) and indeed in the Greenland ice core record (Dansgaard et al 1993). In addition, this proxy is the only one that unequivocally records the progression through one Bond Cycle between GIS8 and GIS4 (H4-H3), the maxima (and minima) reaching progressively higher values with each (D-O) cycle before % lithics falls to its lowest value in the whole core interval (9.9%) during GIS4 (Figure 4.3). GIS4 is not actually associated with particularly high foraminiferal concentrations in the >150μm fraction so this dramatic decrease to 9.9% can only be attributed to an abrupt and pronounced decrease in the delivery of lithics >150μm to the core site following H3. The overall pattern is likely to be due to the coupling of two factors: an increase in glacial debris delivered to the site due to the expansion of the British Ice Sheet both through each stadial period and over the entire course of the Bond Cycle and decreasing productivity through each cooling period,

reducing the foraminiferal concentration. Studying the size evolution of lithic grain sizes at high-resolution through these D-O cycles would provide important data on changing bottom current strength in the event of insufficient benthic foraminifera for isotopic analysis.

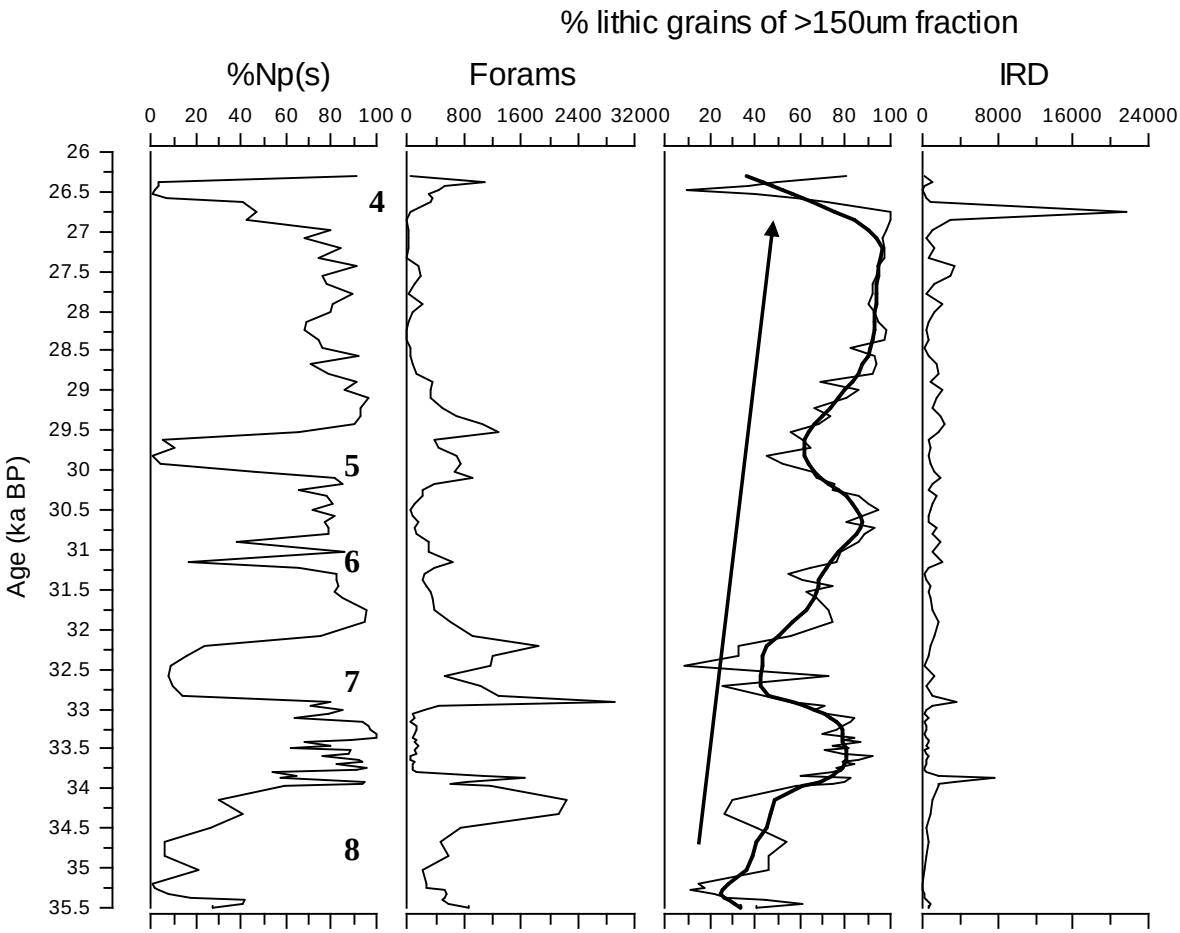

Figure 4.3: The Bond Cycle between GIS 8 and GIS 4 in MD95-2006. Proxies shown are % *N. pachyderma(s)* with Greenland Iterstadial numbers, planktonic foraminifera concentration (tests >150μm g^{-1} of sediment), % lithic grains of total grain counts >150μm (with smoothed trend line and arrow showing the progression of the Bond Cycle) and IRD concentration (grains g^{-1}).

Although the IRD concentration continuously fluctuates at relatively low background levels (average <1000 grains g^{-1}, the regional IRD contribution) throughout MIS 3 reflecting the reduced extent of the BIS, the absolute IRD concentration also records this Bond Cycle: a progressive increase in the maximum of each 'cycle' from 32.5-26.8 ka BP.

The sediment sand content (>63μm fraction) is generally higher during stadials during MIS3, coinciding with higher sediment MS. The MS signal at this site is most likely to be recorded in the terrestrially-derived lithic fraction, sourced from the British land mass and indeed lithic concentration is higher during the stadials. Hence, the background bulk lithic delivery seems to originate from the British landmass. This is in contrast to the MS signal in the Norwegian seas which records changing strength of NADW formation rather than terrestrial sediment delivery (Elliot *et al.* 1998, 2001). It seems that the sand fraction correlated well with the climatic signal, being reduced during warmer periods, however, the short-lived nature of the interstadials within the MD95-2006 %*N. pachyderma (s)* record precludes any detailed examination of this. Both the sand fraction and lithics >150μm do increase progressively through the longer GIS8 but then so too does the planktonic foraminiferal conentration. This is in agreement with the sedimentation rates which increase from a minimum in MIS3 during GIS8, to a maximum into the stadial just following GIS8, then falling during the latter part of this stadial.

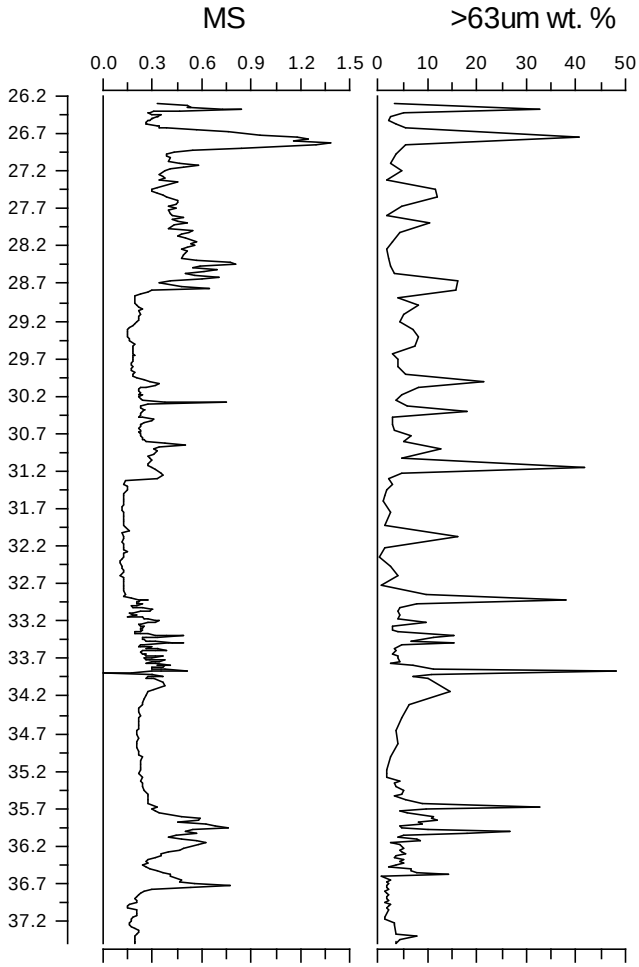

Figure 4.4: Bulk sediment magnetic susceptibility (SI units) and sediment weight % >63μm from 26-38 ka BP in MD95-2006.

Discrete peaks in lithic grains >150μm occur during MIS 3. Due to its reduced extent during MIS3, the BIS had significantly less influence on sediment delivery to the Barra Fan at this time. Thus the discrete intervals of high lithics >150μm are unlikely to be related to slope processes and thus may be assumed to be IRD events. This is supported by the shape of the peaks: sharp base and top, the maximum usually consisting of only one data point (i.e. short duration of <ca.30yr). These IRD events recorded are likely to correlate to those in the open Atlantic, most likely sourced from the already extensive LIS as any stochastic, more continuous IRD delivery from the BIS is unlikely to produce such dispersed, well-defined peaks in such an ice-proximal site.

Continental margin sites are therefore able to reveal more regional information, if examined at times of reduced ice extent on the adjacent margin. This is facilitated by the high sedimentation rates characteristic of such sites. The additional advantage is that the influence of the changing glacio-sedimentary regime can be charted as the local ice sheet expands and site-specific sedimentary processes start to interact with and overwhelm the regional IRD signal. In combination with on-shore glaciological studies, correlated to a common chronology, better understanding of all these processes may be achieved.

4.3 MIS 3/2 Transition

The MIS3/2 transition occurs over a period of ca.1.23 ka, spanning most of the period between and including GIS 4 and 3 (25.34-26.57ka). The increased stochastic variability of most proxies after this time most likely reflects the British Ice Sheet expanding across the continental shelf, increasing the relative influence of glacio-sedimentary factors on the MD95-2006 record, complicating the recorded signals. This is seen particularly in the increase in lithic concentration in all grain sizes (Figure 3.4) and in the increase in sediment magnetic susceptibility, reflecting the dominant contribution from British terrestrial material. This places new constraints on the timing of the main Scottish Ice Sheet expansion. Studies show that ice build up on the NW Scottish mainland occurred after ca.26 ka BP (Atkinson *et al.* 1986, Lawson 1984) and this study seems to agree with this. The increase in clay from MIS3-2 may reflect the overall cooling (as revealed in the $\delta^{18}O$ record) as clay% in the Barra Fan record has

been suggested to correlate to temperature cycles, higher clay% coinciding with cold stages (Knutz *et al.* 2001). However, enhanced ventilation during the interstadials of MIS 3 (Curry *et al.* 1999) may have led to increased bottom current strengths and hence reduced clay contents. Most likely the clay signal will reflect a combination of these, and other, factors.

4.4 Marine Isotope Stage 2

There is an overall decrease in the duration of interstadials from GIS8-GIS2 with each progressive interstadial from GIS8-2 records revealing progressively increasing sedimentation rates. Both the increasing sedimentation rates and decreasing duration of successive interstadials from 36ka to 21ka indicate an increasing influence of the growing BIS on modifying the climatic, oceanographic and sedimentological signals at this location. Any warmer intervals towards the LGM are likely to be shorter in duration as the climate temporarily stabilises into a cold state. However the influence of the proximity of the BIS to the core site as it expands to its maximum extent may have led to ice discharges and injections of fresher water and terrestrial sediment sufficient to abruptly terminate any warmer intervals. It is likely that such ice advances were triggered by slight climatic warming at this site due to the position if the BIS in the path of prevailing wetter (and warmer) air masses from the south west mid-Atlantic. Although the north Atlantic current is thought to have been vastly reduced in strength during the LGM, it is still thought to have operated (Piotrowski et al 2004), transporting sub-tropical waters further north. Warmer air is able to hold more moisture and thus slightly increased temperatures would lead to higher precipitation levels in the NE Atlantic and hence cause ice advance. The smaller size of the British Ice Sheet would reduce its response time to such climatic fluctuations and the Barra Fan record should record these signals relatively instantaneously.

Interstadials as recorded in the % N. pachyderma (s) records appear longer in open ocean sites both outwith (e.g. Rasmussen and Thomson 2004) and within (e.g. Bond et al 1999) the IRD Belt. The contrast between the length of interstadials between and ice-proximal site and an open ocean site is seen if the Barra Fan record is compared with that of ODP 609, a site in the centre of the IRD Belt (Figure 4.5).

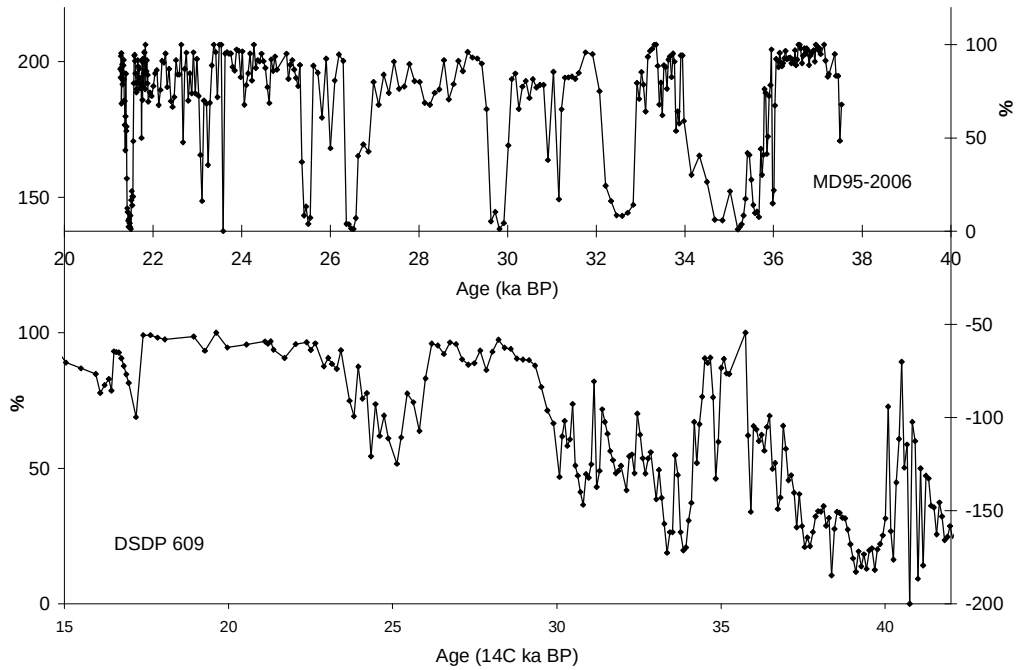

Figure 4.5: A comparison of the length of interstadials as recorded in the % N. pachyderma (s) in an ice-proximal site (MD95-2006; this study: age in ka BP) and an open ocean, IRD belt site (DSDP 609; Bond et al 1999: age in ^{14}C yr BP).

The coincidence of cycles in planktonic foraminiferal concentration and %*N. pachyderma (s)* observed in MIS3 breaks down within MIS 2. Foram concentration does continue in cycles and peaks are observed within GIS 4 and 3, however these are more than half the magnitude of the peaks during MIS3 interstadials. The unnumbered warm interval betwwen GIS 3 and 2 also coincides with a small peak in foram abundance however the two most pronounced maxima in foraminiferal concentration (1400 g^{-1} and 2520 g^{-1}) occur during times of high %*N. pachyderma (s)* between GIS 3 and 2.

The progressive increase in sedimentation rates during interstadials may be an indirect expression of the climate signal and short response time of marginal ice to the warming. Coastal ice streams and outlets respond rapidly to climatic warming. As discussed, in the case of the BIS during MIS2 and 3, this expression is likely to be a marginal ice advance or ice shelf collapse, triggering the delivery of large volumes of sediment to the continental slope, both from that trapped within terrestrial ice and that ploughed down from the continental shelf by advancing ice. Progressive ice sheet advance would have

delivered more sediment to the continental slope throughout MIS2 making available increasing volumes of material able to be delivered to the site of MD95-2006. The expression of this within the core record is in both the increasing sedimentation rates not only through progressive interstadials but in general from before GIS8 to after GIS2. The point at which the BIS is likely to have crossed the shelf break is after ca.25.14ka where a dramatic increase in both the sediment sand fraction and more importantly in concentration of lithic grains >150μm is observed (Figure 4.6). This ice advance would have ploughed the large volumes of terrestrial material which had accumulated on the continental shelf through MIS3 into the Barra Fan system. This horizon also coincides with an increase in MS, (seemingly independent of the previous climate-driven cycles in this proxy), a possible indication of the British origin of this lithic material. The continuation of cycles in planktic foraminiferal concentration through MIS2, independent of changes in surface hydrography, indicates that the lithic signal at this time is likely to be a reflection of glaciological and sedimentological rather than climatic factors as during MIS3.

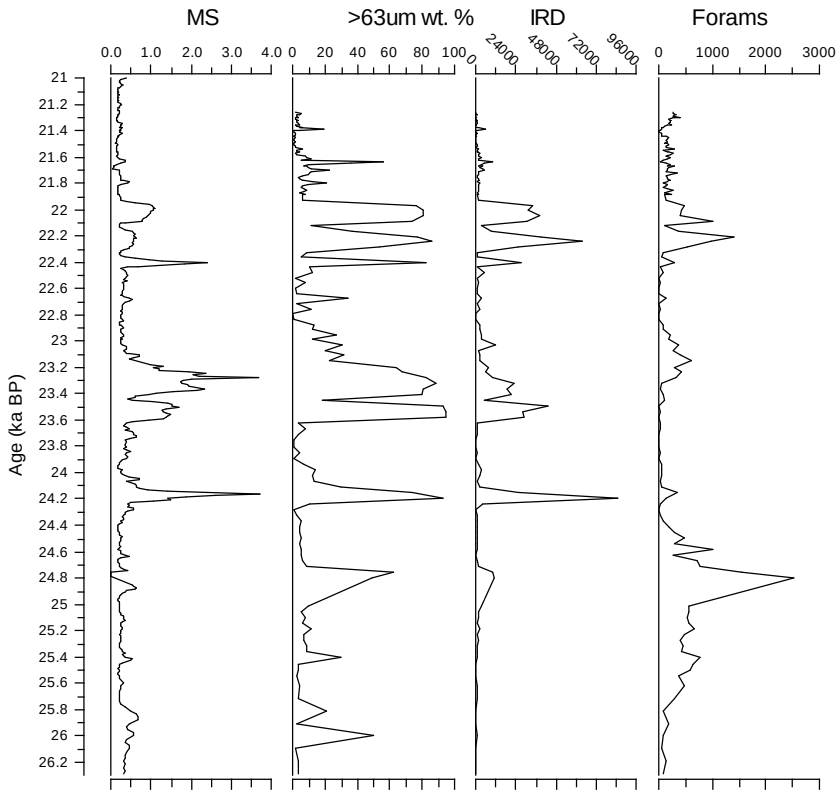

Figure 4.6: MIS 2 in MD95-2006: bulk sediment magnetic susceptibility (SI units), sediment weight % >63μm, IRD concentration (grains g^{-1}), planktonic foraminifera concentration (tests >150μm g^{-1} sediment).

The interaction of these factors can be determined through examination of the grain size distributions and shapes of the curves through the interval after 25.14ka and their relationship with other proxies. This contrasts to open ocean sites where specific grain size variations are mainly a reflection of changing current strength. At this time in MD95-2006, sortable silt and silt fractions fall to lower concentrations as they are diluted by the sand-sized sediment fractions. The sortable silt fraction is highly variable throughout the interval of enhanced sand delivery to the core site. This suggests that the influence of sediment winnowing and reworking is greater during intervals of reduced lithic sediment delivery to the core site as % sortable silt is generally lower during intervals of high >63 weight % and high concentrations of lithic grains >150μm. This is most likely to be due to the large input of terrestrial sediment swamping the sedimentary record and producing horizons of more poorly-sorted material. Indeed, the two intervals of high lithic concentration at 22.2 and 23.4ka BP (1706cm and 1830cm) contain much larger grain sizes in the >150μm fraction than any

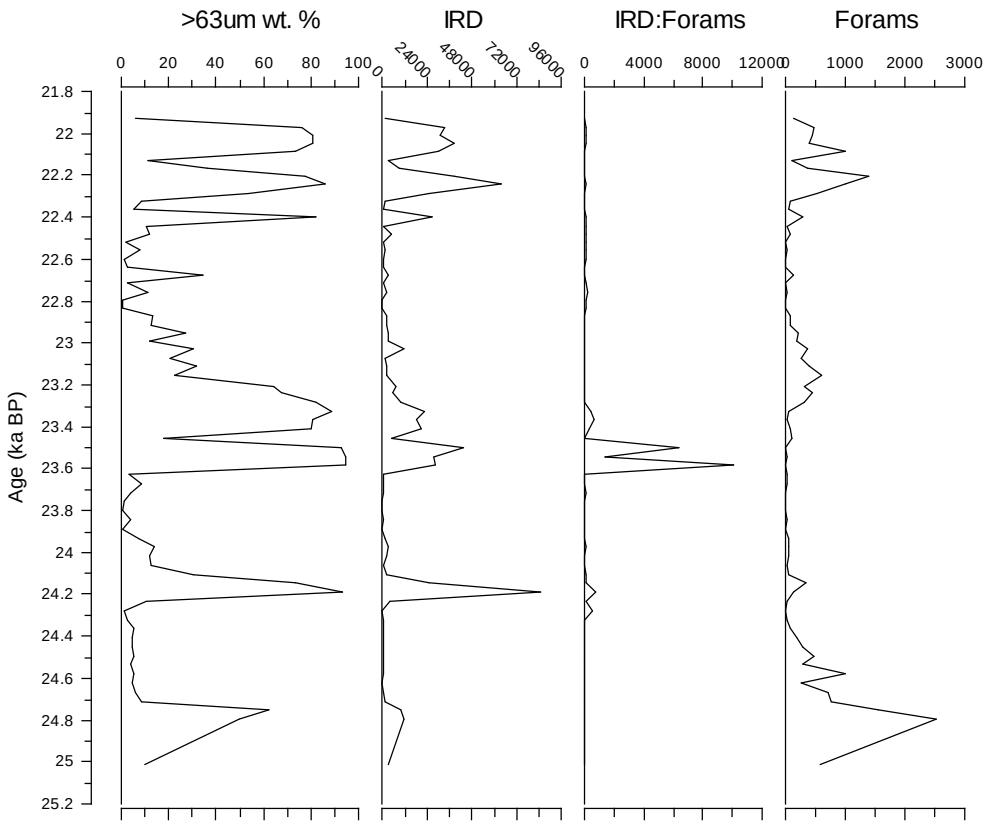

Figure 4.7: The main interval of turbidite activity recorded with MD95-2006: sediment weight % >63μm, IRD concentration (grains g^{-1}), IRD:foram ratio and planktonic foraminifera concentration (tests >150μm g^{-1} sediment).

of the other lithic events. The intervals of high lithic concentration around these two peaks indicate that these events are of much longer duration that the previous IRD events. Both these events appear to be turbidites. Figure 4.7 illustrates the main interval of turbidites within MIS2. The former peak (1830cm) coincides with the interval of highest IRD:Foram ratios in the whole core interval but IRD:Foram ratios then fall rapidly to remain relatively low through to H2. This indicates that after the initial pulse of tubiditic material, instantaneously swamping the sedimentary record, the turbiditic horizon continues, tailing off to a finer-grained tail with cycles in productivity, revealed in planktic foraminiferal concentration, robust through this interval. Within MIS 2, maxima in % lithics do not necessarily coincide with peaks in IRD, indeed the coincidence of peaks in these two proxies may be one indication of a true IRD event as opposed to a turbidite pulse.

Distinguishing between turbidite layers and 'true' IRD events within the interval can be problematic. Ice-proximal IRD events are generally observed to have sharp bases and tops (van Kreveld *et al.* 2000, Elliot *et al.* 2001), confirming the discrete nature of the pulse of sediment discharged from the icebergs that released it. This seems to apply to the IRD events earlier in the core record. This is particularly the case as the overall volumes of sediment available on the continental shelf at this time would have been vastly reduced and thus any slope destabilisation that did occur is unlikely to have produced a large enough sediment volume for the coarse fraction of the sediment plume to have reached the core site. This is not the case during the period of maximum BIS extent. There seems to be only one event after 25.24ka BP and before H2 that have this characteristic shape, at 24.19ka BP (Figure 4.7).

During the initial growth of the BIS at the start of MIS2, ice shelves were probably able to form and thus earlier coarse lithic events are likely to be related to ice shelf processes including sediment delivery sourced from icebergs calved from the marginal ice. However, at the time of maximum BIS extent (LGM), the BIS most likely extended over the continental slope, as is evident from this study, so no ice shelves could have formed at this time and thus later lithic events are more likely to be related mass transport processes from the ploughing of material from the shelf by the extensive ice sheet. The event at 24.19ka BP may therefore reflect the final calving/ice-rafting event from the collapsing western BIS ice shelves before this collapse triggered a period of

sub-marine mass movement facilitated by the large amount of glacially-derived sediment that had been building up under the ice sheet on the continental shelf over the previous 6-10ka.

IRD events have a bimodal size distribution (>63μm and very fine:<2μm; Moros *et al.* 2002). It is difficult to construct a numerical equation to fulfil the identity of IRD events versus turbidites as the absolute values of the parameters would depend so much on the stage of the glacial cycle of the local ice sheet. With further studies into grain size distributions and relationship with oceanographic proxies, it may be possible to define a more complicated, calculus-based equation based on the rate of change of and relationship between certain parameters over a certain depth/time.

Glaciological studies (see Section 1.6.1) have dated the time of BIS maximum extent to a maximum of >22 ka BP (Sejrup et al. 1984) and a minimum of 17 ka BP (Wilson et al. 2002). If it is assumed that the peak lithic delivery to the Barra Fan occurs at the time of maximum ice sheet extent, this study places the LGM in NW Scotland at 22-24 ka BP, agreeing with the oldest estimates from previous studies.

4.5 Heinrich Events

The link between cooling phases and Heinrich Events in the North Atlantic has been made frequently (e.g. Bond et al 1999), the Heinrich Event falling at the coldest phase of the cooling cycle. Placing the HEs in this context relies on the proxies being examined to imitate the saw-toothed shape of long-term cooling and sudden warming. This is very rarely the case with most oceanic proxies. This study demonstrates the occurrence of Heinrich Events during times of high %*N. pachyderma* (s), H4, H3 and H2 all occurring just prior to the warming transition into the following interstadial. However it seems that the proxy revealing the most robust cycles is that of % lithic grains >150μm.

H3 occurs at 26.74 ka BP, coincident with the start of the transition into GIS 4. This event seems to herald the beginning of the increase in lithic fraction significantly with a maxima of 21755g^{-1} lithic grains >150μm. This may have been the initial trigger for the

main period of submarine mass movement down the continental slope leading to the interval of turbidites seen after ca.24.5 ka BP (Figure 4.7).

The longest interstadials follow H4 and H2. This indicates that it is these two Heinrich Events that had the most influence on the general Atlantic climate compared to H3 which is known to have been less pronounced in extent and magnitude, lacking in the large input of LIS-derived material that the 'typical' Heinrich Events are characterised by (Gwiazda *et al.* 1996b, Snoeckx *et al.* 1999). In general the planktic $\delta^{18}O$ record seems to be most influenced by the SST signal at this site as most of the transitions coincide with those in %*N. pachyderma (s)*.

The new chronology for MD95-2006 has also placed better age constraint on the Heinrich Events. Compared to the age model of Knutz *et al.*, this study makes the age of H2 >3ka younger, H3 >2ka younger and H4 >1ka younger. This is likely to be, in part, due to the fact that the new age model is tied to an updated GRIP ice core age model as opposed to the less accurate GISP2 age model employed in other studies. Indeed the younger ages for the Heinrich Events agrees more with those from nearby core VM23-81 (Bond *et al.* 1999). The increasing agreement in HE ages with age is likely to be due to better constraints on the age model during MIS3 with a greater number of tie-points during this interval. It is also complicated by increasing sedimentation rates into MIS2 with the highest sedimentation rates occurring during the period with the fewest tie-points (ca.25-20 ka BP) hence the age model is much more ambiguous at this time.

H4 occurs at a time of overall cold surface water conditions indicated by positive $\delta^{18}O$, very stable, high % *N. pachyderma (s)* and low overall foraminiferal abundance (Figure 4.8). The sub-polar front at H4 is marked by an abrupt transition between waters with high and low % Np(s) and was located around 45°N (Cortijo et al 1997), corresponding to a summer SST of ca.8-10°C (Ruddiman and McIntyre 1981). Hence fluctuations seen in this proxy in DSDP 609 recording the temperature variations over H4 are not observed in the more northerly location of MD95-2006 recording an overall high % *N. pachyderma (s)* i.e. polar waters.

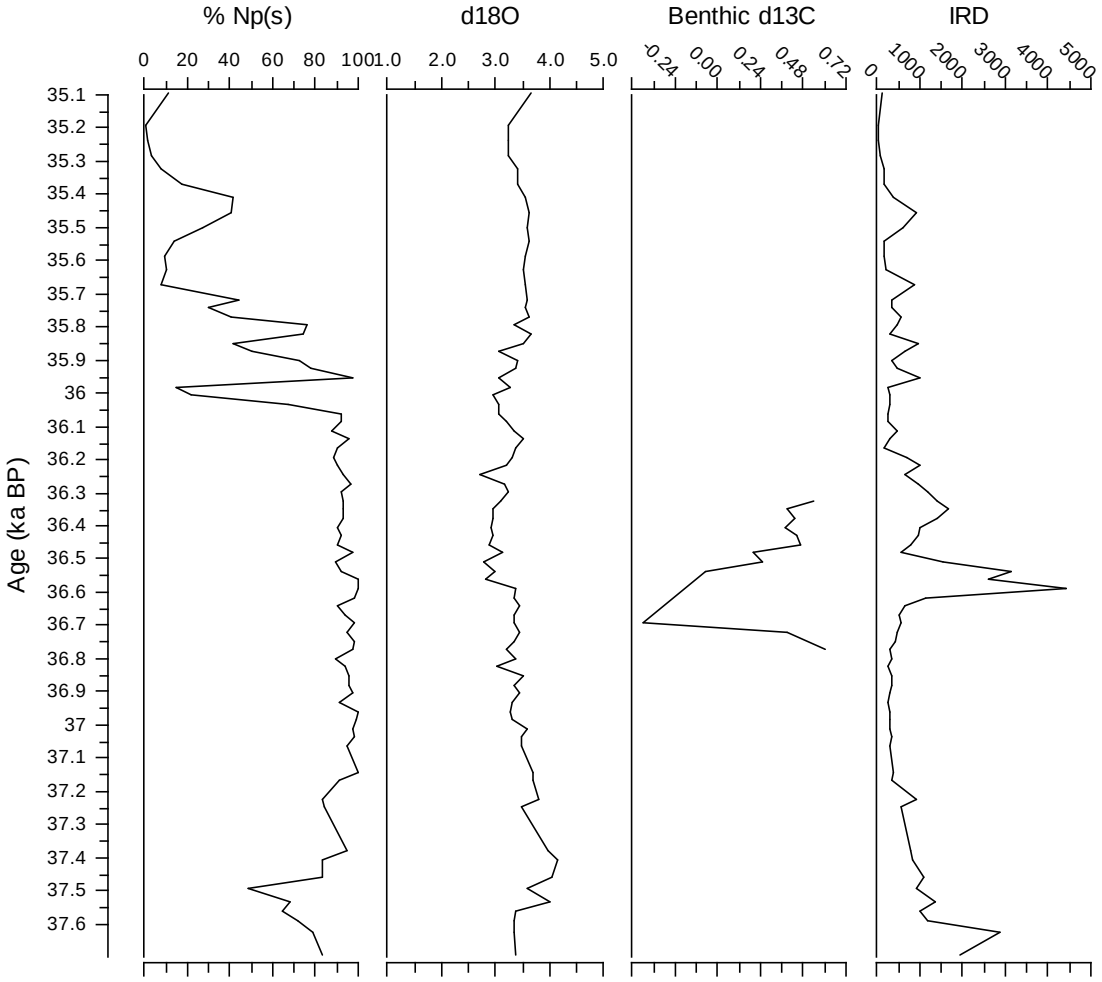

Figure 4.8: Heinrich Event 4 in MD95-2006: % *N. pachyderma* (s) showing the transition into GIS 8, planktonic $\delta^{18}O$ (‰), benthic (*C. wullestorfi*) $\delta^{13}C$ (measured by L. Wilson) and IRD concentration (grains g^{-1} sediment).

Other North Atlantic records cite H4 as being initiated within GIS9 (e.g. Cortijo *et al.δ* 1997, Bond *et al*. 1999) however this is not seen in MD95-2006. GIS9 ends at ca.37.46kaBP (2516cm), revealed in an increase to the pre-H4 high %s *N. pachyderma (s)* and an increase in planktic $\delta^{18}O$ values delimiting the cooling and migration of the polar front over the core site (base of Figure 4.8). However the stadial following GIS9, prior to H4 is characterised by steadily decreasing planktic $\delta^{18}O$ by ca.0.78‰ from ca.37.4ka – 36.59ka BP. This is likely to reflect a progressive decrease in strength of the north Atlantic current. This transports warmer, higher salinity waters northwards, a significant limb of this current flowing across the central Atlantic in a northeasterly direction through the Faraoe-Shetland channel, directly past the site of MD95-2006

(Figure 1.7) and into the Nordic seas prevailing even within the last glacial period. SST fluctuations of 3-4°C have been recorded in the subtropical western Atlantic coincident with D-O cycles in the Greenland ice core records, in addition to deep water delivery alternating between a northern and southern source (Hagen and Keigwin 2002). This supports the assertion that the North Atlantic Current was significantly weakened during cold stadials.

Bond et al (1999) demonstrated for both open Atlantic, IRD Belt (DSDP 609) and NE Atlantic (VM23-81) sites the lead in surface cooling prior to Heinrich Events 2 and 4 coincides with an increase in the percentage of haematite-stained grains and volcanic glass (Figure 4.9). They take this to confirm the presence of European precursor events before these two Heinrich Events and their link to climatic factors and that this cooling and/or sea level rise associated with the precursors is one mechanism which may have destabilised coastal LIS ice producing the following Heinrich Event.

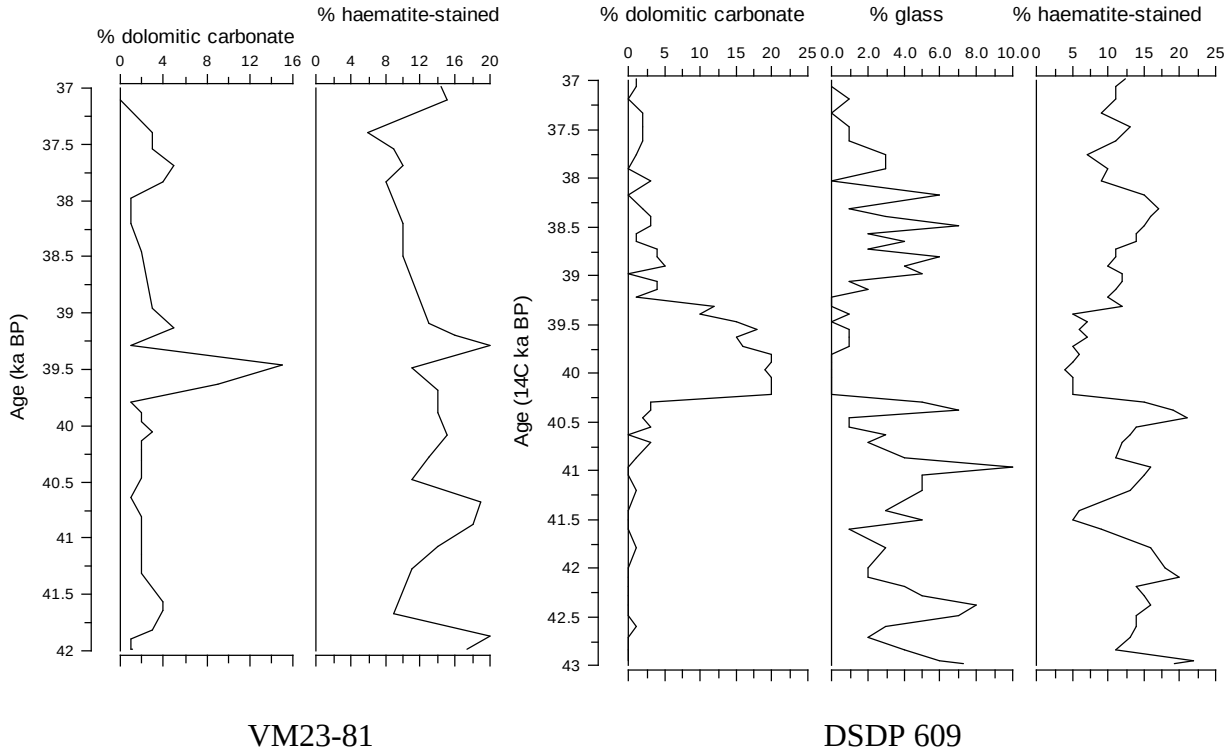

Figure 4.9: Main petrologic tracers recorded across the H4 window within cores from the IRD belt (DSDP 609) and the NE Atlantic (VM23-81) showing the sequencing between IRD delivery from different North Atlantic ice sheets (Bond et al 1999).

Both H4 and H2 in MD95-2006 demonstrate a similar pattern with the main cooling episode prior to H2 (at ca.21.85 ka BP) and that prior to H4 (at ca.37.46 ka BP) coinciding with an increase in both of these petrologic tracers. However, on examination of the data of both Bond et al (1999) and this study, it appears that although the percentages of each of these petrologic tracers increase as stated, there is no significant peak in IRD at these times: both 'precursors' occurring on the increasing limb of the IRD curve into the main Heinrich Layer peak. In addition, the cooling prior to H4 is actually the transition out of GIS 9 and thus any IRD event which did occur at that time is most likely to be part of the 1-2 ka cycle rather than a separate 'precursor' event.

A step towards lighter average $\delta^{18}O$ at ca.36.83ka BP (Figure 3.11) in MD94-2006 is accompanied by higher abundances of certain lithologies (volcanic fragments and glass, plagioclase, dark quartz grains, metamorphic fragments) within the >150μm fraction (Figure 4.10). The lack of corresponding increase in IRD in both MD95-2006 and the aforementioned two cores (Bond et al 1999) suggests that this may be due to a change in sediment provenance delivered by sea ice rather than icebergs. Although the bulk sediment mineralogy seems to remain consistent across this interval there is a small peak in Fe/Al, suggesting a brief influx of clays. A significant lightening of planktic $\delta^{13}C$ at this stage suggests a meltwater influence or terrestrial input of lighter carbon. A relative decrease in calcite may indicate the latter. A lack of a signal in the >63μm fraction indicates that a plume of terrestrially derived meltwater (e.g. glacio-fluvial meltwater/river water) may have reached the core site at this time bringing terrestrial clays in suspension.

The main H4 event at 36.56 ka BP is marked by a pronounced increase in IRD and IRD:Foram ratio. The H4 IRD event shows a double peak, followed ca.200yr later by a smaller and broader IRD peak. This pattern is similar to that seen in SU90-08 (Revel et al 1996, Cortijo et al 1997). However some cores from the European margin (Snoeckx et al 1999) show a two step evolution of H4 with an initial IRD peak of European origin prior to a second of LIS origin. This has been attributed to an initial surge of the European ice sheets producing icebergs which are then transported south along the

European margin reaching core sites before LIS icebergs transported eastwards via the IRD belt, some surviving to the European margin (Snoeckx et al 1999).

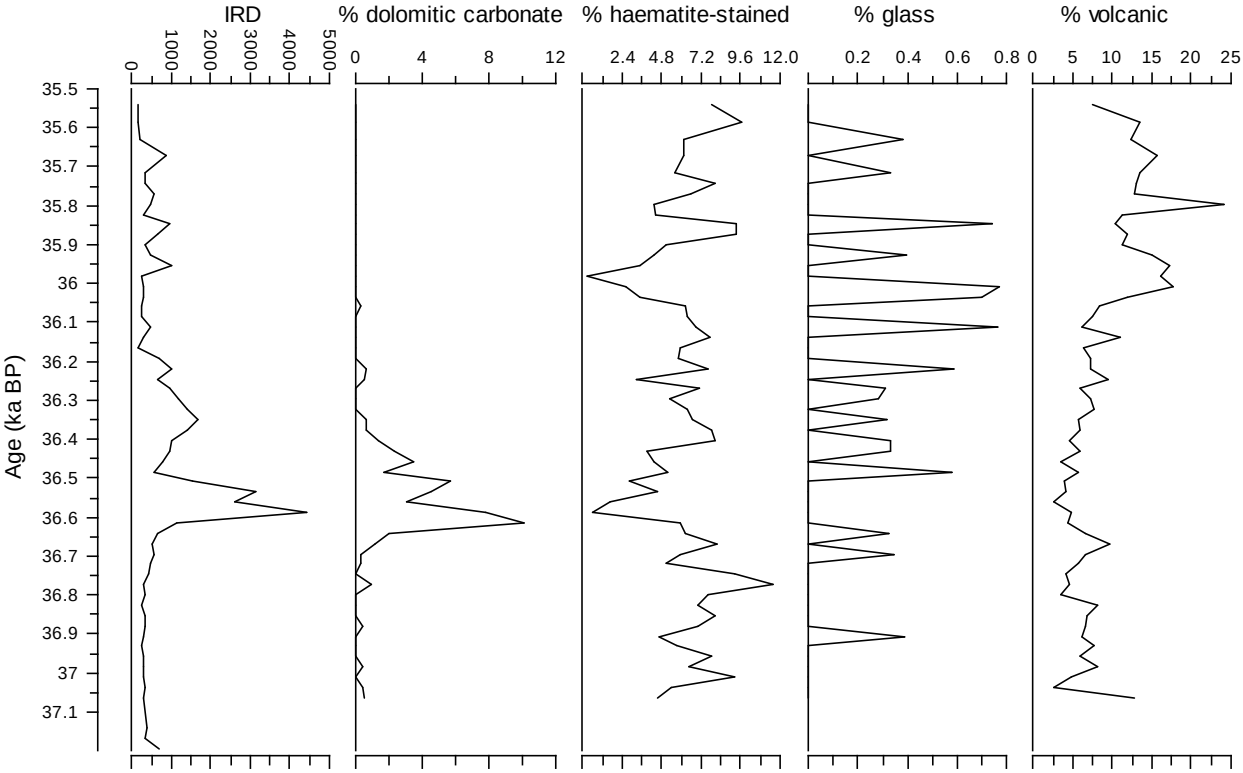

Figure 4.10: IRD concentration (grains g^{-1} sediment) and main petrologic tracers from the H4 window in MD95-2006.

This is not observed on the Barra Fan where the main, dolomite-bearing IRD peak occurs prior to the secondary IRD peak, the latter being dolomite-free. The distinct step to lower $\delta^{18}O$ at 36.59ka BP (2483cm) directly coincides with the IRD pulse, signifying the injection of a meltwater plume. The gradual freshening after GIS 9 may have triggered a short-lived shutdown of the North Atlantic Current, indicated by the sudden decrease in benthic $\delta^{13}C$ just prior to H4 (Figure 4.8). The H4 IRD event in MD95-2006 lasts for ca.500 years. This agrees with the lowest estimations of Cortijo et al (1997) who assert that the main iceberg discharge during H4 continued for about 0.5-2kyr in a cold polar setting. The shorter duration of H4 on the British continental margin is likely to be due to the large cyclonic gyre which existed at the time, leading to the zone of maximum melt being in the SW North Atlantic when icebergs reached warmer waters at around 45-50°N (Cortijo et al 1997).

The main iceberg-related meltwater spike directly coincides with the peak in ice-rafted material, although the main dolomitic carbonate peak occurs just prior to this. The relative pattern of the three main lithilogical tracers (dolomite, Icelandic glass and haematite-stained grains) is remarkably similar to sites both further to the east (VM23-81) and within the IRD belt itself (DSDP 609), with peaks in haematite-stained grains just prior to (and just following) the main dolomitic carbonate peak during which the influx of this lithology dilutes the other tracers.

As observed in other locations, the dolomitic carbonate peaks twice and although the H4 event at the core site consists of a double IRD peak, both IRD peaks occur between the dolomite peaks (Figure 4.10). The main IRD peak consists of lithologies with a crustal origin (quartz, feldspars) with an additional contribution from clay-sized calcite. This is verified by the εNd(0) and $^{206}Pb/^{204}Pb$ ratios (>63μm) which both reveal a significant increase in the contribution of material from much older terrains within the main H4 event compared to the 'background' (Figures 4.11 and 4.12). As the British Ice Sheet was still relatively small, and the lowest Pb-ratios coincide with the second peak in dolomitic carbonate, this change in provenance is likely to indicate a sudden influx of 'foreign' material, overprinting the background European/British radioisotopic signal. The $^{87}Sr/^{86}Sr$ of the carbonate leachate from this interval is significantly lower (0.708126) than the background levels (0.708734-0.709041; reflecting the composition of glacial seawater). Dolomitic limestone sourced from around Hudson Bay has been found to have lower $^{87}Sr/^{86}Sr$ (ca.0.7084-0.7086; Heinrich 1988, Grousset *et al.*. 2001). Therefore the main H4 event seems to be dominated by a Laurentide provenance, the Pb isotope ratios reflecting a shift towards a Churchill Province source. This is verified by the position of the εNd(0) and $^{87}Sr/^{86}Sr$ values from H4 plotted relative to a compilation of eNd(0) and $^{87}Sr/^{86}Sr$ measured from samples around the North Atlantic (Figure 4.12): the main IRD peak tending towards values characteristic of Baffin Bay.

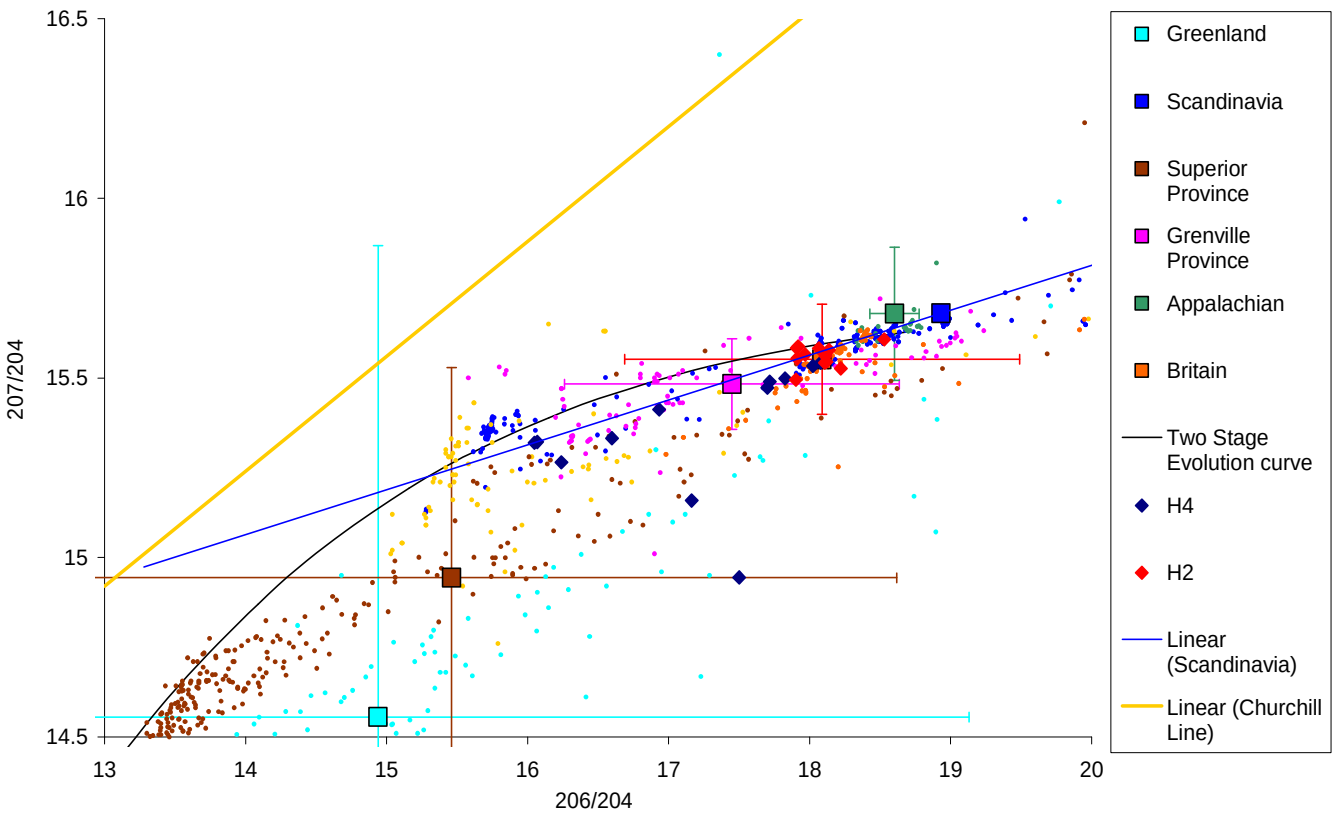

Figure 4.11: Isotopic Composition of the main North Atlantic source areas compared to MD95-2006 H2 and H4 samples.

- Isotopic data from north Atlantic source areas has been collected from the literature and compiled into mean values (Large squares) with their respective standard deviations (Error bars = 2σ).
- The sample-type of source-area data vary from mineral separates (feldspar, galena) to whole rock samples, to sediments, in order to approximate a true apparent isotopic composition with which to compare sample ages within MD95-2006.
- The overall distribution of isotopic ratios around the mean is shown by small pixels with corresponding colour to their respective mean value.
- The Churchill Province is best defined by a line of slope 0.32 representing an Archean Province, metamorphosed during the early Proterozoic.
- A similar mixing line has been plotted for Scandinavia due to the high influence of metamorphism and inclusions of radiogenic material (Klein and Hurbut 1985, Romer and Wright 1993).
- The Two-Stage Mantle Evolution curve is also shown.
- Error bars for MD-952006 samples are smaller than symbols.

For Data sources see Appendix 2.

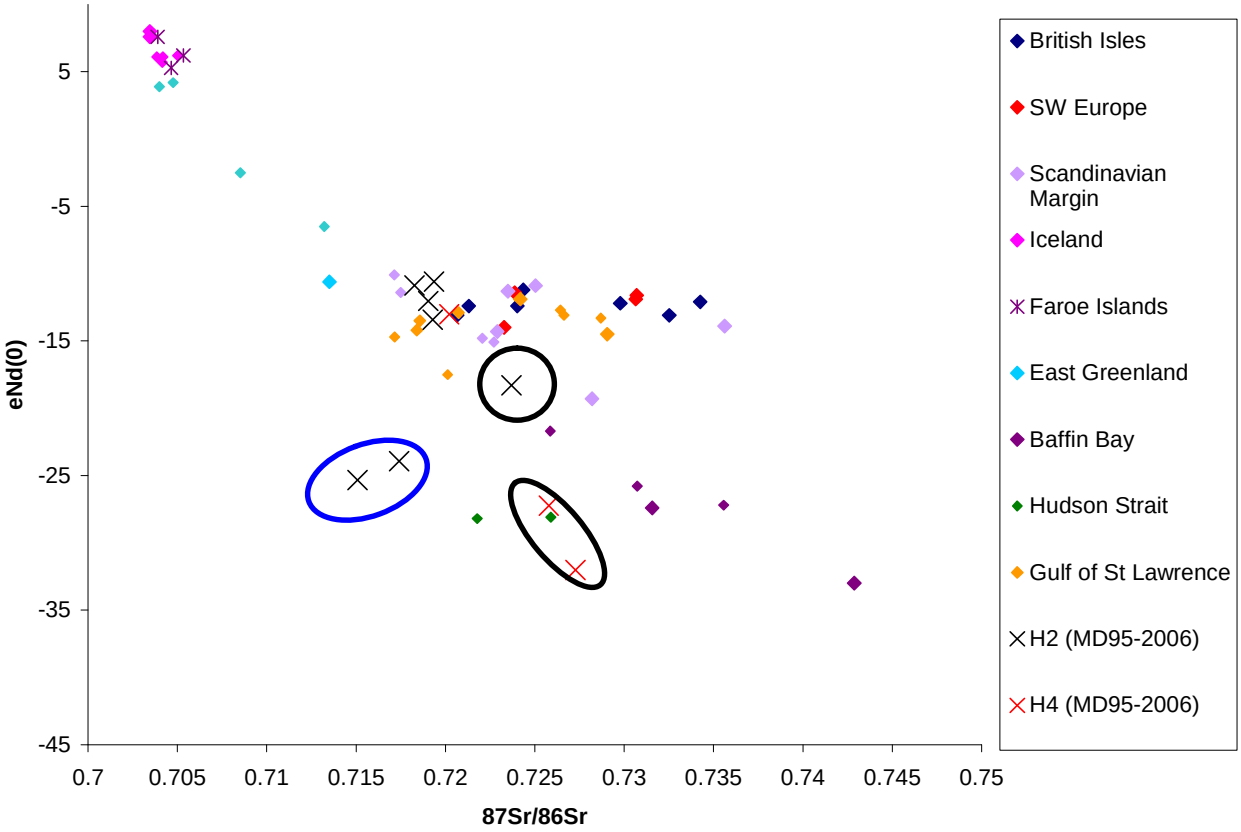

Figure 4.12: $^{87}Sr/^{86}Sr$ vs. εNd(0) plot of the composition of the main North Atlantic source areas compared to MD95-2006 H2 and H4 samples. Small diamonds represent samples >63µm, large diamonds represent samples >150µm. Ringed samples are peak IRD levels from H2 (the two ringed in blue being the secondary IRD peak) and H4. Data from Goldstein and Jacobson 1988, Revel et al 1996 and Grousset et al 2001.

Following H4, $\delta^{18}O$ starts to rise, indicating a recovery of surface salinity as the meltwater lid dissipates and the strength of the NAC starts to increase once more. The $\delta^{18}O$ in MD95-2006 is approximately the same after the discharge as before which is similar to most North Atlantic cores (Cortijo et al 1997). The salinity signal is then overtaken by the warming trend into GIS 8 after ca.35.78ka BP revealed in the subsequent trend to lower $\delta^{18}O$ above this horizon.

As the climate warms into Interstadial 8, the polar front moved over the core site with significant latitudinal fluctuations due to the instability of this climatic transition; the start of this transition marked with a brief, extreme warm event at 35.98kaBP. The

polar front is associated with a boundary between warmer, more saline waters, change in foraminiferal assemblage with the northern watermass dominated by *N. pachyderma (s)* and the locus of iceberg/sea ice melt. Thus the core records fluctuations in $\delta^{18}O$, %*N. pachyderma (s)* and pulses of IRD delivery over this period. An increase in Ti/Al between 36.59 and 35.98 ka BP (Figure 3.13) indicates stronger bottom currents, possibly forced by the constant movement of water masses across the site. Large variation in delivery of >63μm sediment suggests that it is mostly sea ice rather than iceberg melt which is controlling the sedimentary regime. The local provenance is supported by a significant increase in metamorphic rock fragments and mica flakes within the >63μm peaks, likely to originate from the NW Scotland metamorphic provinces and a slight decrease in Pb-ratios (ie specifically British not European) at 35.67kaBP, coinciding with the main >63μm peak. This event is likely to be caused by the warm event at 35.98kaBP. $\delta^{13}C$ lightens significantly at these levels indicating the presence of meltwater lids reducing ventilation, and/or delivery of terrestrial DOC in (glacio-)fluvial water pulses.

This brief warm excursion at the start of Interstadial 8 seems to be a robust feature of North Atlantic records, seen in the open IRD belt (Site DSDP609; occurring ca.500-600yr prior to the start of warming into IS8) and NE open Atlantic (site VM23-81; Bond et al 1999). In the central Atlantic, this warm excursion is associated with a lightening in $\delta^{18}O$ of ca.1‰ compared with 0.6‰ in MD95-2006. In the latter record the lightening in $\delta^{18}O$ starts prior to the warming in %Np(s) suggesting that the total decrease reflects a combination of meltwater and temperature. The difference between the two locations may reflect a greater salinity contribution in the open Atlantic < 50°N during and after H4 (Cortijo et al 1997). This makes sense with respect to the $\delta^{18}O$ variations as the average decrease in temperature for H4 is 2 degrees corresponding to 0.5per mil recovery after the event (ie. the MD95-2006 signal is mostly recording temperature variations).

After ca.35.45ka BP, temperature becomes the dominant control on $\delta^{18}O$ as the climate stabilises into IS8. The calcium carbonate content of the now dominantly clay-sized sediment increases and crustally-derived minerals and lithologies fall to trace levels.

H4 is an unusual IRD event with regards to the MD95-2006 record as it coincides with peaks in %$CaCO_3$ and absolute Ca content indicating that within H4, these proxies are recording a carbonate-rich lithic event rather than high sediment biogenic carbonate content. This additional carbonate is likely to be sourced from the LIS, with H4 IRD revealing a high percentage of dolomitic carbonate grains and high absolute sediment calcite and dolomite content, despite having similar lithic quartz concentrations to the other IRD events recorded in MD95-2006 (Knutz *et al.* 2001). Bulk sediment XRD analysis reveals that quartz content is much lower within H4 than within the rest of MIS3, increasing by an average of 1.5 times the magnitude at ca.33.6ka BP with peak values reaching over twice the magnitude of peaks prior to 33.6ka BP.

The structure of H2 is vastly different from that of H4 as the former occurs at a time of maximum BIS extent and during the peak cold stage of the last glacial cycle and therefore maximum glaciation in the North Atlantic. This is in stark contrast to the time of H4 where the circum-North Atlantic ice sheets were all at different stages of their growth: the BIS was limited in extent whereas the LIS was already highly expanded (Marshall and Clarke 1997, 1999).

At the base of the H2 window, the cold surface conditions are recorded in glacial seawater values of average $\delta^{18}O$ and high % *N. pachyderma (s)* (Figure 4.13). Extreme cold conditions maintain the high $\delta^{18}O$ however a background IRD delivery reflects the pervasive iceberg/sea ice presence over the core site. This possibly designates the position of the polar front near the core site, its fluctuations reflected in those of %*N. pachyderma (s)* and IRD concentration. Discrete turbiditic pulses (indicated in peaks within the >63μm fraction) occur at 21.7 and 21.8 ka BP. The latter peak has high MS and high concentrations of quartz and K-feldspar, low concentrations of volcanic grains and a high quartz/plagioclase ratio indicating the British provenance of this material, NW Scotland geology being dominated by

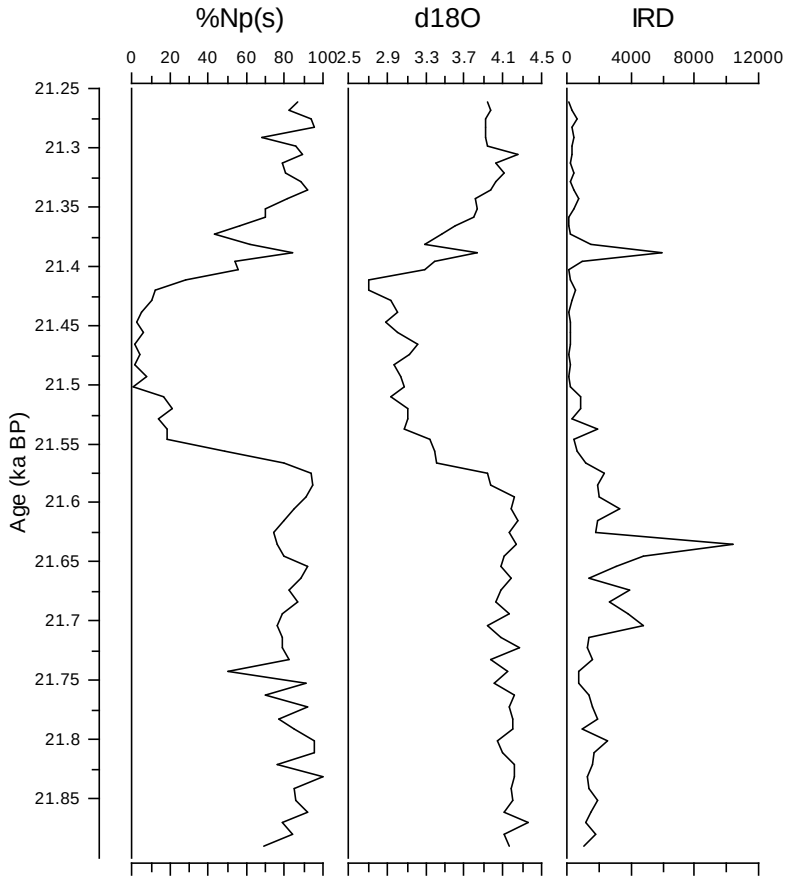

Figure 4.13: Heinrich Event 2 window within MD95-2006 as recorded in % N. pachyderma (s) and planktonic $\delta^{18}O$ (‰), showing the entire GIS 2 and IRD concentration showing the main two IRD events at 21.63 ka BP and 21.29 ka BP.

A southerly shift in the polar front is reflected in the stabilisation of %*N. pachyderma (s)* to >80%. This directly coincides with the main H2 event at 21.63 ka BP, recorded in a significant increase and large peaks in the IRD concentration. Lower Pb-ratios (Figure 3.19) indicate a change in provenance. However, although significant, the relatively small magnitude of the change in Pb-ratios precludes an exact provenance to be defined; the signature most likely to result from a combination of sources with a more significant contribution from northeastern Laurentide-derived material supported by the double peak in dolomitic carbonate. This interval represents the main H2 event during which the core records two IRD peaks: an initial smaller, broad peak and the subsequent major peak. MD95-2006 also records a double peak in % dolomitic carbonate (Figure 4.14). This double peak in dolomitic carbonate may represent the two-stage, pulsed delivery of LIS-sourced icebergs to the North Atlantic observed in

other studies (e.g. Bond et al 1999) and the former IRD peak representing a separate IRD pulse.

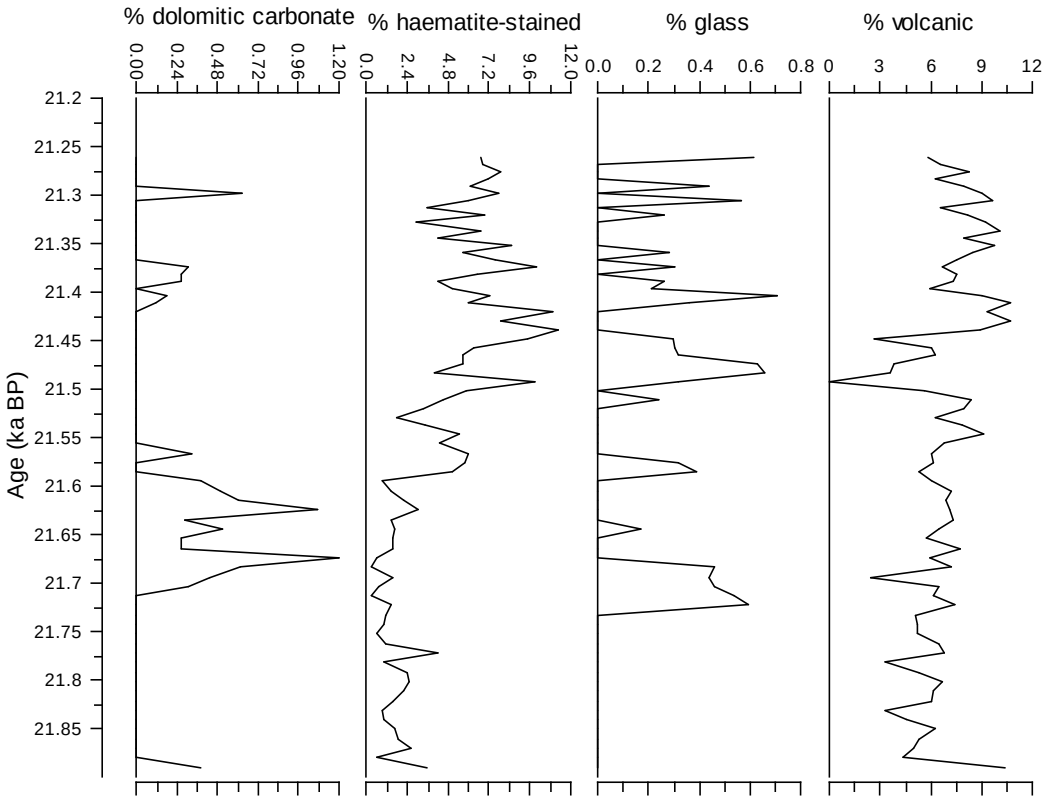

Figure 4.14: Main petrologic tracers from the H2 window in MD95-2006.

A similar pattern is also seen in VM23-81 (Figure 4.15), suggesting that this former IRD peak, is not unique to the Barra Fan site and is a robust feature of the North Atlantic record. This event, however, is unlikely to correlate with the 'precursor' event to H2 observed at other sites (Scourse et al 2000, Grousset et al 2001) as it occurs <100 years before the main H2 IRD peak. Despite the initial peaks in IRD and dolomite occurring in succession, the initial increase in these two proxies occurs simultaneously. This indicates that although the LIS did contribute to the H2 sediment on the British margin, it was significantly swamped by material from European/British sources during the two IRD peaks. The extremely low percentage dolomitic carbonate (1.2%) within the main peak, despite a relatively high overall concentration (30 grains g^{-1}) confirms this assertion. In contrast, the more open ocean location of VM23-81 (Bond et al 1999) sees lower dolomitic carbonate concentrations but a higher percentage in the main H2

IRD peak indicating the relative influence of this dilution of LIS material at the ice-proximal location of MD95-2006.

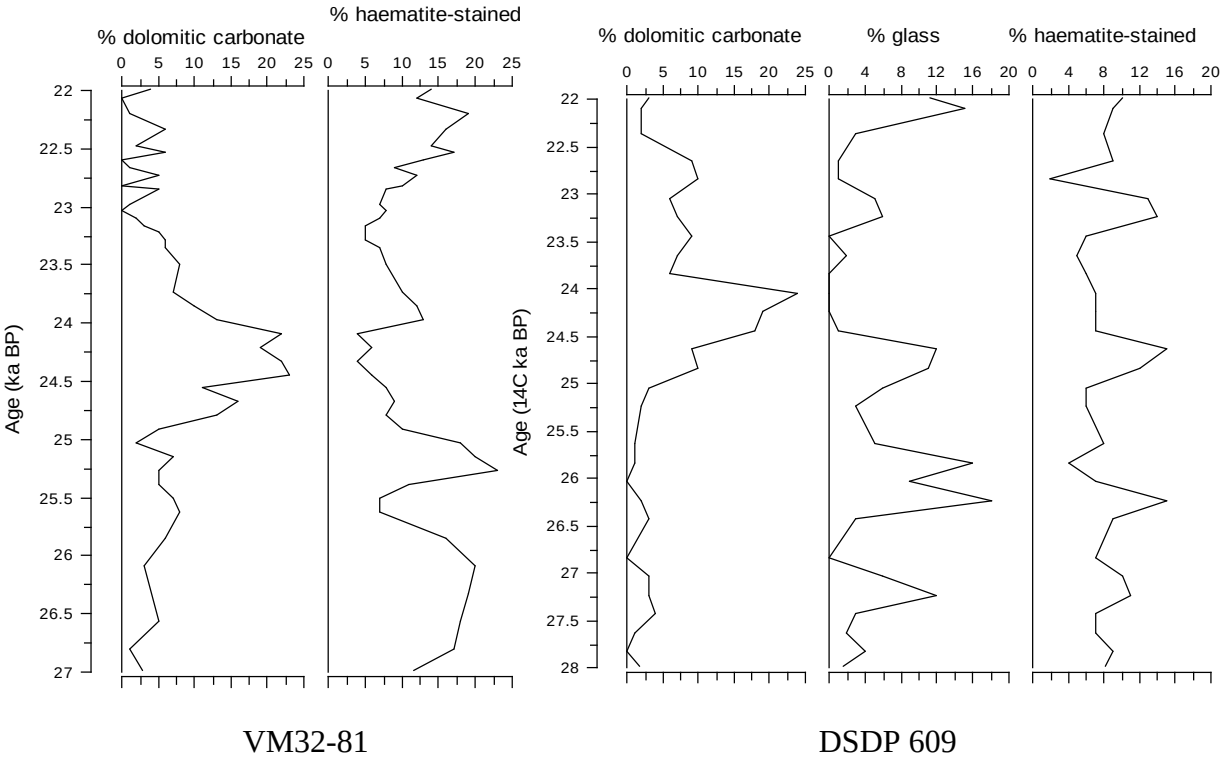

Figure 4.15: Main petrologic tracers recorded across the H2 window within cores from the IRD belt (DSDP 609) and the NE Atlantic (VM23-81) showing the sequencing between IRD delivery from different North Atlantic ice sheets (Bond et al 1999).

In VM23-81 the initial IRD peak is preceded by a peak in % Icelandic glass which in turn is preceded by a peak in % haematite-stained grains. DSDP 609 records simultaneous peaks in the two tracers (Icelandic glass and haematite-stained grains) prior to the main IRD peak (Figure 4.15; Bond et al 1999). This suggests a sequence of a Greenland surge prior to an Icelandic event delivered into a cyclonic oceanic gyre: Icelandic icebergs reaching the proximal site of VM23-81 before those from Greenland but the icebergs reaching the central Atlantic simultaneously. A subsequent European surge then occurred, possibly coeval with initial LIS surge but dolomite peak is slightly delayed due to time lag of LIS icebergs reaching the NE Atlantic core sites. The second, main IRD peaks are due to mainly LIS icebergs, hence the coherence of the main IRD peak and the second dolomite peaks in these records. (Although DSDP 609 has low resolution and may therefore not resolve the finer details). The pattern in

MD95-2006 is slightly different with only a small peak in glass occurring coeval with the initial IRD peak. The dolomitic carbonate peaks do reveal the contribution of LIS material but the significant absence of the peaks in Iceland- and Greenland-derived lithologies confirm the dominating influence of British material at this time. The percentages of both volcanic and haematite-stained grains increasing fivefold after 21.6 ka BP, coinciding with the end of the main H2 IRD event indicating the dramatic increase in the influence of these other North Atlantic sources outwith the heart of the Heinrich Layer.

There is no clear meltwater pulse recorded within H2. Instead $\delta^{18}O$ follows a decreasing trend, initially due to surface water freshening (occurring before the decrease in % *N. pachyderma (s)*) but subsequently reinforced by increasing sea surface temperatures. This shift is accompanied by a discrete interval of lighter planktonic $\delta^{13}C$ (Figure 3.6) possibly reflecting the meltwater lid and hence reduced surface water ventilation. A discrete peak in $\delta^{18}O$ around 1643cm is accompanied by a slight decrease in % *N. pachyderma (s)* indicating that it may be related to the transient influence of higher salinity surface waters from the south during a minor warming event. This warm event could have triggered a small BIS melting hence producing the surface water freshening recorded in $\delta^{18}O$ (ca.1640cm).

There is a sudden surface water warming at 21.58 ka BP (1638cm) indicated by decrease in % *N. pachyderma (s)*. This marks an interval of an overall lightening in $\delta^{18}O$ into GIS 2. Around a third of the way through the interstadial, $\delta^{18}O$ stabilises at values of ca. 3.2‰ indicating a balance between warm temperatures and the influence of higher salinity, warm water masses at a time of stronger THC. The amplitude of $\delta^{18}O$ change in MD95-2006 into interstadial associated with H2 (ca.1.5‰) is about twice as much as that within VM23-81 (ca.0.7; Bond et al 1999) even though they start at the same glacial value of ca.4‰. This may be explained by less of a warming at this location as %Np(s) only falls to ca.20% cf <10% within MD95-2006 or the effects of bioturbation upon a lower-resolution record.

Cooling out of the interstadial is reflected in a gradual increase in %*N. pachyderma (s)*, however at the same time $\delta^{18}O$ remains heavy with an excursion to even lower values.

This appears to coincide with the start of an interval with low overall planktic foram abundance. This may signify the influence of meltwater at that time, however, there is no corresponding IRD peak until significantly later. Hence this signifies that this interval represents a cooling and coincident reduction in the influence of higher salinity water masses from the south. As the polar front shifted southwards, increasing the dominance of *N. pachyderma (s)* in the foraminifer assemblage, the locus of iceberg/sea ice melt passed over the core site, producing the recorded IRD event at 21.39 ka BP; subsequently followed by colder northern water masses. The IRD peak is coincident with a brief cold interval seen in both the %*N. pachyderma (s)* and the $\delta^{18}O$ records prior to the more prolonged cold interval at the top of the H2 window, possibly indicating a fluctuation in the polar front before finally moving to stabilise further south once more. The coarse sediment within this IRD peak appears to have a significantly different provenance to the main H2 event with higher Pb-ratios and a higher contribution of metamorphic rock fragments and metamorphic minerals such as biotite, altered (dark) quartz and metamorphic rock fragments. Thus although the two separate IRD peaks may both contain similar crustally-derived sediment, the difference in Pb-ratios between the IRD events can be explained by the greater concentration of metamorphic grains and hence can quantify the difference in provenance.

One alternative and plausible explanation for this secondary IRD event is that it represents a BIS response to the main LIS-sourced Heinrich Event. A rise in regional sea level caused by the melting of LIS icebergs and subsequently sea ice during GIS 2 could have destabilised the marginal ice of the NW BIS (at this time reaching across the continental shelf) and calving icebergs from the margin. This response is likely to have been accompanied by a debris flow event triggered by the break-up of coastal ice, delivering reworked sediment and foraminifera to the core site. This could explain the short-lived peaks in % *N. pachyderma* (s) and $\delta^{18}O$ coeval with the lithic peak.

Planktonic foraminiferal $\delta^{18}O$ returns to near glacial sea water values above ca.1610cm reflecting the background conditions across the North Atlantic approaching the LGM.

There is an interesting distinction between the εNd(0) and Sr ratios of H2 compared to H4 samples, not only within MD95-2006 but within cores taken from across the whole

North Atlantic (Figure 4.16). H2 samples have a greater spread of values, indicated by the wider scatter of data points in Figure 4.16, indicating an IRD contribution from a larger number of different areas compared to H4 whose samples plot mainly towards higher $^{87}Sr/^{86}Sr$ and lower εNd(0). The only exceptions are H4 samples originating North of ca.60^{0}N, particularly those from the Norwegian Sea (Farmer et al 2003). This indicates that although the Fennoscandian Ice Sheet was of large enough extent at the time of H4 to participate, the volume of IRD was low enough to be swamped by the larger contribution from the LIS in areas distal to the FIS. This, along with the data from MD95-2006 (proximal to the BIS) show that at the time of H4, the LIS was by far the dominant contributor to the event resulting in the much lower εNd(0) signifying the sediment's origin from the ancient Canadian Shield areas of North America (Figure 4.12). Clearly at the time of H2, all circum-North Atlantic ice sheets were approaching maximum extent and this is reflected in the spread of the data in Figure 4.16, with ice-proximal samples having εNd(0) and $^{87}Sr/^{86}Sr$ values tending towards those characteristic of the landmass they are closest to (Figure 4.12) and IRD belt samples reflecting the now less dominant but still significant contribution of LIS-sourced icebergs.

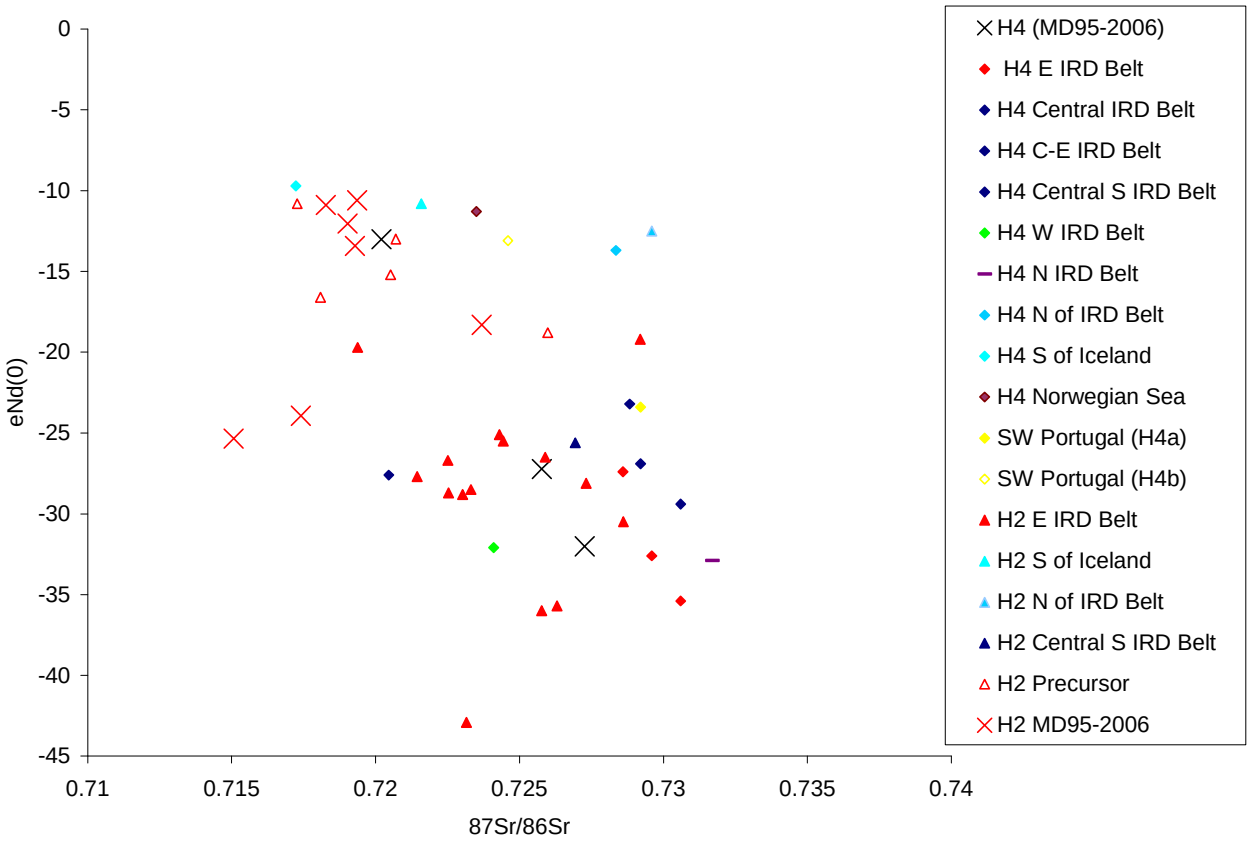

Figure 4.16: $^{87}Sr/^{86}Sr$ vs. εNd(0) plot of core samples taken from H2 (triangles) and H4 (diamonds) horizons taken from different locations across the North Atlantic along with all samples from the H2 and H4 windows within MD95-2006. Data is from Revel et al 1996, Hemming et al 1998, Snoeckx et al 1999, Grousset et al 2001, Farmer et al 2003).

5. Summary and Conclusions

This study has provided new data constraining the timing and dynamics of the growth of the British Ice Sheet during MIS 3 and MIS 2 (ca.40-20 ka BP). At the time of Heinrich Event 4, placed at 36.2-36.7 ka BP, the BIS was of limited extent, at least as regards the lateral ice sheet limits in NW Scotland, proximal to the Barra Fan. Significant ice sheet expansion only occurred after ca.26.5 ka BP, coinciding with the MIS3/2 transition in the MD95-2006 record. At this time the BIS most likely expanded laterally and in volume, extending out across the continental shelf. IRD delivery increased at this time due to the break-up of increasingly unstable maritime ice shelves and increased iceberg discharge. It appears that the margin of the BIS reached the continental slope around 25 ka BP as MD95-2006 records a pronounced interval of turbidite activity at this time, produced through slope sediment destabilisation and mass flow triggered by the ploughing/bulldozing activity of the marginal ice. It is likely that this period (21.5-25 ka BP) represents the maximum extent of the NW Scottish ice sheet (if not the BIS as a whole) as the lithic delivery to the Barra Fan is significantly reduced subsequently.

This background signal of BIS growth is punctuated by discrete events in the sedimentary record, the most significant being the Heinrich Events. The nature of the Heinrich Events as recorded in MD95-2006 reflects a combined signal of the relative influence of the Barra Fan's ice-proximal location (i.e. the local signal), that of the general North Atlantic glacial stage and the contribution from other circum-North Atlantic ice sheets. At the time of H4 (dated at 36.59 ka BP), the BIS is of limited extent whereas the LIS was already significantly expanded, thus the dominant signal seen in H4 in MD95-2006 is that of LIS icebergs, overcoming the BIS contribution. This is revealed in the discrete peak of IRD that defines the position of in H4 compared to low background concentrations at the time, the significantly lower Pb-ratios and εNd(0) of this IRD peak compared to the background and the overall lower IRD concentration of IRD in the H4 peak compared to the other Heinrich Events. In contrast, H2 (dated at 21.63 ka BP) occurs at a time of high background lithic delivery and sees much higher peak IRD concentrations with relatively little difference in radioisotopic ratios compared to the background. This indicates the increased delivery of icebergs to the site from all North Atlantic ice sheets but also the dominating influence of BIS icebergs both

in the increased background level of IRD delivery and the correspondence of background and peak IRD radioisotopic ratios tending towards British provenance.

It seems that throughout the studied period, the palaeoceanographic conditions at the location of MD95-2006 are in direct response to the dynamics of the polar front: there is coeval variation of planktonic $\delta^{18}O$ and % *N. pachyderma* (s); foraminiferal concentration peaks during the transitions in and out of each interstadial reflecting the transitional presence of the frontal high-productivity zone; the coincidence of many IRD peaks with transitions in $\delta^{18}O$ and % *N. pachyderma* (s). Frontal movements reflect changes in the relative influence of warmer, more saline southern waters delivered by the North Atlantic Current and colder northern water masses. Thus the location of the Barra Fan, combined with the high sedimentation rates, makes it an ideal site to investigate the balance between these water masses over the last glacial cycle, capturing the high-resolution, millennial- and centennial-scale dynamics. A major influence on the dynamics of water masses and thus the position of the polar front is the strength of the North Atlantic overturning circulation, which in turn influences the wider climate of the region. Therefore the assumptions behind the correlation of the core's *N. pachyderma* (s) record with the GRIP temperature record in order to produce the new age model, are likely to be highly accurate.

Future work should aim to extend this high-resolution study to the rest of the core. Focus should be placed on the Heinrich Event and Detrital Events, in particular further constraining their provenance through quantitative techniques and how this provenance signature may change within different sediment grain-size fractions related to their transport to the core site. Efforts should be made to carry out similar studies on cores across the North Atlantic, in both open ocean sites and locations proximal to all the main North Atlantic ice sheets, in order to correlate and compare records. This should provide invaluable information on the relative timing and dynamics of the circum-North Atlantic ice sheets and the relationship with the background climatic and oceanographic conditions throughout a glacial cycle.

Appendix 1:

Two-Stage Model Age Equation and Parameters

Mantle Evolution Curve is plotted from the solutions of the following equations from time t = 4.56Ga to t = 0.

$$^{206}Pb/^{204}Pb_{(t)} = {}^{206}Pb/^{204}Pb_{(T)} + (^{238}U/^{204}Pb)^{\lambda(T-t)} \quad (1)$$

$$^{207}Pb/^{204}Pb_{(t)} = {}^{207}Pb/^{204}Pb_{(T)} + (^{235}U/^{204}Pb)^{\lambda(T-t)} \quad (2)$$

Where:

- $^{206}Pb/^{204}Pb_{(t)}$ or $^{207}Pb/^{204}Pb_{(t)}$ = Isotopic Ratio at time t.
- $^{206}Pb/^{204}Pb_{(T)}$ or $^{207}Pb/^{204}Pb_{(T)}$ = Initial Isotopic Ratio at time T.

Ratio	Initial Isotopic Ratios at T =4.56Ga taken from the Troilite (PbS) phase in the Canyon Diablo iron Meteorite (Tatsumoto et al 1973)
$^{206}Pb/^{204}Pb$	9.307
$^{207}Pb/^{204}Pb$	10.294
$^{208}Pb/^{204}Pb$	29.476

- λ = Decay Constant

Isotope	Decay Constant
^{238}U	1.55125×10^{-10}
^{235}U	9.8485×10^{-10}
^{232}Th	0.49475×10^{-10}

- $^{238}U/^{204}Pb = \mu$ = initial mantle reservoir value and $^{235}U/^{204}Pb = (^{238}U/^{204}Pb)/137.88$

When calculating values for the $^{206}Pb/^{204}Pb$ Two-Stage Age Model:

- From 4.56 Ga to t = 3.70 Ga, T=4,56Ga and $^{238}U/^{204}Pb = 7.19$.
- From 3.70Ga to t=0, T = 3.7Ga and $^{238}U/^{204}Pb = 9.74$.

Appendix 2:

Average Lead Isotopic Ratios for the Main North Atlantic Terranes

Province		$^{206}Pb/^{204}Pb$	$^{207}Pb/^{204}Pb$	$^{208}Pb/^{204}Pb$
Churchill	Mean	24.46758	16.21877	40.09748
	σ	14.0715	1.599655	7.703807
Superior	Mean	15.46163	14.94341	35.04941
	σ	3.15458	0.585497	2.686861
Appalachian	Mean	18.60134	15.67876	38.60296
	σ	0.174998	0.198527	0.356974
Grenville	Mean	17.44838	15.48276	37.34087
	σ	1.186755	0.126429	1.408053
Greenland	Mean	14.94014	14.55614	34.95204
	σ	4.189353	1.312011	4.212616
Scandinavia	Mean	18.93026	15.67971	37.94086
	σ	3.692747	0.474304	2.512572
Britain	Mean	18.60134	15.67876	38.6029
	σ	0.174998	0.198527	0.356974
Scotland	Mean	17.32294	15.44568	37.54031
	σ	2.545154	0.105157	0.531436
Ireland	Mean	18.35173	15.5885	38.0935
	σ	0.48008	0.15157	1.41328

Sources of Data

Churchill Province: Doe (1967), Robertson and Cumming (1968), Sinha (1970), Sangster (1978), Cumming and Krstic (1991)

Superior Province: Tilton and Steiger (1969), Steiger and Wasserburg (1969), Gariepy and Allegre (1985), Brevart et al (1986), Deloule et al (1989), Tilton and Kwon (1990), Carignam et al (1993), Carignan and Gariepy (1993)

Appalachian: Vitrac et al (1981), Wilbur et al (1990)

Grenville Province: Doe (1962), Zartman and Wasserburg (1969), Fletcher and Farquhar (1982)

Greenland: Taylor et al (1980), Baadsgaard et al (1986), Kalsbeek et al (1988)

Scandinavia: Sundblad and Stephens (1983), Duane and de Wit (1988), Romer and Wright (1993), Birkland et al (1993), Bjorlykke et al (1993)

Britain: Blaxland et al (1979), Dixon et al (1990), Vitrac et al (1981), Duane and de Wit (1988)

Scotland: Blaxland et al (1979), Dixon et al (1990), Duane and de Wit (1988)

Ireland: Dixon et al (1990), Duane and de Wit (1988)

6. References

Abouchami W., and Zabel M., 2002, The Pb isotopic record of terrigenous input into the tropical Atlantic, *Geochimica et Cosmochimica Acta* **66**, A6

Alley R.B., 1998, Icing in the North Atlantic, *Nature* **392**, pp.335-336

Alley R.B., 2000, Continuity comes first: recent progress in understanding subglacial deformation. *In*: Maltman A.J., Hubbard M.J., Hambrey M.J., (Eds), Deformation of Glacial Material, *Geological Society Special Publication* **176**, pp.171-180

Alley R.B. and MacAyeal D.R., 1994, Ice-rafted debris associated with binge-purge oscillations of the Laurnetide Ice Sheet, *Palaeocenaography* **9**, pp.503-511

Alley R. B., Clark P. U., Keigwin L. D., Webb R. S., 1999, Making sense of millennial-scale climate change, In: Mechanisms of Global Climate Change at Millennial Time Scales, P.U. Clark et al (eds), *Geophysical Monograph* **112**, pp.385-394

Anderson B. G., 1981, Late Weichselian ice sheets in Eurasia and Greenland. In: Denton G. H., and Hughes T.J., (eds), *The Last Great Ice Sheets*, Wiley, New York, pp.1-65

Andersen T., Andresen A., Sylvester A. G., 2001, Nature and distribution of deep crustal reservoirs in the southwestern part of the Baltic Shield: evidence from Nd, Sr and Pb isotope data on late Sveconorwegian granites, *Journal of the Geological Society London* **158**, pp.253-267

Andrews J.T., 2000, Icebergs and iceberg rafted detritus (IRD) in the North Atlantic: facts and assumptions, *Oceanography* **13**, pp.100-108

Andrews J. T., and Barber D. C., 2002, Dansgaard-Oeschger Events: is there a signal off the Hudson Strait Ice Stream?, *Quaternary Science Reviews* **21**, pp.443-454

Andrews J.T., and Maclean B., 2003, Hudson Strait ice streams: a review of stratigraphy, chronology and links with North Atlantic Heinrich events, *Boreas* **32(1**), pp.4-17

Andrews, J.T. and K. Tedesco, 1992, Detrital carbonate-rich sediments, Northwestern Labrador Sea: Implications for ice-sheet dynamics and iceberg rafting (Heinrich) events in the North Atlantic, *Geology* **10**, pp.1087-1090

Andrews J. T., Jennings A. E., MacLean B. C., Mudie P. J., Praeg D., Vilks G., 1991, The surficial Geology of the Canadian eastern Arctic and polar continental shelves, *Continental Shelf Research*, pp.111-819

Andrews J. T., Erlenkeuser H., Tedesco K., Aksu A., Jull A. J. T., 1994, Late Quaternary (stage 2 and 3) meltwater and Heinrich Events, Northwest Labrador Sea, *Quaternary Research* **41**, pp.26-34

Andrews J. T., Jennings A. E., Cooper T. A., Williams K. M., Mienert J., 1996, Late Quaternary sedimentation along a fjord to shelf (trough) transect, east Greenland (ca.68^{0}N), in: Andrews J. T., Austin W. E. N., Bergsen H., Jennings A. E. (eds), Late Quaternary Palaeoceanography of the North Atlantic Margins, *Geological Society of London Special Publication*, pp.153-166

Andrews J.T., Cooper T.A., Jennings A.E., 1998, Late Quaternary iceberg-rafted detritus events on the Denmark Strait Southeast Greenland continental slope (similar to 65 degrees N): Related to north Atlantic Heinrich events? *Marine Geology* **149(1-4)**, pp.211-228

Atkinson F. W., Lawson T. J., Smart P. L., Harmon R. S., Hess J. W., 1986, New data on speleothem deposition and palaeoclimate in Britain over the last forty thousand years, *Journal of Quaternary Science* **1**, pp.67-72

Auffret G. A., Boelart A., Vergnaud-Grazzini C., Muller C., Kerbrat R., 1996, Identification of Heinrich Layers in core KS01 North Eastern Atlantic (46^{0}N, 17^{0}W), implications for their origin, *Marine Geology* **131**, pp.5-20

Austin W. E. N., and Kroon D., 1996, Late glacial sedimentology, foraminifera and stable isotope stratigraphy of the Hebridean Continental Shelf, Northwest Scotland. *In* Andrews J. T., Austin W. E. N., Bergsten H and Jennings A. E., (eds) Late Quaternary Palaeoceanography of the North Atlantic Margins. *Geological Society, London, Special Publications* **111**, pp.187-213

Austin W.E.N., Wilson L.J., Hunt J.B., 2004, The age and chronostratigraphical significance of North Atlantic Ash Zone II, *Journal of Quaternary Science* **19(2)**, pp.137-146

Baadsgaard H., Nutman A. P., Rosing M., Bridgewater D., Longstaffe F. J., 1986, Alteration and metamorphism of Amitsoq gneisses from the Isukasia area, west Greenland: Recommendations for isotope studies of the early crust, *Geochimica et Cosmochimica Acta* **50**, pp.2165-2172

Ballantyne C.K., Hallam G.E., 2001, Maximum altitude of Late Devensian glaciation on South Uist, Outer Hebrides, Scotland, *Proceedings of the Geologists Association* **112**, pp.155-167

Ballantyne C.K., McCarroll D., Nesje A., Dahl S.O., Stone J.O., 1998, The last ice sheet in North-West Scotland: Reconstructions and implications, *Quaternary Science Reviews* **17**, pp.1149-1184

Bamber J.L., Vaughan D.G., Joughin I., 2000, Widespread complex flow in the interior of the Antarctic Ice Sheet, *Science* **287**, pp.1248-1250

Behl R. J., and Kennet J. P., 1996, Brief interstadial events in the Santa Barbera basin, NE Pacific, during the past 60kyr, *Nature* **379**, pp.243-246

Bentley C.R., and Giovinetto M.B., 1991, Mass balance of Antarctica and sea level change. *In*: Weller G., Wilson C.L., Sevberin B.A.B. (Eds), International Conference on the Role of the Polar Regions in Global Change: Proceedings of a conference held June 11-15, 1990 at the University of Alaska Fairbanks, Vol II, Geophysical Institute/Centre for Global Change and Arctic Systems Research, Fairbanks, pp.481-488

Bennett M.R., 2003, Ice streams as the arteries of an ice sheet: their mechanics, stability and significance, *Earth-Science Reviews* **61**, pp.309-339

Bertram C. J., Elderfield H., Shackleton N. J., MacDonald J. A., 1995, Cadmium/calcium and carbon isotope reconstruction of the glacial northeast Atlantic Ocean, *Palaeoceanography* **10(3),** pp.563-578

Bianchi G. G., and McCave I. N., 1999, Holocene periodicity in North Atlantic climate and deep-ocean flow south of Iceland, *Nature* **397**, pp.515-517

Bigg G.R., Wadley M.R., 2001, The origin and flux of icebergs released into the Last Glacial Maximum Northern Hemisphere oceans: the impact of ice-sheet topography, *Journal of Quaternary Science* **16(6)**, pp.565-573

Birkland A., Ihlen P. M., Bjorlykke A., 1993, The sources of metals in sulphide deposits in the Helgeland nappe Complex, north-central Norway: Pb isotopic evidence, *Economic Geology* **88**, pp.1810-1829

Biscaye P. E., Grousset F. E., Dasch E. J., Huon S., 1996, Rb-Sr isotope system as a tracer of provenance in marine sediments and aerosols: Atlantic Ocean, Marine Geology

Biscaye P.E., and Ettreim S.L., Suspended particulate loads and transports in the nepheloid layer of the abyssal Atlantic Ocean, *Marine Geology* **23**, pp.155-172

Bjorlykke A., Vokes F. M., Birkland A., Thorpe R. I., Lead isotope systematics of strata-bound sulphide deposits in the caledonides of Norway, *Economic Geology* **88**, pp.397-417

Blankenship D.D., Bell R.E., Hodge S.M., Studinger M., Behrendt J.C., Finn C.A., 1993, Active volcanism beneath the West Antarctic Ice Sheet and implications for ice-sheet stability, *Nature* **361**, pp.526-529

Blankenship D.D., Morse D.L., Finn C.A., Bell R.E., Peters M.E., Kempf S.D., Hodge S.M., Studinger M., Behrendt J.C., Brozena J.M., 2001, Geologic controls on the initiation of rapid basal motion for West Antarctic ice streams: a geophysical perspective including new airborne radar sounding and laser altimetry results. *In*: Alley R.D., Bindschadler R. (Eds), The West Antarctic Ice Sheet: Behaviour and Environment. *Antarctic Research Series*, **77**, American Geophysical Union, Washington DC, pp.105-121

Blaxland A. B., Aftalion M., Van Breemen O., 1979, Pb isotopic composition of feldspars from Scottish Caledonidian granites, and the nature of the underlying crust, *Scottish Journal of Geology* **15**(2), pp.139-151

Blunier T., Chappellaz J., Schwander J., Dallenbach A., Stauffer B., Stocker T. F., Raynauld D., Jouzel J., Clausen H. B., Hammer C. U., Johnsen S. J., 1998, Asynchrony of Antarctic and Greenland climate change during the last glacial period, *Nature* **394**, pp.739-743

Bond G. C., and Lotti R., 1995, Iceberg discharges into the North Atlantic on millennial time scales during the last deglaciation, *Science* **267**, pp.1005-1010

Bond G. C., Heinrich H., Broecker W., Labeyrie L., McManus J., Andrews J., Huon S., Jantschik R., Clasen S., Simet C., Tedesco K., Klas M., Bonani G., Ivy S., 1992, Evidence for massive discharges of icebergs into the North Atlantic Ocean during the last glacial, *Nature* **360**, pp.245-249

Bond G. C., Broecker W., Johnsen S., McManus J., Labeyrie L., Jouzel J., Bonani G., 1993, Correlations between climate records from North Atlantic sediments and Greenland ice, *Nature* **365**, pp.143-147

Bond G. C., Showers W., Cheseby M., Lotti R., Almasi P., de Menocal P., Priore P., Cullen H., Hadjas I., Bonani G., 1997, Apervasive millennial-scale cycle in North Atlantic Holocene and Glacial climates, *Science* **278**, pp.1257-1266

Bond G. C., Showers W., Elliot M., Evans M., Lotti R., Hadjas I., Bonani G., Johnsen S., 1999, The North Atlantic's 1-2kyr Climate Rhythm: Relation to Heinrich Events, Dansgaard-Oeschger Cycles and the Little Ice Age, In: Mechanisms of Global Climate Change at Millennial Time Scales, P.U. Clark et al (eds), *Geophysical Monograph* **112**, pp.35-58

Boulton G.S., 1972, The role of thermal regime in glacial sedimentation, *Instit. Br. Geogr. Spec. Publ.* **4**, pp.1-19

Boulton G.S., Smith G.D., Jones A.S., Newsom J., 1985, Glacial geology and glaciology of the last mid-latitude ice sheets, *Journal of the Geological Society, London* **142**, pp.447-474

Boulton G.S., Caban P.E., Vangijssel K., 1995, Groundwater flow beneath Ice Sheets. 1.Large-scale patterns, *Quaternary Science Reviews* **14(6)**, pp.545-562

Boulton G.S., Donglemans P., Punkari M., Broadgate M., 2001, Palaeoglaciology of an ice sheet through a glacial cycle: the European ice sheet through the Weichselian, *Quaternary Science Reviews* **20**, pp.591-625

Bowen D.Q., Rose J., McCabe A.M., Sutherland D.G., 1986, Correlation of Quaternary glaciations in England, Ireland, Scotland and Wales, *Quaternary Science Reviews* **5**, pp.299-340

Bowen D. Q., Phillips F. M., McCabe A. M., Knutz P. C., Sykes G. A., 2002, New data for the Last Glacial Maximum in Great Britain and Ireland, *Quaternary Science Reviews* **21**, pp.89-101

Brevart O., Dupre B., Allegre C. J., 1986, Lead-ages of komatiitic lavas and limitations on the structure and evolution of the Precambrian mantle, *Earth and Planetary Science Letters* **77**, pp.293-302

Briner J.P., Miller G.H., Davis P.T., Finkel R.C., 2005, Cosmogenic exposure dating in arctic glacial landscapes: implications for the glacial history of northeastern Baffin Island, Arctic Canada, Canadian Journal of Earth Sciences, 42(1), pp. 67-84

Broecker W.S., 1992, Climate Cycles – Upset for Milankovich Theory, *Nature* **359**, pp.779-780

Broecker W. S., 1994, Massive iceberg discharges as triggers for global climate change *Nature* **372**, pp.421-424

Broecker W. S., Bond G., Klas M., Bonani G., Wolfli W., 1990, A salt oscillator in the glacial North Atlantic?: 1. The Concept, *Palaeoceanography* **5**, pp.469-477

Broecker W.S., Bond G., McManus J., Klass M., Clark E., 1992, Origin of the North Atlantic's Heinrich Events, *Climate Dynamics* **6**, pp.265-273

Carignan J., and Gariepy C., 1993, Pb-isotopic geochemistry of the Silidor and Launay gold deposits: Implications for the source of Archean Au in the Abitibi subprovince, *Economic Geology* **88**, pp.1722-1730

Carignan J., Gariepy C., Machado N., Rive M., 1993, Pb-isotopic geochemistry of granitoids and gneisses from the late Archean Pontiac and Abitibi subprovinces of Canada, *Chemical Geology* **106**, pp.299-316

Chapman M. R., and Shackleton N. J., 1999, Global ice volume fluctuations, north Atlantic ice-rafting events and deep ocean circulation changes between 130 and 70ka, *Geology* **27(9)**, pp.795-798

Chappell J., 2002, Sea level changes forced ice breakouts in the Last Glacial Cycle: new reults from coral terraces, *Quaternary Science Reviews* **21(10),** pp.1229-1240

Charlesworth J. K., 1966, The Geology of Ireland, Oliver and Boyd (Pub), London, UK

Chassery S., Grousset F.E., Lavaux G., et al., 1998, Sr-87/Sr-86 measurements on marine sediments by inductively coupled plasma-mass spectrometry, *Fresenius Journal of Analytical Chemistry*, **360(2),** pp.230-234

Chi J., Mienert J., 1996, Linking physical property records of quaternary sediments to Heinrich events, *Marine Geology* **131(1-2**), pp.57-73

Chough S.K., and Hesse R.,1987, The Northwest Atlantic midocean channel of the Labrador Sea. 4. Petrography and Provenance of the sediments, *Canadian Journal of Earth Sciences* **24(4)** pp.731-740

Clark P. U., 1987, Subglacial sediment dispersal and till composition, *Journal of Geology* **95**, pp.527-541

Clarke G. K. C., Marshall S. J., Hillaire-Marcel C., Bilodeau G., Viega-Pires C., 1999, A glaciological perspective on Heinrich Events, In: Mechanisms of Global Climate Change at Millennial Time Scales, P.U. Clark et al (eds), *Geophysical Monograph* **112**, pp.243-262

Cortijo E., Labeyrie L., Elliot M., Blabon E., Tisnerat N., 2000, Rapid climate variability of the North Atlantic Ocean and global climate: a focus of the IMAGES program, *Quaternary Science Reviews* **19**, pp.227-241

Croudace I.W., Anders R., Rothwell R.G., submitted, ITRAX: description and evaluation of a new X-ray core scanner

Cumming G. L., and Krstyc D., 1991, Geochronology of the Namew Lake Ni-Cu deposit, Flin Flon area, Manitoba, Canada: A pb/Pb study of whole rocks and ore minerals, *Canadian Journal of Earth Sciences* **28**, pp.1328-1339

Dansgaard W., Johnsen S. J., Clausen H. B., Dahl-Jensen D., Gundestrup N. S., Hammer C. U., Hvidberg C. S., Steffensen J. P., Sveinbjornsdottir A. E., Jouzel J., Bond G., 1993, Evidence for general instability of past climate from a 250-kyr ice-core record, *Nature* **364**, pp.218-220

Darby D.A., and Bischof J.F., A statistical approach to source determination of lithic and Fe oxide grains: An example from the Alpha Ridge, Arctic Ocean, *Journal of Sedimentary Research* **66 (3)**, pp599-607

Dasch E.J., 1969, Sr isotopes in weathering profiles, deep-sea sediments and sedimentary rocks, *Geochimica et Cosmochimica Acta* **33**, pp.1521-1552

Deloule E., Gariepy C., Dupre B., 1989, Metallogenesis of the Abitibi Greenstone Belt of Canada: A contribution from the analysis of trace lead in sulphide minerals, *Canadian Journal of Earth Sciences* **26**, pp.2529-2540

Denton G. H., and Hendy C. H., Younger Dryas age advance of Franz Joseph glacier in the Southern Alps of New Zealand, *Science* **264**, pp.1434-1437

Denton G.H., Heusser C.J., Lowell T.V., Moreno P.I., Andersen B.G., Heusser L.E., Schluchter C., Marchant D.R., 1999, Interhemispheric linkage of palaeoclimate during the last glaciation, *Geografiska Annaler* **81A**, pp.107-153

Dickin A. P., 1997, Radiogenic Isotope Geology, Cambridge University Press, UK.

Dixon P. R., LeHuray A. P., Rye D. M., 1990, Basement geology and tectonic evolution of Ireland as deduced from Pb isotopes, *Journal of the Geological Society London* **147**, pp.121-132

Doe B. R., 1962, Relatioships of lead isotopes among granites, pegmatites and sulphide ores near Balmat, New York, *Journal of Geophysical Research* **67**(7), pp.2895-2906

Doe B. R., 1967, The bearing of Lead isotopes on the source of granitic magma, *Journal of Petrology* **8**(1), pp.51-83

Dowdeswell J.A., 1986, The distribution and character of sediments in a tidewater glacier, southern Baffin Island, N.W.T., Canada, *Arctic and Alpine Research* **18**, pp.45-46

Dowdeswell J.A., and Murray T., 1990, Modelling rates of sedimentation from icebergs. *In*: Glacimarine Environments: Process and Sediments. J.A. Dowdeswell and J.D., Scourse (Eds), *Geological Society Special Publication*, pp.121-137

Dowdeswell J.A., Elverhoi A., Spielhagen R., 1998,Glacimarine sedimentary processes and facies on the Polar North Atlantic margins, *Quaternary Science Reviews* **17(1-3)**, pp.243-272

Dowedswell J.A., and Siegert M.J., 1999, The dimensions and topographic setting of Antarctic sub-glacial lakes and implications for large-scale water storage beneath continental ice sheets, *Geological Society of America Bulletin* **111**, pp.254-263

Dowdeswell J. A., Maslin M. A., Andrews J. T., McCave I. N., 1995, Iceberg production, debris rafting and the extent and thickness of Heinrich layers (H1, H2) in North Atlantic sediments, *Geology* **23**(4), pp.301-304

Dowdeswell J.A., Whittington R.J., Hodgkins R., 1992, The sizes, frequencies and freeboards of East Greenland icebergs observed using ship radar and sextant, *Journal of Geophysical Research-Oceans* **97(C3)**, pp3515-3528

Dowdeswell J. A., Elverhoi A., Andrews J. T., Hebbeln D., 1999, Asynchronous deposition of ice-rafted layers in the Nordic Seas and North Atlantic Ocean, *Nature* **400**, pp.348-351

Drewry D., 1986, Glacial Geologic Processes, London, Edward Arnold

Duane M. J., and de Wit M. J., 1988, Pb-Zn ore deposits of the northern Caledonides: Products of continental-scale fluid mixing and tectonic expulsion during continental collision, *Geology* **16**, pp.999-1002

Ehlers J., Gibbard P.L., Rose J., (eds), 1991, *Glacial Deposits in Britain and Ireland*, Balkema, Rotterdam.

Elliot M., Labeyrie L., Bond G., Cortijo E., Turon J. L., Tisnerat N., Duplessy J-C., 1998, Millennial-scale iceberg discharges in the Irminger Basin during the last glacial period: relationship with Heinrich Events and environmental settings, *Palaeoceanography* **13(5),** pp.433-446

Elliot M., Labeyrie L., Dokken T., Manthe S., 2001, Coherent patterns of ice-rafted debris deposits in the Nordic regions during the last Glacial (10-60ka), *Earth and Planetary Science Letters* **194**, pp.151-163

Elverhoi A., Hooke R., Le B., Solheim A., 1998, Late Cenozoic erosion and sediment yield from the Svalbard-Barents Sea Region: implications for understanding erosion of glacierised basins, *Quaternary Science Reviews* **17**, pp.119-125

Farmer G. L., Barber D., Andrews J., Provenance of Late Quaternary ice-proximal sediments in the North Atlantic: Nd, Sr and Pb isotopic evidence, *Earth and Planetary Science Letters* **209**, pp.227-243

Fettes D. J. and Mendum J. R., 1987, The evolution of the Lewisian Complex in the Outer Hebrides. *In:* Park R. G. and Tarney J. (eds), Evolution of the Lewisian and comparable PreCambrian High-grade terrains, *Geological Society of London Special Publication* **27**, pp.27-44

Fillon R.H., Miller G.H., Andrews J.T.,1981, Terrigenous sand in Labrador Sea hemipelagic sediments and paleoglacial events on Baffin island over the last 100,000 years, *Boreas* **10(1)**, pp.107-124 1981

Fitton, J. G., Saunders, A. D., Larsen, L. M., Hardarson, B. S., & Norrey M. J., 1998. Volcanic Rocks from the southeast Greenland Margin at 63°N: composition, petrogenesis, and mantle sources, *Proceedings of the Ocean Drilling Program Scientific Results* **152**, pp.331-350

Fletcher I. R., and Farquhar R. M., 1982, The protocontinental nature and regional variability of the central metasedimentary belt of the Grenville Province: Lead isotopic evidence, *Canadian Journal of Earth Science* **29**, pp.239-253

Francois R., and Bacon M. P., 1994, Heinrich events in the North Atlantic: radiochemical evidence, *Deep-Sea Research* **41**(2), pp.315-334

Francois R., Altabet M.A., Yu E.F., et al., 1997, Contribution of Southern Ocean surface-water stratification to low atmospheric CO2 concentrations during the last glacial period, *Nature* **389(6654)**, pp.929-935

Fronval T., Jansen E., Bloemendal J., Johnsen S., 1995, Oceanic evidence for coherent fluctuations in Fennoscandian and Laurentide ice sheets on millennial timescales, *Nature* **374**, pp.443-446

Gariepy C., and Allegre C. J., 1985, The lead isotope geochemistry and geochronology of late-kinematic intrusives for late-Archaean crustal evolution, *Geochimica et Cosmochimica Acta* **49**, pp.2371-2383

Grimm E. C., Jacobson G. L., Watts W. A., Hansen B.C.S., Maasche K. A., 1993, A 50,000-yr record of climate oscillations from Florida and its temporal correlation with the Heinrich Events, *Science* **261**, pp.198-200

Grootes P. M., and Stuiver M., 1997, Oxygen 18/16 variability in Greenland snow and ice with 10^{-3} to 10^{5} year time resolution, *Journal of Geophysical Research* **102 (C12),** pp.26455-26470

Grootes P. M., Stuiver M., White J. W. C., Johnsen S., Jouzel J., 1993, Comparison of oxygen isotope records from the GISP2 and GRIP Greenland Ice Cores, *Nature* **366**, pp.552-554

Grousset F. E., Biscaye P. E., Zindler A., Prospero J., Chester R., 1988, Neodymium isotopes as tracers in marine sediments and aerosols, *Earth and Planetary Science Letters* **87**, pp.367-378

Grousset F. E., Biscaye P. E., Revel M., Petit J. R., Pye K., Joussaume S., Jouzel J., 1992, Antarctic (Dome C) ice-core dust at 18kyr BP: isotopic constraints on origins, *Earth and Planetary Science Letters* **111**, pp.175-182

Grousset F. E., Labeyrie L., Sinko J. A., Cremer M., Bond G., Duprat J., Cortijo E., Huon S., 1993, Patterns of ice-rafted detritus in the glacial north Atlantic (40-55°N), *Palaeoceanography* **8**, pp.175-192

Grousset F. E., Pujol C., Labeyrie L., Auffret G., Boelaert A., 2000, Were the North Atlantic Heinrich Events triggered by the behaviour of European Ice Sheets?, *Geology* **28**, pp.123-126

Grousset F. E., Cortijo E., Huon S., Herve L., Richter T., Burdloff D., Duprat J., Weber O., 2001, Zooming in on Heinrich Layers, *Palaeoceanography* **16**, pp.240-259

Goldstein S. L., O'Nions R. K., Hamilton P. J., 1984, A Sm-Nd isotopic study of dusts and particulates from major river systems, *Earth and Planetary Science Letters* **70**, pp.221-236

Gwiazda R. H., Hemming S. R., Broecker W. S., 1996a, Tracking the sources of icebergs with lead isotopes: The provenance of ice-rafted debris in Heinrich layer 2, *Palaeoceanography* **11**, pp.77-93

Gwiazda R. H., Hemming S. R., Broecker W. S., 1996b, Provenance of icebergs during Heinrich Event 3 and the contrats to their sources during other Heinrich episodes, *Palaeoceanography* **11(4),** pp.371-378

Hagelberg T. K., Bond G., DeMenocal P., 1994, Milankovich band forcing of sub-Milankovich climate variability during the Pleistocene, *Palaeoceanography* **9(4),** pp.545-558

Hagen S., and Keigwin L.D., 2002, Sea-surface temperature variability and deep-water reorganisation in the subtropical North Atlantic during Isotope Stage 2-4, *Marine Geology* **189(1-2)**, pp.145-162

Hall A.M., 1995, Was north-west Lewis glaciated during the Devensian? *Quaternary Newsletter* **76**, pp.1-7

Hall A.M., 1996, Quaternary glaciation of Orkney and the surrounding shelves, In: *The Quaternary of Orkney: Field Guide*, Quaternary Research Association, London, pp.4-15

Hall I. R., and McCave I. N., 1998, Late Glacial to recent accummulation fluxes of sediments at the shelf edge and slope of NW Europe, 48-50^{0}N, *Special Publication of the Geological Society, London* **129**, pp.339-350

Hebbeln D., Mangerud J., Dokken T.,et al., 1998, Fluctuations of the Svalbard Barents Sea Ice Sheet during the last 150000 years, *Quaternary Science Reviews* **17(1-3)**, pp.11-42

Heinrich H., 1988, Origin and consequences of cyclic ice-rafting in the northeast Atlantic Ocean during the past 130,000 years, *Quaternary Research* **29**, pp.142-152

Hemming S.R., and Rasbury E.T., 2000, Pb isotope measurements of sanidine monitor standards: implications for provenance analysis and tephrochronology, *Chemical Geology* **165(3-4)**, pp.331-337

Hemming S. R., and Hadjas I., 2003, Ice-rafted detritus evidence from ^{40}Ar/^{39}Ar ages of individual hornblende grains for evolution of the eastern margin of the Laurentide Ice Sheet since 43 ^{14}C kyr, *Quaternary International* **99-100**, pp.29-43

Hemming S. R., Broecker W. S., Sharp W. D., Bond G. C., Gwiazda R. H., Ma Manus J. F., Klas M., Hajdas I., 1998, Provenance of Heinrich layers in core V28-82, northeastern Atlantic: ^{40}Ar/^{39}Ar ages of ice-rafted hornblend, Pb isotopes in feldspar grains and Nd-Sr-Pb isotopes in the fine sediement fraction, *Earth and Planetary Science Letters* **164**, pp.317-333

Hemming et al 2002

Heese R., and Khadabakhsh S., 1998, Depositional facies of late-Pleistocene Heinrich Events in the Labrador Sea, *Geology* **26**, pp.103-106

Higgins S. M., Anderson R. F., McManus J. F., Fleisher M. Q., 1995, A high-resolution ^{10}Be/^{230Th} study of Heinrich Events over the last 130k-yr in a North Atlantic deep sea core, *EOS Transactions AGU* **76(17)** Spring Meet Suppl., S170

Hillaire-Marcel et al 1994

Hinnov L. A., Schulz M., Yiou P., 2002, Interhemispheric space-time attributes of the Dasgaard-Oeschger oscillations between 100 and 0ka, *Quaternary Science Reviews* **21**, pp.1213-1228

Hinrichs J, Schnetger B, Schale H, et al., 2001, A high resolution study of NE Atlantic sediments at station Bengal: geochemistry and early diagenesis of Heinrich layers, *Marine Geology* **177(1-2)**, pp.79-92

Howe J. A., Harland R., Hine N. M., Austin W. E. N., 1998, Late Quaternary stratigraphy and palaeoceanographic change in the northern Rockall Trough, North Atlantic Ocean. *In* : Stoker M. S., Evans D., Cramp (eds) Geological Processes on continental margins: Sedimentation, mass wasting and stability. *Geological Society of London Special Publication* **129**, pp.269-286

Hulbe C.L., 1997, An ice shelf mechanism for Heinrich Layer production, *Palaeoceanography* **12**, pp.711-717

Huon S., and Janschik R., 1993, Detrital silicates in northeast Atlantic deep-sea sediments during the late Quaternary – Major Element, REE and Rb-Sr isotopic data, *Eclogae Geologicae Heletiae* **86(1)**, pp.195-218

Huon S., and Ruch P., 1992, Mineralogical, K-Ar and $^{87}Sr/^{86}Sr$ isotope studies of Holocene and late Glacial sediments in a deep-sea core from the northeast Atlantic ocean, *Marine Geology* **107(4)**, pp.275-282

Innocent C, Fagel N, Hillaire-Marcel C, 2000, Sm-Nd isotope systematics in deep-sea sediments: clay-size versus coarser fractions, *Marine* Geology 1**68(1-4)**, pp.79-87

Jantschik R., and Huon S., 1992, Detrital silicates in Northeast Atlantic deep-sea sediments during the late Quaternary: Mineralogical and K-Ar isotopic data, *Ecologae Geologicae Helvetiae* **85**, pp.195-212

Johnsen, S.J., H.B. Clausen, W. Dansgaard, N.S. Gundestrup, C.U. Hammer, U.Andersen, K.K. Andersen, C.S. Hvidberg, D. Dahl-Jensen, J.P. Steffensen, H.Shoji, A.E. Sveinbjörnsdóttir, J.W.C. White, J. Jouzel, D. Fisher, 1997, The $\delta^{18}O$ record along the Greenland Ice Core Project deep ice core and the problem of possible Eemian climatic instability, *Journal of Geophysical Research* **102**, pp.26397-26410.

Johnson Y. Park R. G., Winchester J., 1987, Geochemsistry, petrogenesis and tectonic significance of the Early Proterozoic Loch Maree Amphibolites, *In:* Pharoah T. C., Beckinsale R. D., Rickard D. T., Geochemistry and mineralisation of Proterozoic volcanic suites, *Geological Society of London Special Publication* **33**, pp.255-269

Kalsbeek F., Taylor P. N., Pidgeon R. T., 1988, Unreworked Archean basement and Proterozoic supracrustal rocks from northeastern Disko Bugt, west Greenland: Implications for the nature of Proterozoic mobile belts in Greenland, *Canadian Journal of Earth Sciences* **25**, pp. 773-782

Kanfoush S. L., Hodell D. A., Charles C. D., Guilderson T. P., Mortyn P. G., Ninnemann U. S., 2000, Millennial-scale instability of the Antarctic Ice Sheet During the last Glaciation, *Science* **288**, pp.1815-1820

Keeling C. D., and Whorf T. P., 2000, The 1,800-year oceanic tidal cycle: a possible cause of rapid climate change, *Proceedings of the National Academy of Sciences*, USA **97**, pp.3814-3819

Keigwin L.D., and Boyle E.A., 1999, Surface and deep ocean variability in the northern Sargasso Sea during marine isotope stage 3, *Palaeoceanography* **14(2)**, pp.164-170

Kirby M.E., and Andrews J.T., 1999, Mid-Wisconsin Laurentide Ice Sheet growth and decay: Implications for Heinrich events 3 and 4, *Palaeoceanography* **14 (2)**, pp.211-223

Kissel C., Laj C., Labeyrie L., Dokken T., Voelker A., Blamart D., 1999, Rapid climatic variations during marine isotope stage 3: magnetic analysis of sediments from the Nordic Seas and North Atlantic, *Earth and Planetary Science Letters* **171**, pp.489-502

Kleman J., Hatterstrand C., Borstrom I., Stroeven A., 1997, Fennoscandian palaeoglaciology reconstructed using a glacial geological inversion model, *Journal of Glaciology* **43**, pp.283-299

Knutz P. C., Austin W. E. N., Jones E. J. W., 2001, Millennial-scale depositional cycles realted to British ice sheet variability and North Atlantic palaeocirculation since 45kyr BP, Barra Fan, UK margin, *Palaeoceanography* **16**, pp.53-64

Knutz P.C., Jones E.J.W., Austin W.E.N., van Weering T.C.E., 2002, Glacimarine slope sedimentation, contourite drifts and bottom current pathways on the Barra Fan, UK North Atlantic margin, *Marine Geology* **188**, pp.129-146

Knies J., Nowaczyk N., Müller C., Vogt C., Stein R., 2000, A multiproxy approach to reconstruct the environmental changes along the Eurasian continental margin over the last 150 000 years, *Marine Geology* **163(1-4)**, pp.317-344

Kroon D., Shimmield G., Austin W. E. N., Derrick S., Knutz P., Shimmield T., 2000, Century- to millennial-scale sedimentological-geochemical records of glagial-Holocene sediement variations from the Barra Fan (NE Atlantic), *Journal of the Geological Society, London* **157**, pp.643-653

Lackschewitz K.S., Baumann K.H., Gehrke B., et al., 1998, North Atlantic ice sheet fluctuations 10,000-70,000 yr ago as inferred from deposits on the Reykjanes ridge, southeast of Greenland, *Quaternary Research* **49(2)**, pp.171-182

Lambeck K., 1993, Glacial Rebound of the British Isles: 2. A high-resolution, high-precision model, *Geophysics Journal International* **15**, pp.960-990

Lambeck K., 1995, Late Devensian and Holocene shorelines of the British Isles and North Sea from models of glacio-hydro-isostatic rebound, *Journal of the Geological Society, London* **152**, pp.437-448

Lambeck K., 1996, Limits on the areal extent of the Barents Sea ice sheet in Late Weichselian time, *Global and Planetary Change* **12(1-4)**, pp.41-51

Langmuir C., Vocke R., Hanson G. N., Hart S. R., 1978, A general mixing equation with applications to Icelandic basalts, *Earth and Planetary Science Letters* **37**, pp.380-392

Lawson T.J., 1984, Reindeer in the Scottish Quaternary, *Quaternary Newsletter* **42**, pp.1-7

Lebel J., Silverberg N., Sundby B., 1982, Gravity core shortening and pore water chemical gradients, *Deep-sea Research Part A-Oceanographic Research Papers* **29(11)**, pp.1365-1372

Little M. G., Kroon D., Schneider R. R., 1997, Heinrich Events in the South Atlantic Ocean: implications for cross-equatorial and Global heat transfer and sub-Milankovich climate, EUG Meeting, Strasbourg, p.613

Lowell T. V., Heusser C. J., Andersen B. G., Moreno P. I., Hauser A., Heusser L. E., Schluchter C., Marchant D. R., Denton G. H., 1995, Interhemispheric correlation of Late Pleistocene glacial events, *Science* **269**, pp.1541-1549

MacAyeal D. R., 1993, Binge/purge oscillations of the Laurentide Ice Sheet as a cause of the North Atlantic's Heinrich Events, *Palaeoceanography* **8**, pp.775-784

Manhes G., Minster J. F., Allegre C. J., 1978, Comparative Uranium-Thorium-Lead and Rubidium-Strontium of St. Severin amphoterite: consequences for early solar system chronology, *Earth and Planetary Science Letters* **39**, pp.14-24

Manighetti B., McCave I. N., Maslin M., Shackleton N. J., 1995, Chronology for Climate Change: Developing age models for the Biogeochemical Flux Study cores, *Palaeoceanography* **10**, pp.513-525

Marchal O., Stocker T. F., Joos F., 1999, Physical and bio-geochemical responses to freshwater-induced thermohaline variability in a zonally-averaged ocean model. In *Mechanisms of Global Climate Change at Millennial Time Scales* (eds. Clark P. U., Webb R. S., Keigwin L. D.), AGU 112, pp.263-284

Marko J.R., Fissel D.B., Wadhams P., et al., 1994, Iceberg severity off eastern North America – its relationship to sea-ice variability and climate change, *Journal of Climate* **7(9)**, pp.1335-1351

Marshall S. J., and Clarke G. K. C., 1997, A continuum model of ice-stream thermomechanics in the Laurentide Ice Sheet 1.Theory, *Journal of Geophysical Research* **102 B9**, pp20599-20613

Marshall G. J., and Clarke G. K. C., 1999, Modelling North American freshwater runoff through the last glacial cycle, *Quaternary Research* **52**, pp.300-315

Marshall S. J., Tarasov L., Clarke G. K. C., Peltier W. R., 2000, Glaciological reconstruction of the Laurentide Ice Sheet: physical processes and modelling challenges, *Canadian Journal of Earth Sciences* **37**, pp.769-793

Marshall S. J., James, T. S., Clarke G. K. C., 2002, North American ice sheet reconstructions at the Last Glacial Maximum, *Quaternary Science Reviews* **21**, pp.175-192

Maslin M., Shackleton N. J., Pflaumann U., 1995, Surface water temperature, salinity and density changes in the northeast Atlantic during the last 45000 years: Heinrich Events, deepwater formation and climatic rebounds, *Palaeoceanography* **10(3),** pp.527-544

Matsumoto K., 1997, Modeled glacial North Atlantic ice-rafted debris pattern and its sensitivity to various boundary conditions, *Palaeocenaogrpahy* **12(2),** pp.271-280

Mayewski P. A., Meeker L. D., Twickler M. S., Whitlow S., Yang Q., Lyons W. B., Prentice M., 1997, Major features and forcing of high-latitude northern hemisphere atmospheric circulation suing a 110,000-year-long glaciochemical series, *Journal of Geophysical Research* **102 (C12)**, pp.26345-26366.

McCabe A. M., Clark P. U., 1998, Ice sheet variability around the North Atlantic Ocean during the last deglaciation, *Nature* **392**, pp.373-377.

McCave I. N., Manighetti B., Robinson S. G., 1995, Sortable silt and fine sediment size/composition slicing: Parameters for palaeocurrent speed and palaeoceanography, *Palaeoceanography* **10(3),** pp.593-610.

McIntrye A., and Molfino B., 1996, Forcing of Atlantic equatorial and subpolar millennial cycles by precession, *Science* **274**, pp.1867-1870.

Moros M., Endler R., Lackschewitz K. S., Wallrabe-Adams H-J., Mienert J., Lemke W., 1997, Physical properties of Reykjanes Ridge sediments and their linkage to high-resolution Greenland Ice Sheet Project 2 ice core data, *Palaeoceanography* **12(5),** pp.687-695.

Moros M., McManus J.F., Rasmussen T., Kuijpers A., Dokken T., Snowball I., Nielsen T., Jansen E., 2004, Quartz content and the quartz-to-plagioclase ratio determined by X-ray diffraction: a proxy for ice rafting in the northern North Atlantic? *Earth and Planetary Science Letters* **218(3-4)**, pp.389-401.

Musgrove, M. and Banner, J. L., 2004, Controls on the spatial and temporal variability of vadose dripwater geochemistry: Edwards aquifer, central Texas, *Geochimica et Cosmochimica Acta* **68**, pp.1007-1020.

Otto J.B., Blank W.K., Dahl D.A., 1988, A Nitrate precipitation technique for preparing strontium for isotopic analysis, *Chemical Geology* **72(2)**, pp.172-179.

O'Nions, R.K., Hamilton, P.J. and Evensen, N.M., 1977, Variations in (super 143) Nd/ (super 144) Nd and (super 87) Sr/ (super 86) Sr ratios in oceanic basalts. *Earth and Planetary Science Letters* **34(1),** pp.13-22.

Paillard D., and Labeyrie L., 1994, Role of the thermohaline circulation in the abrupt warming after Heinrich Events, *Nature* **372**, pp.162-164

Park R. G., 1991, The Lewisian Complex, *In:* The Geology of Scotland 3rd Ed, Craig G. Y. (ed), The Geological Society, UK, pp.25-64

Parker W.R., and Sills G.C., 1990, Observation of corer penetration and sample entry during gravity coring, *Marine Geophysical Reseaches* **12(1-2)**, pp.101-107

Payne A.J., and Baldwin D.J., 1999, Thermomechanical modelling of the Scandinavian ice sheet: implications for ice-stream formation, *Annals of Glaciology* **28**, pp.83-89

Peacock J.D., 1984, Quaternary Geology of the Outer Hebrides, *British Geological Survey Reports* **16/2**, p.26

Peacock J.D., 1991, Glacial Deposits of the Hebridean Region. In: Ehlers J., Gibbard P.L., Rose J., (eds), *Glacial Deposits of Great Britain and Ireland*, Balkema, Rotterdam, pp109-119

Peacock J.D., Austin W.E.N., Selby I., Graham D.K., Harland R., Wilkinson I.P., 1992, Late Devensian and Flandrian palaeoenvironmental changes on the Scottish continental shelf wets of the Outer Hebrides, *Journal of Quaternary Science* **7**, pp.145-161

Peltier W.R., 1994, Ice-age Palaeotopography, *Science* **265**, pp.195-201

Piotrowski, A,M., Goldstein S.L., Hemming S.R., Fairbanks R.G., 2004, Intensification and variability of ocean thermohaline circulation through the last deglaciation, Earth and Planetary Science Letters 225(1-2), pp.205-220

Piper D.J.W., and DeWolfe M., 2003, Petrographic evidence from the eastern Canadian margin of shelf-crossing glaciations, *Quaternary International* **99-100**, pp.99-113

Piper D.J.W., Mudie P. J., Fader G.B., Josenhans H.W., MacLean B., Vilks G., 1991, Quaternary Geology, in: Keen M.J., Williams G.L. (eds), Geology of the continental margin of eastern Canada, Geological Society of America, Boulder CO, pp.475-607

Pollard D., 1982, A Coupled climate-ice sheet model applied to the Quaternary ice ages, *Journal of Geophusical Research-Oceans and Atmospheres* **88(NC12)**, pp.7705-7718

Quetel C. R., Thomas B., Donard O. F. X., Grousset F. E., 1997, Factorial optimisation of data acquisition factors for lead isotope ratio determination by inductively coupled plasma mass spectrometry, *Specrochimica Acta* **B 52**, pp.177-187

Ran E.T.H., 1990, Dynamics of vegetation and environment during the middle pleniglacial in the Dinkel Valley (The Netherlands), *Mededelingen Rijks Geologische Dienst* **44**, pp.141-205

Rasmussen T. L., Thomsen E., van Weering T. C. E., Labeyrie L., 1996a, Rapid changes in surface and deep water conditions at the Faeroe margin during the last 58,000 years, *Palaeoceanogrpahy* **11**, pp.757-771

Rasmussen T. L., van Weering T. C. E., Labeyrie L., 1997, Climatic instability, ice sheets and ocean dynamics at high northern latitudes during the last glacial period (58-10ka BP), *Quaternary Science Reviews* **16**, pp.71-80

Revel M., 1995, Dynamique des courants profonds en Atlantique nord, depuis 200ka, Thesis, Universite Bordeaux I.

Revel M., Sinko J. A., Grousset F. E., Biscaye P. E., 1996a, Sr and Nd isotopes as tracers of North Atlantic lithic particles: Palaeoclimatic implications, *Palaeoceanography* **11**, pp.95-113

Revel M., Cremer M., Grousset F. E., Labeyrie L., 1996b, Grain-size and Sr-Nd isotopes as tracer of palaeo-bottom current strength, Northeast Atlantic Ocean, *Marine Geology* **131**, pp.233-249

Rietveld, H.M., 1967, Line profiles of neutron powder-diffraction peaks for structure refinement, *Acta Crystallography* **22**, pp.151-2.

Rietveld, H.M., 1969, A profile refinement method for nuclear and magnetic structures, *Journal of Applied Crystallography* **2**, pp.65-71.

Richter T.O., Lassen S., van Weering T.C.E., de Haas H., 2001, Magnetic susceptibility patterns and provenance of ice-rafted material at Feni Drift, Rockall Trough: implications for the history of the British–Irish ice sheet, *Marine Geology* **173(1-4)**, pp.37-54

Robertson D. K., and Cumming G. L., Lead and sulphur isotope ratios from the Great Slave Lake area, Canada, *Canadian Journal of Earth Sciences* **5**, pp.1269-1276

Robinson S. G., Maslin M. A., McCave N., 1995, Magnetic susceptibility variations in upper Pleistocene deep sea sediments of the NE Atlantic: implications for ice-rafting and palaeocirculation at the Last Glacial Maximum, *Palaeoceanography* **10**, pp,221-250

Romer R. L., and Wright J. E., 1993, Lead mobilisation during tectonic reactivation of the western Baltic Shield, *Geochimica et Cosmochimica Acta* **57**, pp.2555-2570

Rose J., 1985, The Dimlington Stadial/Dimlington Chronozone: a proposal for naming the main glacial episode of the Late Devensian in Britain, *Boreas* **14**, pp.225-230

Rosell-Melé A., Maslin M.A., Maxwell J.R., Schaeffer P., 1997, Biomarker evidence for "Heinrich" events, *Geochimica et Cosmochimica Acta* **61(8)**, pp.1671-1678

Ruddiman W. F., 1977, Late Quaternary deposition of ice-rafted sand in the sub-polar north Atlantic (40-60°), *Geological Society of America Bulletin* **88**, pp.1813-1821

Sancetta C., 1992, Primary Production in the glacial North Atlantic and North Pacific Oceans, *Nature* **360**, pp.249-251

Sanchez-Goni M. F., Turon J-L., Eynaud F., Gendreau S., 2000, European climatic responses to millennial-scale changes in the atmosphere-ocean system during the last glacial period, Quaternary Research 54, pp.394-403

Sangster D. F., 1978, Isotopic studies of ore-leads of the circum-Kisseynew volcanic belt of Manitoba and Saskatchewan, *Canadian Journal of Earth Sciences* **15**, pp.1112-1121

Sarnthein M., Stattegger K., Dreger D., Erlenkeuser H., Grootes P., Haupt B. J., Jung S., Kiefer T., Kuhnt W., Pflaumann U., Schafer-Neth C., Schulz H., Schulz M., Seidov D., Simstich J., van Kreveld S., Vogelsang E., Volker A., Weinelt M., 2001, Fundamental modes and abrupt climate changes in North Atlantic circulation and climate over the last 60 kyr – Concepts, reconstructions and numerical modelling, In: *The Northern North Atlantic: A Changing Environment*, edited by P. Shafer et al., Springer-Verlag, New York, pp.365-410

Schulz H., von Rad U., Erlenkeuser H., 1998, Correlation between Arabian Sea and Greenland climate oscillations of the past 110,000 years, *Nature* **393**, pp.54-57

Schulz M., 2002, On the 1470-year pacing of Dansgaard-Oeschger warm events *Palaeoceanogrpahy* **17(2)**, p.1014

Schulz M., Berger W. H., Sarnthein M., Grootes P. M., 1999, Amplitude variations of 1470-year climate oscillations during the last 100,000 years linked to fluctuations of continental ice mass, *Geophysical Research Letters* **26(22)**, pp.3385-3388

Scource J. D., Hall I. R., McCave I. N., Young J. R., Sugden C., 2000, The origin of Heinrich layers: Evidence from European Precursor events, *Earth and Planetary Science Letters* **182**, pp.187-195

Sejrup H.P., Haflidason H., Aarseth I., King E., Forsberg C.F., Long D., Rokoengen K., 1994, Late Weichselian glacial history of the northern North Sea, *Boreas* **23**, pp.1-13

Sejrup H.P., Larsen E., Landvik J., King E.L., Haflidason H., Nesje A., 2000, Quaternary glaciations in southern Fennoscandia: evidence from southwestern Norway and the northern North Sea region, *Quaternary Science Reviews* **19(7)**, pp.667-685

Severinghaus J. P., and Brook E. J., 1999, Abrupt climate change at the end of the last glacial period inferred from trapped air in polar ice, *Science* **286**, pp.930-934

Shackleton N. J., Hall M. A., Vincent E., 2000, Phase relationships between millennial-scale events 64000-24000 years ago, *Palaeoceanography* **15(6)**, pp.565-569

Shackleton N. J., Fairbanks R.G., Tzu-chien C., Parrenin F., 2004, Absolute calibration of the Greenland timescale: implications for Antarctic time scales and for $\Delta^{14}C$, *Quaternary Science Reviews* **23**, pp.1513-1522.

Shoemaker E.M., 1992, Water sheet outburst floods from the Laurentide Ice Sheet, *Canadian Journal of Earth Sciences* **29**, pp.1250-1264

Sinha A. K., 1970, Model lead and radiometric ages from the Churchill Province, Canadian Shield, *Geochimica et Cosmochimica Acta* **34**, pp.1080-1106

Sinha A. K., and Tilton G. R., 1973, Isotopic Evolution of common lead, *Geochimica et Cosmochimica Acta* **37**, pp.1823-1849

Sinko J. A., 1994, Les flux de particules issues des eaux de surface de l'Atlantique Nord depuis 250,000 ans: variabilite et implications paleo-climatique, Thesis, Universite Bordeaux I.

Singer A., 1984, The palaeoclimatic interpretation of clay minerals in sediments: A review, Earth Science Reviews 21, pp.251-293

Skinner L.C., and McCave I.N, 2003Analysis and modelling of gravity- and piston coring based on soil mechanics, *Marine Geology* **199(1-2)**, pp.181-204

Slatt R.M., and Eyles N., 1981, Petrology of glacial sand: implications for the origin and mechanical durability of lithic fragments, *Sedimentology* **28**, pp.171-183

Smythe F.W., Ruddiman W.F., Lumsden D.N., 1985, Ice-rafted evidence of long-term North Atlantic circulation, *Marine Geology* **64(1-2)**, pp.131-141

Snoeckx H., Grousset F. E., Revel M., Boelaert A., 1999, European contribution of ice-rafted sand to Heirich layers H3 and H4, *Marine Geology* **158**, pp.197-208

Solheim A, Faleide J.I., Andersen E.S., et al., 1998, Late Cenozoic seismic stratigraphy and glacial geological development of the East Greenland and Svalbard Barents Sea continental margins, *Quaternary Science Reviews* **17(1-3)**, pp.155-184

Steiger R. H., and Wasserberg 1969, Comparative U-Th-Pb systematics in $2.7x10^9$yr plutons of different geoloical histories, *Geochimica et Cosmochimica Acta* **33**, pp.1213-1232

Stein R., Man S-I., Grobe H., Hubberten H., 1996, Late Quaternary glacial history and ice-rafted debris fluctuations along the East Greenland continental margin. In: Late Quaternary palaeoceanography of the North Atlantic margins, J.T. Andrews, W.A. Austen, H. Bergsten and A.E. Jennings (eds), London Geological Society

Stoker M.S., 1995, The influence of glacigenic sedimentation on slope-apron development on the continental margin off northwest Britain. In: Scrutton R.A., Stoker M.S., Shimmield G.B., Tudhope A.W. (eds), The Tectonics, Sedimentation and Palaeoceanography of the North Atlantic Region, *Geological Society of London Special Publication* **90**, pp.159-277

Stoker M.S., and Holmes R., 1991, Submarine end moraines as indicators of Pleistocene ice limits off north-west Britain, *Journal of the Geological Society of London* **148**, pp.431-434

Stoker M.S., Hitchen K., Graham C.C., 1993, The geology of the Hebrides and West Shetland shelves and adjacent deep-water areas, *British Geological Survey United Kingdom Offshore Regional Report*. HMSO, London

Stoner J. S., Channell J. E. T., Hillaire-Marcel C., 1996, The magnetic signature of rapidly deposited detrital layers from the deep Labrador Sea: relationship to north Atlantic Heinrich Layers, *Palaeoceanography* **11**(3), pp.309-325

Sundblad K., and Staphens M. B., 1983, Lead-isotope systematics of strata-bound sulphide deposits in the higher nappe complexes of the Swedish Caledonides, *Economic Geology* **78**, pp.1090-1107

Sutherland D.G., 1984, The Quaternary deposits and landforms of Scotland and the adjacent shelves: a review, *Quaternary Science Reviews* **3**, pp.157-254

Sutherland D.G., 1991, Late Devensian glacial deposits and glaciation in Scotland and the adjacent offshore region. In: Ehlers J., Gibbard P.L., Rose J., (eds), *Glacial Deposits of Great Britain and Ireland*, Balkema, Rotterdam, pp.53-60

Sutherland D.G., and Walker M.J.C., 1984, A Late Devensian ice-free area and possible interglacial site on the Isle of Lewis, Outer Hebrides, *Nature* **309**, pp.701-703

Sutherland D.G., Ballantyne C.K., Walker M.J.C., 1984, Late Quaternary glaciation and environmental change on St Kilda, Scotland and their palaeoclimatic significance, *Boreas* **13**, pp.261-272

Syvitski J.P.M., Andres J.T., Dowdeswell J.A., 1996, Sediment deposition in an iceberg-dominated glacimarine environment, East Greenland: basin fill implications, *Global and Planetary Change* **12**, pp.251-270

Tamburini F., Huon S., Steinmann P., Grousset F. E., Adatte T., Follmi K. B., 2002, Dysaerobic conditions during Heinrich Events 4 and 5: Evidence from phosphorus distribution in a North Atlantic deep-sea core, *Geochimica et Cosmochimica Acta* **66(23)**, pp.4069-4083

Taylor P. N., Moorbath S., Goodwin R., Petrykowski A. C., 1980, Crustal contamination as an indicator of the early Archean continental crust: Pb isotopic evidence from the late Archean gneisses of west Greenland, *Geochimica et Cosmochimica Acta* **44**, pp.1437-1453

Thomas R.H., and Bentley C.R., 1978, Model for Holocene retreat of West Antarctic Ice Sheet, *Quaternary Research* **10(2)**, pp.150-170

Thomson J., Higgs N.C., Clayton T., 1995, A geochemical criterion for the recognition of Heinrich Events and estimation of their depositional fluxes by the $^{230}Th_{excess}$ profiling method, *Earth and Planetary Science Letters* **135**, pp.41-56

Thouveny N.A., Moreno E., Delanghe D., et al., 2000, Rock magnetic detection of distal ice-rafted debris: clue for the identification of Heinrich Layers on the Portuguese margin, *Earth and Planetary Science Letters* **182(2)**, pp.197

Tilton G. R., and Steiger R. H., 1969, Mineral ages and isotopic composition of primary lead at Manitouwadge, Ontario, *Journal of Geophysical Research* **74**(8), pp.2119-2132

Tilton G. R., and Kwon S. T., 1990, Isotopic evidence for crust-mantle evolution with emphasis on the Canadian Shield, *Chemical Geology* **83**, pp.149-163

Todt W., Cliff R. A., Hanser A., Hofman A. W., 1996, Evaluation of a ^{202}Pb – ^{205}Pb Double Spike for High-Precision Lead Isotope Analysis, *In* Basu and Hart, Earth processes: Reading the Isotopic Code. *Geophysical Monograph* **95**, American Geophysical Union, Washington DC 429-437

Valen V., Larsen E., Hufthammer A.K., 1996, Sedimentology and stratigraphy in the cave Hamnsundhelleren, western Norway, *Journal of Quaternary Science* **11**, pp.185-201

Van Kreveld S., Sarnthein M., Erlekevser H., Grootes P., Jung S., Nadeau M. J., Pflaumman U., Voelker A., 2000, Potential links between surging ice sheets, circulation

changes and the Dansgaard-Oeschger cycles in the Irminger Sea, 60-18kry, *Palaeoceanography* **15(4),** pp.425-442

Viega-Pires C. and Hillaire-Marcel C., 1999, U and Th isotope constraints on the duration of Heinrich Events H0-H4 in the southeastern Labrador Sea, *Palaeoceanography* **14**, pp.187-199

Vitrac A. R., Albarede F., Allegre C. J., 1981, Lead isotopic composition of Hercynian granitic K-feldspars constrains continental genesis, *Nature* **291**, pp.461-464

Voelker, A.H.L., Sarnthein, M., Grootes, P., Erlenkeuser, H., Laj, C., Mazaud, A., Nadeau, M.-J. and Schleicher, M., 1998, Correlation of marine ^{14}C ages from the Nordic Seas with the GISP2 isotope record: implications for ^{14}C calibration beyond 25 ka BP, *Radio-carbon* **40**, pp. 517–534.

Vorren T.O., and Laberg J.S., 1997, Trough mouth fans - Palaeoclimate and ice-sheet monitors, *Quaternary Science* Reviews **16(8)**, pp.865-881

Vorren TO, Laberg JS, Blaume F, et al., 1998, The Norwegian Greenland Sea continental margins: Morphology and late Quaternary sedimentary processes and environment, *Quaternary Science* Reviews **17(1-3)**, pp.273-302

Wang L., Sarnthein M., Erlenkeuser H., Grimalt J., Grootes P., Heilig S., Ivanova E., Kienast M., Pflaumann U., 1999, East Asian monsoon climate during the last Pleistocene: High-resolution sediment records from the South China Sea, *Marine Geology* **156**, pp.245-284

Whittington G., and Hall A.M., 2002, The Tolsta Interstadial, Scotland: correlation with D-O cycles GI-8 to GI-5? *Quaternary Science Reviews* **21**, pp.901-915

Wilbur J. S., Mutschler F. E., Friedamn J. D., Zartman R. E., 1990, New chemical, isotopic and fluid inclusion data from zinc-lead-copper veins, Sawangunk mountains, New York, *Economic Geology* **85**, pp.182-196

Wilson L.J., and Austin W.E.N., 2002, Millennial and sub-millennial-scale variability in sediment colour from the Barra Fan, NW Scotland: implications for British ice sheet dynamics, 2002, *In*: Glacier-influenced sedimentation on High Latitdue Continental Margins, Dowdeswell J.A., and Cofaigh C (eds), *Geological Society London Special Publication* **203**, pp.349-365

Wilson L. J., Austin W. E. N., Jansen E., 2002, The Last British Ice Sheet: growth, maximum extent and deglaciation, *Polar Research* **21**, pp.243-250

Wintle A.G., 1981, Thermoluminescence dating of sediments, *Geophysical Journal of the Royal Astronomical Society* **65(1)**, pp.280

Wunsch C., 2000, On sharp spectral lines in the climate record and the millennial peak, *Palaeoceanography* **15**, pp.417-424

Zahn R., Schonfeld J., Kudrass H-R., Park M-H., Erlenkeuser H., Grootes P., 1997, Thermohaline instability in the North Atlantic during meltwater events: stable isotopes and detritus records from core SO75-26KL, Portuguese margin, *Palaeoceanogrpahy* **12(5),** pp.696-710

Zartman R. E., and Wasserburg G. J., 1969, The isotopic composition of lead in potassium feldspars from some 1.0b.y. old North American igneous rocks, *Geochimica et Cosmochimica Acta* **33**, pp.901-942